Rapid Vaccine Development using a Micro-scale Platform

A thesis submitted to University College London for the degree of

ENGINEERING DOCTORATE

by

Tarit K. Mukhopadhyay

The Advanced Centre for Biochemical Engineering, Department of Biochemical Engineering, University College London, Torrington Place, WC1E 7JE, United Kingdom

ProQuest LLC
789 East Eisenhower Parkway
P.O. Box 1346
Ann Arbor, MI 48106-1346

THE ADVANCED CENTRE FOR BIOCHEMICAL ENGINEERING

24th May 2008

Curriculum Development and Examiners
Registry
UCL

Dear Examiners Section

Revised EngD Thesis of Mr Tarit Mukhopadhyay – Two Year Restriction of Access

This letter accompanies the revised version of the above thesis which has now been approved by the UCL Internal Examiner. Also attached is a letter dated 8th February which accompanied the examiner nomination forms.

Since the work described in the thesis is currently being pursued for commercial exploitation I would request a restriction of access to the thesis for a period of 2 years. Please could you confirm that appropriate steps are taken to ensure this happens for the copy of the thesis to be retained by the UCL Library? I need to pass this confirmation on to the collaborating company that sponsored the EngD project.

Regards

Gary Lye
EngD Supervisor

Department of Biochemical Engineering
UCL, Torrington Place, London WC1E 7JE, UK
Tel: +44 (0)20 7679 7942 Fax: +44 (0)20 7209 0703
Email: g.lye@ucl.ac.uk, Website: www.ucl.ac.uk/biochemeng

Gary J Lye, BSc, PhD, CEng, CSci, MIChemE
Professor of Biochemical Engineering
MSc Programme Co-ordinator

8th February 2008

Curriculum Development and Examiners
Registry
UCL

Dear Examiners Section

EngD Candidate Mr Tarit Mukhopadhyay – Restriction of Access to Thesis

Please find attached examiner nomination forms for the above candidate. The content of this cover letter follows a conversation with Helen Notter at the end of last year.

The work described in the thesis is currently being pursued for commercial exploitation by the company that sponsored the EngD project. In order to protect their interests, and still enable the student to complete his doctoral programme, I would like to request the following:

- A restriction of access to the thesis for a period of 2 years for reasons of commercial exploitation of the results.
- It be made clear to the examiners that the viva is held under conditions of strict confidentiality with regard to the results presented in the thesis.
- A modification of the recorded thesis title from "Rapid vaccine development using a micro-scale platform with applications to meningitis serogroup B and anthrax vaccines" (as it appeared on the thesis submission forms) to "Rapid vaccine bioprocess development using a microscale platform" to avoid any indication of the specific applications.

Let me know if there is any further information I need to supply.

Regards

Gary Lye
EngD Supervisor

Department of Biochemical Engineering
UCL, Torrington Place, London WC1E 7JE, UK
Tel: +44 (0)20 7679 7942 Fax: +44 (0)20 7209 0703
Email: g.lye@ucl.ac.uk, Website: www.ucl.ac.uk/biochemeng

Gary J Lye, BSc, PhD, CEng, CSci, MIChemE
Professor of Biochemical Engineering
MSc Programme Co-ordinator

Abstract

Vaccine research and development is becoming increasingly important because of the potential to create a blockbuster drug, such as Prevnar®. However, the development pipeline continues to be a limiting factor in commercialising a vaccine. In this thesis a micro-scale platform is created to mimic the key features of a unit operation so that it is possible to calculate the impact of a commercial manufacturing process using this scaled down platform. Two model vaccines were applied to the micro-scale platform, a new Meningitis serogroup B vaccine based on the outer membrane vesicle proteins of *Neisseria lactamica* and the licensed UK Anthrax vaccine.

To create the platform, cultures of *Neisseria lactamica* in microwells have been combined with statistical techniques such as Design of Experiments to increase biomass production by four fold and antigen yields by 165%. Microwell experiments were coupled with SELDI-TOF mass spectroscopy to enable a detailed insight into the changing vaccine composition with culture conditions. Microwell results here were scaled up to 2, 8 and 50 litre fermentations using dimensionless analysis based on the oxygen mass transfer co-efficient, k_La.

The effects of pilot scale downstream processing were investigated using ultra scale down tools and models. It was possible to characterise product losses and the robustness of the process stream by conducting shear experiments. Furthermore, final product filter sterilisation was investigated using a microwell platform coupled with statistical analysis, particle sizing and DLVO theory. Through these studies it was possible to minimise aggregation and increase antigen transmission through the membrane from 35% to 78%.

The platform was applied to cultures of *Bacillus anthracis* Sterne $34F_2$, the Anthrax vaccine strain. Microwells were used to mimic Thompson bottle cultures and ascertain the main factors which effect *B. anthracis* growth and antigen production. The cell density dependent

signalling mechanism, known as quorum sensing was found to control growth and antigen production in *B. anthracis* and that a protein below 5kDa may be involved in the quorum sensing mechanism along with the auto inducer molecule, AI-2.

Finally, transfer of *B. anthracis* vaccine production from static culture to a homogenous stirrer tank culture environment was investigated using a miniature bioreactor. It found that transfer was possible and that doing so reduced the culture time from 28 hours to just 14 hours, increasing production of PA and LF vaccine antigens by 25% and 78% respectively. Aeration of the culture showed that biomass production could be improved upon, but it had a detrimental effect on antigen expression.

"It is a far, far better thing that I do, than I have ever done; it is a far, far better rest that I go to than I have ever known."

Charles Dickens – A Tale of Two Cities

Acknowledgements

I am convinced that the pursuit of a doctorate in any discipline should not be as enjoyable as this was. Even while slaving away in the depth of a research laboratory till the small hours of the morning, shielded from sunlight, my spirit never faltered. The reason for this is solely down to the privilege of having such a large network of friends and family who care deeply for me.

I am grateful. I am grateful to my family. To my mother and father whose love and belief in me kept my course true; encouraging and supporting me until the final hurdle. To my sister, nephew, niece and brother-in-law; my Sundays with them provided the escape I needed to stop me from falling apart.

I am grateful to my friends in the Anthrax Vaccine team, who provided the excellent comedy required whenever working with a Class 3 pathogen. Their camaraderie and friendship helped me to survive my exile in Salisbury.

Special thanks to Professor Gary Lye for his guidance, tutelage and of course, his comprehensive corrections. I am grateful also to Susana Levy, John Ward, Nigel Allison, Sue Charlton, Karen Reddin and Andy Gorringe for their knowledge and supervision.

Finally, to my friends at University College London:

It was the best of times.

Table of Contents

List of Figures

List of Tables

List of Abbreviations

a	interfacial mass transfer area
AI-1	autoinducer type 1
AI-2	autoinducer type 2
A_S	effective aeration
cfu	colony forming units
C_L	oxygen concentration in liquid phase
C*	oxygen concentration in gas phase
CPP	critical process parameter
CQA	critical quality attribute
D_i	impeller diameter
DOE	design of experiments
DOT	dissolved oxygen tension
DSW	deep square wells
EF	oedema factor
FDA	Food and Drug Administration
fur-1	(5Z)-4-bromo-5-(bromomethylene)-3-butyl-2(5H)-furanone
GMP	Good Manufacturing Practice
h	hours
HPA	Health Protection Agency
IND	Investigational New Drug
IMP	Investigational Medicinal Product
k_La	oxygen mass transfer coefficient
LF	lethal factor
MHRA	Medicines and Healthcare products Regulatory Agency
min	minutes
MS	mass spectroscopy
n	revolution per second

OD	optical density
OMV	outer membrane vesicle
PA	protective antigen
rLF	recombinant lethal factor
rPA	recombinant protective antigen
RO	reverse osmosis
Rpf's	Resuscitation protein factors
rpm	revolutions per minute
SELDI	surface enhanced laser desoprtion and ionisation
SSPS	sterile stationary phase supernatant
TOF	time of flight
USD	ultra-scale down
vvm	volume of air per volume of liquid per minute

1 Introduction

1.1 Vaccines and vaccination

Vaccination is perhaps the most successful and significant medical accomplishment of the 20th century. It is because of vaccination that over two million deaths a year have been prevented (World Health Organisation). This has resulted in an increased life expectancy of thirty years; saving over $1 billion per year. It is because of vaccination that Smallpox has been eradicated (Fenner *et al.* 1988) and Polio is soon to follow (www.polioeradication.org).

It should be noted however that vaccination is not a marvel of the 20th century. Indeed, as early as the 18th century Edward Jenner and later Louis Pasteur in the 19th century have both used vaccination in the fight against disease. Towards the end of the twentieth century though, there was a slow down in vaccination and vaccine research due to three main problem areas. These were legal, social and financial; the last cause being perhaps the main driver for the lack of vaccine research in recent years. The legal or regulatory requirements of vaccine research are strict and stringent for safety reasons but essentially have proved to be a limit on the time scale for a vaccine to be launched on the commercial market. These regulations take the form of a Code of Federal Regulations, Chapter 21 (21CFR) in the United States, and are enforced by the Food and Drug Administration (FDA). The equivalent organisation in the United Kingdom is the Medicines and Healthcare products Regulatory Agency (MHRA) which is a member through association of a greater European Union agency, the European Medicines Agency (EMEA). In order to launch a product in any market the vaccine manufacturing company must meet the legally required safety standards set by each authority in the respected national markets which is both costly and time consuming. There is also a social aspect to consider, as routine vaccination involves the administering of vaccine to otherwise healthy individuals in the hope that they

might not catch a disease. This in itself is not an issue until the patient concerned develops side effects to the vaccine, which can then lead to mistrust in both the vaccine and the pharmaceutical community. The final aspect is one of financial needs. Due to a poor guarantee on the uptake of vaccine plus the costs associated with regulatory compliance, vaccines have traditionally yielded very modest returns on investment. Furthermore, there is also a high perceived legal liability, as seen in the recent TGN 1412 clinical trials (Mukhopadhyay 2006). As a result since 1967, the number of vaccine manufactures in the United States has fallen from thirty-seven to less then ten, while the number of vaccines approved by the FDA has decline from 380 to approximately a few dozen (Miller 2003). This has resulted in less competition and investment into new technologies and consequently vaccines are becoming more expensive. So much so that recently the FDA demanded Wyeth reduce its unit price for their new pneumococcal vaccine from $58 per unit by $12 (Stolberg 2000).

However, a new precedent has been set with the release of Gardasil (Merck) and Prevenar (Wyeth) both of which are expected to reach blockbuster status, yielding over $1 billion revenue per annum (Smith 2007). They have demonstrated that vaccines need not give poor returns, which has caused resurgence in vaccine research. This interest falls into two categories; investment into new vaccines, and the improvement of existing vaccines. Vaccine development itself is changing in order to create vaccines that are more potent, tolerable and safe. The results is a better product but with a more demanding manufacturing process. In order to better appreciate exactly what is required for this to be achieved the vaccine development pipe line must be understood.

1.2 Vaccine Development Pipeline

It is important to make clear and understand that vaccines are not created at point of discovery, but that there is a long process of development. From the start of discovery to

the end of development, the entire process can take 8-15 years. The cost of vaccine development varies depending on the type of vaccine manufacture, but usually requires millions of pounds of investment.

Figure 1.1 outlines the most common steps of vaccine development. Basic research focuses on the biological mechanisms pathogenic bacteria use to cause damage. Such research also takes into account physical characteristics of an organism, which might be used as a vaccine component, or as a drug to prevent or interrupt the disease process. To develop a candidate vaccine preparations of cell-culture are tested. If initial results are promising, the candidates are further tested in laboratory animals such as mice, guinea pigs or monkeys. In some cases, computers can help visualise the vaccine candidates in three dimensions to gain speculative pharmacokinetic data. If the vaccine candidate performs well throughout these preclinical evaluations, it can become an investigational vaccine for use in human volunteers in clinical trials.

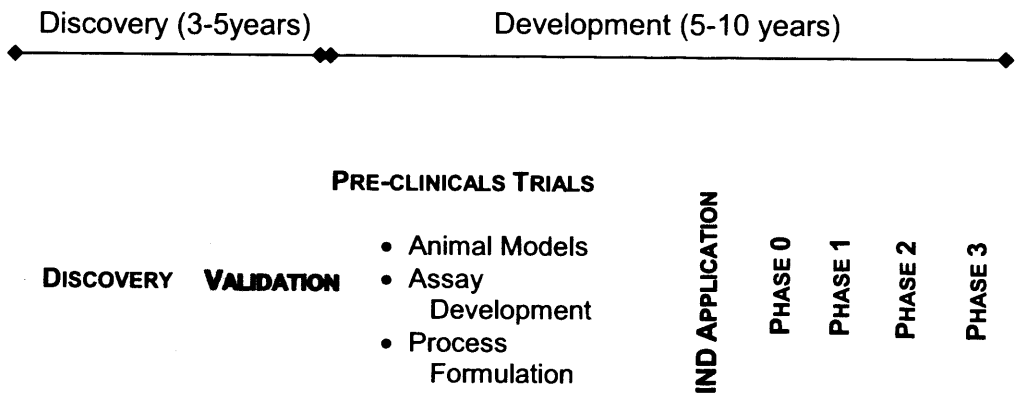

Figure 1.1 The vaccine development pipeline, segmented into the distinct phases of research and development

Traditionally, clinical trials have been divided into three distinct phases, but this has now been expanded to five phases following FDA recommendations on new guidance's for investigational new drug (IND) applications (Food and Drug Administration - CDER 2006).

Phase zero is a first in man study conducted to determine very early pharmacokinetic and pharmacodynamic data. Sample groups are no larger then fifteen persons and are used to expedite the clinical trial process. In these trials, full doses are not yet administered to this population. Phase one is normally a small number of patients suffering from the disease for whom all other treatments have been exhausted. These sample groups are larger then phase zero trials and can consist of up to 30 persons. During this phase the dosage is investigated and can be escalated from a safe starting dose to a maximum treatment dose. These data should provide information on the safety and tolerability of the investigational medicinal product (IMP). Studies are also conducted to increase the pharmacokinetic and pharmacodynamic data and provide preliminary evidence of efficacy. Phase one trials last less then one year and for this only a relatively small amount of clinical material needs to be manufactured. Once an IMP enters phase two, the sample groups used increases from 30-50 patients to one approximately hundred patients and are designed to provide proof of efficacy with a manageable safety profile. This phase can take one to two years and is usually randomised. Most IMP's fail at the end of phase two, allowing for only a one in three chance of progression to phase three.

Phase three is the largest and most expensive phase of vaccine development requiring on average approximately £50million to conduct (Antisoma). It uses a sample group of several hundred patients to confirm efficacy and may take several years. This phase is used to establish the complete safety profile of the IMP and is often used as the basis of regulatory information. Most products have an 80% success rate at the end of phase three (Ernst & Young). Following phase three and the launch of the product onto the market phase four

commences, which monitors for any long term post market release side effects of the product.

From a research and development viewpoint, the fermentation and downstream processing route should already be established by the end of phase two, leaving time for the optimisation of the process during phase three clinical trials. However, as phase two trials are most risky, offering only a 30% success rate, it is desirable to limit the amount of money spent on the process at the end of phase two. However, if the process has not been defined by the end of phase two, this then consequently may result in a non-optimised process being rushed for commercial manufacture, or worse, a delay in launch. The reason why it is so important to have a well defined process stems from a regulatory perspective. In order to launch a product onto market the key operating parameters of the process must be defined in accordance with cGMP manufacture, (U.S. Code of Federal Regulations, Chapter 21, 21CFR210-211, 21CFR600-680), clearly stating the written procedures in forms of standard operating protocols (SOP's), the critical quality attributes (CQA) and critical process parameters (CPP) of the process. Failure to have GMP documentation ready which defines the process SOP's, CQA and CPP delays the launch of the product, resulting in loss of revenue and potential loss of market share.

1.3 Micro-scale approaches to vaccine process development

As highlighted in a review of the subject by Micheletti and Lye, there has been a significant development of microtitre plates as a platform technology for bioprocess development over the past five years (Micheletti and Lye 2006). Many are already familiar with the concept of microwell or microtitre plates for use in assays and high throughput screening (Hajduk and Greer 2007), but their application until recently had not been expanded to include bioprocess evaluation and scale-up. Yet, the benefits of this methodology would be

considerable. By using small volumes the cost of materials could be reduced as could the time taken to perform each experiment, as replicates could be conducted on the same plate. There is also an added safety benefit, as the application of the microwell platform could be expanded to include experiments on dangerous pathogens, working volumes of which should be intentionally minimised for safety reasons. This class of organism could be investigated without the need for expensive, specialist containment level three manufacturing facilities. Instead the whole process could be investigated in a flexible film isolator or cabinet.

There is already a precedent for unit operations being performed in microwell format. Several microbial fermentations have been conducted in microwells using *E.coli* (Kostov *et al.* 2001;Micheletti *et al.* 2006) and some investigations into enzyme biocatalysis (Ferreira-Torres *et al.* 2005;Schmidt and Bornscheuer 2005) and even tissue culture (Girard *et al.* 2001). Other organisms include yeast (Kensy *et al.* 2005) and filamentous *S. erythraea* (Elmahdi *et al.* 2003). Work on the downstream processing aspect has been limited. Jackson *et al* has investigated the interaction between fermentation and primary recovery using a micro scale filtration device coupled to a vacuum manifold (Jackson *et al.* 2006).

What gives the micro scale platform a significant advantage is its ease of automation. Automated liquid handling systems have illustrated the suitability of the microwell plate for automation, (Ferreira-Torres *et al.* 2005;Jackson *et al.* 2006). The result of which is the reduction in operator error and increase in throughput meaning reproducible and accurate results. Yet to fully benefit from the microwell platform a good understanding of fluid mixing is required as well as a better understanding of statistical methods to produce reliable quantitative data.

1.3.1 Hydrodynamics and mass transfer in microwell systems

Ideally, scaled-down fermentations should replicate large-scale fermentations in order to be truly indicative of microbial metabolic function, physiology, and strain productivity. Puskeiler *et al.* (2005) demonstrated physiological and metabolic reproducibility between discrete miniature bioreactors for dry cell weight and glucose metabolic profiles for *Escherichia coli* in parallel, fed-batch, fermentations at 6mL scale. Reproducible fermentations of *S. cerevisiae* by dissolved oxygen, pH, and optical density profiles in both 50µL and 150µL scale micro bioreactors for growth physiology and global gene expression analysis have also been established (Boccazzi *et al.* 2006). However, there are associated problems with such operations.

As stated previously, scale down fermentations should be able to replicate large scale fermentations. Yet to accomplish this it is necessary to attain comparable oxygen transfer. Oxygen transfer has always been a prime concern in microtitre plates. The reason for this is that microwell plates are aerated using a shaking platform; there is no impeller system to facilitate mass transfer. It has been shown that the rate of oxygen transfer can be controlled in a 96-well plate by altering the shaking frequency and amplitude (Büchs 2001). Increases in shaker throw change the liquid height, thus increasing the area available for gas transfer. The phenomenon has already been well characterised in shakeflasks (Büchs *et al.* 2000a;Büchs *et al.* 2000b).

However, when moving to the small volumes of a microtitre well, another effect not previously characterised comes into force. This is surface tension. The surface tension acts as another barrier to gas transfer as it can have a direct effect on the liquid displacement height, thus affecting the oxygen mass transfer co-efficient ($k_o$la). When considering the classic example of oxygen transfer from an air bubble into the liquid medium of a bioreactor it is often described by Equation 1.1 (Stanbury and Whitaker 1984a):

$$\frac{dC_L}{dt} = k_L a\left(C^* - C_L\right) \qquad \text{(Eq. 1.1)}$$

Where $\frac{dC_L}{dt}$ is the rate of oxygen transfer, (C^* - C_L) is the oxygen gradient, k_L is the oxygen mass transfer co-efficient and 'a' is the area available for mass transfer. In reality it is very difficult to separate k_L and a, thus they are usually thought of as a combined mass transfer coefficient, k_La. In shaken bioreactors such as microwells, the surface tension affects the area component of the k_La reducing the liquid displacement height in the microwell and consequently reducing the diffusivity of the system as described by Ficks Law.

However, surface tension also has a secondary effect when considered in the context of two-film theory (Doran 2003). A mass transfer boundary layer forms at the contact point between two immiscible phases, in this case a gas and liquid. If C_{O1} represents the bulk concentration of oxygen in the gaseous phase and C_{O2} represents the bulk oxygen concentration in the liquid phase, then the two film resistance can be described as in Figure 1.2. According to the theory, a relatively stagnant boundary layer films exists on either side of the interface and mass transfer through molecular diffusion is hindered through the film layers. The resistance to oxygen transfer is increased if conditions at the interface are less turbulent as this generates larger film boundaries.

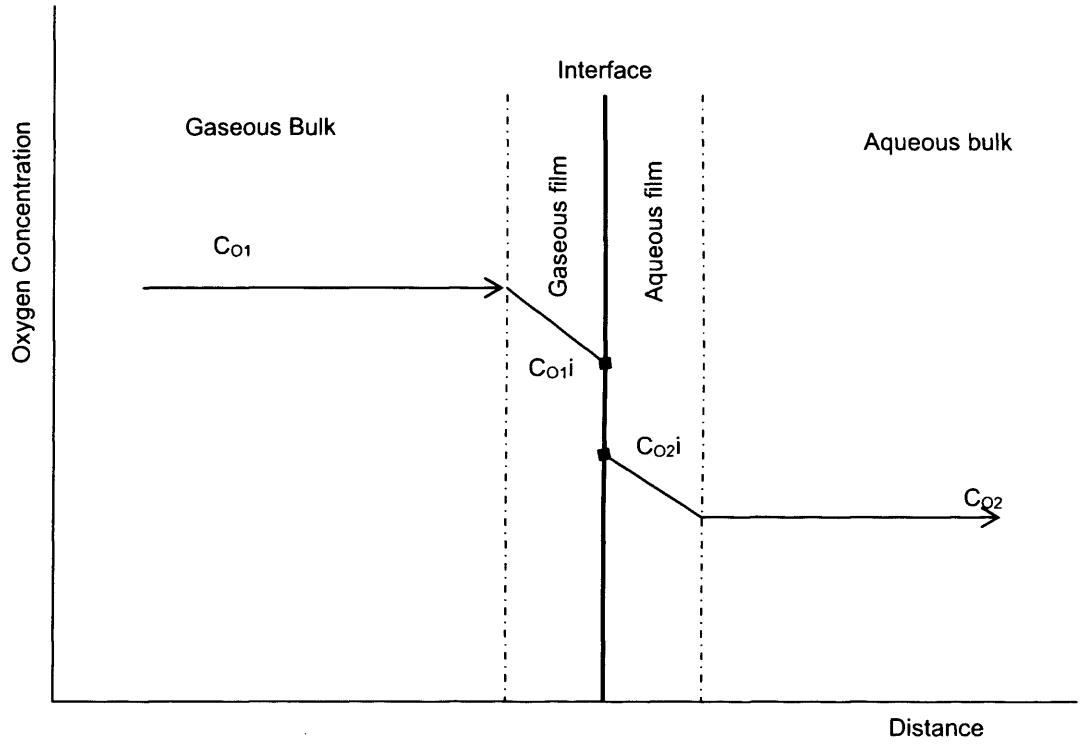

Figure 1.2 Two-film theory of oxygen mass transfer describing the molecular diffusion of oxygen from the gaseous phase to the liquid phase being hindered through resistive film layers. CO1 represents the bulk gaseous oxygen concentration; CO1i represents the bulk gaseous phase oxygen concentration at the interface. CO2i represents the bulk aqueous phase oxygen concentration at the interface; CO2 bulk aqueous phase oxygen concentration.

For practical reasons it is generally assumed that there is no resistance at the interface itself as the two phases are at equilibrium and have uniform properties. This assumption is an oversimplification, especially as the properties of the system such as density, concentration, dielectric constant etc. change abruptly at the interface. The molecules at the interface are subject to strong fields causing orientation due to interfacial tension, interfacial electro-potential differences and adsorption. With the addition of surface active molecules, such as salts, these have the effect of increasing the surface tension and thus

the interface resistance (R_i) to mass transfer across the film. The total resistance (R_T) can be summarised as the sum effect of the gaseous film resistance (R_G), fluid film resistance (R_F) and the interface resistance (R_i), Equation 1.2 (Meares 1984).

$$R_T=R_G+R_F+R_i \qquad \text{(Eq. 1.2)}$$

Surface tension itself is a measure of a wide range of intermolecular forces such as van der Waals forces, electrostatic and dipole moments. In practical terms these forces can be affected by medium ionic strength, the microwell material of construction and temperature. Increasing the temperature has the effect of reducing the surface tension based upon the Eötvös rule as increasing the temperature increases the entropy of the system (Tornberg 1977). The choice of microtitre plate construction, either glass (hydrophilic) or plastic (hydrophobic) will impact upon the way molecules align themselves on the surface (Büchs 2001), with hydrophobic surfaces increasing the surface tension, similar to water droplets upon a waxed leaf. The presence of inorganic salts and electrolytes such as sodium chloride often increase the surface tension. These electrolytes usually are surface active as they have a very strong attraction to the solvent, water, and are most easily described by a Gibbs isotherm (Alexander and Posner 1950).

The effect of shaker amplitude, frequency and surface tension upon the microwell plate changes dependent upon the shaker platform used and the culture medium and thus should be evaluated empirically until better understood.

1.4 Experimental Design

The use of statistical experimental design or Design of Experiments (DOE) is an efficient procedure which economically maximises information gained with each experimental run and evaluates the statistical significance of the data. It is common to define a process

model for DOE, categorising the model as a 'black box.' That is to say the mechanism of the model is unknown but the inputs and outputs can be measured and related to each other (NIST/SEMATECH 2003).

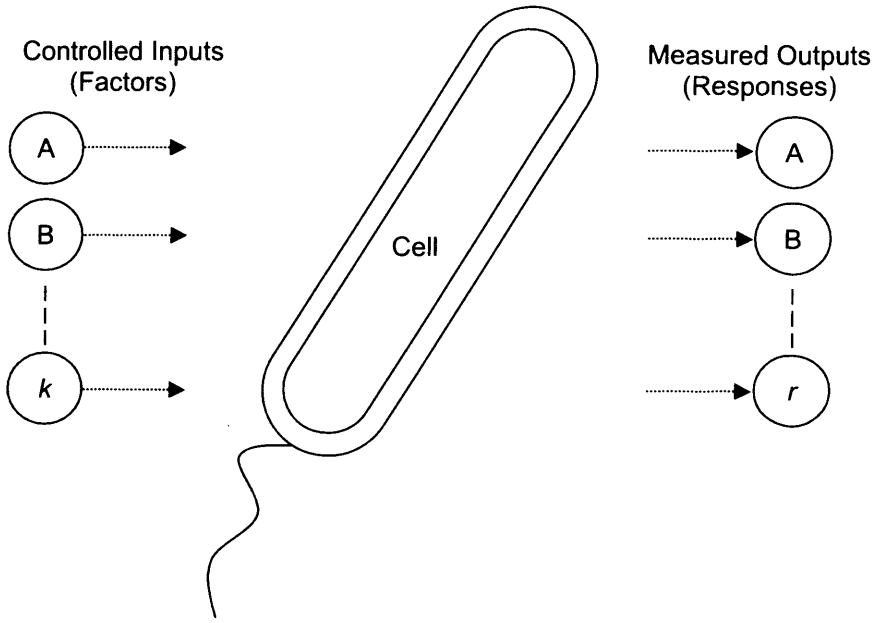

Figure 1.3 A 'black box' process model schematic. The internal workings of the box are unknown, however the controlled inputs to be tested (factors) can be varied and the desired outputs (responses) measured to evaluate which factors are responsible for specific responses

For example, as shown in Figure 1.3, let the black box be thought of as a single bacterium. The exact genetics and metabolic pathways are unknown; however it is possible to measure the inputs into the model, such as glucose, amino acids and the outputs, enzyme activity, acid formation and so on. This experimental data are used to derive an empirical model linking the inputs to the outputs and can be expressed as either a first order linear

model (Equation 1.3) or a second order quadratic model, though the quadratic model is usually reserved for response surface DOE to optimise a process. Equation 1.3 identifies the main effects of the model as single factor terms and interaction effects as two factor terms (NIST/SEMATECH 2003).

$$y_{ri} = \beta_{ki} X_{ki} + \varepsilon_0$$
$$Y = \beta_0 + \beta_A X_A + \beta_B X_B + \beta_{AB} X_A X_B + \varepsilon_0 \quad \text{(Eq. 1.3)}$$

Where Y is the response, β is the co-efficient effect, ε_o is the experimental error and X represents the factor investigated.

DOE can be used for several purposes and as a result there are several designs and methodologies to choose from. The choice of design is dependent upon the number of factors required and the purpose of the experiment. Table 1.1 summarises the choice and methods available. The purpose of comparative experimentation is to focus on one factor out of many and identify if that principal factor is significant to the desired response. Screening experiments are designed to screen out the main effects from other less important factors, while response surface experiments are used to find optimal process settings. Most of the experiments conducted will be limited to four factors and will focus mainly on discovery rather then optimisation, thus the next section will focus on factorial design.

1.4.1 Factorial Design

A common experimental design is one with all input factors set at two levels each. These levels are called `high' and `low' or `+1' and `-1', respectively. A design with all possible high/low combinations of all the input factors is called a full factorial design in two levels. If there are k factors, each at 2 levels, a full factorial design has 2^k runs (Mathews 2004).

A factorial experiment allows for estimation of experimental error through replication. Replication is a very reliable way of assessing experimental error. When the number of factors is large (typically more than 5 factors) replication of the design can become operationally difficult. In these cases, it is common to only run a single replicate of the design, and to assume that factor interactions of more than a certain order (say, between three or more factors) are negligible. Under this assumption, estimates of such high order interactions are estimates of an exact zero, thus really an estimate of experimental error (Mathews 2004).

Number of Factors	Comparative Design	Screening Design	Response Surface Design
1	1-factor, completely randomised	-	-
2-4	Randomised block design	Full or half factorial design	Central composite of Box-Behnken design
5+	Randomised block design	Fractional factorial or Plackett-Burman design	Screen first to reduce number of factors

Table 1.1 Summary table for choosing an experimental design for comparative, screening or response surface experiments (NIST/SEMATECH 2003)

When there are many factors, many experimental runs will be necessary, even without replication. For example, experimenting with 10 factors at two levels each produces 2^{10}=1024 combinations. At some point this becomes unfeasible due to high cost or insufficient resources. In this case, fractional factorial designs may be used. As with any statistical experiment, the experimental runs in a factorial experiment should be randomised to reduce the impact that bias could have on the experimental results. In practice, this can be a large operational challenge (NIST/SEMATECH 2003).

Factorial experiments can be used when there are more than two levels of each factor. However, the number of experimental runs required for three-level (or more) factorial designs will be considerably greater than for their two-level counterparts. Factorial designs are therefore less attractive if two or more levels are to be considered. Factorial design experiments are most commonly analysed using analysis of variance (ANOVA).

1.4.2 Factorial ANOVA

This is also known as two-way ANOVA and is used to determine the effects of two or more factors on the response variable and, if there are interaction effects, determine the nature of the interactions. Key to implementing ANOVA is understanding the total sum of squares methodology used. By expanding the total sum of squares (SS_{TOTAL}) expression, it shows that the total variance in the data is partitioned into two parts, variance within each treatment and variance between each treatment. The error sum of squares (SSE) measures the variance of each data point from its treatment level mean. This is the measure of variance *within* treatments and so must be random error. The treatment sum of squares relating to the factors A and B (SSA, SSB, SSAB) provide a measure of variance *between* treatments by considering the deviation of each treatment mean from the grand mean. The total sum of squares and its constituent parts are expanded in Equation 1.4 to 1.8 (Stephens 2004).

$$SS_{TOTAL} = SSA + SSB + SSAB + SSE \quad \text{(Eq. 1.4)}$$

$$SSA = \sum_{i=1}^{a}\left(\bar{x}[A]_i - \bar{\bar{x}}\right)^2 \quad \text{(Eq. 1.5)}$$

$$SSB = \sum_{j=1}^{b}\left(\bar{x}[B]_j - \bar{\bar{x}}\right)^2 \quad \text{(Eq. 1.6)}$$

$$SSAB = \sum_{i=1}^{a}\sum_{j=1}^{b}\left(\bar{x}[AB]_{ij} - \bar{x}[A]_i - \bar{x}[B]_j + \bar{\bar{x}}\right)^2 \quad \text{(Eq. 1.7)}$$

$$SSE = \sum_{i=1}^{a}\sum_{j=1}^{b}\sum_{k=1}^{r}\left(x_{ijk} - \bar{x}[AB]_{ij}\right)^2 \quad \text{(Eq. 1.8)}$$

Where $\bar{x}[AB]_{ij}$ is the mean of the response in the ij^{th} treatment (mean of the treatment when the factor A level is *'i'* and the factor B level is *j*), $\bar{x}[A]_i$ is the mean of the responses when the factor A level is *'i'*, $\bar{x}[B]_j$ is the mean of the responses when the factor B level is *'j'*, $\bar{\bar{x}}$ is the mean of all responses and 'a' is the number of factor A levels, 'b' is the number of factor B levels and 'c' is the number of replicates.

By calculating the total sum of squares and identifying the degrees of freedom an ANOVA table can be generated. The general form of the two factor factorial is shown in Table 1.2.

Source of Variance	Degrees of Freedom	Sum of Squares	Mean Squares	F-statistic
Factor A	a-1	SSA	MSA = SSA/(a-1)	F = MSA/MSE
Factor B	b-1	SSB	MSB = SSB/(b-1)	F = MSB/MSE
Factor AB	(a-1)(b-1)	SSAB	MSAB = SSAB/(a-1)(b-1)	F = MSAB/MSE
Error	n-ab	SSE	MSE = SSE/(n-ab)	
Total	n-1	SS(total)		

Table 1.2 A summary ANOVA table based upon two factor experiments (Stephens 2004).

The test statistic used relies upon an F-distribution from which the *p*-value can be found as it is the area in the upper tail of this distribution. Hence the F-statistic is used to allude the *p*-value which dependent upon the degrees of freedom of the model and can be obtained through reference (NIST/SEMATECH 2003). The *p*-value itself is the probability of the test statistic being at least as extreme as the one observed given that the null hypothesis is true. A small *p*-value is an indication that the null hypothesis is false (Mathews 2004).

As the number of factors investigated increases, so does the number of terms in the model, so computer programs are used to easily calculate and plan DOE factorial design experiments. The statistical software 'Minitab' was used as the statistical package for DOE planning and analysis as it incorporates the sum of squares form outlined above with graphical outputs (Mathews 2004).

Several groups have recently applied DOE to investigate protein expression but most studies focus upon only a narrow range of factors, broadly grouped into either media formulation (Nikerel *et al.* 2005;Ren *et al.* 2006) or protein induction conditions (Cao

2006;Swalley *et al.* 2006;Urban *et al.* 2003) with no consideration of the engineering environment under which cell growth and protein synthesis occurs.

1.5 Vaccine application systems

1.5.1 Meningitis Serogroup B vaccine

The clinical disease known as meningitis can be caused by several means; however, infection through the pathogenic bacteria, *Neisseria meningitidis* is most frequent. There are five common serogroups of *N.meningitidis*, (A, B, C, Y and W135) which are responsible for most of the disease, though in Europe and North America it is serogroups B and C which are most prevalent (Pollard and Moxon 2002).

Neisseria meningitis serogroup B infection remains a significant global public health problem (Gorringe *et al.* 2005a). Since the introduction of the conjugated meningococcal serogroup C vaccine in 1999, the incidence of serogroup C infection in the United Kingdom has fallen, yet at the same time, the numbers of serogroup B cases have increased. In 2004/2005, the number of reported serogroup B infections in England and Wales alone reached 1288 confirmed cases, compared to only 43 group C infections. (Figure 1.4). Today, serogroup B infections account for over 85% of total meningitis infections, thus remaining a high priority in the UK as *Neisseria meningitidis* remains one of the leading causes of childhood death in many industrialised nations (Pollard and Moxon 2002). It is a serious disease as the clinical features of infection are mostly indistinguishable. Death can only be prevented through the timely administration of antibiotics. This however can not always be guaranteed and thus there is a clear need to develop an effective serogroup B vaccine (Morley and Pollard 2001).

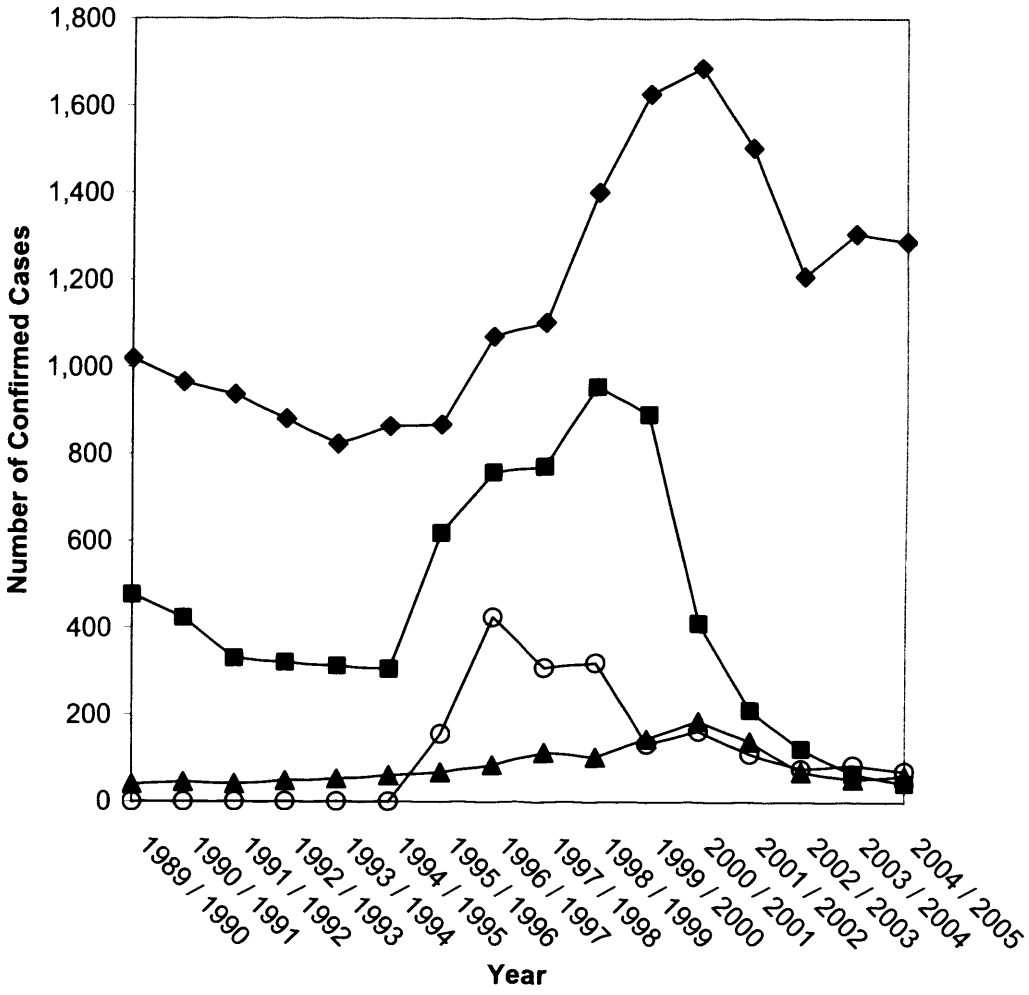

Figure 1.4 Incidence of confirmed cases of meningococcal disease by year in England and Wales (source Health Protection Agency). (◆) Serogroup B infection, (■) Serogroup C infection, (▲) other serogroups, (○) unclassified.

Around the world, serogroup B *N. meningitidis* infections account for approximately 50% of all meningococcal disease. Capsular polysaccharide based vaccine exist for most serogroups of *N. meningitidis* apart from serogroup B. It is the only serogroup whose infection cannot be prevented by capsular polysaccharide based vaccines because the capsule is a polymer of α(2–8)-linked N-acetyl-neuraminic acid (polysialic acid), which is also present in human tissues, including the neural cellular adhesion molecule involved in cell-to-cell adhesion (Griffiss *et al.* 1991). An attempt was made at developing a conjugated

vaccine using group B capsular polysaccharide in which the N-acetyl groups of the sialic acid residues had been replaced with N-propionyl groups (Sanofi-Pasteur). The vaccine was tested in a Phase I trial on adult volunteers and found to be safe, but the antibodies induced were devoid of functional activity (Bruge *et al.* 2004). Consequently, vaccine research against serogroup B meningococcus has mostly focused on cell-surface protein antigens contained in outer-membrane vesicles (OMVs). Native OMVs consist of intact outer membrane and contain outer membrane proteins (OMP's) and lipooligosaccharides. They readily can be prepared by detergent extraction from the bacteria (Fredriksen *et al.* 1991).

One of the outer meningococcal OMP's, PorA, was identified as a major inducer of and target for serum bactericidal antibodies. This protein is expressed by almost all meningococci. However, there is a large number of PorA proteins with different antigenic specificities so that eliciting an immune response against one PorA antigen does not confer protection against strains with heterologous PorA antigens. In a study of the prevalence of serogroup B strains in the USA, it was found that 20 different PorA proteins would have to be incorporated in a group B OMV vaccine to cover 80% of circulating strains (Tondella *et al.* 2000). OMV vaccines are thus strain-specific vaccines that can only be used against colonal disease outbreaks but not for prevention of sporadic disease caused by diverse strains.

PorB is a more promising OMP vaccine candidate as it was suggested that only a limited number of combinations of these proteins would be needed in a vaccine (Urwin *et al.* 2004). The two currently best studied group B OMV vaccines have been produced in response to national outbreaks in Norway and Cuba, respectively. The Norwegian vaccine has been developed in collaboration between the Norway Institute of Public Health and Chiron whereas the Cuban vaccine was developed in collaboration between the Finlay Institute in Cuba and GSK. Both vaccines have been used for epidemic control in their

respective countries and, in the case of the Cuban vaccine, in Brazil and Chile. These PorA vaccines were found to be 50%–80% effective, but they did not provide protection in children less than 4 years of age (Jodar *et al.* 2002), the immune response was of short duration, and the vaccine did not seem to have an impact on nasopharyngeal carriage.

In an effort to develop a vaccine against the New Zealand group B strain (NZ), the National Institute for Public Health and the Environment (RIVM) in The Netherlands has used recombinant technology to produce both a monovalent NZ PorA vaccine and a hexavalent vaccine containing 6 PorA proteins, including that of the NZ strain. The performance of the NZ PorA antigen in the hexavalent formulation administered as a three dose series was only modest in infants, but it was shown to stimulate a satisfactory immune response after a fourth dose in children under 4 (Cartwright *et al.* 1999;Longworth *et al.* 2002). This vaccine has now been tested in Phase II trials (GSK).

An OMV vaccine containing PorA and PorB as well as LPS from the New Zealand serogroup B strain was developed by Chiron in partnership with the New Zealand Ministry of Health and the University of Auckland (O'Hallahan *et al.* 2004). The vaccine, MeNZB, was successfully tested in Phase I and a series of successive Phase II trials in school children then in children under 12 years. A three dose regimen of immunization was found to elicit bactericidal antibodies in 70% of children 6–24 months of age as well as in 8–12 years old children. The vaccine elicited a 90% response in teenagers. Strain-specific anti-OMP immune responses also were generated in infants. Sequential, nationwide introduction of the vaccine in the under 20 years of age population is currently ongoing with intensified Phase III/IV monitoring. Of note is the fact that a prototype OMV vaccine against Group A meningococcus that was able to efficiently induce bactericidal antibodies in mice, was shown to contain, in addition to the major OMP's PorA and PorB, other proteins such as RmpM and small amounts of NspA , as well as lipooligosaccharides (Norheim *et al.* 2005).

A subunit vaccine based on purified *Neisserial* surface protein A (NspA) has been developed by Shire Pharmaceuticals (Moe *et al.* 2001) and (O'Dwyer *et al.* 2004b) and evaluated in a Phase I clinical trial. Other OMP's, such as the transferrin-binding protein (Danve *et al.* 1993) and (West *et al.* 2001), also are being explored as possible meningococcal vaccines. A member of the OMP family, lipoprotein LP2086, which is displayed on the surface of 91% meningococcal strains, could serve as an immunogen to induce protective serum bactericidal activity against a broad variety of meningococcal strains (Pillai *et al.* 2005).

1.5.1.1 Neisseria lactamica

Natural immunity to Meningitis serogroup B infection has been documented and reviewed (Pollard and Frasch 2001). Protection against Meningitis serogroup B infection can be attained through the presence of serum antibodies which are progressively acquired during the early years of childhood. During this period carriage of *N.meningitidis* is low, while the carriage rates of other commensal *Neisseria* species are high. It is believed that the colonisation of the nasopharynx with non-pathogenic commensal *Neisseria* species may provide immunity. Carriage of non pathogenic commensal *Neisseria lactamica* is especially prevalent in early childhood and is associated with a rise in antibody titres against *N.meningitidis* (Goldschneider *et al.* 1969;Mitchell *et al.* 1965). 3.8% of 3 month old and 21% of 18 month old carried *N. lactamica*. By age 14-17 years this carriage rate had dropped to less than two percent (Gold *et al.* 1978). However, during the same time frame, only 0.71% of infants between the age of 0-4 years and 5.4% of teenagers were carriers of *N.meningitidis*, with approximately 66% of the group developing immunity to meningococci of serogroups A,B and C (Gold *et al.* 1978). Studies in the Faeroe Islands have also demonstrated that those children who had previously been exposed to *N. lactamica* have a reduced chance of developing meningococcal disease (Olsen *et al.* 1991), findings which have since been supported through mathematical modelling (Coen *et al.* 2000).

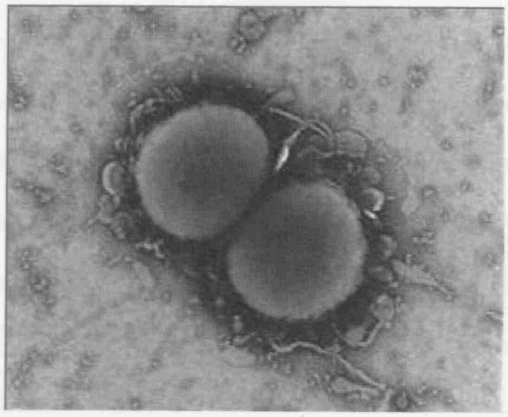

Figure 1.5 An image of an *N. lactamica* diplococcus showing OMV being created on the cell surface. This image was produced using a scanning electron microscope. (Image from hpa.org.uk)

An investigation into the efficacy of an *N. lactamica* vaccine has been carried out through experimentation with the protein components of the outer membrane vesicles (OMVs) and protection has been demonstrated in mouse models (Gorringe *et al.* 2005b;Troncoso *et al.* 2002). In particular, an outer membrane protein pool between 0-43kDa has been shown to provide the greatest protection to mice when challenged with *N.meningitidis* of diverse serogroup and serotype (Oliver *et al.* 2002) . Furthermore, *N. lactamica* does not produce the highly variable outer membrane protein PorA (Kim JJ *et al.* 1989) hence the resulting vaccine may not be sero-subtype specific and may offer protection from meningococci of diverse serotype and serogroup (Gorringe *et al.* 2005a;O'Dwyer *et al.* 2004a). This information provides the basis for an *N. lactamica* OMV vaccine against meningococcal disease. It is this production process for the current vaccine that forms the basis for part of the studies reported in this thesis.

1.5.2 Anthrax Vaccine

Anthrax has been a prominent feature in bio-defence since World War 2, thought recently brought to the forefront by the notorious mail attacks of 2001 (Brachman 2002). As a result the United States government has significantly increased bio-defence funding through the BioShield projects (Dudley and McFee 2005). This renewed interest in anthrax exposed limitations in current vaccine production methods (Smith 2005). The causative agent of anthrax is the rod shaped, non-motile, spore forming bacterium, *Bacillus anthracis*. It is a Gram positive bacteria (Mock and Fouet 2001) and usually grows aerobically but is actually a facultative anaerobe (Wenner and Kenner 2004). Anthrax has two main virulence factors, the polyglutamic acid capsule and the toxins themselves which are encoded on two plasmids separate from the bacterial chromosome. Plasmid pX01 is a 182kb plasmid which encodes for the proteins Protective Antigen (PA), Lethal Factor (LF) and Oedema Factor (EF) (Guidi-Rontani *et al.* 1999). Proteins PA and LF combine to form lethal toxin (Beall *et al.* 1962) and PA and EF combine to form oedema toxin (Stanley and Smith 1961) in a bi-partite arrangement (Figure 1.6).

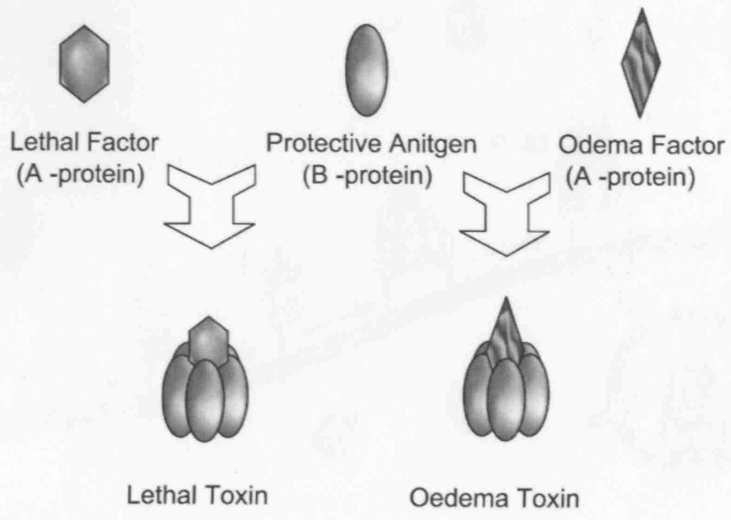

Figure 1.6 Arrangement of the two principle anthrax toxins, lethal toxin and oedema toxin from the constituent proteins, lethal factor, protective antigen and lethal factor (Grabenstein 2003).

Plasmid pX02 is 93kb in size and encodes several genes which combine to form a polyglutamic acid capsule which inhibits phagocytosis (Zwartouw and Smith 1956). The vaccine strain used in current UK production is *B. anthracis* Sterne $34F_2$ which lacks the pX02 plasmid. It still possesses pX01 and expresses PA which is the main component of the vaccine. PA has been well established as the main protective component of both the US and UK acellular vaccines through a variety of lethal challenge experiments with mice (Grabenstein 2003;Hambleton *et al.* 1984). It is an 83kDa protein which is cleaved by furin at the cell surface to produce two subunits, PA_{63} and PA_{20}. LF and EF are also produced but in smaller amounts and are both considered to be important contributors to the potency of the UK vaccine. LF is a 90kDa Zn^{2+} metalloprotease, which cleaves and inactivates mitogen activated protein kinase kinases (Duesbery *et al.* 1998). EF is an intracellular active enzyme, which is a calmodulin-dependent adenylate-cyclase (89kDa) that causes a dramatic increase of intracellular cAMP levels (Leppla 1984). PA_{63} combines to form a heptamer which creates a porin like structure to which lethal factor, oedema factor or both attach itself. The toxin is then internalised resulting in toxic a effect on the cell (Figure 1.7).

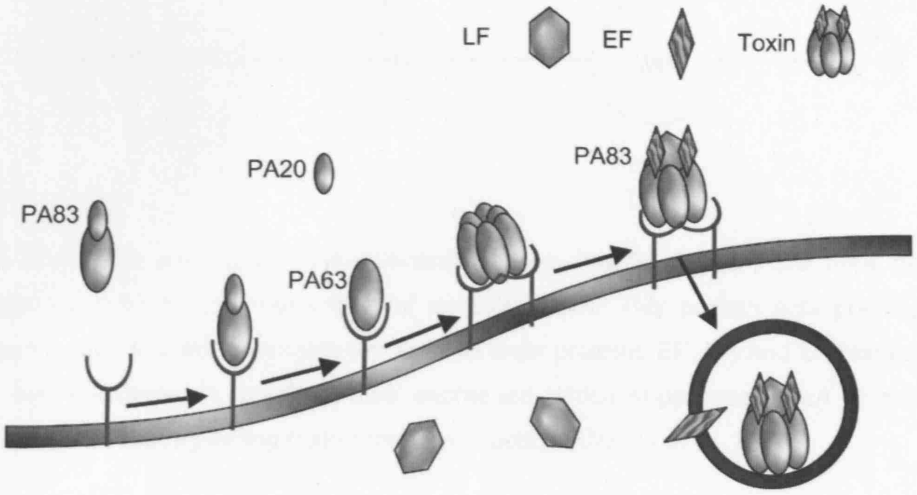

Figure 1.7 Schematic of the internalisation of the anthrax toxins, showing the cleavage and heptamerisation of PA to form a pore like structure to which LF and EF bind to (Mock and Mignot 2003).

Also encoded on pX01 is the anthrax toxin attenuator protein (AtxA). It is a central regulator that interferes with the expression of 70 genes *in vivo* and is thought to control PA, LF and EF expression as well as capsule expression (Mock and Mignot 2003). Key to this regulon is the necessity for an elevated carbon dioxide environment. Optimal production of toxins requires the bacteria to be grown under high CO_2-tension at 37℃ (Sirard *et al.* 1994). The current hypothesis is that the high carbon dioxide tension has a positive effect on AtxA expression which in turn triggers the expression of anthrax virulence factors (Uchida *et al.* 1993;Uchida *et al.* 1997).

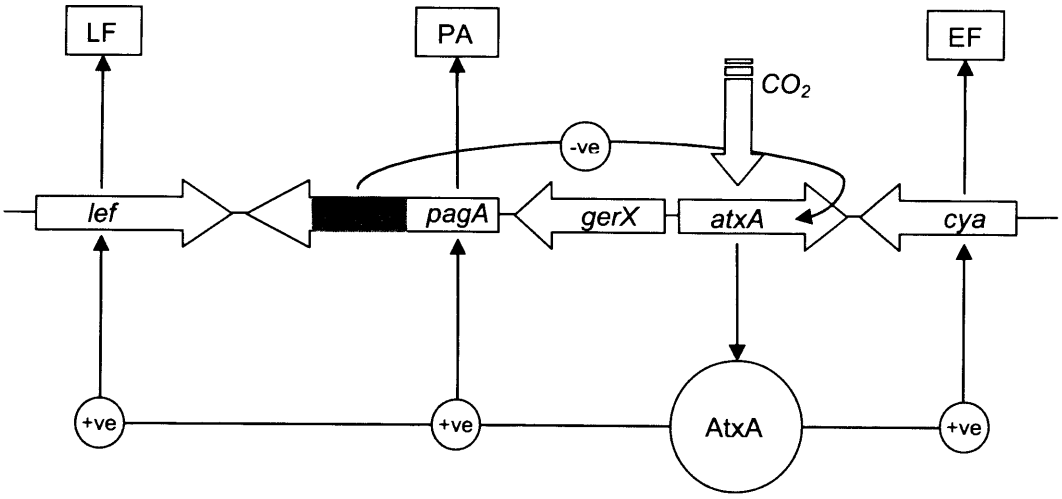

Figure 1.8 In the presence of an elevated carbon dioxide tension, the *atxA* gene is expressed to produce the transcriptional activator AtxA. This protein acts positively on genes *cya*, *pagA* and *lef* to produce the anthrax toxin proteins EF, PA and LF respectively. During *pagA* expression, *pagR* is also expressed which suppresses *atxA* in sufficient concentrations, thus regulating toxin protein production (Uchida *et al.* 1997).

The current UK anthrax vaccine (AVP) has been manufactured under licence at the Health Protection Agency for in excess of 40 years. There has been limited process modification during this time. AVP is a cell free alum precipitate of the anthrax culture supernatant containing the vaccine antigens. Briefly, *B. anthracis* Sterne $34F_2$ is grown in Thompson

bottles with a 500mL working volume under static conditions for 24-28 hours. The culture is then passed through a 0.2 µm filter after which the sterile supernatant is combined with potassium aluminium sulphate and acidified to create a precipitate which is left to settle for approximately one week. This precipitate forms the basis of the anthrax vaccine (Hambleton *et al.* 1984). A typical vaccine runs consists of 228 bottles, which takes approximately 2 hours to inoculate under containment level 3 conditions, which could lead to some batch to batch variability. The bottles are considered ready to harvest after a characteristic change in the culture pH profile is observed where the pH drops below a value of 7.6 and then recovers slightly. It is licensed under special consideration by the Secretary of State for the Department of Health.

1.5.2.1 Quorum Sensing

The control of pathogenicity in *B. anthracis* may not be limited to the activation of the AtxA regulon. The cell density communication phenomenon known as quorum sensing may also be involved. Quorum sensing relies on a signalling mechanism based on small molecules called auto-inducers (Kaprelyants and Kell 1996). Individual bacterial cells produce auto-inducer molecules that pass into the surrounding medium, but initially their concentration is too low to stimulate a general culture response. When sufficient bacteria are present, all producing the auto-inducer molecule; the concentration passes a threshold level allowing the bacteria to sense that a critical population density has been reached. This, then, has the effect of up-regulating or down-regulating targeted genes. Quorum sensing itself is not normally associated with growth but rather regulates the activation of certain phenotypes, such as pathogenic relationships (Joyce *et al.* 2004;Miller *et al.* 2002;Sircili *et al.* 2004).

Two main classes of auto-inducer molecules have been identified. The first, auto-inducer 1 (AI-1), has been identified as a N-acyl-homoserine lactone in Gram negative bacteria (Bassler 1999;Fuqua *et al.* 1996;Parsek and Greenberg 2000). When in sufficient concentrations the molecules bind and trigger a transcriptional activator, which in turn

induces the expression of target genes. However, there are no reports of gram positive bacteria, such as *B. anthracis*, producing N-acyl-homoserine lactones (de Kievit *et al.* 2001). Instead, Gram positive bacteria make use of a post-translationally processed peptide signal molecule. These peptide signals interact with a two component histidine kinase sensor element which up regulates gene expression (Kleerebezem *et al.* 1997). An AI-1 type signalling molecule has yet to be detected or identified in *B. anthracis*; however, research conducted on *B. subtilis* has identified two such signalling molecules. One is the competence and sporulation factor (CSF) (Solomon *et al.* 1995;Solomon *et al.* 1996) and the other is a competence pheromone, ComX (Magnuson *et al.* 1994). Both accumulate during exponential growth and are required to stimulate a transcription factor ComA. CSF utilises an oligopeptide permease as a signalling sensor while the ComX pheromone uses a hisitidine protein kinase, ComP (Lazazzera and Grossman 1998).

The second class of auto-inducer molecules, AI-2, is widely found in the bacterial kingdom. It was initially discovered as a molecule required for bioluminescence in the marine bacterium *V. harveyi* (Bassler *et al.* 1993) but since has been identified in several other bacteria. The AI-2 molecule is a furanosyl borate diester (Chen *et al.* 2002) coded for by the *luxS* gene (Schauder *et al.* 2001) and which is excreted by the bacteria. The AI-2 molecule is then detected by two proteins, LuxP and LuxQ, (Bassler *et al.* 1994) which combine to form the sensor. LuxP is similar to periplasmic ribose binding protein, while LuxQ is a two component histidine kinase sensor (Neiditch and Hughson 2007). The LuxPQ sensor element creates a signal cascade to luxR, which is required for the expression of the target genes in the quorum sensing regulon (Showalter *et al.* 1990). This signal cascade is based upon the production of luciferase in *V.harveyi*. While AI-2 systems have been identified in many bacteria, its method of signal transduction has only been established in *V. harveyi*, *V. cholerae*, and *S. enterica* serovar Typhimurium (Xavier and Bassler 2005). In *B. anthracis*, luxPQ has not been identified; however, luxS and luxR are present in the genome (Jones and Blaser 2003).

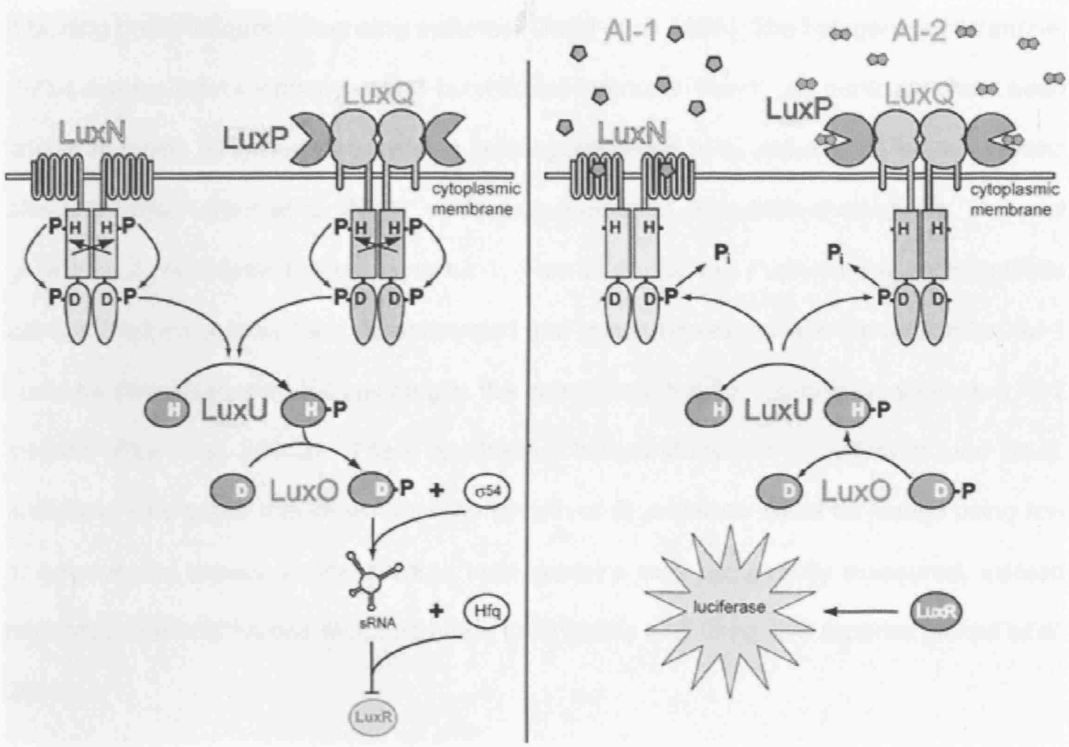

Figure 1.9 *V.harveyi* quorum-sensing signal transduction circuit. Under conditions of low cell density, LuxN and LuxPQ act as kinases that catalyze histidine (H) phosphorylation. Phosphate is then transferred to a conserved aspartate (D) in the receiver domains of LuxN or LuxQ, and then to histidine and aspartate residues on LuxU and LuxO, respectively. LuxO-phosphate, in conjunction with the sigma factor s54, promotes transcription of genes encoding small regulatory RNAs (sRNAs). The sRNAs, together with the chaperone Hfq, destabilize the mRNA encoding the transcription factor LuxR. Under high-cell-density conditions, LuxN and LuxPQ bind their respective autoinducer ligands (AI-1: pentagons; AI-2: double pentagons) and are converted from kinases to phosphatases. Phosphate is stripped from LuxO and LuxU and is hydrolyzed to inorganic phosphate (Pi). Because dephosphorylated LuxO is inactive, LuxR is produced and activates the expression of the luciferase operon. As a result, the bacteria produce light. (Neiditch *et al.* 2006)

1.5.2.2 Quorum Sensing Inhibition

It has been documented that the effects of quorum sensing can be inhibited by certain furanones. The red marine algae *Delisea pulchra* was one of the first micro-organisms

identified as being able to produce a halogenated furanone which had the effect of inhibiting bacterial quorum sensing systems (Gram et al. 1996). The halogenated furanone, (5Z)-4-bromo-5-(bromomethylene)-3-butyl-2(5H)-furanone (fur-1) in particular has been shown to inhibit AI-2 mediated quorum sensing pathways in *E. coli* and *V. harveyi* without affecting growth (Ren *et al.* 2001), while experiments in *B. subtilis* showed that bacterial growth could be effected when using fur-1, (Ren *et al.* 2004a). Furthermore, investigations using a DNA microarray have demonstrated that genes repressed with the addition of fur-1 could be stimulated with AI-2, leading to the conclusion that fur-1 should be seen as a AI-2 inhibitor (Ren *et al.* 2004b). There has been a limited study into the effect of fur-1 on *B. anthracis*. One paper has shown that the growth of *B. anthracis* could be limited using fur-1; however its impact on the anthrax toxin proteins was not directly measured, instead transcriptional *lacZ* fusions attached to the toxin genes was used as a reporter (Jones *et al.* 2005).

1.6 Thesis Aim and Objectives

The aim of this thesis is to develop and explore the abilities and limitations of a microwell based platform when applied to vaccine research and development. With the new financial climate and a renewed popularity of vaccine research, the application of the microwell platform is two fold; one is to apply the platform to a new vaccine candidate in very early development and the second is to apply the platform to already licensed vaccines to increase of understanding of the vaccine system, with hopes of making process improvements. Therefore two very different vaccine candidates were chosen to test the ability of the platform to adapt and perform. The first was a new Meningitis B vaccine based on the outer membrane vesicles of the bacteria *Neisseria lactamica,* as described in Section 1.5.1.1. The second was the current licensed UK anthrax vaccine which is difficult to experiment on due to safety requirements and about which, there is limited process understanding, (Section 1.5.2). The specific objectives of this thesis are therefore:

Micro-scale Process Creation: *N. lactamica* fermentation (Chapter 3)

The objective of the work described was to create a microwell based bacterial culture system to facilitate the rapid optimisation and scale-up of fermentation conditions. It would require the coupling of the two themes previously discussed in the introduction, the combination of the microwell platform with statistical DOE to create a platform capable of media optimisation verifiable at larger scales of fermentation.

Micro-scale Process Creation: Downstream Processing of *N. lactamica* outer membrane vesicles (Chapter 4)

The micro-scale platform was combined with ultra-scale down (USD) tools to investigate the downstream processing requirements of the vaccine. The specific objectives of primary recovery, vesicle extraction, ultra centrifugation and end product filtration were all to be investigated to create a potential purification route for a commercial vaccine.

Micro-scale Process Application: Investigation into the growth kinetics and antigen production of *B. anthracis* (Chapter 5)

The work described here was to use the newly created microwell platform from Chapter 3 and to test its limitations through application to *B. anthracis* fermentations. It will require the new platform to mimic the current vaccine production process and investigate the culture medium and identify main factors which may affect vaccine production. The presence of intercellular signalling pathways based on quorum sensing will also be investigated.

***B. anthracis* fermentations and Anthrax vaccine production in a stirred miniature bioreactor (Chapter 6)**

With the increased understanding of *B. anthracis* culture requirements using data obtained from the previous chapter, *B. anthracis* growth and antigen production will be considered in

a homogeneous stirred culture system. Specifically, the culture condition will be examined so that static and stirred culture conditions may be directly compared.

2 Materials and Methods

2.1 Chemicals and Media

All chemicals used were of analytical grade or higher and purchased from the Sigma-Aldrich chemical company, (Dorset, UK). Yeast extract powder and tryptone soya agar were purchased from Oxoid Ltd., (Basingstoke, UK), while some additional chemicals were purchased from BDH Lab Supplies Ltd (Poole, UK). Reverse osmosis (RO) water was used throughout for media preparation. A summary table of the media used and their supplier is provided in Appendix A.

2.2 Bacterial Strains

2.2.1 *Neisseria lactamica* Y92 NL1009

Neisseria lactamica Y92 NL1009 was provided by the Meningococcal Reference Unit, Manchester Public Health Laboratory, UK. Strains were cultured from a frozen seed stock on Tryptone Soya Agar plates (Oxoid Ltd., Basingstoke, UK). Bacteria were grown overnight (37℃, 5% CO_2) and half the growth from an agar plate was transferred to 10 mL of MC7 medium (5.8 g L^{-1} NaCl, 1 g L^{-1} ammonia, 10 g L^{-1} glucose, 3.9 g L^{-1} L-glutamic acid, 0.1 g L^{-1} L-cystine.HCl, 0.4 g L^{-1} $MgCl_2.6H_2O$, 0.8 g L^{-1} yeast extract powder, 4g L^{-1} K_2HPO_4, 1 g L^{-1} K_2SO_4, 0.03 g L^{-1} $CaCl_2.2H_2O$). Glycerol (30% w/v) was added to the 10 mL MC7 suspension for cryo-preservation at -80℃. W orking cell banks were created from the 11^{th} passage of the bacteria.

2.2.2 *Bacillus anthracis* Sterne $34F_2$

Safety Note: All work with *Bacillus anthracis* was conducted in a containment level 3 laboratory at the Health Protection Agency. *Bacillus anthracis* Sterne $34F_2$ was provided

by the Health Protection Agency, Porton Down, UK. A working cell bank consisting of *B. anthracis* spores was created for use in subsequent fermentations. *B. anthracis* was cultured overnight at 37℃ on Tryptone Soya Agar (TSA) plates (Oxoid Ltd., Basingstoke, UK). These colonies were resuspended in 100 µL of phosphate buffered saline (PBS) and grown to a thin layer on sporulation agar (Health Protection Agency, Porton Down, UK) plates for 48 hours, or until sporulation had occurred. Spores were harvested by washing the surface with 10 mL of sterile deionised water (SDW), washed twice in SDW by centrifugation at 3000x*g* for 10 min at 4-8℃ and resuspended in 5 mL SDW. This suspension was then heated at 60℃ for 40 min to kill any vegetative cells present. Glycerol (30% v/v) was added to the 5mL SDW spore suspension and was sub-divided into 500 µl aliquots to create a working spore bank stored at -80℃.

2.2.3 *Bacillus cereus* ATCC 10876

B. cereus ATCC 10876 was provided by the Health Protection Agency, Porton Down, UK. Strains were cultured from solid Tryptone Soya Agar plates (Oxoid Ltd., Basingstoke, UK) stored at 4℃. As work with this organism was limited no frozen cell bank was created. Colonies were resuspended in nutrient-broth (Oxoid Ltd., Basingstoke, UK) and grown overnight at 37℃ to create an inoculum for further experimentation.

2.3 Fermentations

2.3.1 *N. lactamica* microwell fermentations

Two types of plates were used for *N. lactamica* microwell fermentations. For media optimisation studies plastic, low protein binding, round 24-well plates, (#3473, Corning Inc., NY, USA) were used. Each well was inoculated with 10% (v/v) transfer from a 6 mL inoculum culture grown for 16 hours overnight using the frozen cell stock described in Section 2.2.1 and had a working volume of 1 mL. For scale-up experiments 96-deep

square well plates (2ML-SQ, Axygen Inc., CA, USA) were used. In the scale-up experiments the fill volume varied, however each well was inoculated with a 10% (v/v) transfer of the total working volume. Sterility was maintained through the use of Breath-Easy™ sealing membrane (RPI Corp., Il, USA) which sealed the microtitre plate while allowing for gas transfer (Micheletti *et al.* 2006). The plates were incubated at 37℃ at 1000 rpm using a Thermomixer Comfort (Eppendorf AG). At given time points the sealing membrane was pulled back and a row of wells were sacrificed, transferring 100 µL into a 96-well microtitre plate (Sterilin) using a multi channel pipette. Optical density readings were then taken at 600 nm using a SpectraCount (Packard Bell) plate reader. The remainder of the well contents were filter sterilised using a 0.2µm syringe filter (Sartorius AG) and retained for further analysis as described in Sections 2.6.9 and 2.6.12.

2.3.2 *N. lactamica* shake flask culture

A 250 mL shake flask containing 75 mL of MC7 medium was seeded with $1x10^4$ cfu mL^{-1} of *N. lactamica* from the frozen cell stock described in section 2.2.1. This culture was incubated overnight at 200 rpm, 37℃. An optical d ensity between 1 OD_{600} and 2 OD_{600} was normally attained after 16 hours. 75 mL of culture was then used to inoculate a 2 L fermenter containing 1.5 L of growth medium as described in Section 2.3.3.

2.3.3 *N. lactamica* 2 litre bioreactor fermentations

A 2 L stirred tank bioreactor (LH Fermentation Inc.) was used for scale-up studies and *N. lactamica* biomass generation. The glass vessel was 13.5 cm in diameter and 21 cm in height. The stainless steel head plate accommodated the impeller shaft which held two equally spaced, top driven, six-bladed Rushton turbine impellers. The vessel had a working volume of 1.5 L and was maintained at 37℃ using an externally applied electrical heating jacket. pH was monitored using a Mettler Toledo probe (Mettler GmbH, Urdorf, Switzerland) and was steam sterilised *in situ* but calibrated outside the vessel using

standards at pH 4.01 and pH 7.00 (BDH). The dissolved oxygen tension (DOT) was measured using a probe made by Ingold Messtechnik AG (Urdorf, Switzerland) and was sterilised *in situ*. The probe was calibrated to 0% DOT by sparging the vessel with nitrogen gas (BOC, Surrey, UK) and 100% DOT by sparging the vessel at the working air flow rate prior to inoculation. The impeller speed ranged between 700-800rpm to ensure that agitation sufficiently dispersed the sparged air. Changes in the pH of the medium were not controlled during fermentation. Exit gas was monitored on-line using an MM8-80S mass spectrometer (VG Gas Analysis Ltd., Winsoworth, UK) for oxygen and carbon dioxide measurements.

2.3.4 *N. lactamica* 8 litre bioreactor fermentations

An 8 L glass bioreactor (New Brunswick) was used for scale up studies and *N. lactamica* biomass generation. The glass vessel was 18 cm in diameter and 40 cm in height. The stainless steel head plate accommodated the impeller shaft which held two equally spaced, top driven, six-bladed Rushton turbine impellers. The vessel had a working volume of 6 L and was maintained at 37℃ using an internal heating element. pH was monitored by aseptically sampling the culture and measuring pH using a Mettler Toledo probe (Mettler GmbH, Urdorf, Switzerland) calibrated using standards at pH 4.01 and pH 7.00 (BDH). The dissolved oxygen tension (DOT) was measured using a probe made by Ingold Messtechnik AG (Urdorf, Switzerland) and was steam sterilised *in situ*. The probe was calibrated to 0% DOT by sparging the vessel with nitrogen gas (BOC, Surrey, UK) and 100% DOT by sparging the vessel at the working air flow rate prior to inoculation. The impeller speed ranged between 200-300 rpm to ensure that agitation sufficiently dispersed the sparged air. An air flow rate of 2 L min^{-1} was used to culture the bacteria. Changes in the pH of the medium were not controlled during fermentation. The vessel was inoculated with a 10% transfer volume, provided by shake flask culture as described in Section 2.3.2.

2.3.5 *N. lactamica* 50 litre bioreactor fermentation

A 72 L bioreactor (Incelltech) was used for scale up studies and *N. lactamica* biomass generation. This was a stainless steel vessel of 35 cm diameter and 55 cm height. A working volume of 50 litres was used. Agitation was achieved though the use of three equally spaced 6-bladed Rushton turbines on a bottom driven stainless steel impeller shaft. There was no external gas analysis and hourly samples were taken aseptically to measure pH using a Mettler Toledo probe (Mettler GmbH, Urdorf, Switzerland) calibrated using standards at pH 4.01 and pH 7.00 (BDH) and optical density at 600nm. The vessel was inoculated with a 10 % transfer volume, provided by 8 L bioreactor culture as described in Section 2.3.4.

2.3.6 *B. anthracis* microwell culture

Pre-sterilised low protein binding, plastic 12-well plates (#3512, Corning Inc., CA, US) were used for microwell cultures. A working volume of 2 mL was used per well. Basal medium was used in microwell cultures. A spore inoculum was first diluted in 200 µL of Addition medium to $2x10^4$ cfu mL^{-1}. This was then added to 1.8 mL of basal medium giving a starting concentration of approximately $2x10^3$ cfu mL^{-1}. Inoculated plates were then placed inside a fanned convection incubator at 37℃ for 24-28 hours, during which time samples were taken to measure viable counts Section 2.6.1 and antigen concentration Section 2.6.6 and 2.6.7. An entire well was sacrificed in order to generate time points and sufficient materials for analysis. The content of each well was removed using a syringe and then sterilised by filtration (0.2 µm syringe filter, Sartorius AG) and the filtrate retained for analysis. Plates were sealed using a plate sealer (Sigma) that did not permit gas transfer; this minimised volume losses due to evaporation.

2.3.7 *B. anthracis* Thompson bottle fermentation

B. anthracis spores were cultured in Thompson bottles as described by the product license for the manufacture of the UK Anthrax Vaccine Precipitate license application (PL 1511/0058). Spores from a pre-prepared glycerol stock (section 2.2.2) were diluted to a concentration of $2x10^4$ cfu mL^{-1} in 50 mL of 'Addition' media, (60 g L^{-1} $NaHCO_3$; 20 g L^{-1} glucose; 10 mg L^{-1} $MnSO_4.4H_2O$). This was used to inoculate pre-sterilised Thompson bottles containing 450 mL of 'Basal' media (5.95 g L^{-1} casamino acids; 0.52 g L^{-1} KOH; 69.5 mg L^{-1} activated carbon; 52 mg L^{-1} DL-serine; 25 mg L^{-1} $MgSO_4.7H_20$; 24.5 mg L^{-1} $CaCl_2.6H_2O$; 20 mg L^{-1} L-cystine; 0.167 mg L^{-1} thiamine hydrochloride). This gave each Thompson bottle a working volume of 500 mL. Each bottle was then sealed with a paper stopper and laid flat in a fanned convection 37℃ incubator. The culture was grown statically for 24-28 hours. Bottles were sequentially sacrificed at each time point in order to gain a bulk value for pH and glucose. When the pH fell below a value of 7.6 the bottles were considered ready for harvest. There was no aeration or agitation. These fermentations were performed by staff at the Health Protection Agency.

2.3.8 *B. anthracis* miniature bioreactor culture

The miniature bioreactor (HEL Ltd, UK) shown in Figure 2.1 comprised a baffled cylindrical glass vessel approximately 70 mm in height and 65 mm in diameter (Gill 2007b). It had a stainless steel head plate which could accommodate probes, gas in and gas out lines as well as a sampling port. A six blade Rushton turbine, (D_i = 20 mm), was located 22 mm from the base. The impeller was magnetically driven from below and consisted of a solid magnetic disc at the base of the shaft. The entire bioreactor was maintained at 37℃ by placing it inside an incubator. Agitation was at 700 rpm and in cases where aeration was used, a peristaltic pump fed air into the reactor through a 0.22 μm filter. The fermenter off gas passed through a 0.22 μm filter in order to maintain sterility. A pH probe (Hamilton, Easyferm 9-6-52) connected to an Applikon ADI1030 controller was used in all bioreactor

runs. A working volume of 80 mL was used utilising the same Basal medium as in Thompson bottles.

Briefly, 72 mL of Basal medium (Table A1.4) was first measured into the bioreactor and the head plate secured. The pH probe was screwed into the head plate and other ports were closed. The sampling port remained slightly open during sterilisation to prevent excess pressure build up but was immediately closed post sterilisation. The entire reactor was autoclaved using steam at 121℃, for 15 min. Once s terilised the bioreactor was allowed to cool and moved into the fanned convection 37℃ incu bator. The pH probe was connected to the data logger and the bioreactor left in the incubator for approximately one hour to equilibrate. It was then inoculated aseptically with a pipette via a secondary port on the top plate using *B. anthracis* spores diluted in 8 mL of Addition medium to give an approximate starting concentration of $2x10^3$ cfu mL^{-1}. The sampling port utilised a septum similar to many commercial bioreactors, so it was not necessary to stop operation or remove the bioreactor from the incubator in order to take a sample. Instead a fixed syringe was used to create a vacuum and draw fermentation broth into collection bottles. Samples were passed through a 0.22 µm filter and assays were conducted upon the sterile culture supernatant. Post fermentation the sampling port was opened and the entire reactor was autoclaved.

2.3.9 *Bacillus cereus* microwell culture

B. cereus was cultured in low protein binding, pre-sterilised 12 well plates, at a working volume of 2 mL using L-broth (Oxoid Ltd.) Each well was equally inoculated with the $2x10^3$cfu mL^{-1} of vegetative *B. cereus* cells and allowed to grow at 37℃ in a fanned convection incubator until reaching the 6^{th} hour of exponential phase. At each hour a pipette was used to extract the contents of each well and monitor the optical density before being returned to the microwell. A total of 24 wells were monitored requiring two plates cultured on different days.

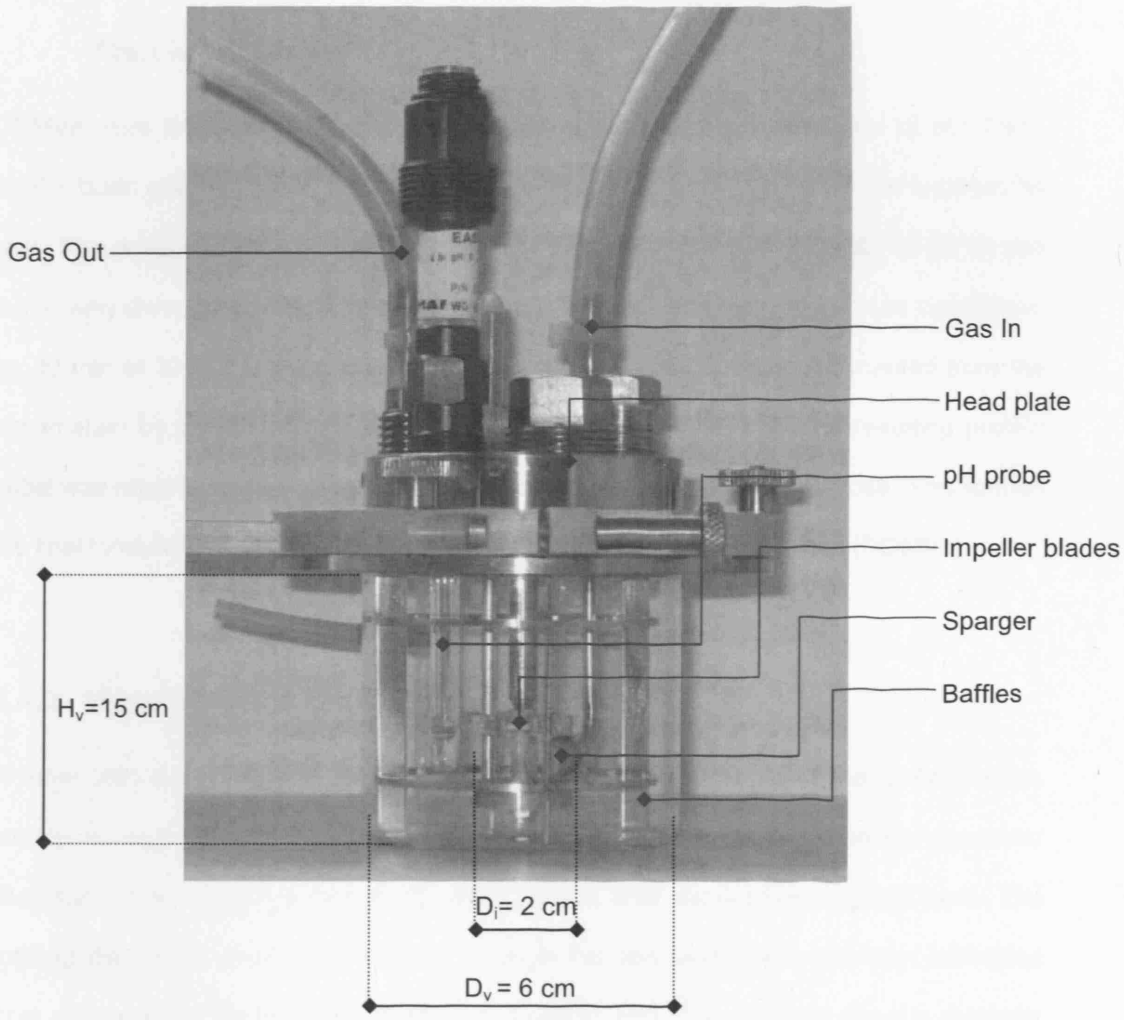

Figure 2.1 Illustration of the miniature bioreactor used in *B. anthracis* cell culture experimentation as described in section 2.3.8.

2.4 Preparation and Processing of *N. lactamica* OMVs

2.4.1 Preparation of Deoxycholate-extracted Outer Membrane Vesicles (DOMVs)

DOMVs were prepared according to the method described by Fredriksen *et al* (1991). Briefly, broth culture from *N. lactamica* was centrifuged at 5,000 x g for 30 min to pellet the cells. The pellet was resuspended in 0.1 M Tris-HCl buffer (pH 8.6) with 0.01 M EDTA and 0.5% (w/v) deoxycholic acid sodium salt (DOC). The resulting suspension was centrifuged for 30 min at 20,000 x g and the supernatant retained. OMVs were sedimented from the supernatant by centrifugation for a further 2 hours at 100,000 x g. The resulting protein pellet was retained and resuspended in 50mM Tris-HCl with 3% (w/v) sucrose. This formed the final formulation for Deoxycholate-extracted Outer Membrane Vesicles (DOMVs).

2.4.2 Ultra Scale Down (USD) shear device

A rotary disk shear device developed in house was used to subject the OMV process stream to varying amounts of shear. The device itself has been previously described (Boychyn *et al.* 2000;Boychyn *et al.* 2001), but a brief description is given here. The rotating disk shear device consisted of a single flat disk and shaft assembly, fabricated from an aluminium alloy (Durell, Smith Ltd., London, UK). The disk was 3 cm in diameter and 0.1 cm in thickness. It was mounted centrally in a cylindrical stainless steel chamber with an air-tight removable flat top and a permanently fixed flat base. The chamber had a diameter of 4 cm and a height of 1.5 cm. The shaft extended through the top cover via an airtight PTFE bearing and was connected to a small high speed motor. The disk was rotated at fixed speeds which were measured and displayed digitally using an optical probe. The whole assembly was mounted on a heavy metal base to reduce vibration during the experiments.

The top and bottom covers of the chamber contained two 1.5 mm diameter ports to siphon out any air trapped in the solution during the filling operation. The chamber was completely filled with the test solution to ensure the elimination of air-liquid interfaces. The chamber was emptied and washed before the start of each time point. Samples of the sheared OMV process stream were removed for analysis as described in Sections 2.6.4, and 2.6.9. All experiments were performed at room temperature.

The USD clarification analysis was calculated as a function of the sigma factor and the flow rate of the process stream through the centrifuge. The performance of two centrifuges can be compared using Equation 2.1:

$$\frac{Q_1}{c_1\Sigma_1} = \frac{Q_2}{c_2\Sigma_2} \qquad \text{(Eq. 2.1)}$$

Where subscripts 1 and 2 denote the two centrifuges, Q (L h^{-1}) is the volumetric flow rate, Σ (m^2) is the sigma factor and c denotes the correction factor for the centrifuge. However, in order the compare a bench scale centrifuge the Equation 2.1 must be modified to Equation 2.2.

$$\frac{Q}{c_1\Sigma_{industrial}} = \frac{V}{c_2 t\Sigma_{lab}} \qquad \text{(Eq. 2.2)}$$

Where V (m^3) is the volume spun and t (s) is the spin time. Equations evaluating the sigma factor are dependent of centrifuge design. The lab sigma factor can be calculated using Equation 2.3.

$$\Sigma_{lab} = \frac{V\omega^2}{2g\ln\left(\frac{2R_2}{R_2 + R_1}\right)} \qquad \text{(Eq. 2.3)}$$

Where, R_1 and R_2 are the inner and outer distances of the fixed angle rotor from the centre of rotation, ω is the angular velocity, V the volume spun. The clarification efficiency was measured using Equation 2.4.

$$\text{Clarification Efficiency}\,(\%) = \frac{OD_{\text{feed}} - OD_{spun}}{OD_{feed} - OD_{well-spun}} \qquad \text{(Eq. 2.4)}$$

This was based on the methodology proposed by Boychyn *et al,* 2004. The optical density of the feed was measured at 600nm, followed the optical density of the well spun sample, created by placing 1 mL *N. lactamica* culture broth in a Eppendorf tube and centrifuging (Beckman Microfuge 11) at 13,000 x *g* for 30 min. Further 1 mL samples of sheared *N. lactamica* culture were centrifuged at different rotational speeds for varying times to create the OD_{spun} value.

2.4.3 Homogenisation of the OMV process stream

Total OMV release from *N. lactamica* was based upon mechanical homogenisation of the cell paste resuspended in 0.1 M Tris-HCl buffer (pH 8.6) with 0.01 M EDTA and 0.5% (w/v) deoxycholic acid sodium salt (DOC). 40 mL of this cell suspension was loaded into the APV Lab 40 (Manton-Gaulin) and homogenised twice at 1200 bar. This assumed total cell breakage. The homogenised suspension was centrifuged for 30 min at 20,000 x g to remove the cell debris and the supernatant retained for analysis as described in Sections 2.6.4 and 2.6.9.

2.4.4 Microwell precipitation

A low protein binding, pre-sterilised 12-well microwell plate (#3512, Corning Inc., CA, USA) was used to precipitate OMV proteins from the homogenised OMV purification stream. 2 mL of homogenised OMV supernatant from Section 2.4.5 was aliquotted into each well.

Then the pH value of the well adjusted to a required acidity (pH range of 7.6 to 3.7) using 5M HCl; pH monitored using a Mettler Toledo probe (Mettler GmbH, Urdorf, Switzerland) calibrated using standards at pH 4.01 and pH 7.00 (BDH). Alternatively, 1 mL of homogenised OMV supernatant from Section 2.4.5 was combined with 1 mL of ammonium sulphate of varying concentrations. Both plates were placed in the Thermomixer Comfort (Eppendorf AG) and shaken for 20 min at 700 rpm. This allowed a precipitate to form. The contents of each well were then transferred to a 2 mL Eppendorf tube and centrifuged (Beckman Microfuge 11) for 5 min at 13000 rpm and the precipitate retained. This pellet was then dissolved in 1 mL Tris-HCL buffer at pH 8 and retained for analysis (Sections 2.6.4 and 2.6.9).

2.4.5 OMV filtration studies

A 1 mL syringe was used to pass a formulated OMV solution at a concentration of 500 µg mL^{-1} total protein through a disposable, single use, cellulose acetate syringe filter (0.2µm, Sartorius AG). The BCA protein assay (Section 2.6.4) was used to measure protein concentration before and after filtration to quantify the total protein loss.

2.5 *B. anthracis* quorum sensing studies

2.5.1 Synthesis and purification of Fur-1

Fur-1 was prepared according to the method described by (Manny *et al.* 1997). Briefly, 3'5-dibromo-levulinic acid was firstly created by combining levulinic acid and bromine, both dissolved in chloroform and then refluxed for an hour to form an oil. Once the oil cooled the resulting crystals of 3'5-dibromo-levulinic acid were combined with sulphuric acid and heated to 120℃ for 20 min. The solution was allowe d to cool to room temperature and then slowly poured over crushed ice to form an emulsion. The emulsion was initially

extracted using dichloromethane and then brine. The resulting solution was dried over sodium sulphate and evaporated create crystals of fur-1.

2.5.2 Molecular weight fractionation of *B. anthracis* culture supernatant

Vivaspin6™ (Sartorius AG) spin filters of varying molecular weight cut offs (5-50 kDa PES membranes) were used to fractionate sterile *B. anthracis* culture supernatant into discrete molecular weight fractions. Each filter unit was filled with 4 mL of supernatant and centrifuged at 4,000 *g* for 15 min, according to the manufacturer's instructions. The permeate from each molecular weight membrane was collected and used in subsequent growth experiments (Section 2.5.3).

2.5.3 Quorum sensing growth profiles of *B. anthracis*

15% or 30% (v/v) additions of sterile *B. anthracis* culture stationary phase supernatants (SSPS) or varying molecular weight fractions from Section 2.5.2 were added to microwell cultures of *B. anthracis* as described in Section 2.3.6. The resulting impact on growth was monitored through viable cell counts as described in Section 2.6.1.

2.6 Analytical methods

2.6.1 *B. anthracis* viable cell counts

Total viable counts of *B. anthracis* culture were determined by plating serial decimal dilutions of 100 µL portions in duplicate onto Tryptone Soya Agar plates (Oxoid Ltd., Basingstoke, UK). These were incubated for 24 hours and only plates with single colony units were counted.

2.6.2 Visualisation of *B. anthracis* cell growth

In some of the microwell cultures of *B. anthracis*, the tetrazolium salt WST-1 (Roche Ltd.) was used to visualise cell proliferation. The reagent was directly added to each well at 1/10 of the culture volume (200 µL into a 2 mL well working volume). The mixture was left to incubate for 20 min before being examined through visually inspected. The areas of the well where there were viable cells turned orange, while areas of no cellular activity remained a light pink colour.

2.6.3 Determination of glucose concentration

Two different methods were used for determination of glucose concentration. In the case of *N. lactamica*, a 10% (w/v) solution of 3,5-dinitrosalicylic acid (DNS) was used to determine glucose concentration (Miller 1959). The method though was adapted to fit a 96-well microtitre plate format. 0.6 mL of filter sterilised fermentation broth sample was mixed with 0.2 mL of DNS reagent in a 2 mL Eppendorf tube and incubated at 97℃ for 5 min. The samples were then placed on ice and serially diluted by a factor of two with RO water in a microtitre plate, after which the absorbance was measured at 570nm. Glucose concentrations were calculated from a standard curve prepared on the same microtitre plate, (Appendix A). All measurements were carried out in duplicate.

In the case of *B. anthracis* a Lifescan® One Touch Ultra® glucose monitor (Johnson & Johnson) was used to determine glucose levels in filtered culture supernatants. Test strips supplied with the monitor were used for each time point assay. After calibration of the meter against a control solution supplied with the kit, 10 µL of supernatant was applied to each test strip and readings in mmol L^{-1} obtained. Readings were carried out in duplicate.

2.6.4 Determination of protein concentration

The bicinchoninic acid protein assay (Pierce, Rockford, IL, USA) was used to determine protein concentrations in all samples. However, the assay was adapted to be performed in a 96-microwell plate format in order to facilitate its use on an automated platform. A standard curve was created using bovine serum albumin ranging from zero to 1 mg mL^{-1}. Samples were loaded on the top row and serially diluted by a factor of two down the plate. Samples were mixed with the working reagent (50:1 ratio of bicinchoninic acid solution to a 4% (w/v) copper sulphate solution) using a ratio of 1:8, sample to reagent and incubated for 30 min at 37℃. The plate was then read at 562 nm, using a Safire II multi-plate reader (Tecan). A sample calibration curve is located in Appendix A.

2.6.5 Antibody production

Hyperimmune sera to PA and LF were produced, purified and conjugated by the Health Protection Agency through the immunisation of rabbits with highly purified recombinant PA or LF. The sera generated were used in Western blot analysis as described in Section 2.6.9 and the purified IgG fraction was used in ELISA assays (Sections 2.6.7 and 2.6.8). Purified IgG was conjugated to HRP using periodate mediated reductive amidation (Hermanson 1996).

2.6.6 Determination of PA concentration

Concentrations of PA in *B. anthracis* fermentations were assessed using an enzyme linked immunosorbent assay (ELISA). 96-well Immulon-2HB plates (Thermo Life Sciences) were coated overnight with 2 μg mL^{-1} of recombinant α-PA at a concentration of 100 μL $well^{-1}$. Plates were washed and blocked for 1 hour using PBST+5%FCS at 37℃. Plates were then subsequently washed with PBST and fermentation broth samples and standards transferred onto the plate and serially diluted by half. The standard was created using rPA

with a starting concentration of 300 ng mL^{-1}. The samples were performed in duplicate. The plates were then incubated for 1h at 37℃ before be ing washed three times in PBST. The conjugate, PA-HRP was diluted 1:5000 and 100 µL was added to each well. Plates were incubated for another hour at 37℃ before being was hed three times in PBST and 100 µL $well^{-1}$ of 3,3',5,5'-tetramethylbenzidine (TMB) liquid substrate (Sigma) was added. The plates were incubated for 30 min before the enzymic reaction was stopped with 50 µL $well^{-1}$ of 2 mol L^{-1} sulphuric acid. The plates were then read at 450nm. A sample calibration curve is available in the appendix. This assay was developed, optimised and validated by the Health Protection Agency.

2.6.7 Determination of LF concentration

Concentrations of LF in *B. anthracis* fermentation broth samples were assessed using an enzyme linked immunosorbent assay (ELISA). 96-well Immulon-2HB plates (Thermo Life Sciences) were coated overnight with 2 µg mL^{-1} of recombinant α-LF at a concentration of 100 µL $well^{-1}$. Plates were washed and blocked for 1 hour using PBST+5%FCS at 37℃. Plates were then subsequently washed with PBST and samples and standards transferred onto the plate and serially diluted by half. The standard was created using rLF with a starting concentration of 300 ng mL^{-1}. The samples were performed in duplicate. The plates were then incubated for 1h at 37℃ before being was hed three times in PBST. The conjugate, LF-HRP was diluted 1:3000 and 100 µL was added to each well. Plates were incubated for another hour at 37℃ before being was hed three times in PBST and 100 µL $well^{-1}$ of 3,3',5,5'-tetramethylbenzidine (TMB) liquid substrate (Sigma) was added. The plates were incubated for 20 min before the enzymic reaction was stopped with 50 µL $well^{-1}$ of 2 mol L^{-1} sulphuric acid. The plates were then read at 450nm. This assay was developed, optimised and validated by the Health Protection Agency.

2.6.8 Western blot analysis

For Western blot analyses, proteins from SDS-PAGE (Section 2.6.10) were transferred to nitrocellulose at a constant voltage of 150 V for 90 min using the NuPAGE western transfer system according to the manufacturer's instructions (Invitrogen Ltd.). Membranes were then blocked with PBST containing 2% (w/v) BSA for 1 hour. The membrane was then washed with PBST and incubated for 1 hour in a diluted primary antibody, rabbit-α-PA or rabbit-α-LF, then washed and incubated in a secondary antibody conjugated to horse radish peroxidase, goat-α-rabbit-HRP (Sigma). Blots were developed using the ECL Plus Kit (GE Healthcare) according to manufacturer's instructions. The chemiluminescent reaction product was visualised using a gel documentation camera using an exposure time of 40 seconds (Amersham Imagemaster VDS-CL, Gel Doc System, GE Healthcare).

2.6.9 SDS-PAGE analysis and quantification

An Invitrogen *XCell Surelock*™ Mini-Cell was used to carry out electrophoresis. Protein samples were mixed with NuPAGE™ LDS sample buffer (Invitrogen Ltd.) in a 3:1 (v/v) ratio and denatured for 10 minutes at 72°C. Pre-cast NuPAGE® 4-12% Bis-Tris gradient gels (Invitrogen Ltd.) were used to characterise the proteins and each well loaded with 10μg of total protein. The MES (Reduced) Electrophoresis Protocol was followed (Invitrogen Ltd.). The gel was run at 200V for 35 minutes and stained using SimplyBlue™ SafeStain (Invitrogen Ltd. UK). The molecular weight was determined by reference to the Mark 12™ (Invitrogen Ltd. UK) unstained protein standard, which was included on each gel. Each gel was duplicated and when required used for further analysis, such as Western blots or SELDI-MS.

SDS-PAGE gels were scanned using a GelDoc 2000 (Bio-Rad Laboratories Inc.) imaging camera and analysed using the densitometry software Quantity One™ version 4.6 (Bio-Rad Laboratories Inc.). Quantification of each lane was achieved by measuring the

intensity of each band and dividing that by the total intensity of all detected bands to obtain a percentage value.

2.6.10 Identification of protease activity

Zymograms of *B. anthracis* culture supernatant samples were performed to detect extracellular protease activity. Supernatant samples were loaded onto a Novex gelatine substrate 10% zymogram gel (Invitrogen Ltd.) according to the manufacturer's instructions using a reducing Tris-Glycine SDS sample buffer (Invitrogen Ltd.). The gel was run at constant voltage at 125V for 90min after which it was incubated for 30min with the Novex Zymogram Renaturing Buffer (Invitrogen Ltd.) under gentle agitation. The gel was then equilibrated for 30min at room temperature using the Zymogram Developing Buffer (Invitrogen Ltd.) with gentle agitation. Fresh Zymogram Developing Buffer (Invitrogen Ltd.) was then added and the gel was incubated overnight at 37℃. The gel was then stained using Simply Blue Safe™ stain (Invitrogen Ltd.) according to the manufacturer's instructions. The gel was scanned using a white light using the Amersham Photoman Direct Gel Doc System (GE Healthcare). These gels were not quantified.

2.6.11 Particle size analysis

A Zetasizer 3000 (Malvern) was used to determine sample particle sizes based on dynamic light scattering. DOMV samples from *N. lactamica* fermentation broth were prepared as described in Section 2.4.1 to a final concentration of 500 μg mL^{-1} and maintained at 20℃. The Zetasizer was firstly calibrated using a 2 μm latex stock solution. Then 1 mL of DOMV sample was added to a 12 mm square polystyrene cuvette and placed into the Zetasizer for analysis. Samples were run in triplicate.

2.6.12 SELDI-TOF-MS analysis of culture supernatants

Surface enhanced laser desorption and ionisation (SELDI) mass spectroscopy (MS) was used to profile the protein antigen profile in both *N. lactamica* and *B. anthracis* culture supernatant fluids. Two different chips, a 'SAX-2' protein chip array and a 'WCX-2' protein chip array were used to analyse *N. lactamica* and *B. anthracis* supernatant samples respectively in the SELDI-TOF Protein Chip reader (PBS-II, Ciphergen® Biosystems Inc.). Each protein chip array comprised an aluminium strip with 8 chemically treated 2 mm diameter spots. The spots had hydrogel bases which were interspaced with quaternary amine groups facilitating anion exchange. Proteins were bound to the chip surface through electrostatic interactions, optimised by the selection of a binding buffer at pH 8 for the SAX-2 chips and pH 6 for the WXC-2 chips.

A 96-well Bioprocessor (Ciphergen® Biosystems Inc.) was used to prepare each protein chip array before it was inserted into the PBS-II reader. The Bioprocessor is a bottomless microwell plate, which when placed on top of the Protein Chip allows the array spots to be exposed to a column of liquid during sample preparation. A binding buffer of 50mM Tris-HCl with 0.1% (v/v) Triton X-100, pH 8, was used in all experiments and the wash buffer consisted of 50mM Tris-HCl without Triton X-100. The Energy Absorbing Matrix (EAM) was composed of 5 mg of EAM1 (Energy Absorbing Molecule 1, a proprietary product of Ciphergen®), dissolved in 250 µL of 0.5% (v/v) tri-fluoric acid and 50% (v/v) acetonitrile.

A protein chip was mounted into the Bioprocessor and each spot incubated with 150 µL of binding buffer and placed on a shaking platform for 5 min, after which the buffer was discarded and the step repeated with fresh binding buffer for a further 5 min. Each well was loaded with 50 µg of either *N. lactamica* or *B. anthracis* protein from a stock concentration of 1 mg mL^{-1}. The stock concentration was determined by using a bicinchoninic acid protein assay (Pierce) calibrated against BSA (Section 2.6.4). 150 µL of binding buffer was placed into each well yielding a total well volume of 200 µL. The Bioprocessor was covered with

parafilm and placed on a shaker for 40 min at room temperature, after which the liquid in each well was disposed of and the well contents washed with 150 µL of binding buffer for 5 min. The washing step was repeated twice more with binding buffer and a further two times with distilled H_2O. The protein chip was left to air dry, following which each spot was encircled with a PAP™ Pen (Zymed® Labatories) and 0.75 µL of EAM1 was added to each spot and allowed to dry. Finally, a further 0.5 µL of EAM1 was added to each spot, the chips were allowed to dry and placed in the PBS-II reader.

The PBS-II reader was externally calibrated using the All-in-One Protein Standard™ (Ciphergen® Biosystems Inc.). Cytochrome C (12.4 kDa), myoglobin (17.0 kDa) and GAPDH (35.7 kDa) were used to calibrate the lower molecular weight range (15-50 kDa) and GAPDH (35.7 kDa), albumin (66.4 kDa) and β-galactosidase (116.4 kDa) for the high molecular weight range (50-150 kDa). Analysis of each protein spot took place in two discrete passes. The first pass was optimised to analyse a molecular weight range between 15 and 50 kDa, using a laser intensity of 215. The second pass analysed proteins in the weight range between 50 and 150 kDa using a laser intensity of 230. During both passes the focus was set by a lag time of 600ns.

2.6.13 Band extraction protocol

This method was employed to extract protein from SDS-PAGE gel bands for analysis. Tris-glycine gels were used to allow efficient separation of the protein bands. Samples were prepared as described in Section 2.6.9. The gel was stained using a Reversible Zinc Stain, (Bio-Rad Laboratories Inc.) a negative staining technique, as more commonly used positive stains, such as blue or silver staining, were unsuitable because they irreversibly fix the protein to the gel matrix. Protein bands of interest were excised from gel and destained. The destaining process was repeated three times until the gel pieces were clear, vortexing during each wash. The destaining buffer was pH neutral, to remove any residual SDS. After destaining, the gel pieces were placed in a test tube and crushed into tiny fragments.

The fragments were sonicated for 30 min in FAPH buffer (50% (v/v) formic acid, 25% (v/v) acetonitrile, 15% (v/v) isopropanol, 10% (v/v) water). Sufficient FAPH buffer was used to completely cover the gel fragments and following sonication, the solution was vortexed at room temperature for 4 hours. The eluted protein was collected into a fresh microfuge tube and the remaining gel fragments were rinsed with an equal volume of fresh FAPH buffer. The solutions were combined and evaporated in a Speed Vac™. The resulting white crystals were dissolved in 10 µL of water and analysed using SELDI-TOF as per Section 2.6.12.

2.6.14 Visualisation of the liquid displacement height in shaken microwells using high speed photography

A model created from Perspex of a single microwell based on the dimensions of a 96 DSW was affixed onto a microtitre plate. A scale was attached to the side of the microwell which indicated the height in centimetres, subdivided in half centimetres. The microwell was placed in a Thermomixer Comfort (Eppendorf AG) and filled with medium to a desired volume and set to agitate at 1000 rpm. A digital camera (Ixus 40, Cannon Inc. Japan) mounted on a stand in front of the shaken microwell was used to take images of the liquid displacement height. A setting of ISO 400 was required using the macro focus setting.

2.6.15 Image analysis using confocal microscopy

Samples of *N. lactamica* fermentation culture were viewed and recorded using a Leica Polyvar microscope connected to an Image Processing and Analysis System, (Leica Ltd, Cambridge, UK). 200 µL of cell culture was transfered onto a glass slide over which a cover slip was placed and viewed at times 40 magnification.

2.6.16 Quantification of DNA

The quantification of DNA in OMV sample preparations was achieved using the Nanodrop ND-1000 Spectrophotometer (Nanodrop Technologies, Wilmington, DE, USA). Briefly, The sampling arm was raised and 1.5 µL of sample was pipetted onto the lower sampling arm. The sampling arm was closed and the spectral measurement was initiated using the operating software on the computer interface. The nucleic acid application protocol was used which measured the sample at a range of absorbances (230 – 260 nm) and calculated the DNA content in ng μL^{-1}, using the Beer-Lambert equation.

$$A = E * b * c \qquad \text{(Eq. 2.5)}$$

Where 'A' is the absorbance, 'E' is the wavelength dependent molar absorptivity coefficient, 'b' is the path length and 'c' is the analyte concentration.

2.6.17 Factorial Design Analysis

The statistical software package Minitab™ (Mintab Inc., USA) was used to design and analyse Design of Experiments (DOE) experiments conduct in this thesis. The STAT > DOE .> Factorial > Create Factorial Design function was used to select the design template used and programmed the number of factors in the experiment. In all cases the design encompassed three replicates and was randomised.

3 Micro-scale Process Creation: *N. lactamica* fermentation

3.1 Introduction

As described in Section 1.5.1.1, immunological and epidemiological evidence suggests that the development of natural immunity to meningococcal disease resulted from colonization of the nasopharynx by commensal *Neisseria* species, particularly with *Neisseria lactamica*. It has been reported previously (Oliver *et al.* 2002) that immunization with *N. lactamica* outer membrane vesicles (OMVs) containing the major outer membrane proteins protected mice against a lethal challenge of meningococci of diverse serogroup and serotype. OMVs thus have the potential to form the basis of a vaccine against meningococcal disease.

Hitherto, little consideration has been given to process reproducibility and optimisation since only small amounts of highly purified materials were required for animal experiments. However, in order to facilitate the transition from research to manufacture, process scale-up and optimisation must be considered. Essentially, the progression from research to commercialisation consists of three phases: (i) strain selection, (ii) bacterial growth and (iii) downstream processing.

Strain selection is based mainly on the requirement to produce the vaccine antigens of interest. The preliminary immunological data available at the start of this project was based on the outer membrane proteins of the bacterium, *N. lactamica;* hence strain selection was already predetermined. In general, cell growth can be separated into two aspects, media selection and optimisation of growth conditions. It is good microbiological practice to prepare a master seed stock and a working seed stock ideally in the same media used for vaccine production (Allison and Tranter 2003). Medium design is an important aspect of

process design and careful consideration at this stage can result in reduced time and costs for later development stages (Allison and Tranter 2003). The majority of standard media recommended for bacterial expression studies (such as L-broth) are useful for early 'proof of principle' experiments but are not suitable for production because of low antigen titre and/or poor biomass yields. For the preliminary immunological studies *N. lactamica* was grown in Frantz media, which produced the vaccine antigens of interest, but resulted in poor growth.

The second aspect of bacterial growth, the optimisation of growth conditions, consists of several factors. Factors that should be examined include; (i) pH, (ii) aeration, (iii) antifoam requirements and (iv) harvest time. Information gained from these studies will provide the basis for process transfer into conventional stirred tank bioreactors. The goal of this stage of development is to produce a scaleable and reproducible process for bacterial growth and expression of the vaccine antigens.

The purpose of using microwells is that they have the potential to be transformed into a quantitative research platform which can provide reproducible results for bacterial growth with the added benefits of replication and potential automation. Previous microwell fermentation studies have shown that bacteria can be culture in these formats (Elmahdi *et al.* 2003;Ferreira-Torres *et al.* 2005). By coupling the microtitre plate with new forms of protein analysis such as SELDI-MS, it will allow more data to be produced in a shorter period of time when compared to studies conducted in shakeflasks, a method that is generally used for such experiments.

3.1.1 Aim and objectives

The overall aim of this chapter is to establish a microwell based bacterial culture system for the rapid optimisation and scale-up of fermentation conditions. This approach will be established here with *N. lactamica* however later chapters will show it has generic

application to other vaccine producing strains and in particular those with requirements for high levels of containment. The specific objectives of this chapter are thus:

- Demonstration of *N. lactamica* growth in microwell culture and identification of optimal medium composition using a statistical Design of Experiment (DOE) approach.

- Investigation of antigen components using SELDI-MS as a new and rapid method of protein analysis to test the hypothesis that media design has an impact on the antigen profile.

- Optimisation of the fermentation requirements of *N. lactamica* based on the factors outlined in Section 3.1 which should focus on (i) pH, (ii) aeration, (iii) antifoam requirements and (iv) harvest time.

- Creation a method of scale-up that allows the correlation of data obtained in microwells to data obtained in commercial stirred tank bioreactors.

3.2 Optimisation of microwell culture conditions

3.2.1 Medium development

As described in Section 3.1 previous studies with *N. lactamica* were performed using Frantz medium to generate material for immunological studies. These results form the basis of microwell development of medium components. Figure 3.1 shows a typical microwell growth profile for the culture of *N. lactamica* on Frantz medium. The culture displays a typical batch fermentation profile with a lag phase of approximately two hours followed by a period of exponential growth at a maximum specific growth rate of 0.03 h^{-1}. The final culture optical density attained was 0.39 OD_{600}.

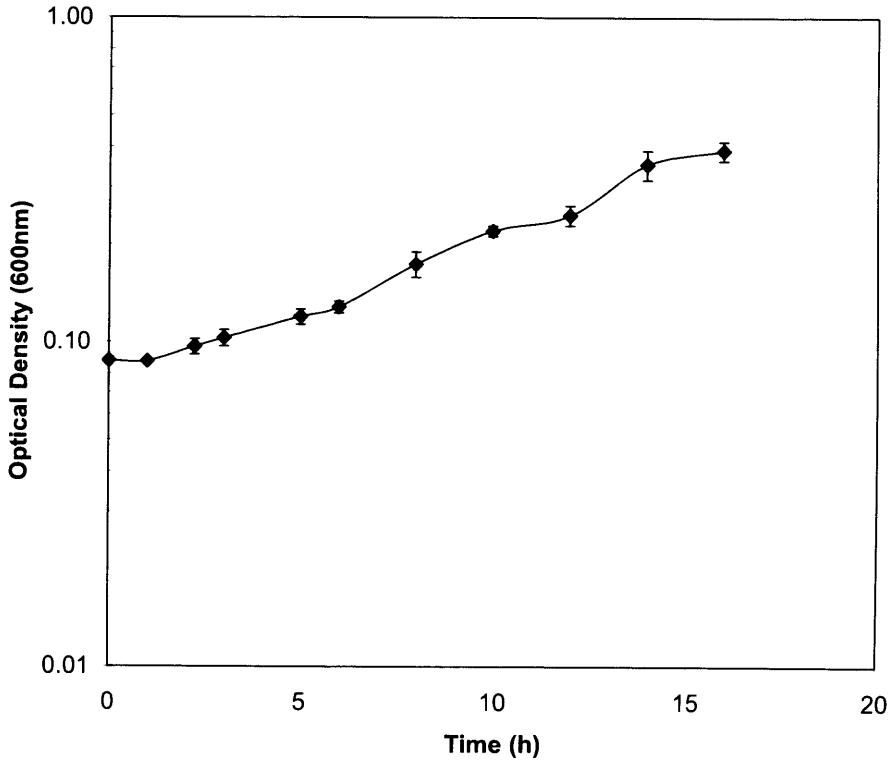

Figure 3.1 Initial microwell growth studies of *N. lactamica* on Frantz medium. Experiments performed as described in Section 2.3.1. Error bars represent one standard deviation about the mean, where n=3.

Normally medium development would begin with a stoichiometric mass balance of the data described in Figure 3.1. This would be based upon the composition of the carbon source and the required product (Stanbury and Whitaker 1984b). However, this strategy is difficult to apply here because the end product is rather undefined consisting of multiple proteins. However, there is some literature available on previous attempts to create a chemically defined medium for *N. lactamica* (Catlin BW. 1973) and so this was used as a starting point for medium development in conjunction with the data presented in Figure 3.1.

3.2.2 Selection of initial experimental design, factors and responses

A factorial design experiment method was chosen because this was still very much early research and the main factors which influenced *N. lactamica* growth had yet to be identified. Furthermore, the number of factors to be investigated in any one run did not exceed five, so a full factorial design run was most appropriate. The purpose of factorial design was to determine the effects of the chosen factors on the response and if there was an interaction between the factors to determine the nature of the interaction. In this case the factors and responses identified are summarised in Table 3.1. The factors chosen are the discrepancy between the original Catlin medium and Frantz medium. The rational for choosing the growth rate was so that lag phase could be taken into account and be excluded as this was variable in some microwell fermentations.

Factor	+1	-1	Response
Carbon source	glycerol	glucose	Growth rate
Amino Acid	8% (v/v) addition	2% (v/v) addition	Growth rate
Yeast Extract	8% (v/v) addition	2% (v/v) addition	Growth rate

Table 3.1 Summary table of factors and responses chosen for factorial design medium development

The fixed response model is used to conduct media development which required the following assumptions; (i) the response is normally distributed (ii) the variance of each treatment is identical and (iii) samples are independent.

Effectively, factorial design can be considered as 2-way ANOVA where the first part is to identify the variance and general error (residuals) of the data while the second part looks at the main effects and interaction effects and measures their significance by comparing them with the error determined from the variance. If the effect or interaction is greater then the variance it is termed significant.

In all of the following factorial experiments the significance was expressed by the alpha value. This is the probability of rejecting the null hypothesis when it is actually true. In these experiments the α-value was set to 0.05, i.e. a 5% chance of the null hypothesis being true.

Table 3.2 shows an example DOE worksheet used for a 2^3 factorial design experiment. This experiment has three factors investigated, carbon source, yeast extract and a chemically defined amino acid solution, each of which had two levels, +1 and -1. As a result, the experiment has eight runs in total ($2^3 = 8$). Each run is represented by a row in the table, representing the unique combination of the factors. The standard order column represents the order in which the levels would be presented if the runs were not randomised. Thus, standard order 1 would be an all negative run while standard order 8 would be an all positive run, with differing levels in between. The run order represents the order in which the experiment was conducted post randomisation. Randomisation provides some protection in removing experimental bias and the influence of unknown variables.

Standard Order	Run Order	Block	Carbon Source	Amino Acids	Yeast Extract	Growth Rate (h^{-1})
4	1	1	+1	+1	-1	0.14
5	2	1	-1	-1	+1	0.24
2	3	1	+1	-1	-1	0.21
3	4	1	-1	+1	-1	0.29
8	5	1	+1	+1	+1	1.35
1	6	1	-1	-1	-1	0.09
7	7	1	-1	+1	+1	1.46
6	8	1	+1	-1	+1	0.09

Table 3.2 Example of a 2^3 factorial design experiment investigating the effect of carbon source, a chemically defined amino acid solution and yeast extract on the growth rate of *N. lactamica*. In this example, the coded values for carbon sources represent glucose (-1) and glycerol (+1). For the amino acid and yeast extract columns, the levels vary between a 2% v/v addition (-1) and a 8% v/v addition (+1).

3.2.3 Analysis of initial factorial experiment results

Once the experiment had been run and replicated as described in Table 3.2, the results are analysed using the statistical software package Minitab (Section 2.6.17). This software can be used to analyse the main effects and any interaction effects between the chosen factors.

A main effects plot is used to visualise the effect of the factors on the response and compare the relative strengths of each effect. Figure 3.2 shows the data means, which are the means of the growth rate for each run. The horizontal reference line represents the overall mean and is calculated as the average of all the data points. The line connecting the two factor level points helps to visualises the main effect. If this line is horizontal, then

the factor is not considered a main effect. If this line is not horizontal it may be considered a main effect. The magnitude of the effect is assessed through the gradient as the greater the slope of the line, the stronger the effect.

The carbon source panel illustrated the effect of changing the carbon source from glucose (-1) to glycerol (+1). It is observed that the change had a slight negative impact on the growth rate, but line response line was approximately horizontal, thus it is not considered a main effect. However, the amino acid panel and the yeast extract panel both recorded a steep increase in the response when the media addition was increased from 2% v/v (-1) to 8% v/v (+1). Thus these two factors are considered as positive main effects on the growth rate.

Having identified the main responses, interaction plots are next used to describe any interaction effects between any two factors on the cell growth rate. In this instance the data means are used. To interpret this plot, if the lines were parallel to each other then this suggests no interaction was present. However, should the lines not be parallel then there may be an interaction effect. The magnitude of the interaction effect can be judged based upon the degree of departure from parallelism.

In Figure 3.3, there appears to be little or no interaction between the carbon source and the amino acid solution or the carbon source and the yeast extract solution. The effects lines in both these panels are approximately parallel to each other. There did however appear to be an interaction effect between the amino acid solution and the yeast extract, as it is only in the presence of the second factor, the amino acid solution, that there is a noted increase in the response. The fact that these two lines have greatly deviated from parallelism suggests that there is a very strong interaction effect.

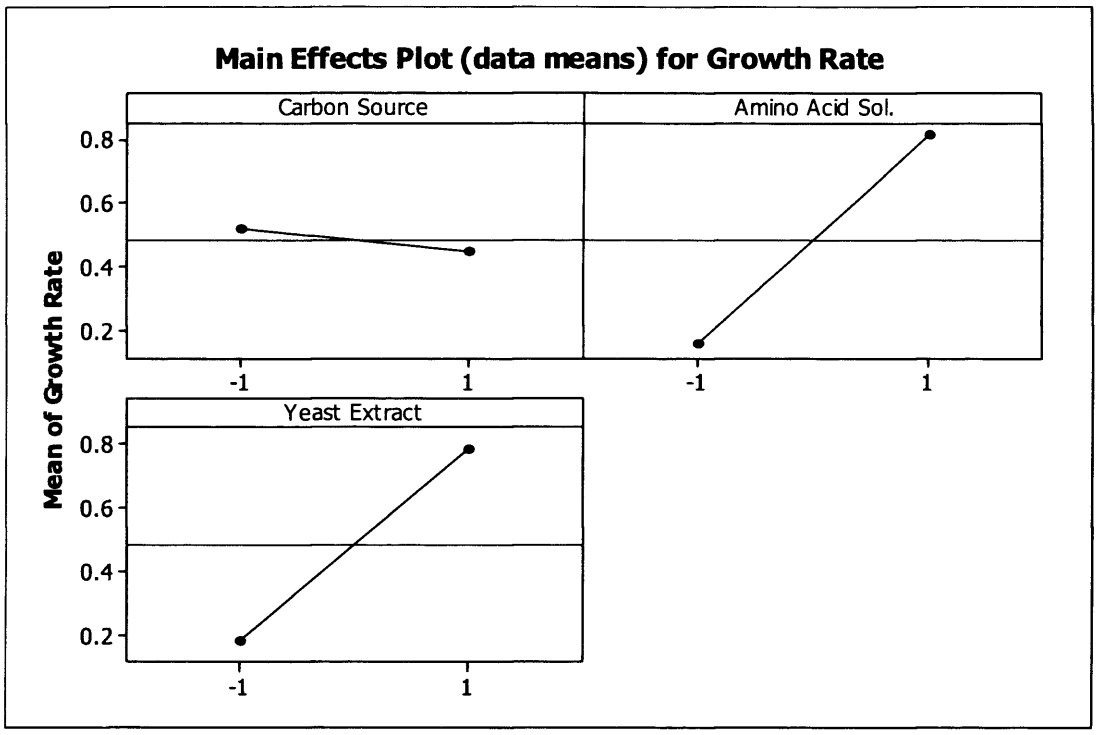

Figure 3.2 Visualisation of the effects of the carbon source, amino acid solution and yeast extract on the mean growth rate. As the carbon source was changed from glucose (-1) to glycerol (+1) there was a slight negative effect on the growth rate. The increase in concentration from 2% v/v (-1) to 8% v/v (+1) of both the amino acid solution and yeast extract had a strong positive effect on the mean growth rate. Analysis performed as described in Section 2.6.17.

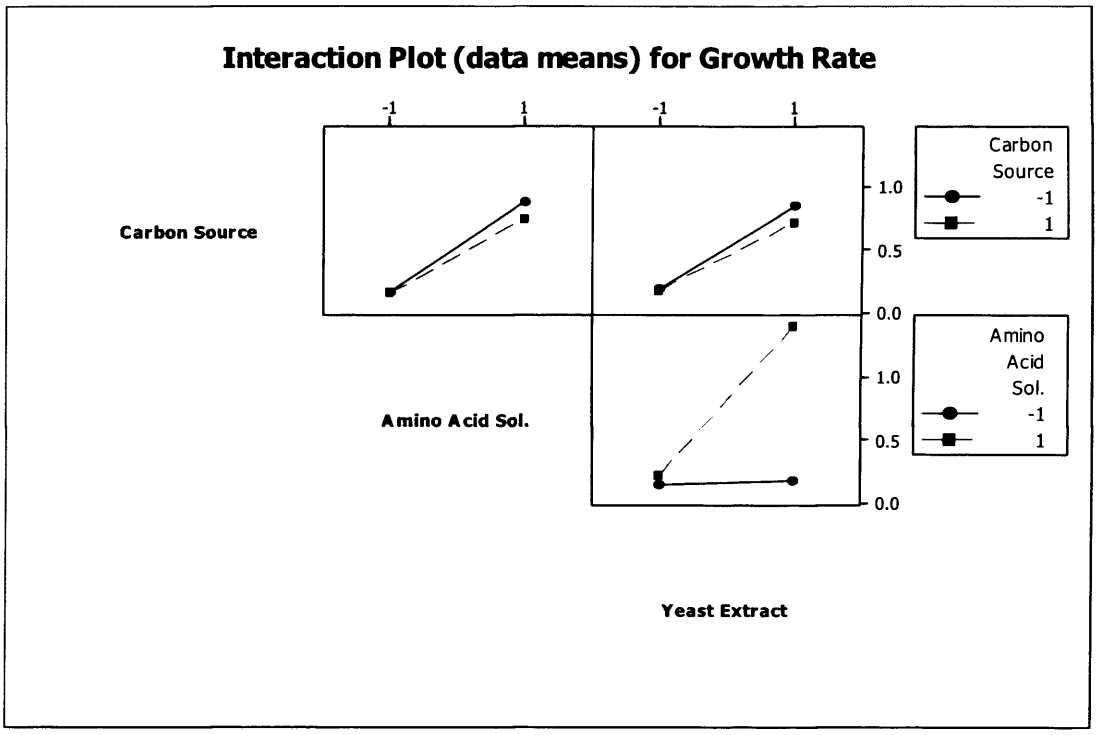

Figure 3.3 An interaction plot of the effects upon the mean growth rate. The top left panel shows the interaction effect between carbon source and the amino acid solution. The top right panel shows the interaction effect between the carbon source and the yeast extract solution, while the bottom panel demonstrates the strong interaction effect between amino acid and yeast extract solutions. Analysis performed as described in Section 2.6.17.

The interaction effect between the defined amino acid solution and the yeast extract is interesting as it indicates possibly that one of the components within the solutions is rate limiting. In further analysis both the defined amino acid solution and yeast extract contained many of the same amino acids, so it is possible that the absence of a vitamin or other component found in yeast extract was responsible.

The normal probability plot allows the comparison of the relative magnitude and the statistical significance of both the main and interaction effects described previously in Figures 3.2 and 3.3 respectively. The solid line in Figure 3.4 indicates where all the points should fall if they had no effect on the growth rate. The plot also indicates the direction of the effect. Those points to the right of the line have a positive effect on the growth rate, while points to the left of the line have a negative impact. As stated previously, the significance level, α, was set to 5%. Significant effects were larger and farther away from the line.

Figure 3.4 confirms the findings from the previous two figures, i.e., that the amino acid solution and the yeast extract both had strong, significant, beneficial effects on the growth rate and that their interaction effect also is significant. The carbon source, while significant, is not a main effect in comparison to the other two factors and remains predominantly in the left hand sector of the plot. Changing the carbon source has a significant negative effect, though it was not a main effect and had no interactions, as points A, AB and AC all line up near the same negative effects score.

From Figure 3.4 three main points of interest, B, C and BC can be identified which have the greatest impact on growth rate. This however does not indicate the impact of these media factors on the antigen profile. Thus with reference to Table 3.1, supernatant samples from well with standard order 3, 5 and 7 representing B, C and BC respectively were analysed using SELDI mass spectroscopy.

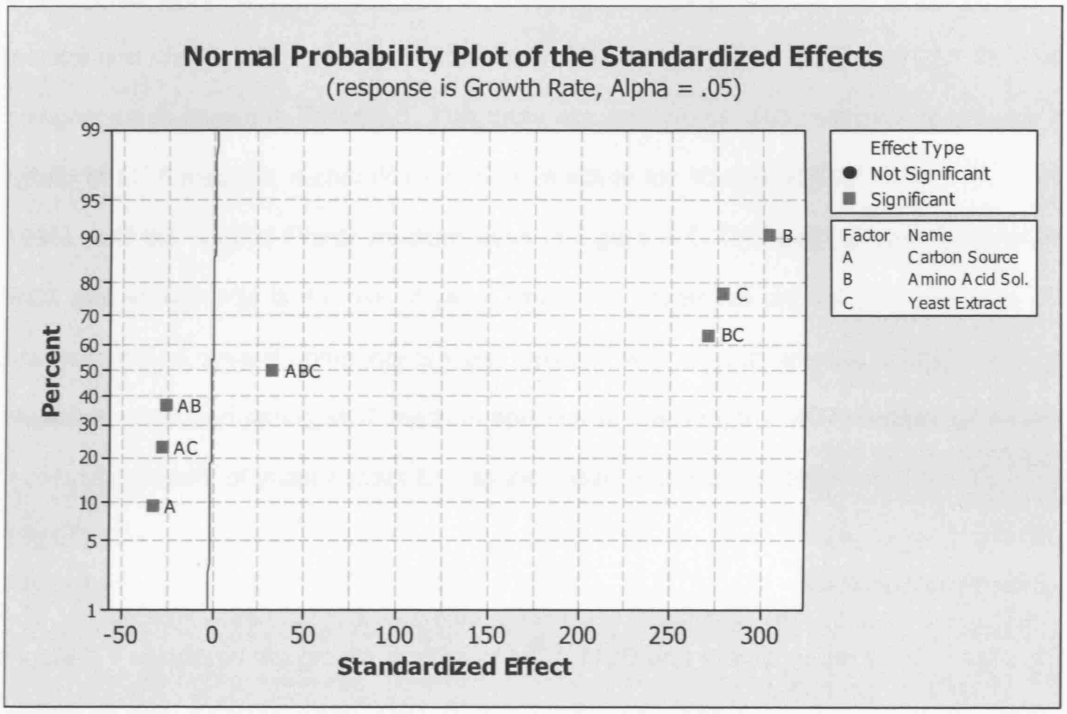

Figure 3.4 Normal probability plot of the effects indicates that there are three runs which had the most positive impact on the growth rate when compared with the whole data set. These runs were the amino acid solution, yeast extract solution and the run where both yeast extract and the amino acid solution were present. The plot also identifies the significance of each factor, and while changing the carbon source is significant, it has a relatively minor effect when compared with the other two factors. Analysis performed as described in Section 2.6.17.

3.2.4 Further medium optimisation

Other factors from the original chemically defined Catlin medium (Catlin BW. 1973) were investigated which excluded the use of thiamine and tryptone but included biotin, myo-inositol and choline chloride into a chemically defined medium designated MCD. Its final composition is shown in Table 3.3. This table also compares MC7 medium, which was a hybrid of MC6 medium, a chemically defined medium for *N. meningitidis* growth (Fu *et al.* 1995), and the original Frantz medium used in Figure 3.1. The main difference between MC7 and MC6 media is the use of yeast extract. *N. lactamica* did not grow well in MC6 medium and so several components were replaced with a small amount of yeast extract. However, when comparing MC7 medium and Frantz medium, the MC7 medium contained a reduced amount of yeast extract and an increased glucose concentration, from 5g L^{-1} to 10g L^{-1}.

Figure 3.5 compared the growth profiles of MC7, MCD and Frantz media in microwells. As previously stated Frantz media generated poor amounts of biomass in shake flask culture, yielding an optical density of 0.7 OD_{600} after 16 hours of culture. In microwells, where oxygen transfer is limiting, *N. lactamica* growth is restricted to an optical density of 0.16 OD_{600} after 16 hours of culture in Frantz media. In MCD media, this is improved upon resulting in a culture optical density of 0.46 OD_{600} after 16 hours of culture. However, MC7 media provided the best culture optical density of 1.13 OD_{600} after 16 hours of culture. While the MCD medium did improve upon the original Frantz medium by increasing the optical density by almost two-fold, it is MC7 medium that produced the best improvement on culture optical density, increasing the yield by six fold.

	Media component ($g\ L^{-1}$)			
Component	**Catlin Media MC6**	**Catlin Media MC7**	**Frantz Media**	**MCD Media**
NaCl	5.8	5.8	6	5.8
NH_4Cl	1	1	1.25	0.2
Glucose	10	10	5	10
L-Glutamic acid	3.9	3.9	1.6	3.7
L-Cysteine.HCl	0.1	0.1	0.012	0.1
$MgCl_2.6H2O$	0.4	0.4	0.6	0.4
Yeast extract	-	0.8	2	-
K_2HPO_4	4.0	4.0	-	4.0
K_2SO_4	1.0	1.0	-	1.0
$CaCl_2.2H2O$	0.03	0.03	-	0.04
L-Arginine	0.15	-	-	0.1
L-Serine	0.5	-	-	0.5
Fe (III) citrate	0.04	-	-	-
Glycine	0.25	-	-	0.25
KCl	-	-	0.09	-
$NaH_2PO_4.2H20$	-	-	2.5	-
$NaHCO_3$	-	-	-	0.04
L - Aspartic acid	-	-	-	0.50
Sodium acetate	-	-	-	2.05
Choline chloride	-	-	-	0.01
Biotin	-	-	-	0.01
myo - Inositol	-	-	-	0.04

Table 3.3 Composition of media investigated in relation to *N. lactamica* growth.

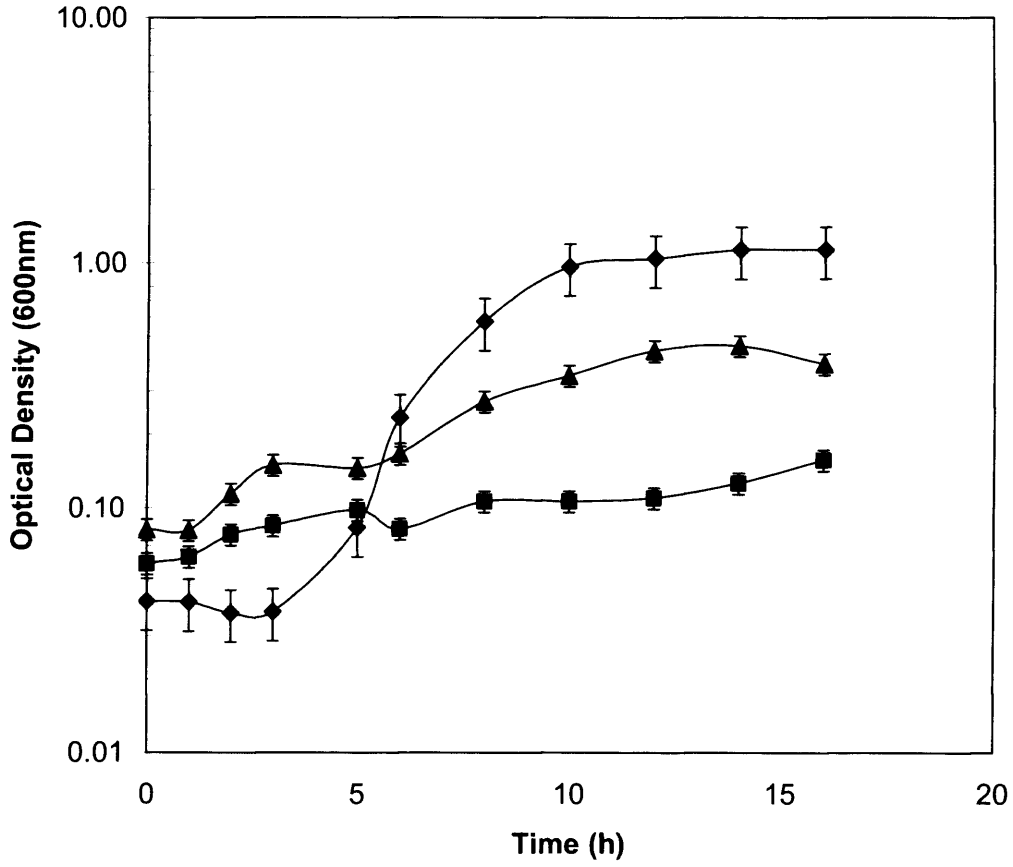

Figure 3.5 Comparison of *N. lactamica* growth kinetics in microwell cultures: (■) Frantz medium, (▲) MCD medium and (◆) MC7 medium. Experiments performed in 96 deep square well plates as described in Section 2.3.1. Error bars represents one standard deviation about the mean, where n=3.

3.2.5 Influence of pH control on *N. lactamica* growth

As described in the introduction to this chapter, pH is an important factor for the optimisation of growth conditions. The control of acidity in the growth medium can be extremely important if optimal productivity is to be achieved. Previous fermentations were conducted in microwells and did not incorporate any pH control; therefore it is desirable to investigate the effect of pH control and the starting pH of the medium on microbial growth. In Figure 3.6 the growth of N. lactamica in shake flasks under different pH conditions is investigated. Using the previous Frantz medium, the culture was begun at pH 7 and then became slowly more acidic over time, reaching a minimum of pH 5 after 16 hours. MC7 medium maintained that same pH range but had a lag phase of six hours and entered early stationary phase by 16 hours. Buffering MC7 medium at constant pH of 7 increased the lag phase to ten hours before the culture entered into exponential phase. However, by reducing the starting pH to 6, the lag phase was reduced to just four hours and the culture then entered early stationary phase by 12 hours. Thus pH control is not desirable in this fermentation and the reduction of the starting pH to 6 helps to reduce the lag phase of the culture. A possible explanation for this is that the seed inoculum used in the shake flasks attained a pH of 6 after overnight incubation, thus by matching the starting conditions of the media with the inoculum, the lag phase was reduced.

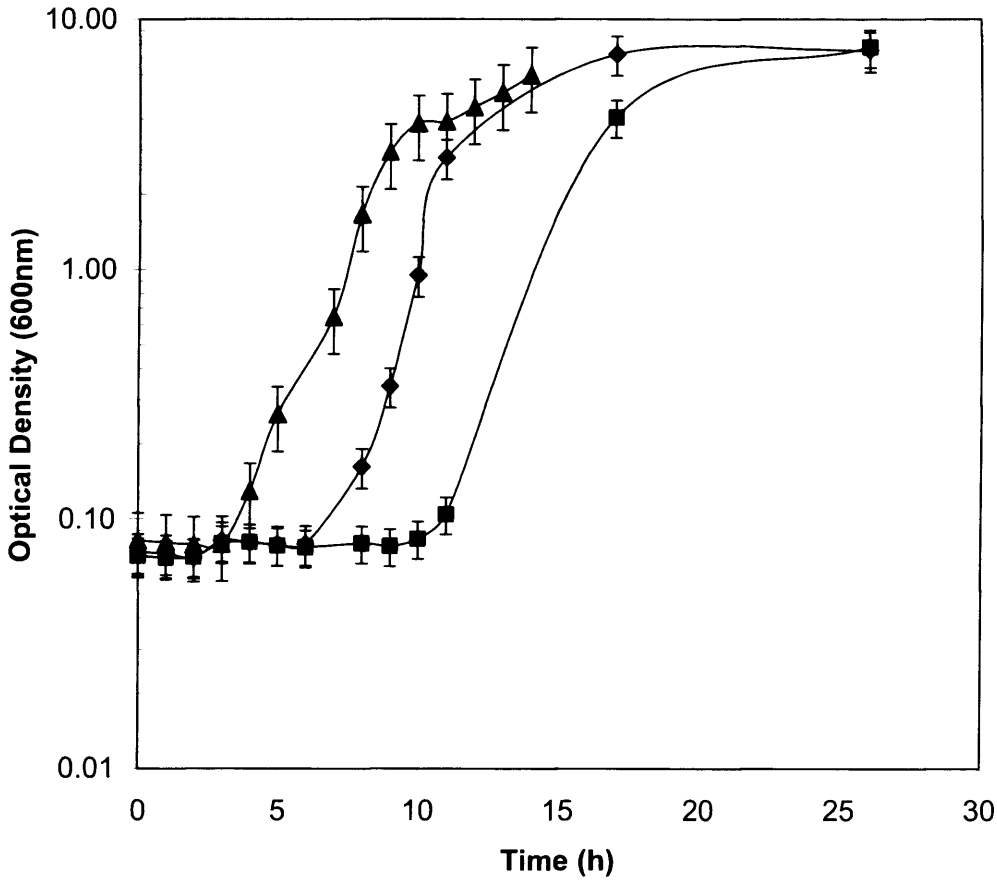

Figure 3.6 The effect of pH on *N. lactamica* fermentation in shake flasks, (■) MC7 medium buffered at pH7, (◆) MC7 medium with no pH control, starting pH 7, (▲) MC7 medium with no pH control, starting pH 6. Experiments performed in shakeflask cultures as described in Section 2.3.2. Error bars represent one standard deviation about the mean, where n=3.

3.3 *Influence of culture conditions on antigen profiles*

3.3.1 Use of SELDI-MS to monitor antigen profiles

In addition to the optimisation of cell growth conditions it is also important to ensure changes in medium composition do not adversely affect the required antigen profile. In this work SELDI-MS was used because of its small sample requirements, speed and most importantly, the fact that it can be used in a semi-quantitative capacity. The amount of protein present in the antigen profile was dependent not solely on peak height, but on the area under the peak. Thus provided sample volumes, sample concentration and incubation times were kept constant, the profiles can be directly compared and used in a semi-quantitative fashion to detect shifts in the antigen profile. This was because protein detection was dependent upon the antigen binding to the chemically treated surface.

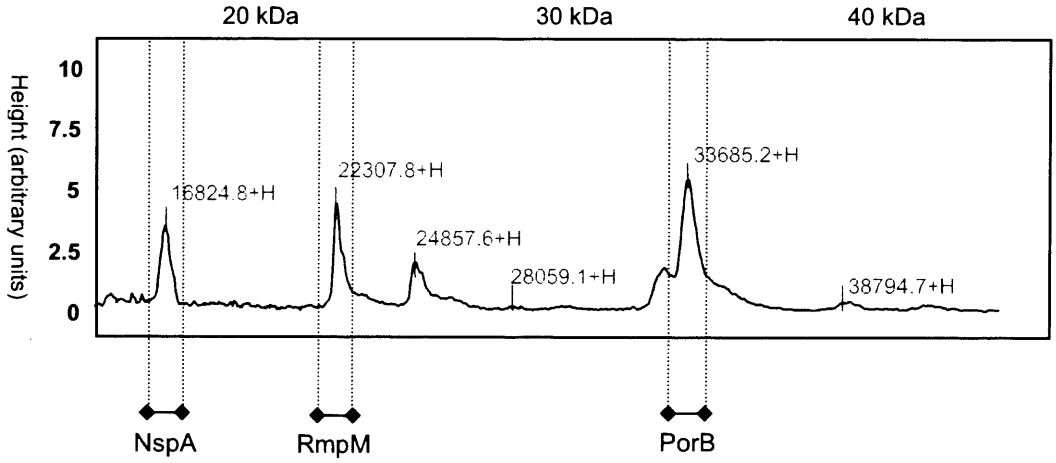

Figure 3.7 shows the SELDI-MS antigen profile generated by *N. lactamica* culture in Frantz medium. SELDI-MS analysis performed as described in Section 2.6.12. Identity of highlighted profile peaks confirmed through band extraction and Western blots (Mukhopadhyay *et al.* 2005).

The established antigen profile based on cell growth in standard Frantz medium shown in Figure 3.1 is shown in Figure 3.7.

Cell culture supernatants from the initial DOE experiments described in Section 3.2.3 were analysed by SELDI-MS to identify potential changes in antigen profile as a result of changes in medium composition. As shown in Figure 3.8 the antigen profile is seen to vary significantly. Each profile was created using equal sample volumes and Bioprocessor incubation times (Section 2.6.12). The antigen profile generated using only the amino acid solution (B) shows the presence of NspA at 16.7kDa and small amounts of PorB at 34kDa but there was no RmpM generated. The middle panel, generated using the yeast extract addition (C), shows the presence of all three antigen of interest, including RmpM at 22.7kDa. The bottom profile was generated with the presence of both a defined amino acid solution and the yeast extract solution (BC). This profile showed the presence of all three key antigens; however, when comparing the height of these peaks with those in panel B more RmpM was produced in BC then in C. However, it was the yeast extract panel that produced more PorB then the other two panels, while both C and BC produced approximately the same amount of NspA. In comparing the yeast extract profile generated in Figure 3.8 to the Frantz profile in Figure 3.7 all of the main antigens of interest have been retained.

Though the defined amino acid solution (B) had the best effect on the growth rate (Figure 3.3), its effect on the antigen profile was poor as it was unable to produce all of the key antigens. Yeast extract (C) on the other hand produced the second best growth effect and retained the key antigen profile while the combined effect of adding the amino acid solution and the yeast extract (BC) still produced an excellent growth rate, but reduced PorB expression. As a consequence of these experiments yeast extract was maintained in this round of development and glucose was retained as the carbon source.

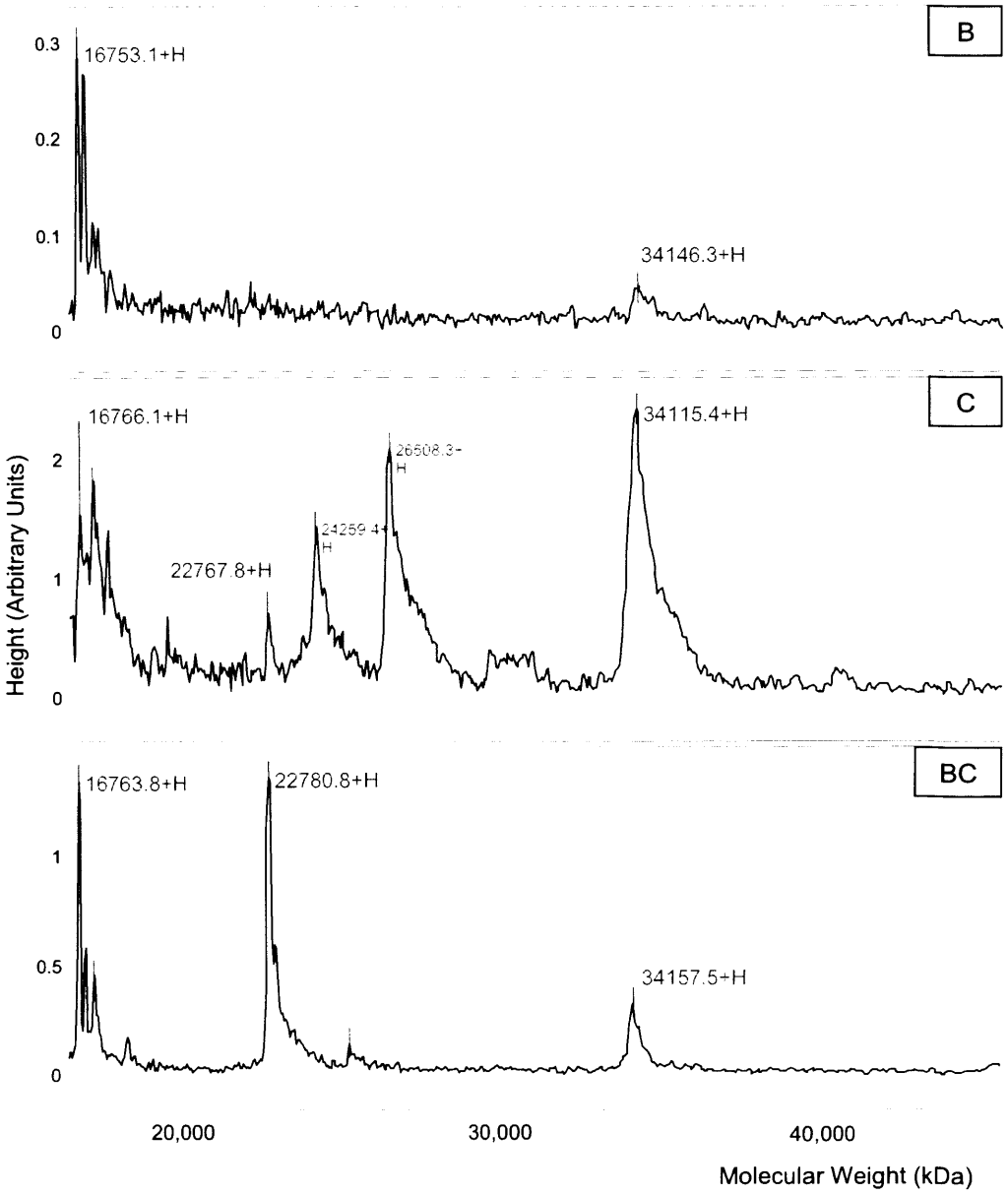

Figure 3.8 Antigen profiles generated by SELDI-MS analysis of culture supernatants from initial DOE experimentation (Section 3.2.3). Labels B, C and BC correspond to the medium composition shown in Figure 3.4. In these antigen profiles, PorB was located at 34kDa, RmpM at 22.7kDa and NspA at 16.7kDa. Fermentations performed as described in Section 2.3.1 and SELDI-MS analysis performed as described in Section 2.6.12. Profiles are indicative of three replicate determinations.

3.3.2 Impact of media composition on antigen profile

As shown in Figure 3.5 MC7 medium provided the best biomass yield when compared with MCD media, however, the media impact on the antigen profile had yet to be assessed. In order to accomplish this SELDI-MS was used in a semi-quantitative capacity.

In Figure 3.9 the antigen profiles generated by MC7 and MCD media are directly compared. Both profiles have been generated using the same sample concentrations, volume and incubation time. Thus by comparing the area under each peak it was observed that both media produced approximately the same amount of NspA, located at 16.3kDa. Both traces produce a sharp narrow peak approximately 10 units high. However, when comparing RmpM at 22.3kDa and PorB at 33.7kDa it was the MC7 medium that produced more of the vaccine antigens. The RmpM peak has a height of 12 units using MC7 medium which was reduced to just 5 units in MCD medium. Furthermore, the height of the PorB peak was 7.5 units in MC7 medium and only 5.5 units in MCD media. Thus it would seem that MC7 medium not only produced higher biomass concentrations but resulted in an improved antigen profile when compared with the chemically defined media, MCD. In this example SELDI-MS has shown itself to be a rapid method of determining the protein profile whilst using only small amount of protein for detection. Due to the unique nature of the chip chemistry used in SELDI-MS, it was possible to bind targeted antigen proteins of interest from the supernatant, requiring little sample purification.

Figure 3.10 is an overlaid profile showing the direct comparison of the final purified OMV product, one generated using MC7 medium and the other using Frantz medium. Biomass was generated using shakeflask culture as described in Section 2.3.2 and the OMVs were prepared as described in Section 2.4.1.

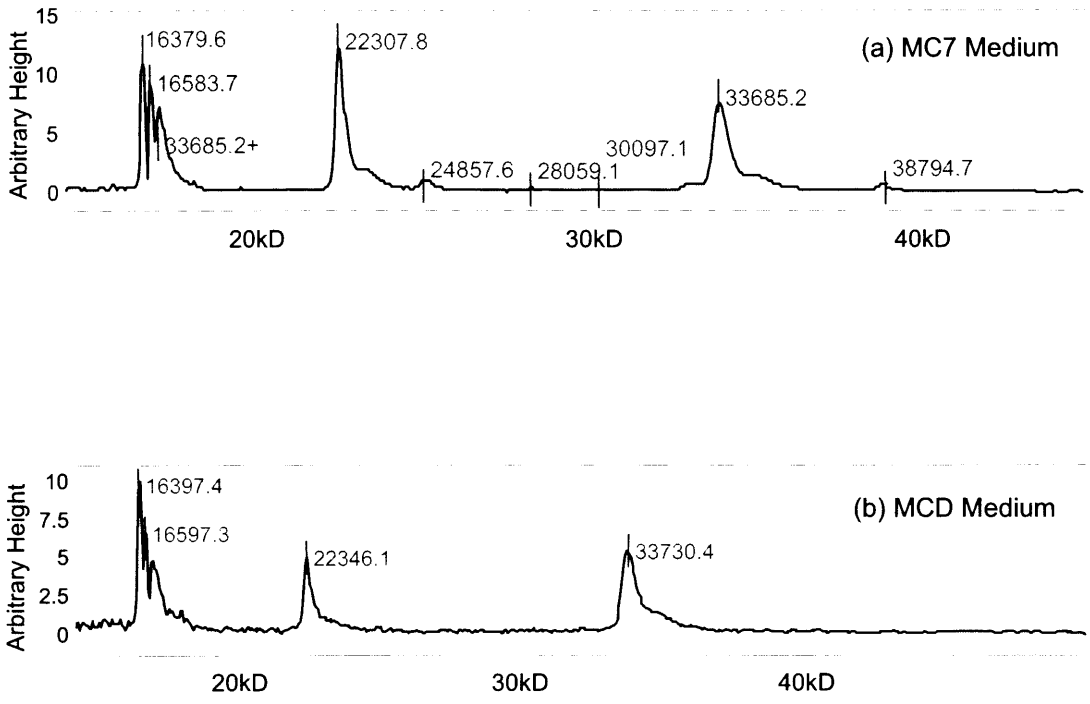

Figure 3.9 SELDI-MS comparison of the antigen profile in culture supernatants generated using (**a**) MC7 media and (**b**) MCD media. PorB is at 33.6kDa, RmpM is at 22.3 and NspA is at 16.4kDa. Both spectra were generated using the same amounts of total protein determined by BCA assay (Section 2.6.4). Fermentations were performed as described in Section 2.3.1 and SELDI-MS analysis performed as described in Section 2.6.12. Profiles are indicative of three replicate determinations.

Each sample was identically prepared. The figure confirmed the hypothesis that the growth media had an impact on the final product as MC7 medium made a noticeable improvement on the original antigen profile generated with Frantz medium. By comparing the area under each peak, NspA titres have been improved by three fold, RmpM titres have increased six fold and PorB titres have been improved upon by three fold.

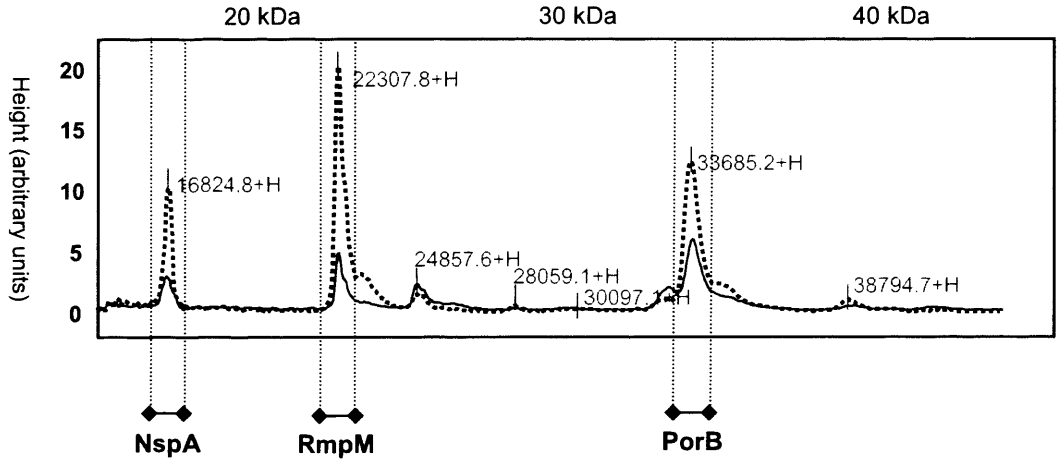

Figure 3.10 Direct SELDI-MS comparison of purified OMV profiles obtained using the original Frantz medium with MC7 medium. The solid line represents the antigen profile generated using Frantz media and the dashed line represented the profile generated using MC7 media. The same starting protein concentration, 150 μg mL^{-1}, was used for each sample. Shakeflask fermentations performed as described in Section 2.3.2 and OMVs prepared and purified as described in Section 2.4.1. SELDI-MS was performed as described in Section 2.6.12.

Finally, to validate the use of SELDI-MS in a semi-quantitative manner an SDS-PAGE gel was run loading 10 µg of total protein onto each well, as shown in Figure 3.11. When comparing the two lanes it was clear that the antigen profile was more intense using MC7 medium and that in particular the bands corresponding to PorB, RmpM and NspA were markedly more intense then the bands generated using Frantz medium.

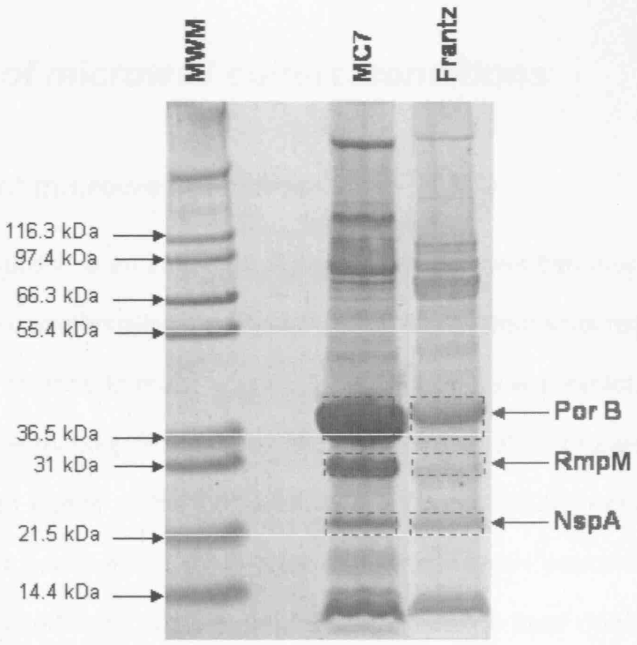

Figure 3.11 Verification of SELDI-MS antigen profiles using a conventional 4-12% Bis-Tris gradient SDS-Page gel. Each lane was loaded with 10 µg total protein and the antigens of interest, PorB, RmpM and NspA, highlighted. Samples taken from shakeflask cultures as described in Section 2.3.2 and purified as in Section 2.4.1 to create OMVs. SDS-PAGE analysis was performed as described in Section 2.6.9.

Interestingly the PorB bands appeared to be much darker in the SDS-PAGE gel then was expected using the SELDI-MS approximation. SELDI-MS predicted a three fold increase in PorB using the MC7 media. However, using gel densitometry scans, a five fold increase in PorB was detected. A possible explanation for this discrepancy could be the trailing shoulder seen in the SELDI-MS profile in Figure 3.10. The base of the PorB peak had a large foot print, possible indicating the presence of a second protein of similar molecular weight. This trailing shoulder was excluded from the PorB analysis as it did not fit the general shape of the peak, however in the gel, this protein would have been stained and may have made the PorB band appear wider and darker.

3.4 Scale-up of microwell culture conditions

3.4.1 Scale-up of microwell cultures

The scale-up of production is an important aspect of any process that makes the transition from development to commercialisation (Banks 1979). Many processes require scale-up to increase production volumes to make vaccine production more economically viable and to adequately supply the market. Scale-up of microbial fermentation processes is normally based on the oxygen needs of the bacterial culture (Doran 2003). Almost all microbial fermentations have a requirement for a high dissolved oxygen concentration and thus scale-up is usually based upon ensuring that the fermentation itself does not exceed the oxygen supply capabilities of the vessel.

The most commonly used gas for aeration during fermentation is air and the transfer of oxygen from an air bubble to the microbial cell can be described in three steps, (Bartholomew *et al.* 1950): (i) Transfer of oxygen from the air bubble to solution, (ii) transfer of the dissolved oxygen from solution into the cell, (iii) uptake of the dissolved oxygen by the cell.

Resistance to oxygen transfer in step two could be overcome through increased agitation. The limiting step to oxygen transfer was identified as the fist step, the transfer of oxygen from gas into the liquid. This rate of transfer is described using the following equation (Stanbury and Whitaker 1984a).

$$\frac{dC_L}{dt} = k_L a\left(C^* - C_L\right) \qquad \text{(Eq. 3.1)}$$

Where $\frac{dC_L}{dt}$ is the oxygen transfer rate, k_L is the oxygen mass transfer coefficient, 'a' is the specific interfacial area available for mass transfer, C* is the saturated oxygen concentration and C_L is the oxygen concentration in liquid.

The oxygen concentration gradient (C^*-C_L), may be regarded as the driving force across the air liquid interface, while k_La can be considered as the volumetric mass transfer coefficient. k_La is commonly used as a measure of a fermenter's aeration capacity. Therefore, to ensure that the fermenter can meet the oxygen demands of the bacterial culture, k_La is commonly used as the scale-up parameter (Banks 1979).

However, there is a specific problem in measuring the k_La in microwells, though some papers have demonstrated methods to overcome them (Doig *et al.* 2005;Hermann *et al.* 2001;Kensy *et al.* 2005). There two standard methods for measuring the k_La in bioreactors, the gassing out method (static and dynamic) and the sulphite method have their own associated problems. The gassing out technique requires a fast probe response time and the ability to control aeration rates to ensure that the dissolved oxygen does not fall below a critical oxygen tension. However, controlling the oxygen tension in a microwell was not

possible and can lead to erroneous results, especially since most shaken 96-well microwell fermentations are oxygen limiting. Furthermore, the ability to obtain an accurate dissolved oxygen sensor for a microwell with a fast probe response time is not always guaranteed. While there have been developments in optical probe technologies, these probes can be very expensive. Therefore, the more common sulphite method has been used to measure the k_La in microtitre plates (Kensy *et al.* 2005), however this was in 48-well plates not 96 well plates. The sulphite method has a tendency to over estimate the k_La (van't Riet 1979). This is because the sulphite method requires perfectly clean conditions in order to function properly as small amount of fatty acids, proteins and amino acids can have a major effect on k_La measurements (Bell and Gallo 1971). Furthermore, the rheology of the sodium sulphate solution is completely different to the fermentation broth.

Predictable scale-up of bacterial cultures from microtitre plates to conventional lab scale and pilot scale fermenters would allow a significant part of the development process to be carried out with reduced time and cost. Thus the key challenge was to form an empirical correlation between biomass yields and a wide range of operating conditions; however this can only be done by establishing first that *N. lactamica* growth was closely related to aeration.

3.4.2 Identification of scale-up basis for *N. lactamica*

A two litre pilot scale fermenter was utilised in order to first establish that *N. lactamica* growth was closely related to aeration. The rational for using a stirred bioreactor for the experiment was that control of aeration was better accomplished in a fermenter then in microtitre plates. The fermenter, with working volume of 1.6 litres, was used to determine the exponential growth rate and biomass production after 12 hours under varying aeration conditions. The impeller speed ranged from 600 rpm to 850 rpm, increased incrementally in order to ensure effective mixing. It was important though to ensure that excessive impeller speeds were not used as *N. lactamica* growth was adversely affected at high shear rates.

Figure 3.12 illustrates that as aeration was increased the growth rate and the final biomass yields also increased. At a starting airflow rate of 1 L min^{-1}, the corresponding growth rate and optical density were measured as 0.3 h^{-1} and 4.11 OD_{600}. This increased to a maximum growth rate of 0.54 h^{-1} and an optical density of 6.38 OD_{600} at an air flow rate of 1.5 L min^{-1}. Beyond this, conditions in the fermenter generate a high shear rate which resulted in a negative impact on *N. lactamica* growth as witnessed when the airflow rate was increased to 1.7 L min^{-1}. In this instance the growth rate diminished to 0.21 h^{-1} giving a final optical density of 3.48 OD_{600}. Note also the close relationship between the growth rate and final biomass yield. Overall the results show that *N. lactamica* cultures are sensitive to changes in aeration and hence this is likely to be a suitable scale-up parameter

3.4.3 Factors influencing aeration in microwells

In contrast to agitation and aeration rates in stirred bioreactors, the key operating parameters in microwells that influence oxygen transfer are the shaking pattern, shaking frequency, shaking amplitude, microwell diameter, liquid fill volume and the fluid properties such as density, viscosity, diffusivity and surface tension (Büchs 2001). To investigate the influence of aeration rates in microwells on *N. lactamica,* growth kinetics experiments were performed in 96 deep square well plates as a function of liquid fill volume using MC7 medium. All other parameters were held constant. Figure 3.13 shows the culture optical density attained after 12 hours of growth in a deep square well microtitre plate with varying fill volumes.

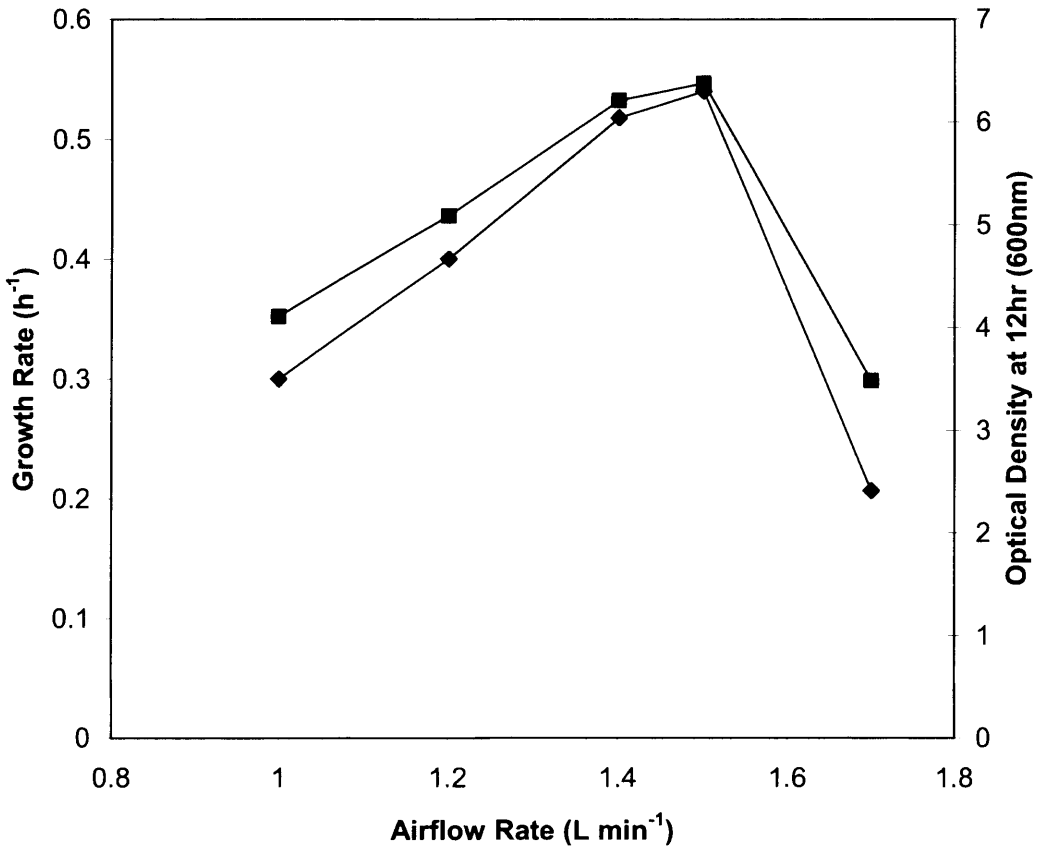

Figure 3.12 The effect of aeration on *N. lactamica* growth kinetics in a 2 L stirred bioreactor. (■) optical density of the culture and (◆) exponential growth rate. Fermentation performed as described in Section 2.3.3.

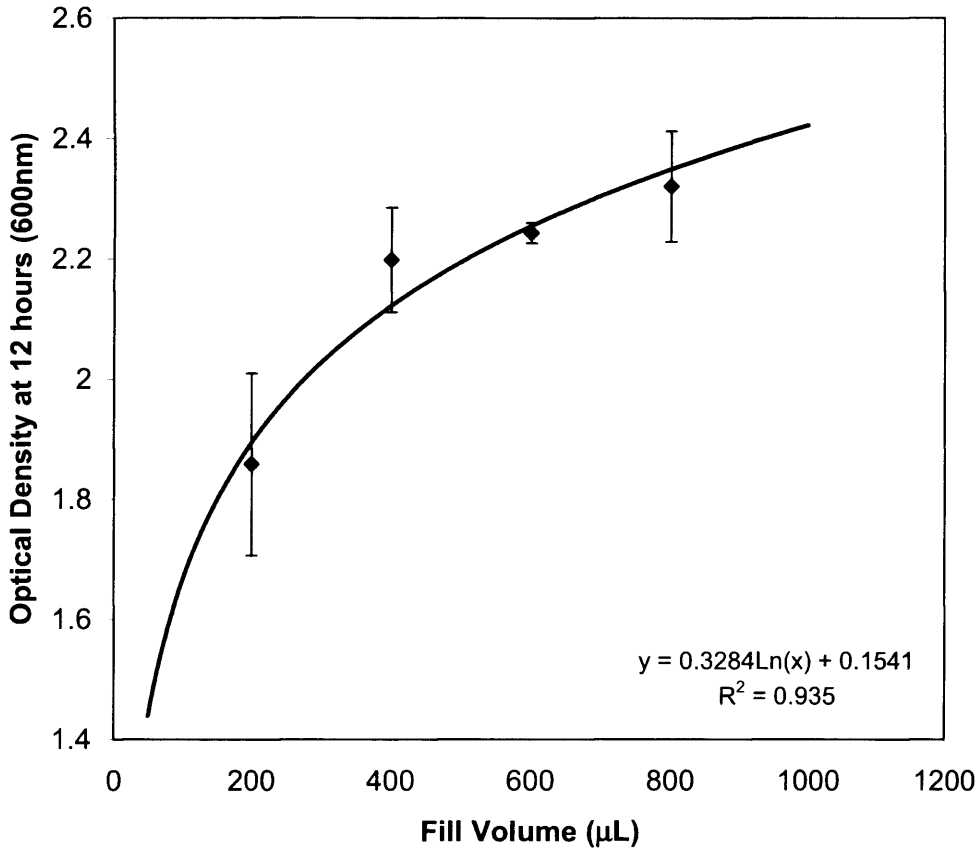

Figure 3.13 *N .lactamica* growth kinetics in 96-DSW plates as a function of fill volume. Experiment was performed as described in Section 2.3.1 with a shaker speed of 1000 rpm. Data fitted using logarithmic trend. Error bars represent one standard deviation about the mean, where n=3.

Based upon pervious work (Hermann *et al.* 2001), as the power input was kept constant for all wells, it would normally be expected that as the well volume increased, the aeration would decrease, based upon a ratio of power per unit volume. As it had been established that *N. lactamica* growth was a function of aeration, increased culture volume should result in reduced biomass yields. Unexpectedly, the exact opposite was observed. As the well volumes increased so did the final biomass yields. A fill volume of 200µl achieved a final optical density of 1.86 OD_{600} after 12 hours. This trend increased logarithmically so that a fill volume of 800µl achieved an optical density of 2.32 OD_{600} after 12 hours of culture.

To better understand this phenomenon high speed photographic images were taken of a model deep square well filled with varying liquid volumes. As in Figure 3.13, the shaking frequency was kept constant at 1000rpm and the same medium, MC7 was used in all experiments. Figure 3.14 shows the high speed images of the microwells shaken at different fill volumes. As the fill volume increased, the displacement height is seen to also increase. Furthermore, as a steady state was reached in the microwells, the gas liquid interface area took the shape of an inverted undulating cone, with the cone tip moving from corner to corner.

The relationship between displacement height and fill volume is plotted in Figure 3.15. The closest fitting trend line was a logarithmic one which is similar to that shown in Figure 3.13. The pre logarithmic factor in both equations is very similar as is the shape. This would perhaps indicate that there is a relationship between the displacement height and aeration as an increase in the displacement height will increase the gas-liquid interface area. This will result in an increase in the oxygen transfer rate and consequently enhance *N. lactamica* growth.

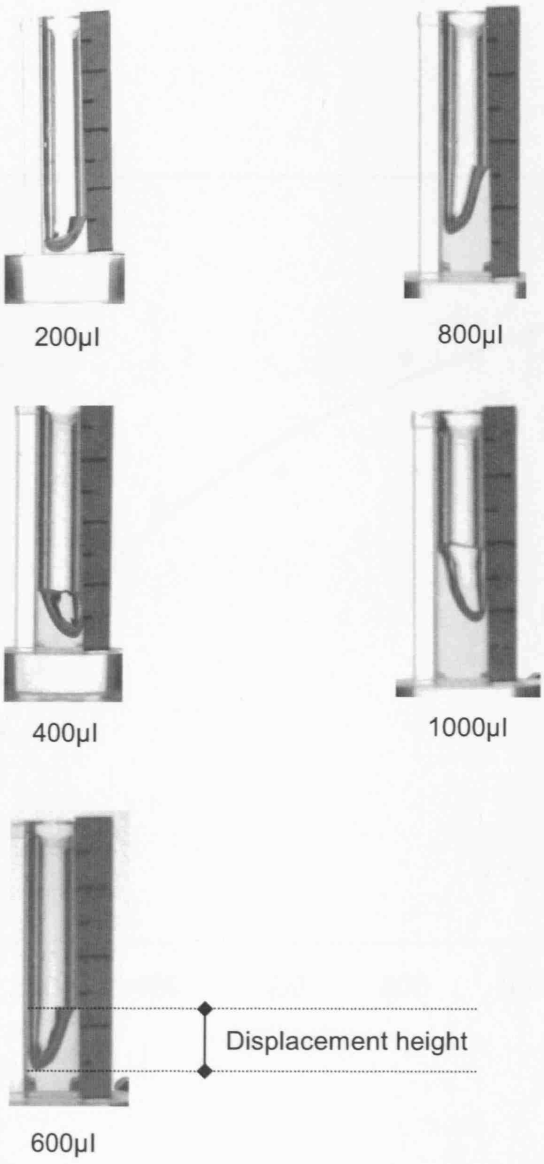

Figure 3.14 High speed photographic images of a single deep square well mimic filled with varying volumes of MC7 medium, at an agitation of 1000 rpm. Experiment performed as described in Section 2.6.14.

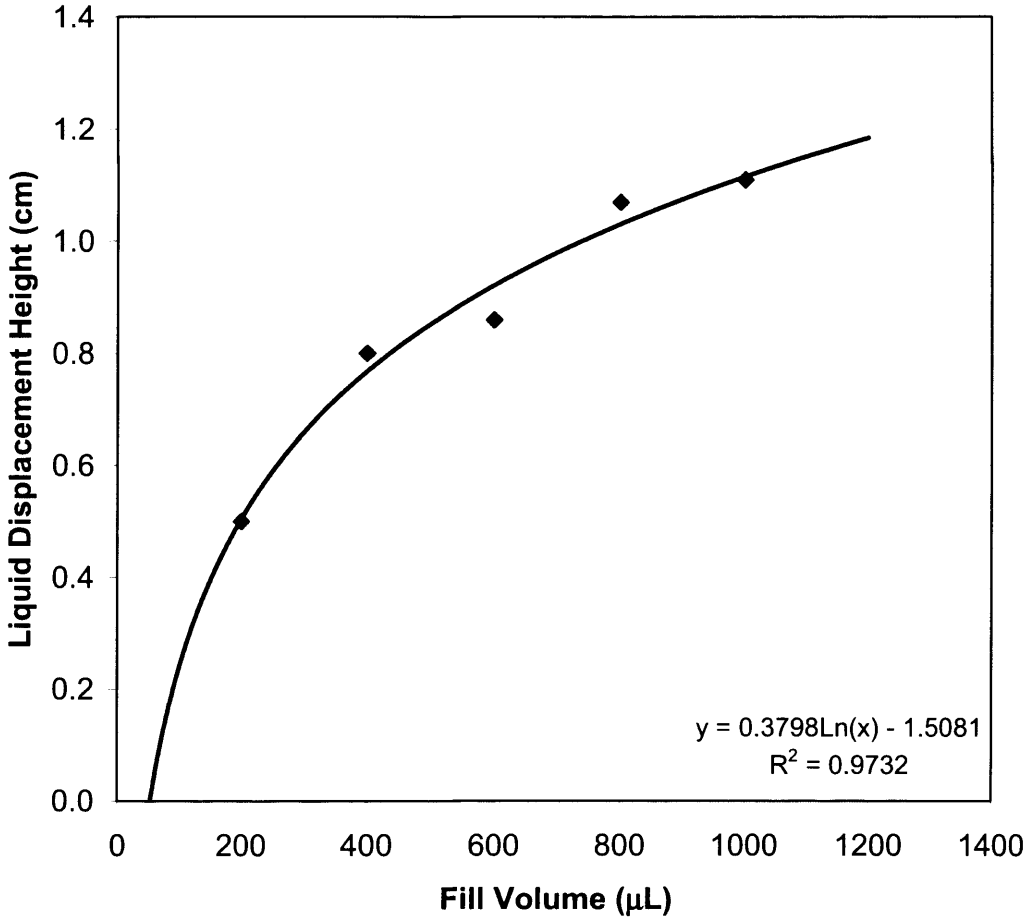

Figure 3.15 Variation of liquid displacement height as a function of well fill volume. Displacements calculated from Figure 3.14. Experiment performed as described in Section 2.6.14.

3.4.4 Modelling aeration in microwells

The term superficial gas velocity has been used to characterise the aeration of a fermenter (Doran 2003). It is described as the volumetric air flow rate (m^3 s^{-1}) divided by the cross sectional area of the fermenter (m^2) and is included in many approximations describing k_La in bioreactors (van't Riet 1979). By deriving an equivalent superficial gas velocity term for microwells, dimensionless analysis will be employed to create a correlation to link aeration in microwells with aeration in stirred bioreactors. Key to this will be linking the biomass attained into the correlation as this has been demonstrated to be a function of aeration.

In the superficial gas velocity term, the key variable is the volumetric gas flow rate. The cross sectional area is related to the diameter of the tank which is normally a fixed constant value. This cross sectional area term needed to be translated for microwells as a description of the surface aeration.

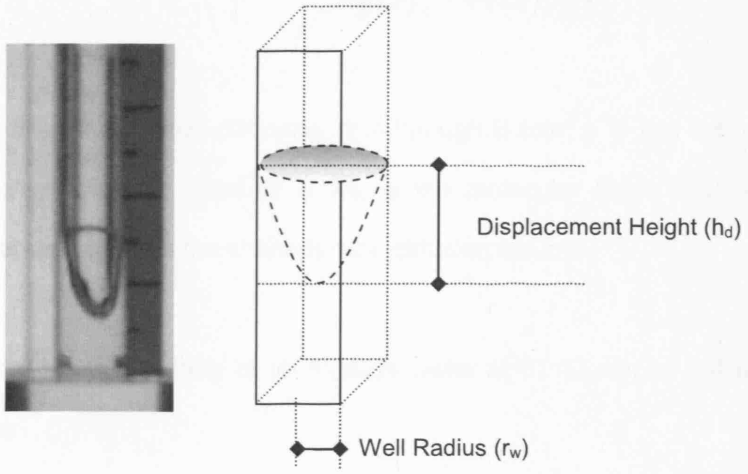

Figure 3.16 Schematic diagram showing how the gas-liquid surface area in a shaken 96 DSW is modelled and calculated. Photographic image capture as described in Section 2.6.14.

The surface area of the gas liquid interface at the top of a microwell can be described as an inverted cone, once the shaking has stabilised as shown in Figure 3.16. The interfacial area (SA_W) can then be calculated according to Equation 3.2.

$$SA_w = \pi r_w \sqrt{r_w^2 + h_d^2} \qquad \text{(Eq. 3.2)}$$

Where r_W is the well radius and h_d is the displacement height as described in Figure 3.16. The driving force of oxygen transfer into a microwell is based upon diffusion and the diffusion coefficient can be used as a measure of the diffusivity of air from the gas phase to the liquid phase in the well, using Equation 3.3 (Fuller *et al.* 1966).

$$D_{AB} = \frac{10^{-3} T^{1.75} \left(\frac{1}{M_A} + \frac{1}{M_B} \right)^{\frac{1}{2}}}{P\left[(\Sigma v)_A^{\frac{1}{3}} + (\Sigma v)_B^{\frac{1}{3}} \right]^2} \qquad \text{(Eq. 3.3)}$$

Where D_{AB} is the mass diffusivity of A through B ($cm^2\ s^{-1}$), T is the temperature in Kelvin, M_A is the molecular mass of A, M_B is the molecular mass of B, P is the pressure in atmospheres and v is the characteristic diffusion volume.

Thus the mass diffusivity of air through water at 37 ℃ can be calculated from Equation 3.3a as:

$$D_{Air-Water} = \frac{10^{-3}(310)^{1.75}\left(\frac{1}{29}+\frac{1}{18}\right)^{\frac{1}{2}}}{(1)\left[(20.1)^{\frac{1}{3}}+(12.7)^{\frac{1}{3}}\right]^2} \qquad \text{(Eq. 3.3a)}$$

$$D_{Air-Water} = 0.269 cm^2 s^{-1}$$

In order to relate microwell and bioreactor aeration a new term was created for microwell fermentation called the effective aeration, A_S, and is described as the mass diffusivity of air through water ($D_{Air\text{-}Water}$) divided by the gas-liquid interface area available for oxygen transfer (SA_w):

$$A_{S\text{-}micro} = \frac{D_{AB}(cm^2 s^{-1})}{SA_w(cm^2)} \qquad \text{(Eq. 3.4)}$$

The A_S microwell term thus has a characteristic dimension of s^{-1}. This dimension is different to the superficial gas velocity. Consequently a corresponding equation for the effective aeration, A_S, was determined for stirred fermenters as described by Equation 3.5.

$$A_{S\text{-}fermenter} = \frac{\text{air flow rate (L s}^{-1})}{\text{volume of liquid (L)}} \qquad \text{(Eq. 3.5)}$$

As described in Section 3.4.2 and 3.4.3 experimental data have been collected for both microwell fermentations and bioreactor fermentations. Though these were at the extremes of scale and utilised different methods of agitation, there were inherent kinematic

similarities and as such dimensionless analysis was used to correlated performance at the different scales.

In the case of stirred bioreactors certain dimensionless groups such as Reynolds number and Froude number are widely used (Welty *et al.* 1995). However, when it is not clear which dimensionless groups apply, as in the case of microwells, a more general procedure can be applied called the Buckingham Pi method. (Buckingham 1914;Vignaux 1991).

The first step is to identify the number of variables in the problem. In this case it was established in Sections 3.4.2 and 3.4.3 that *N. lactamica* growth is a function of aeration.

Growth = *f* (aeration)

Growth = *f* (power, volume, oxygenation)

The relationships are then expressed as a dimensionless matrix, shown in Table 3.4.

	M	L	T
Growth Rate	1	-1	-1
Oxygenation (A_S)	0	0	-1
Volume	0	3	0
Power	1	1	-2

Table 3.4 Dimensionless matrix of the key variables that influence *N. lactamica* growth expressed in fundamental dimensions, M, L and T.

The number of dimensionless groups to be formed was based on the number of variables minus the rank of the matrix (Welty *et al.* 1995). In this case there was only one dimensionless group (Π_1) to be formed:

$$\Pi_1 = GA_S{}^a V^b P^c \qquad \text{(Eq. 3.6)}$$

Resolving for the unit balance, the exponents are:

a=1, b=2/3, c=-1

Thus:

$$\Pi_1 = \frac{GA_S V^{2}{}_{3}}{P} \qquad \text{(Eq. 3.7)}$$

Equation 3.7 can be rearranged to so that growth is made the principle.

$$G \propto \frac{P}{A_S V^{2}{}_{3}} \qquad \text{(Eq. 3.8)}$$

As with effective aeration, A_S, different equations are required to calculate the power input for bioreactors and microwell fermentation. In bioreactors the gassed power consumption was used to calculate the power input, as described by Equation 3.9 (Hughmark 1980).

$$\frac{P_g}{P_0} = 0.10\left(\frac{F_g}{N_i V}\right)^{-0.25}\left(\frac{N_i^2 D_i^4}{g W_i V^{2/3}}\right)^{-0.20} \qquad \text{(Eq. 3.9)}$$

Where P_g is the gassed power, P_0 is the ungassed power, F_g is the volumetric gas flow rate, N_i is the impeller speed, D_i is the impeller diameter, W_i is the impeller width, V is the volume.

The power input for the microwell plate was approximated using kinetic energy. The units of power are joules per second, thus if a basis of one second was used then the power input into the microtitre plate can be approximated to the kinetic energy input per second.

$$\text{Kinetic Energy} = \tfrac{1}{2} mv^2 \qquad \text{(Eq. 3.10)}$$

$$\text{Kinetic Energy} = \tfrac{1}{2} (\rho V)[(n)(0.012)]^2 \qquad \text{(Eq. 3.11)}$$

Where n is the revolutions per second of the shaken platform, ρ is the density of the fluid, V is the fill volume of the microwell. The 0.012 term was calculated as the path length of each revolution. The Thermomixer used a shaking motion with an amplitude of 3 mm. Thus each revolution has a path length of 12 mm. The dimensionless group shown in Equation 3.8 thus provides a basis for scale comparison where growth is related to power input, aeration and volume, all of which can be determined independently.

3.4.5 Verification of scale-up predictions

The utility of the dimensionless relationship obtained in Equation 3.8 was tested, based on *N. lactamica* growth kinetics obtained for fermentations performed at up to 50 L stirred bioreactor scale. Example fermentations of 2 L, 8 L, and 50 L fermentations are given in Figure 3.17. They show that as the scale increases, it is possible to attain higher growth rates. The 2 L growth profile shows a lag phase of approximately 4 hours before entering exponential phase. The lag phase in the 8 L and 50 L fermentations appear to have been reduced to 40 minutes. Consequently, the exponential growth rates increase with

increasing scale. The 2 L fermentation achieves an exponential growth rate of 0.49 OD hr^{-1}, while the 8 L and 50 L fermentations attain exponential growth rates of 0.67 and 0.92 OD hr^{-1} respectively. Experimental data from Figure 3.17 and further fermentations carried out at various scales were used to create Figure 3.18. The $P/A_S V^{2/3}$ term was plotted on the x-axis and calculated for a variety of different fermentations. A relationship between the growth rate and the optical density yield at 12 hours has already been established in Figure 3.12, thus the culture optical density was plotted on the y-axis. The result of the semi-log plot indicates that it is possible to relate microwell growth data with that found in bioreactors. The data was used to project a line of best fit, these data points were represented by diamonds in Figure 3.18. Further fermentations were conducted using shake flasks, two litre and eight litre fermentations to verify the model. These points were represented by squares and aligned themselves closely to the line of best fit.

The data points are aligned in order of aeration. For example, examining the two litre data points used in the model, the point farthest to the left was the fermentation with the lowest aeration of 0.67 vvm. The data point next to it on the right used an aeration of 0.8 vvm and so forth until the final two litre model data point which utilised the highest aeration rate of 0.93 vvm. The same was true with regards to the eight litre fermentation data points, where upon the point furthest left used the lowest aeration, while the point furthest right used the highest aeration. It may be that the figure is indicative of a scale effect, as there were no data points in the bioreactor runs which over lapped. That is to say, a two litre data point did not run into an eight litre data point, though they attained the same optical density. Effectively, the $P/A_S V^{2/3}$ value should be seen as a measure of culture aeration and thus should only be applicable to strict aerobes such as *N. lactamica.*

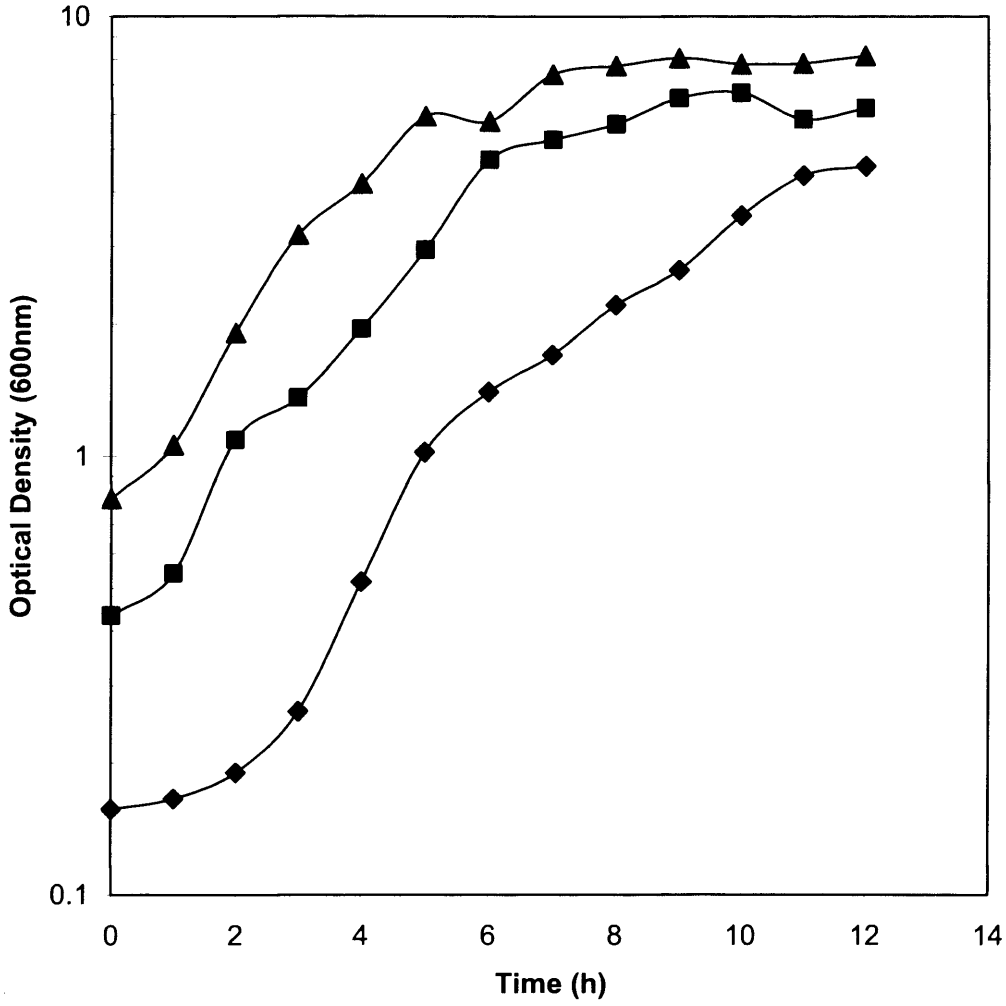

Figure 3.17 Example of bioreactor fermentation of *N. lactamica* growth in MC7 medium at (◆) 2 L, (■) 8 L and (▲) 50 L scales. The measured exponential growth rates, μ, were 0.49, 0.67 and 0.92 hr-1 for 2 L, 8 L and 50 L scales respectively. 2 L fermentations conducted as described in Section 2.3.3 using an air flow rate of 1.2 L min-1. 8 L fermentation conducted as described in Section 2.3.4 using an air flow rate of 2 L min-1. 50 L fermentation conducted as described in Section 2.3.5 using an air flow rate of 20 L min-1.

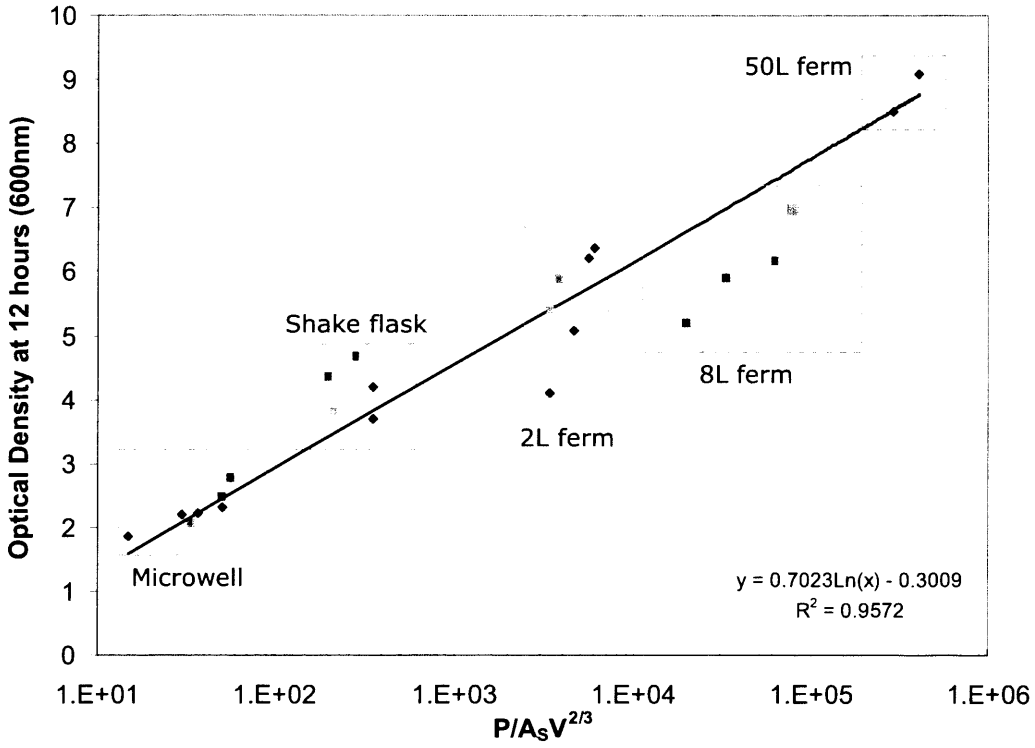

Figure 3.18 Correlation of *N. lactamica* growth (OD_{600}) with the dimensionless group $P/A_SV^{2/3}$ over a range of scales. Points included in model development are plotted using diamonds (◆), while the squares (■) represent fermentations carried out to test the relationship. Solid line fitted by linear regression. N. lactamica cultured on MC7 medium as described in Section 2.3.1 for microwell culture, Section 2.3.2 for shakeflask culture and Section 2.3.3 for 2 L fermentations. 8 L and 50 L fermentations were conducted as described in Sections 2.3.4 and 2.3.5.

3.5 Summary

In this chapter the statistical technique, factorial design, was effectively applied as a scouting tool for media components (Section 3.2.2). The range of the media concentrations for the positive and negative coded values was based on earlier work into the nutritional profiles of *Neisseria* (Catlin BW. 1973). Occasionally, when creating a factorial design experiment to study a variable, a nuisance variable is identified which cannot be held constant or randomised. This nuisance variable was found to be the heating block of the Thermomixer used to conduct the media development experiments. This heating block did not evenly distribute the heat which led to the creation of hot spots. This had a corresponding effect on the response, the growth rate. Hence in order to accommodate the error generated by this nuisance variable the microtitre plate was divided into blocks, each block large enough to accommodate a complete replicate of the experimental run. This allowed for the isolation of the nuisance variance caused by the heating block.

The ability to couple SELDI mass spectroscopy to media development, shown in Section 3.3, greatly increased the speed of the research and development process as it accurately identified key antigens in each supernatant sample in their relative quantities. Due to the unique nature of the chemically treated sample spots, it was possible to bind and identify the key vaccine antigens of interest without the need for downstream processing. The appropriate binding buffers, pH and chip chemistry must be determined first; but because SELDI-MS is semi-quantitative and fits the microtitre plate foot print it allows the use of the micro-scale platform to shift from a qualitative tool to a quantitative one.

As stated previously in Section 3.4.1, k_La has been traditionally used as a scale-up parameter. However, measurement of this value can be complicated in a microtitre plate without specialist optical probes. Therefore dimensionless analysis (Section 3.4.4) was applied based upon the terms which could be accurately measured, relating the growth to the power, volume and effective aeration of the system. The data obtained (Figure 3.18)

demonstrated that it was possible to relate these microwell fermentations to those carried out in stirred bioreactors. However, upon closer examination of the available literature this dimensionless group is analogous to the k_La, but is easier to estimate.

Van't Riets review suggested the k_La in bioreactors can be expressed in the following general terms:

$$k_L a = \mathrm{K}\left(\frac{P}{V}\right)^a (v_s)^b \qquad \text{(Eq. 3.12)}$$

Where the values for K, *a* and *b* are determined experimentally and depend upon factors such as vessel geometry, ionic strength of the media, fill volumes and impeller arrangements. Thought the superficial gas velocity (v_s) term was not used in the dimensionless correlation, its function remained the same; to describe the aeration of the culture media and was measured by dividing the gas flow rate by the cross sectional area of the vessel instead of the working volume, as described by the effective aeration (A_S).

The dimensionless relationship is not a true model but an empirical correlation which was specific only to *N. lactamica*. Correlations involving other aerobic micro-organisms would have to be empirically determined. However, this work does show it was possible to relate microwell fermentation data to bioreactor runs using dimensionless analysis.

In summary the aims outlined at the beginning of the chapter have been met. The use of statistical DOE has led to the development of two new media, MCD and MC7, both of which surpassed the original Frantz medium used at the beginning of this study in terms of growth. By coupling the microwell platform with SELDI-MS, it was possible to monitor the impact on the antigen profile during media development and chose MC7 medium that increased titres of PorB, RmpM and NspA have increased by three, six and three fold

respectively. The fermentation culture conditions were optimised and by choosing not to control the pH the lag phase was reduced resulting in a fermentation time of 12 hours. Finally, through micro-scale studies into the fluid dynamics of microwell mixing, it was possible to relate microwell fermentation to stirred bioreactor fermentations of various scale using dimensionless analysis.

There were some limitations to the micro-scale approach. For example, it was only through bioreactor runs that the impact of foaming could be properly assessed, a problem not identified in the small scale. However, it has allowed the development of a dimensionless correlation which provided for robust and reproducible scale-up. As a consequence of the micro-scale approach the amount of time spent conducting pilot scale fermentations has been reduced allowing fermentation development to be more cost effective and rapid.

4 Micro-scale Process Creation: Downstream processing of *N. lactamica* outer membrane vesicles

4.1 Introduction

The *N. lactamica* fermentation process established in Chapter 3 yielded a final broth that contains a mixture of spent medium, metabolic by-products and product components in dilute solution. The downstream processing of this broth requires the concentration and purification of the outer membrane vesicles for use in the final Meningitis B vaccine formulation. The initial downstream purification method used at the HPA was a lab-scale manufacturing method which was utilised to produce sufficient material for pre-clinical trials. This process was based on the methods of Fredriksen and co-workers (Fredriksen *et al.* 1991;Helting *et al.* 1981;Zollinger *et al.* 1978) in the manufacture of a Meningitis B OMV vaccine. It has several disadvantages having been established solely for lab scale production. If clinical trails of the meningitis B vaccine proved to be successful, then this initial process would be impractical for commercial production. The Fredriksen method requires a series of batch centrifugation steps which limit the process volume per batch and have low throughput, as each step took up to two hours.

The most significant hurdle to overcome is the final sterility of the product because all the buffers used in the Fredriksen purification process required the use of thimerosal (Fredriksen *et al.* 1991). Thimerosal is a bacterio-static preservative which prevents bacterial growth during and after the purification process. It is the primary method used to ensure the sterility of the product and prolonged its shelf life after package into vials. Thimerosal contains 50% mercury by weight and when injected into the body thimerosal is

broken down into ethyl-mercury. It was thought to have similar effects as methyl-mercury, which is a potent neurotoxin (U.S. Pharmacopoeia, 2004), but in reality has undetermined toxic effects. Several studies have been commissioned to investigate the toxicity of thimerosal but have led to contradictory conclusions (Axton 1972;Ball *et al.* 2001;Pichichero *et al.* 2002). As thimerosal is routinely used in many childhood immunisations there was a concern that it may accumulate in the body. Therefore, the FDA and other regulatory bodies have now decided to withdraw the use of thimerosal from childhood immunisations as a precautionary measure. This decision is based on the use of methyl-mercury toxicity data for ethyl-mercury thimerosal (FDAMA 1997, http://www.fda.gov/cber/vaccine/thimerosal.htm). Hence finding a new method to maintain end product sterility has become a recent concern requiring modification of the Fredriksen method. Other chemicals could be used instead of thimerosal, such as phenol, but in order to expedite the regulatory process the MHRA recommends the use of filtration, heat or radiation to maintain sterility of the product (MHRA 2002).

4.1.1 Potential downstream processing routes

The downstream processing of the Meningitis B OMV vaccine can be split into three distinct stages. The first stage is primary recovery, used to harvest the cell suspension from the fermentation broth. In the Fredriksen method this is achieved by batch centrifugation post fermentation. The second stage was to resuspend the cell paste in a deoxycholate buffer, which is a detergent used for stripping outer membrane vesicles from the cell wall; this stage is referred to as vesicle extraction. The final stage is concentration and purification of the outer membrane vesicles using ultra-centrifugation.

In Figure 4.1, processing route A represents the Fredriksen method. It consisted of a series of centrifugation and ultra-centrifugation steps. Following primary recovery the cell paste is gently resuspended in a deoxycholate buffer in a water bath at 37℃.

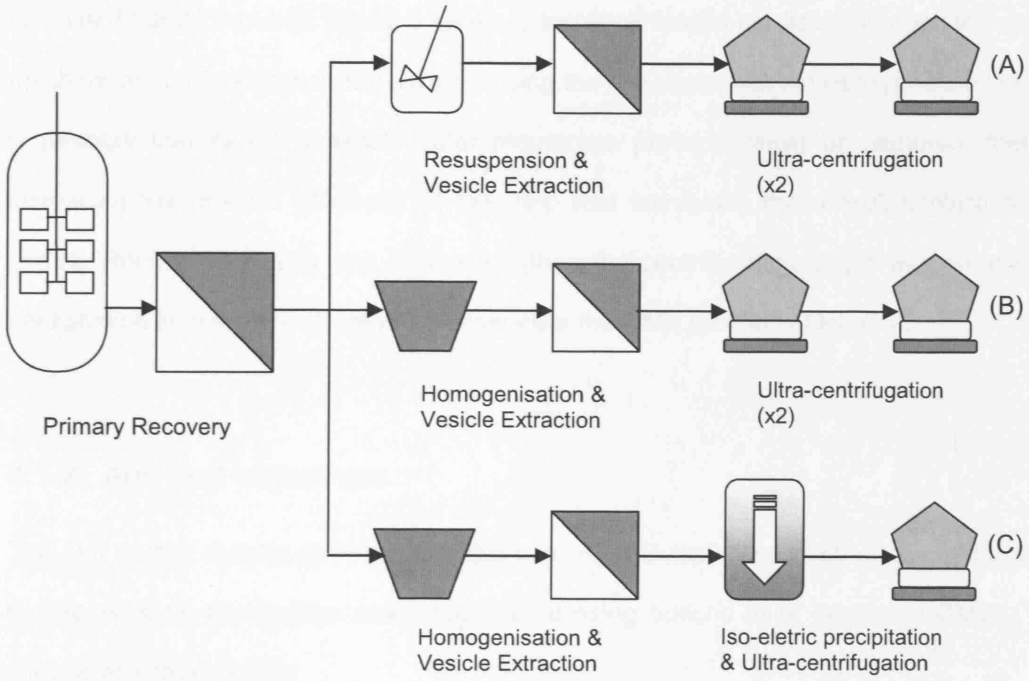

Figure 4.1 Outline of the three potential downstream processing routes evaluated in this chapter. Route (A) is the Fredriksen method (Fredriksen *et al.* 1991), route (B) replaces resuspension with homogenisation and route (C) replaces one of the ultra-centrifugation steps with iso-electric precipitation.

This is followed by centrifugation to pellet and discard the biomass and retain the supernatant containing the OMVs. After this, two ultra centrifugation steps concentrated and purified the OMVs, each time pelleting and resuspending them in a smaller buffer volumes. The final OMV pellet was resuspended in a 3% (w/v) sucrose solution which contained 50mM Tris-HCl. Route B seeks to increase vesicle extraction through the use of mechanical homogenisation. By homogenising the cell paste with the deoxycholate buffer it is possible that all the available outer membrane proteins would be captured, thereby increasing the process efficiency of this step and increasing the overall capture of the OMVs. Route C replaces one of the lengthy ultra-centrifugation steps with iso-electric precipitation in order to capture and concentrate the OMV proteins of interest.

4.1.2 Aim and objectives

The aim of this chapter is to explore the use of USD tools and micro-scale methods to rapidly evaluate the vaccine downstream processing options of *N. lactamica* OMVs. The specific objectives are to:

- Investigate the robustness of the process stream in primary recovery and its tolerance to shear using USD tools. This would be necessary in order to consider continuous centrifugation for biomass harvest.

- Study the detergent assisted vesicle extraction step and identify its effectiveness using a micro-scale platform as this would uncover areas of vesicle loss during the purification process.

- Explore options to the ultra centrifugation step as it is both time consuming and rate limiting using a micro-scale platform. A secondary aspect of this is to produce a purification process that minimises process stream contaminants such as DNA.

- Study the aggregation of OMVs using DLVO theory so that end production filtration could be used as an alternative to thimerosal to sterilise the final vaccine product.

4.2 Influence of shear on primary recovery

4.2.1 Application of USD tools on the shear sensitivity of the process stream

Post fermentation, the first step in the downstream process is the recovery of cells from the fermentation broth. This is because the majority of the outer membrane vesicles were attached to the cell wall (Fredriksen *et al.* 1991). Under the Fredriksen method, solid separation is achieved using batch centrifugation, each with a volume capacity of three litres per run. In a commercial environment these centrifuges would probably be replaced with continuous centrifuges. In order to evaluate which continuous centrifuge, if any, might be suited to cell recovery two issues need first to be resolved.

The first is the response of the cell suspension to shear forces. A common issue with many continuous centrifuges is the high levels of shear generated in the feed zones, as liquid entering the centrifuge is rapidly accelerated from near zero speeds to the centrifuge bowl speed (Boychyn *et al.* 2001). Shear forces of this magnitude may be sufficient to detach the OMVs from the surface of the cell wall resulting in a decrease in the step yield. Consequently a rotating disk shear device (20 mL) was used to evaluate the shear sensitivity of the culture supernatant at harvest. The shear device has been previously used to predict the performance of industrial centrifuges and its application is well understood (Boychyn *et al.* 2004). Culture samples were loaded into the shear device and subjected to different shear rates and residence times, as described in Section 2.4.2. Figure 4.2 shows the normalised protein released into the fermentation broth as a function of the applied shear rate. The calculated protein release result of OMV loss or cell

breakage represents the difference between the protein content of the supernatant sample before and after shearing. As expected, the amount of protein released increased with increasing shear rates and residence time. However, the process stream appeared to be very robust as there seemed to be little loss of OMVs from the cells. Shear rates of greater than 25,000s^{-1} were required to detect any measurable product loss. The maximum shear rate varies depending on the type of centrifuge used and the mode of operation. For example, in a basket centrifuge (30 L Rousselt) the solid fraction is subject to a continued maximum shear rate of 18,000 s^{-1} at the basket wall (Boulding *et al.* 2002). In continuous disk stack centrifuges, such as the Westfalia SAMR 3036, a maximum shear rate has been identified at the solids discharge point, subjecting the processed solids to a few seconds of shear at 10,000 s^{-1} (Neal *et al.* 2003). The highest shear rate measured in tubular bowl centrifuges such as the Carr Powerfuge™, under normal, non flooded, operating condition is 20,000 s^{-1} in the feed zone, for a duration of a few seconds (Boychyn *et al.* 2001). This means that it is possible to choose from a range of centrifuge designs for the recovery of *N. lactamica* from culture.

The second issue is the clarification efficiency. It is desirable to have a high clarification efficiency, in excess of 90%, as the supernatant is to be discarded as waste. High clarification efficiency thus indicates the proportion of cells and OMVs captured in the solids product stream of centrifugation. Figure 4.3 shows the clarification of the *N. lactamica* cell suspension as a function of residence time and exposure to different levels of hydrodynamic shear. As expected, the supernatant clarification increases as the residence time inside the centrifuge bowl increases. In this case solids had more time to settle inside the centrifuge bowl. However, what is unusual about these data is that sheared samples attained a higher clarification than unsheared samples. Previous literature data suggested that shearing a cell suspension generated fine debris which is characteristically difficult to sediment, resulting in poor clarification (Maybury *et al.* 1998).

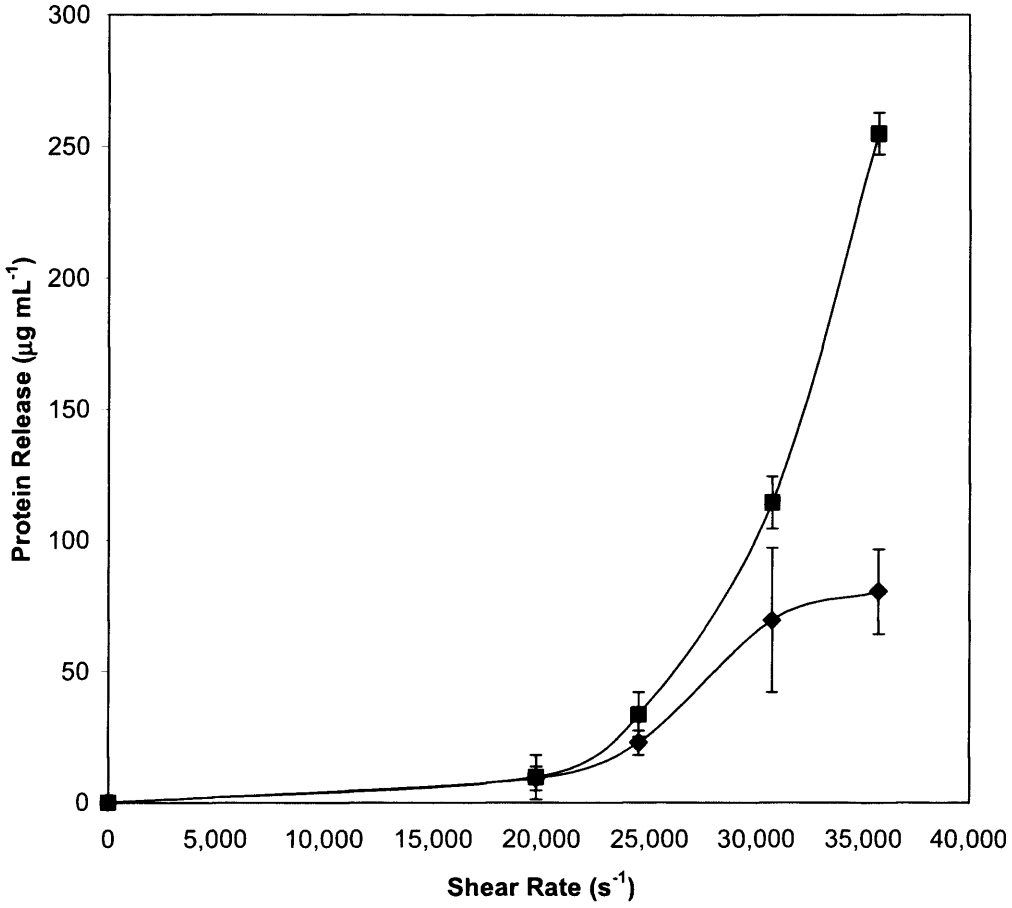

Figure 4.2 Protein release from *N. lactamica* fermentation broth suspension subjected to varying shear rates for (◆) 20 and (■) 40 seconds. The protein release is the difference in measured protein concentration in culture supernatants pre and post shearing. *N. lactamica* cultured in shakeflasks (Section 2.3.3) using MC7 medium. USD shear experiments conducted as described in Section 2.4.2 and protein concentration determined using BCA assay (Section 2.6.4). Error bars represent one standard deviation about the mean, where n=3.

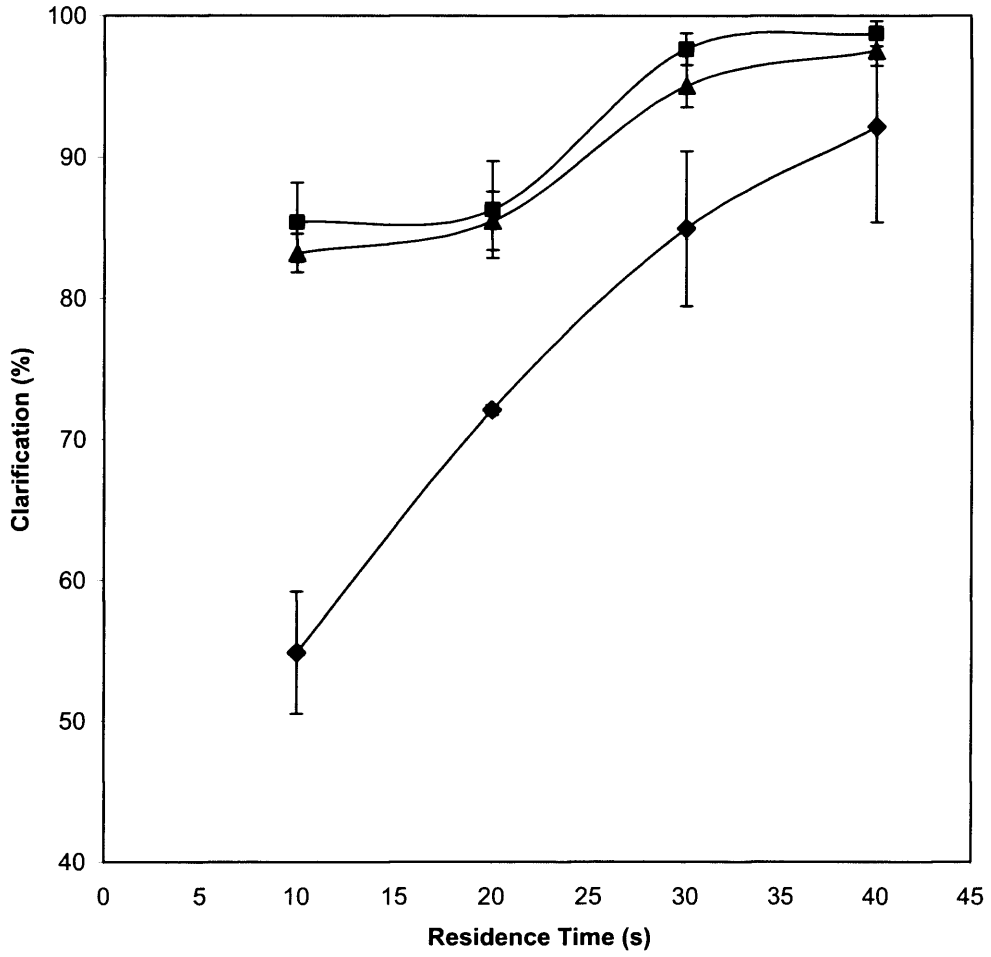

Figure 4.3 Clarification of the *N. lactamica* fermentation broth suspension subjected to varying residence time: (◆) unsheared process stream, (■) process stream subjected to an average shear rate of 15,000s^{-1} for 40 seconds, (▲) process stream subjected to an average shear rate of 20,000s^{-1} for 40 seconds. *N. lactamica* cultured in shake flasks (Section 2.3.2) using MC7 medium. USD shear experiments and clarification determination conducted as described in Section 2.4.2. Error bars represent one standard deviation about the mean, where n=3.

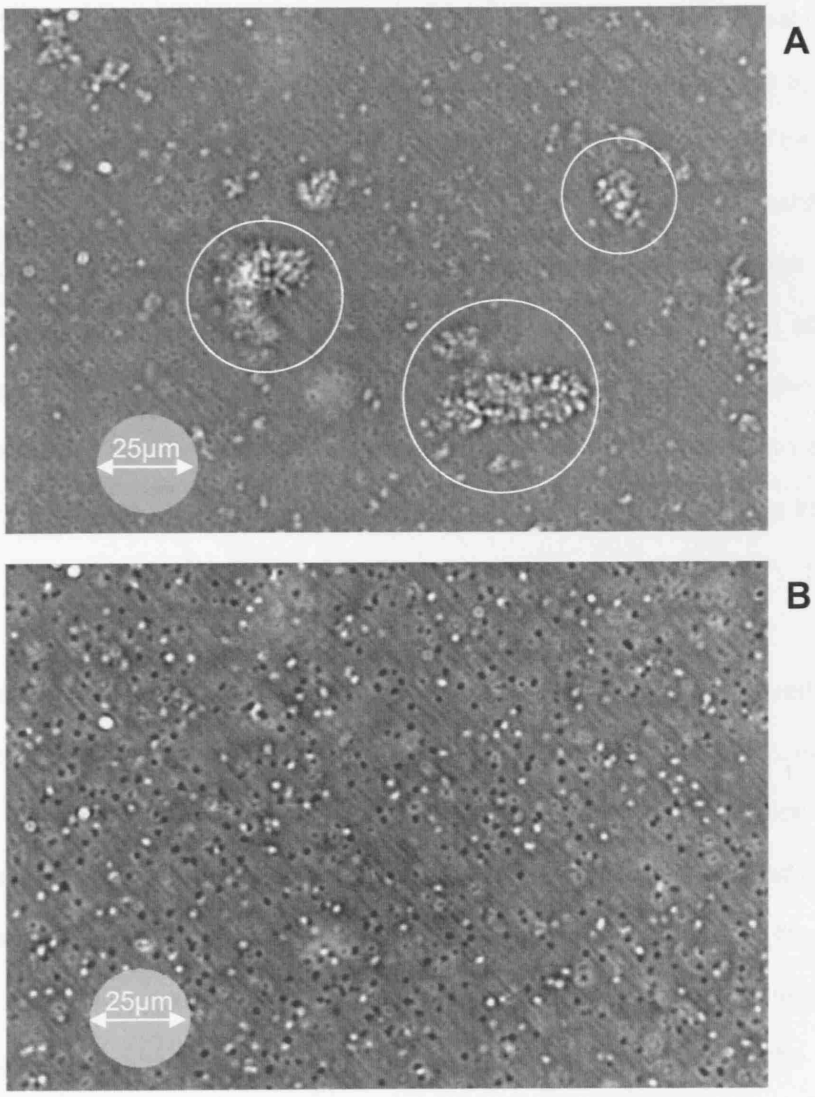

Figure 4.4 Confocal microscopy images of *N. lactamica* fermentation broth samples. (A) Normal fermentation broth harvested from a bioreactor culture, where the white circles identify areas of aggregation. (B) Sample subjected to an average shear rate of 15,000s^{-1} for 40 seconds. *N. lactamica* fermentation conducted in a 2 L bioreactor (Section 2.3.3) using MC7 medium. *N. lactamica* fermentation broth samples sheared using USD shear device (Section 2.4.2). Images taken with confocal microscopy (Section 2.6.15)

In order to understand this phenomenon better, samples were analysed using confocal microscopy. Figure 4.4(a) shows an unsheared fermentation broth sample of *N. lactamica*. This shows discrete diplococci approximately 2-4μm in diameter. The individual OMVs are too small to be visualised. However the image also shows a number of large aggregates. These aggregates form most probably as a result of non-specific interactions between the cell wall and the lipid membranes produced by the cell (Israelachvili and Pashley 1982). The aggregates observed here have diameters of 30μm and so are over ten times the sizes of individual cells. In contrast, Figure 4.4(b) shows the sheared cell suspension indicating that none of these large aggregates are present. This might explain the improved clarification efficiency seen in Figure 4.3 as the individual cells are able to form a compact pellet during centrifugation which, most probably due to a decrease in drag in line with Stokes' Law.

Figure 4.5 takes the experimental clarification data from Figure 4.3 and converts it into a log-probability plot of clarification efficiency as a function of a new term, V/ctΣ. In this term the flow rate (V) divided by the sigma factor (Σ) residence time (t) and correction factor (c). This term is used to allow the comparison of bench scale centrifuges employed in the USD model to laboratory and commercial scale centrifuges. By selecting the required fermentation broth clarification from the y-axis the corresponding V/ctΣ is selected and used to determine centrifuge bowl speeds and flow rates. For example, the operating conditions required in a tubular bowl centrifuge, such as the Carr Powerfuge P6 (Boychyn *et al.* 2004), selected due to the ease with which the cell paste can be harvested and its high dewatering (Salte *et al.* 2006), can be calculated using V/ctΣ from Figure 4.5.

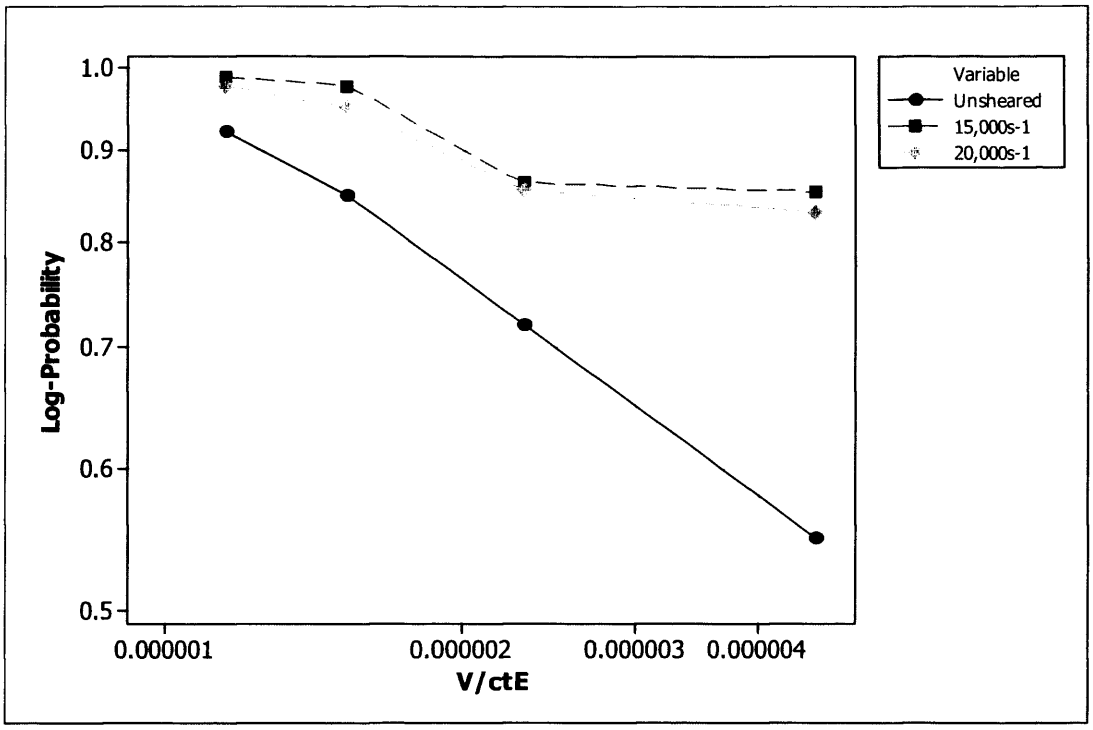

Figure 4.5 Probability plot of clarification versus V/ctΣ. In order to achieve a clarification above 90% the V/ctΣ value must be below 1.25×10^{-6} for an unsheared sample or below 2×10^{-6} if the sample was sheared. Log-probability clarification calculated according to Equation 2.4 based upon the experimental data shown in Figure 4.3.

$V/ct\Sigma$ ($m\ s^{-1}$)	RPM	Σ (m^2)	Q ($L\ h^{-1}$)
$9x10^{-7}$	1,000	3.02	8.81
	2,000	12.01	35.24
	3,000	27.20	79.29
$1x10^{-6}$	1,000	3.02	9.79
	2,000	12.01	39.16
	3,000	27.20	88.10
$2x10^{-6}$	1,000	3.02	19.58
	2,000	12.01	78.31
	3,000	27.20	176.20

Table 4.1 Predicted flow rates for the Carr Powerfuge, P6, under a range of bowl rotations and V/ctΣ values calculated details. Calculations based on data presented in Figure 4.5

Table 4.1 demonstrates that the sigma factor (Σ) is dependent on the bowl speed, measured in revolutions per minute (rpm), while the flow rate (Q) is affected by both the V/ctΣ and the sigma factor itself. In order to achieve 90% clarification in unsheared fermentation broth a V/ctΣ value of $1x10^{-6}$ m s^{-1} should be used in which case a flow rate of 39L h^{-1} can be used with a bowl speed of 2,000 rpm. Interestingly, if the process stream was sheared, then almost double the flow rate could be used in order to achieve the same clarification using the same bowl speed. This would effectively half the time required for the primary recovery step in the overall downstream processing sequence (Figure 4.1). Since

the process stream appeared to take little time to clarify, throughput is no longer a constraint. In which case, the clarification efficiency could be increased to 99%, which resulted in a $V/ct\Sigma$ of $9x10^{-7}m\ s^{-1}$. Using the previous bowl speed of 2000rpm, a flow rate of 35 L h^{-1} could be used to ensure maximum biomass retention and product recovery. Thus it would seem that shear has little influence on the primary recovery of biomass from the fermentation broth and modest levels shear improve recovery.

4.3 Influence of shear on vesicle extraction

After recovery of *N. lactamica* from culture the next downstream processing step is normally resuspension of the cell paste and vesicle extraction. In the Fredriksen method (Figure 4.1(a)), the cell paste is resuspended in a deoxycholate buffer and then centrifuged to pellet and discard the biomass. The resuspension process itself takes approximately 30 minutes and requires the constant mixing of the cell paste into the buffer at 37℃ to create a homogeneous mixture. The deoxycholate buffer was used to extract the vesicles from the surface of the cell wall and retain them in the supernatant fluid post centrifugation. It is an anionic membrane detergent used to solublise membrane components. In order to measure the efficiency of this process and the detergent's ability to efficiently extract the OMVs, the BCA total protein assay (Section 2.6.4) was used to quantify the total protein captured in this step and relate this information to the antigens captured by SDS-PAGE band densitometry (Section 2.6.9). SELDI-MS was not used to quantify protein capture because the deoxycholate detergent interfered with the binding of outer membrane proteins to the protein chip.

To determine the maximum possible amount of protein release, a small sample of resuspended cell paste was passed twice through a homogeniser (Section 2.4.3) at a pressure of 1,200 bar. This assumes that all the cells were lysed and consequently all OMVs released into the supernatant fluid. This homogenised sample was subsequently

centrifuged for 10 minutes at 13,000 rpm in a microfuge to sediment cell debris. In comparing the resuspended vesicle recovery supernatant with the total protein release value, it is observed that resuspension was able to recover 88% of the total protein available (Table 4.2). In fact, if resuspension is replaced with homogenisation and then centrifuged under the same conditions this would only increase recovery by five percent to 93%. This seven percent loss in protein is lost in the process as the buffer suspension is handled from one unit operation to another.

The antigen composition of the two supernatant fluids was quantified using SDS-PAGE. Gels were loaded with 15 μg of total protein in each well and subsequent band densitometry analysis revealed the proportions present of each of the three main OMV protein antigens, PorB, Rmp and NspA. Table 4.3 shows the results of this analysis. The extract produced by the homogenised vesicle recovery route contained 15% PorB, 8% Rmp and 4% NspA. In comparison the resuspended supernatant contained 14%, 7% and 4% respectively. Thus homogenisation offers little advantage in antigen capture compared with the original method as the antigen profile is the same in both methods.

Homogenisation can also be undesirable as cell breakage often leads to the introduction of extra intracellular contaminants into the process stream, such as protein and nucleic acids. Consequently, the shear device used in Section 4.2 was further used to asses what levels of shear would be required to facilitate vesicle capture without homogenisation. Figure 4.6 shows the effect of subjecting the deoxycholate buffer cell suspension to a range of shear rates, prior to centrifugation. In order to increase protein capture by ten percent, shear rates of $35{,}000s^{-1}$ are required. This is a large shear rate and the subsequent protein release probably reflects overall cell breakage rather then vesicle release. In summary the deoxycholate buffer appeared to very efficient at removing the OMVs from the cell paste (Tables 4.2 and 4.3). Homogenisation would only marginally increase antigen recovery (Table 4.3).

Treatment	*Resuspended*	*Homogenised*
Total protein pre centrifugation (mg mL^{-1})	240	580
Protein recovered post centrifugation (mg mL^{-1})	210	540
Loss (%)	12	7
Recovery (%)	**88**	**93**

Table 4.2 Total protein recovery from the cell paste based on gentle resuspension or total homogenisation. The percentage recovery values are based on amount of protein measured before and after centrifugation. *N. lactamica* generated using 2L fermentation conducted as in Section 2.3.3 using MC7 medium. Cell recovery and protein assay performed as described in Sections 2.4.1, 2.4.3. and 2.6.4 respectively.

Sample	*MW (kDa)*	*Name*	*Quantity (%)*
Homogenised supernatant	39	PorB	**15**
	29	Rmp	**8**
	22	NspA	**4**
Resuspended supernatant	39	PorB	**14**
	29	Rmp	**7**
	22	NspA	**3**

Table 4.3 Densitometry analysis of SDS-PAGE gel of the process supernatants based on resuspension or homogenisation. Each well was loaded with 15 µg total protein. *N. lactamica* generated using 2L fermentation conducted as in Section 2.3.3 using MC7 medium. Cell recovery and protein assay performed as described in Sections 2.4.1, 2.4.3. and 2.6.4 respectively. SDS-PAGE analysis conducted as in Section 2.6.9.

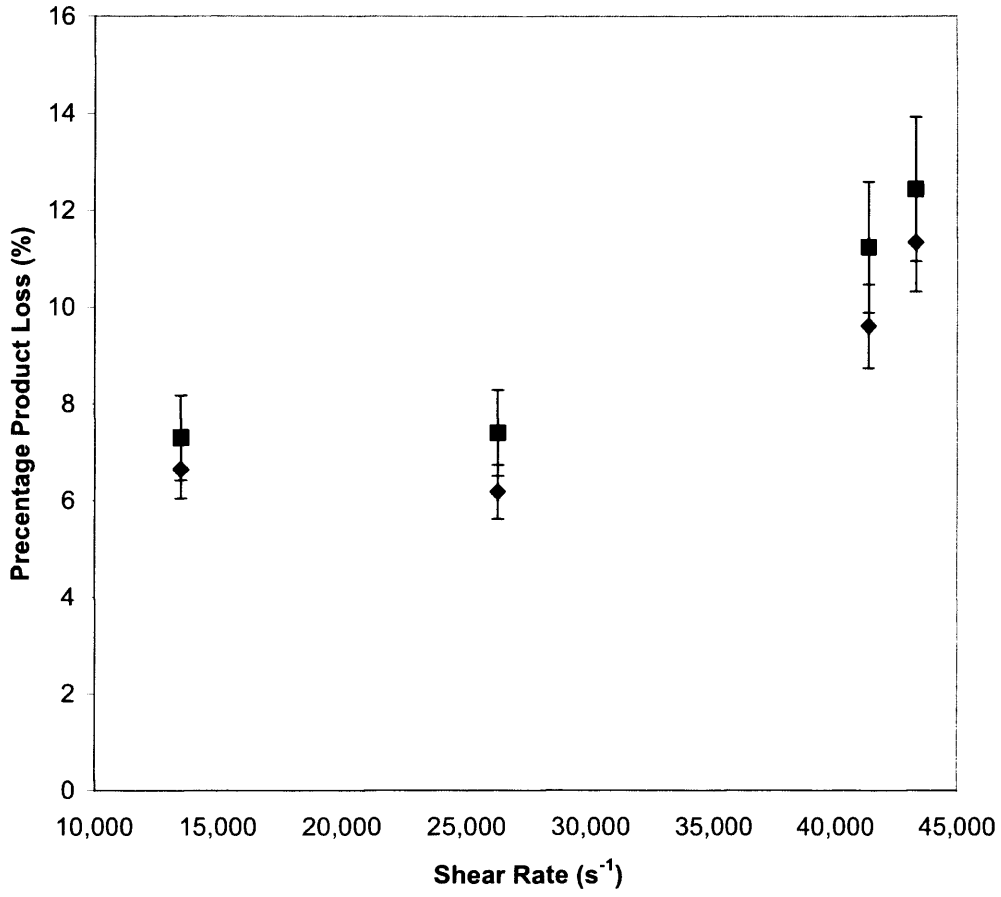

Figure 4.6 Percentage protein release of the cell paste deoxycholate buffer suspension under a range of shear rates: (◆) residence time of 20 seconds, (■) residence time of 40 seconds. *N. lactamica* fermentation conducted in a 2 L bioreactor (Section 2.3.3) using MC7 medium. *N. lactamica* fermentation broth samples sheared using USD shear device (Section 2.4.2) and protein release determined using BCA assay (Section 2.6.4). Error bars represent one standard deviation about the mean, where n=3.

4.4 Investigation of a protein precipitation step

In the standard process route purification and concentration of the supernatant from resuspended vesicles is achieved via ultra-centrifugation, which pellets the OMVs (Figure 4.1(a)). This pellet is resuspended in a smaller buffer volume and the process repeated. Ultra-centrifugation is both time consuming and inefficient due to the low process volumes that can be handled. In order to reduce the duration of this purification stage, precipitation was evaluated to create an insoluble fraction of the OMV proteins (Figure 4.1(c)). This also addresses a secondary concern of product contamination with host cell DNA. The sedimentation coefficients of the OMVs and contaminant DNA were very similar, thus ultra-centrifugation pelleted both OMVs and DNA. Therefore, by using precipitation it was hoped to increase the sedimentation coefficient of the OMVs, thereby allowing the use of a lower centrifugal force to pellet just the insoluble protein component. Two methods of protein precipitation were assessed, ionic precipitation and iso-electric precipitation.

Figure 4.7 shows the effect of ionic precipitation using ammonium sulphate, also known as salting out. Ammonium sulphate is commonly used for protein precipitation mainly due to its high solubility, which facilitates the creation of high ionic strength solutions (Harris 1989). Increasing the ionic strength of the buffer increases the amount of protein precipitated; however, this method offers no selectivity and furthermore complicates the purification route as dialysis may be required subsequently to remove excess salt. In contrast, Figure 4.8 shows the iso-electric precipitation of the process stream achieved by adjusting the pH by acid addition. This offers a more selective precipitation so that it is possible to isolate the main proteins of interest while avoiding smaller media component proteins. At pH 6.6 PorB was precipitated from the medium. By reducing the pH of the process stream to 5.2, it is possible to precipitate all the main proteins of interest. This insoluble fraction is then pelleted and resuspended in a Tris-HCL buffer at pH 8 which fully re-dissolved the protein precipitate pellet.

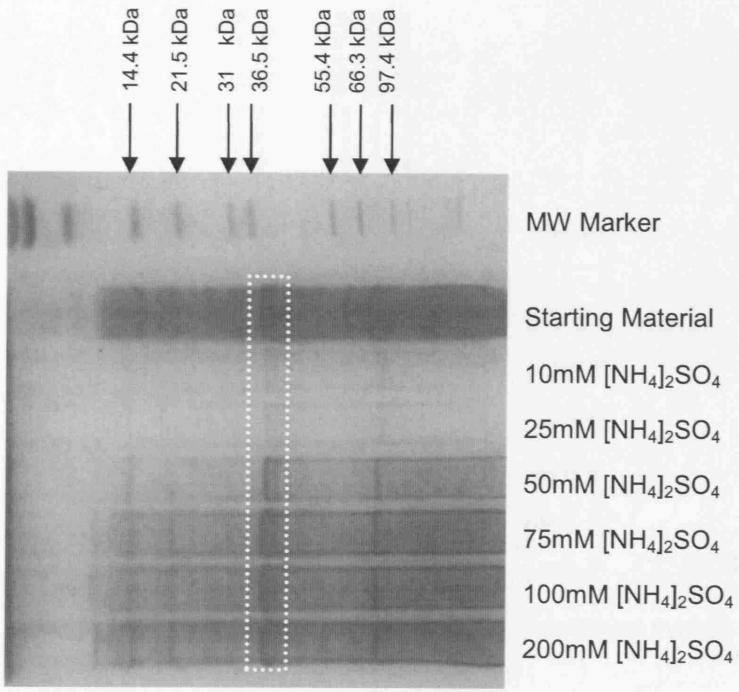

Figure 4.7 Ionic precipitation of the outer membrane proteins from *N. lactamica* OMVs. The dashed box represents the location of the outer membrane protein, PorB. Biomass produced by *N. lactamica* 2 L fermentation (Section 2.3.3) and ammonium precipitation conducted as in Section 2.4.4. SDS-PAGE analysis performed as described in Section 2.6.9.

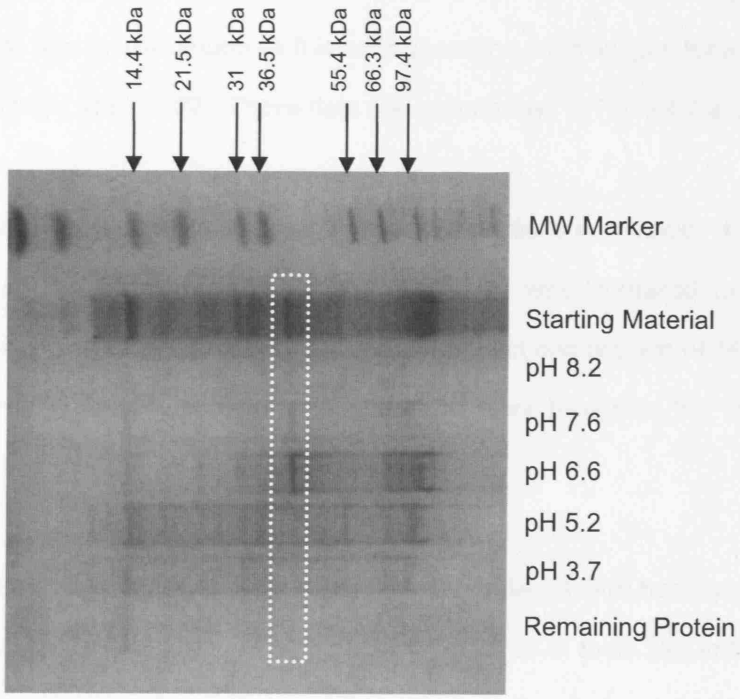

Figure 4.8 Iso-electric precipitation of the outer membrane proteins from *N. lactamica* OMVs. The dashed box represents the location of the outer membrane protein, PorB. Biomass produced by *N. lactamica* 2 L fermentation (Section 2.3.3) and iso-electric precipitation conducted as in Section 2.4.4. SDS-PAGE analysis performed as described in Section 2.6.9.

4.5 Overall downstream process mass balance

Based on each of the downstream processing routes outlined in Figure 4.1, the final product compositions were evaluated and the process efficiencies calculated. This was accomplished by combining BCA total protein assay data (Section 2.6.4) with SDS-PAGE gel densitometry (Section 2.6.9) to evaluate the total amount of PorB entering and leaving each stage. PorB was focused upon as it is considered the main antigen for a Meningitis B OMV vaccine (Wright *et al.* 2002). These data are summarised in Table 4.4 and Figure 4.9.

Route (A), which represents the normal Fredriksen purification method, achieved 22% PorB recovery in the first ultra-centrifugation step. This was increased to 62% in the second ultra-centrifugation step and attained a final product composition of 14% PorB, 7% Rmp and 4% NspA. These percentage compositions were based on the UCF2 – Final Product lane in the SDS-PAGE gel shown in Figure 4.9.

Route (B), where resuspended vesicle recovery was replaced with homogenisation also underwent the same two step ultra-centrifugation process as in route (A). In this instance, PorB recovery was increased to 76% in the first ultra-centrifugation step and to 86% in the second ultra-centrifugation step. This resulted in a final product composition of 21% PorB, 6% Rmp and 1% NspA.

Route (C), which was similar to route (B), replaced the first ultra-centrifugation step with iso-electric precipitation. Iso-electric precipitation increased PorB capture from 76% to 89% when compared with route (B). This was followed by an ultra-centrifugation step which recovered 71% of all the PorB entering the step. The effect of which was a final product composition of 26% PorB, 8% Rmp and 2% NspA.

PorB Step Recovery	Route (A) Ultra-centrifugation1	Route (B) Ultra-centrifugation 1	Route (C) Iso-electric precipitation
Initial (μg mL^{-1})	16034	92002	1702
Discard (μg mL^{-1})	12557	22393	185
Retained(μg mL^{-1})	3477	69609	1517
Lost (w/w)	78%	24%	11%
Recovery (w/w)	**22%**	**76%**	**89%**
	Ultra-centrifugation 2	Ultra-centrifugation 2	Ultra-centrifugation
Initial (μg mL^{-1})	732	25430	1772
Discard (μg mL^{-1})	277	3625	508
Retained(μg mL^{-1})	454	21804	1263
Lost (w/w)	38%	14%	29%
Recovered (w/w)	**62%**	**86%**	**71%**
End Product Composition	Route (A)	Route (B)	Route (C)
PorB	14%	21%	26%
Rmp	6.9%	6.1%	7.8%
NspA	4.3%	1.1%	1.8%

Table 4.4 Summary table showing the final purification mass balance, based on PorB recovery for the various downstream processing routes shown in Figure 4.1. Each purification step shows the efficiency of PorB capture expressed as a precentage based on the amount of PorB entering the step minus the amount of PorB lost. The end product composition shows the relative amounts of the three membrane proteins present in the final product. Biomass produced by *N. lactamica* 2 L fermentation (Section 2.3.3) and downstream processing conducted as in Sections 2.4.1, 2.43 and 2.4.4. SDS-PAGE analysis performed as described in Section 2.6.9.

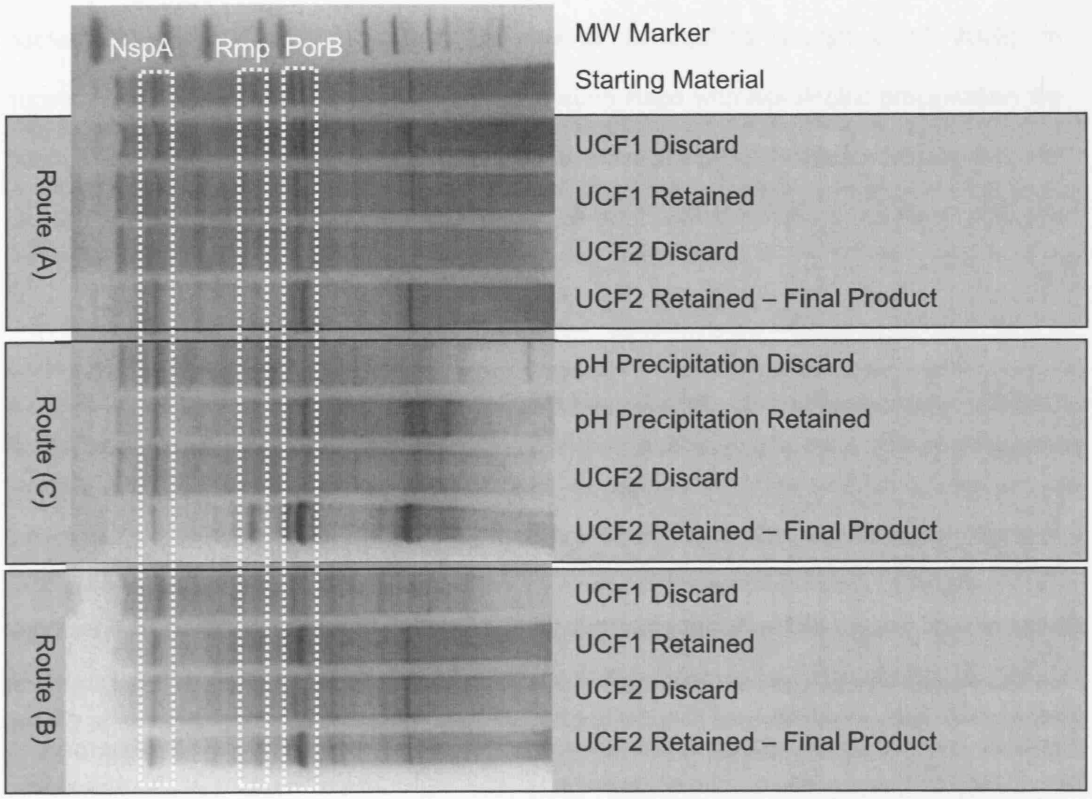

Figure 4.9 SDS-PAGE of the final purification streams, routes A, B and C. As illustrated in Figure 4.1, the first ultra-centrifugation (UCF) step was replaced with iso-electric precipitation in route B. The three main OMV proteins of interest are highlighted. Each well was loaded with 15 µg total protein.

In comparing route (A) with route (C), the final percentage composition of PorB and Rmp have been increased by 87% and 13% respectively. However, the NspA content was reduced by 59%. However, this may not be a setback as it is believed that the main vaccine antigen is PorB, purified recombinant forms of which have been used to induce a bactericidal immune response against *Neisseria meningitidis* (Wright *et al.* 2002). In summary, by replacing one of the ultracentrifugation steps with iso-electric precipitation the overall recovery the OMVs has been improved, increasing the PorB content of the final product and reducing the processing time by two hours when compared to the Fredriksen method (Route (A)).

4.5.1 DNA contamination

Before any vaccine can be released for use, it must undergo characterisation and quality control (MHRA 2002). Part of this control is the evaluation of host derived DNA in the final vaccine. For the Folkehelsa OMV vaccine the acceptable range of DNA in the final vaccine is 0.16 – 0.5 µg per 100µg of protein. This same constraint is assumed to apply here for outer membrane protein vaccines for *Neiseria meningiditis* serogroup B infection as they belong to the same vaccine class. Figure 4.10 illustrates the amount of DNA visible in the final product, prior to sterile filtration for each of the process routes investigated. Route (A), the Fredriksen method had 0.64 µg DNA per 100 µg protein, slightly outside the Folkehelsa limit. Route (B), which included homogenisation had more then ten times the amount of DNA of route (A) at 7.45 µg DNA per 100 µg protein. However, route (C), which included both homogenisation and iso-electric precipitation only had 0.11 µg DNA per 100 µg protein. These results demonstrated that the iso-electric precipitation step was effective in precipitating the target proteins of interest while excluding the contaminant DNA, which remained in solution.

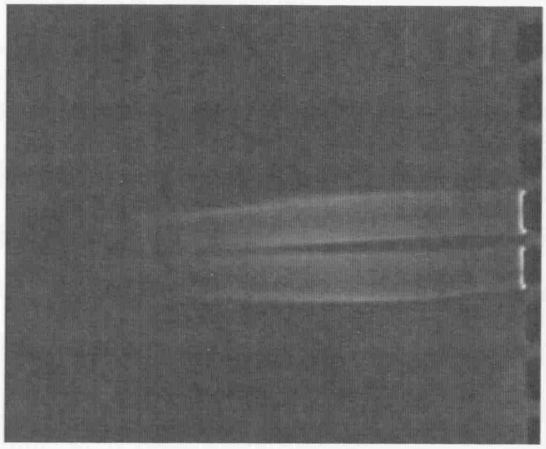

Figure 4.10 DNA quantification of the final vaccine formulation. In the Folkehelsa OMV vaccine the acceptable range of DNA in the final product was between 0.16-0.5µg of DNA per 100µg of protein. The DNA present in the final purifcation routes as described in Figure 4.1 was quantified as described in Section 2.6.16.

4.6 End Product Sterilisation

4.6.1 Sterile filtration of outer membrane vesicles

Sterilisation of the original Folkehelsa OMV vaccine was achieved by the addition of the mercury based preservative, thimerosal (Fredriksen *et al.* 1991). Its inclusion is now discouraged because of the potential harm from mercury and so is now removed from all childhood vaccines as a precautionary measure (www.fda.gov/cber/vaccine/thimerosal.htm). Consequently, for the *N. lactamica* Meningitis B OMV vaccine filtration through a 0.22µm membrane was chosen as the preferred method of sterilisation (MHRA 2002). However, the OMVs were found to form large aggregates which made the filtration step very difficult. Figure 4.11 shows the particle size distribution of OMVs formulated in a 3% (w/v) sucrose solution, as in the Fredriksen method. This shows 95% of the OMVs formed aggregates larger then 0.22 µm. This figure increased to 98% when the sample was freeze thawed. Approximately 65% (w/w) product loss occurred in this final sterilisation step, which indicated that at least some of the smaller aggregates could be forced through the filter.

4.6.2 Valency affects vesicle aggregation

Aggregation is a common problem in many biological systems, including membrane vesicles, and in order to investigate these phenomenon further experiments were performed to study OMV aggregation based on Derjaguin, Landau, Verwey and Overbeek (DLVO) theory. DLVO theory has been widely used to predict the interaction of colloidal particles, but its application to biological systems has been limited thus far. DLVO theory is the interplay between repulsive electrostatic forces and attractive van der Waals forces. These forces have a short range less than 15nm, and are based on non-specific interaction.

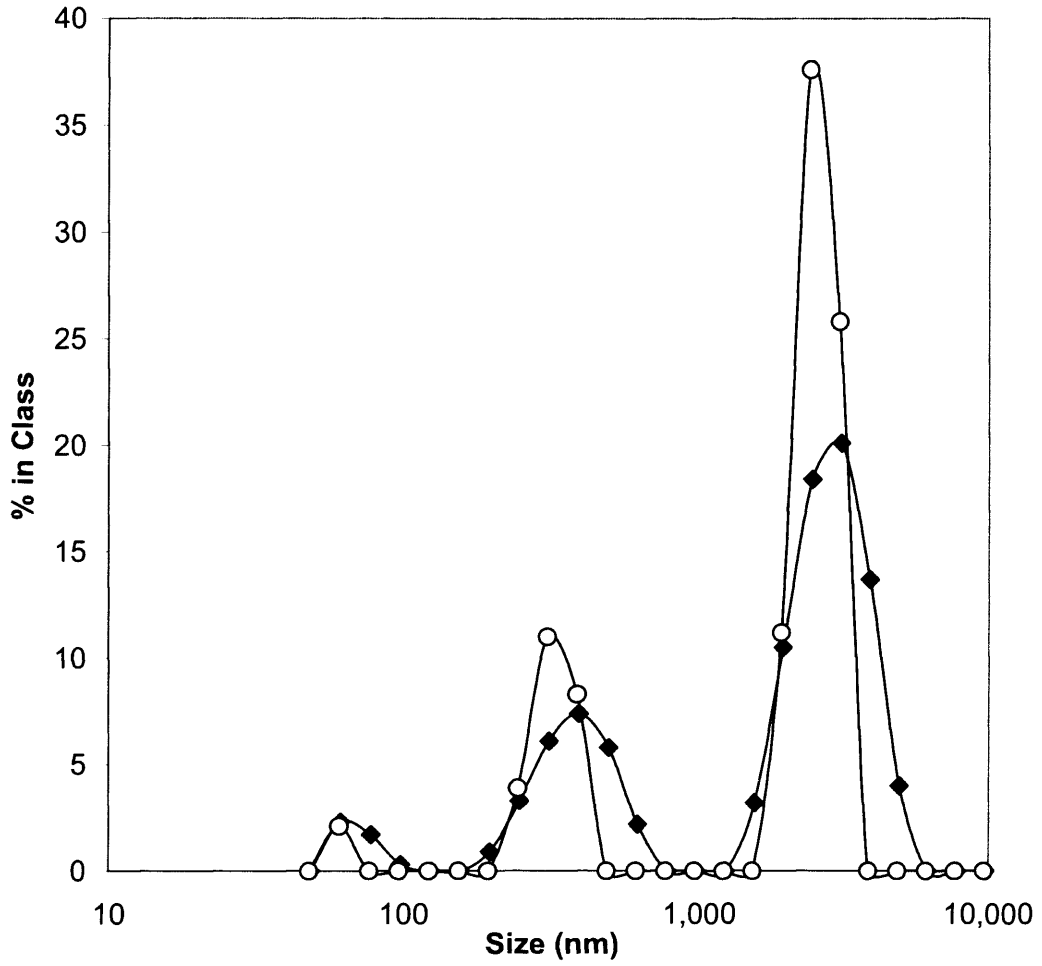

Figure 4.11 Particle size distribution of OMVs formulated in 50 mM Tris-HCL with 3% (w/v) sucrose: (◆) normal OMV sample (○) freeze thawed OMV sample. OMVs prepared as described in Section 2.4.1. Particle size analysis conducted as described in Section 2.6.11.

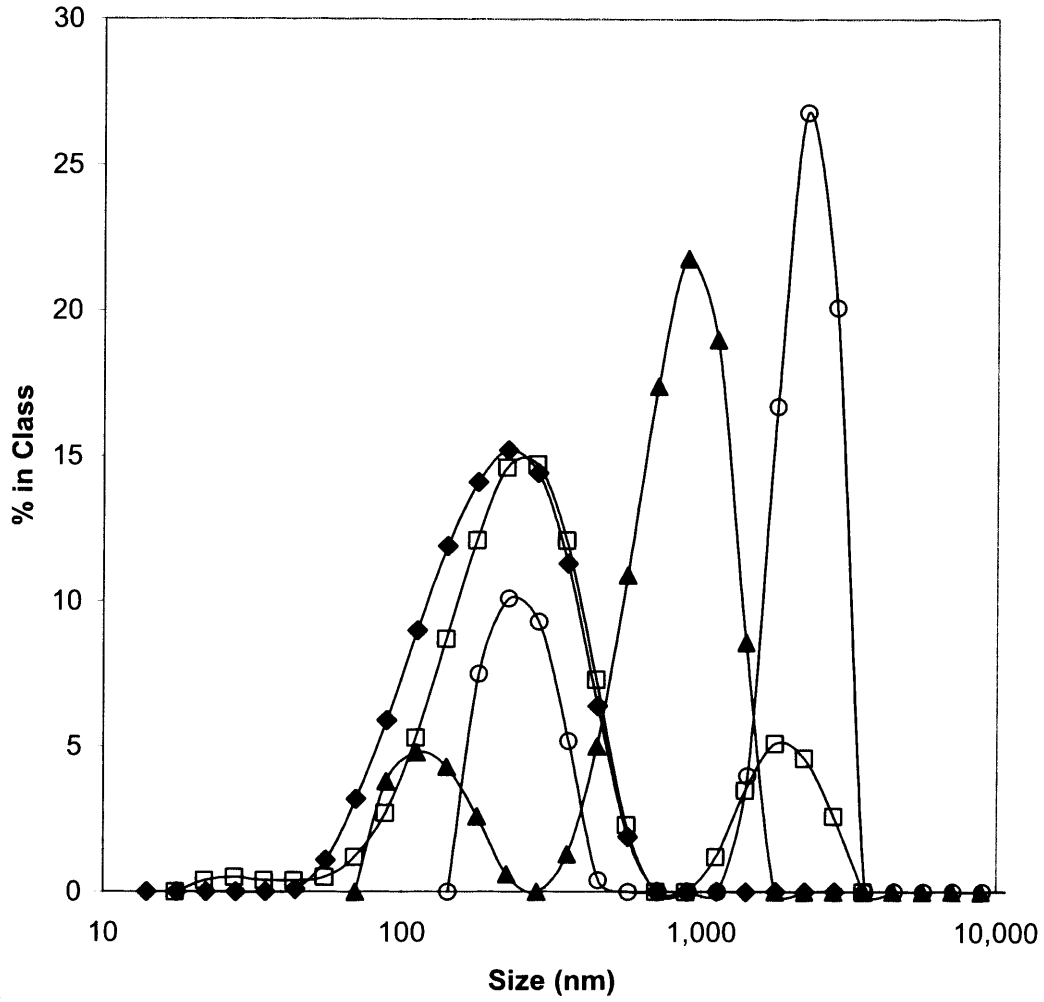

Figure 4.12 Particle size distribution of OMV formulated in differing salt solutions all of 1.0mM concentration: (○) magnesium chloride, (▲) calcium chloride, (□) sodium chloride, (◆) lithium chloride. OMVs prepared as described in Section 2.4.1. Particle size analysis conducted as described in Section 2.6.11.

One of the main predictions of DLVO theory is the influence of valency on aggregation. Figure 4.12 shows the average particle size distribution of the OMVs in different salts, all at the same salt (1 mM) and vesicle concentrations (500μg mL^{-1}). Within the four particle size distributions there seems to be two distinct size groups, those with peaks below 1,000nm and a second group above 10,000nm. The differences between these two groups can be put down to the valency of the cation causing a shift in the surface charge of the vesicle. This is consistent with DLVO theory. The ability of divalent cations in biological membrane systems to reduce repulsive force has been well characterised (Marra 1986), however sometimes the presence of divalent ions can make OMVs more attractive then DLVO theory can account for, (Khan *et al.* 1985), which may explain why magnesium and calcium chloride caused the vesicles to flocculate. In this case it is seen that both sodium chloride and lithium chloride were able to produce OMV preparations with the lowest size distributions. However, the use of lithium chloride is undesirable in vaccine formulation due to its chemically irritant nature (lithium chloride MSDS); consequently sodium chloride was selected for subsequent experiments.

Figure 4.13 shows the effect of decreasing NaCl ionic strength on the particle size distribution. By reducing the salt concentration it is possible to shift the size distribution so that 75% of the OMVs has a particle diameter below 0.22μm. Once again, this was consistent with DLVO theory. By reducing the salt concentration the repulsive electrostatic forces were increased by increasing the Debye length. The Debye length is a measure of the diffuse layer surrounding each vesicle. By increasing the size of the diffuse layer the vesicles will tend to repel each other at longer distances. Therefore, in order to minimise OMV aggregation a low salt concentration should be used with a small monovalent cation.

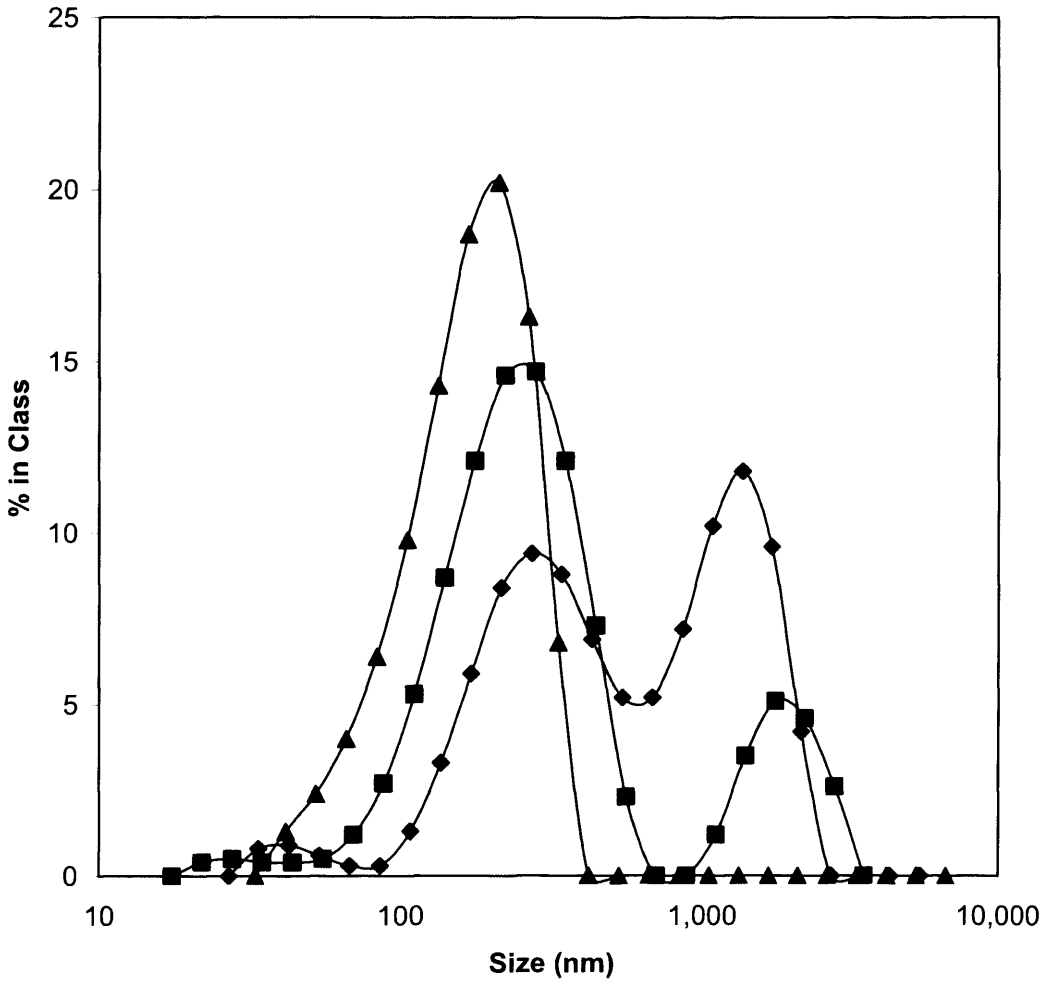

Figure 4.13 Particle size distribution of DOMV samples formulated in NaCl of varying concentration: (◆) 10mM, (■) 1.0mM, (▲) 0.1mM. OMVs prepared as described in Section 2.4.1. Particle size analysis conducted as described in Section 2.6.11.

4.6.3 Entropic nature of electrostatic interactions

Most of the experiments performed have so far focused exclusively on cation selection. It was also important to consider the anion as well. In Figure 4.14 it is observed that as the size of the anion increased the average OMV diameter also decreased. In order to understand why this is so, the nature of the repulsive electrostatic interaction was considered. If sodium chloride salt were added to the OMV preparation suspended in water, the salt would dissociate from its crystalline structure and the entropy of the system be increased. The positive sodium salts would be drawn towards the negatively charged surface of the vesicles, while the chlorine ions would move into the bulk solution, even though attractive Coulombic forces attempt to pull them back (Israelachvili 1991). On bringing two vesicles together, the chlorine ions would effectively be forced to combine with the sodium ion surface against their preferred equilibrium state, which is favoured Coulombically but not entropically, thus resulting in a net repulsive force (Israelachvili 1991). Therefore, it is hypothesised that increasing the anion size would enhance the repulsive forces by making it further entropically unfavourable for OMVs to aggregate. In this case, the return of further aggregate size reduction diminished beyond nitrate.

4.6.4 Final sterile filtration conditions

Based on the results in Section 4.6.2 and 4.6.3, in order to minimise aggregation of OMV preparations, it is important to use a very low ionic strength formulation coupled with a monovalent salt with a relatively large anion. This is confirmed by the post filtration recovery data shown in Table 4.5. The original formulation in 3% sucrose results in only 35% (w/w) transmission through a hydrophilic 0.22μm cellulose acetate membrane. However, using a low monovalent salt of increasing anion size has the effect of increasing membrane transmission to a maximum of 80% (w/w) when using 0.1mM sodium citrate, which is a GRAS (Generally Recognised As Safe, FDA, Code of Federal Regulations, Chapter 21) reagent that can be used in vaccine formulation.

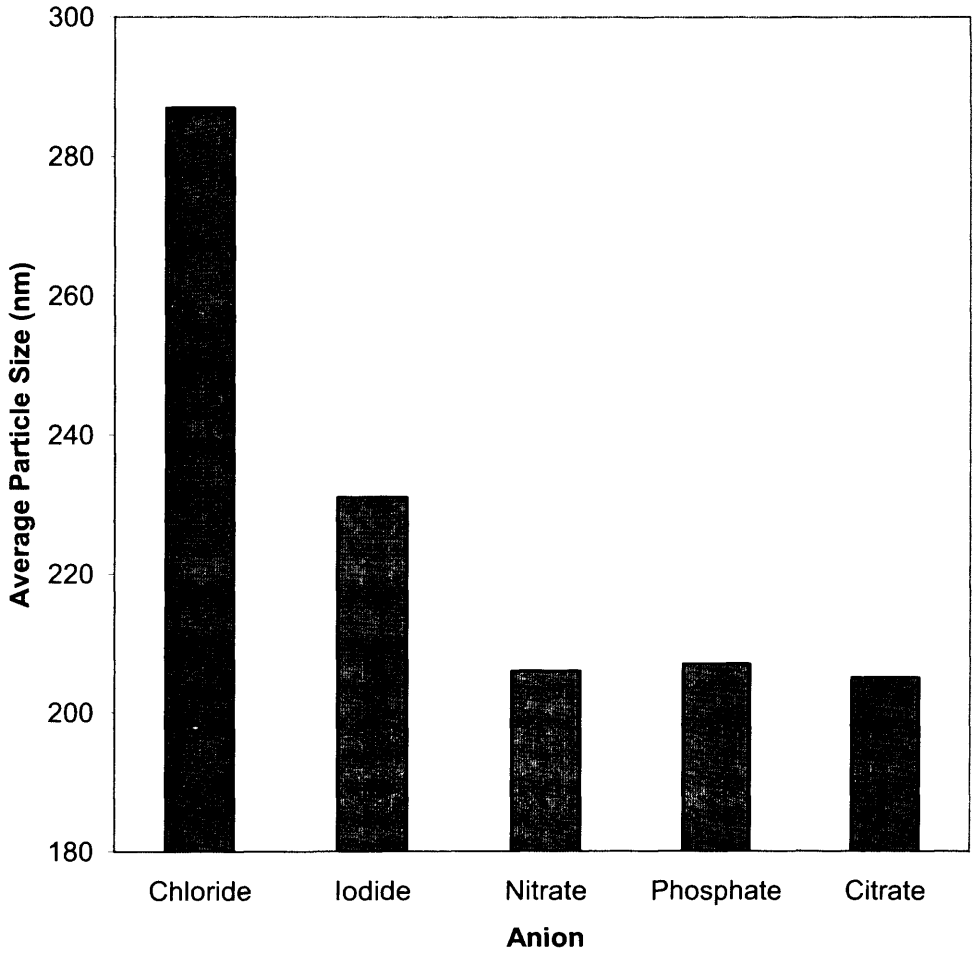

Figure 4.14 The influence of anions on mean OMV particle size. The average particle size was measured in different 0.1mM sodium salts. The general effect observed was as the anion size increased, the average particle size decreased. OMVs prepared as described in Section 2.4.1. Particle size analysis conducted as described in Section 2.6.11.

Formulation	OMV Recovery (%) (w/w)
50mM Tris -HCl 3% sucrose	35
0.1 mM Sodium chloride	72
0.1 mM Sodium iodide	73
0.1 mM Sodium nitrate	76
0.1 mM Sodium phosphate	77
0.1 mM Sodium citrate	78

Table 4.5 Influence of *N. lactamica* OMV formulation on transmission through a 0.22µm cellulose acetate syringe filter. OMVs prepared as described in Section 2.4.1 and formulated as above. Filtration performed as described in Section 2.4.5 and recovery based on measurement of total protein present before and after filtration, measured using the BCA assay (Section 2.6.6).

4.7 Summary

Most of the experiments conducted in this study used a microwell format, either in 96-well or 24-well microtitre plate, creating a platform technology. There were limitations to the capabilities of the micro-scale platform as it was not possible to conduct experiments relating to centrifugation in microtitre plates. However, new rotors are now arriving on the market for the centrifugation of microtitre plates, thus even these experiments could be transferred onto the micro-scale platform. In this case, for protein precipitation, only 10 µL per sample were required for each well in SDS-Page and 100 micro-litres for the microplate BCA protein assay. The extensive use of the microwell platform means that the entire process could easily be automated using robotic liquid handling systems, such as the Tecan Genesis FE 500^{TM} and with the use of a vacuum manifold, it is now possible to screen for different membranes and buffer conditions using the microwell foot print (Jackson *et al.* 2006). This undoubtedly would increase throughput and reduce costs, though it is important to devise experiments with care, as the measure of success for high throughput screening lies in the number of positive results obtained rather then the throughput volume.

DLVO theory was not a new concept in itself as it has been traditionally associated with colloids and emulsions. Its application into biological sciences has been limited for two reasons, the first was limited understanding of the topic itself by biologists, but the second was its limited application to biological systems. There are four main forces which occur in colloidal systems which are further sub-divided into long and short range forces. The long range forces are attractive van der Waals forces and repulsive electrostatic forces; hydration forces and steric forces constitute the short range forces. The interplay of the attractive and repulsive long range forces constitute DLVO theory, which is understood very well. The short range forces are less understood and essentially must be determined empirically for any novel system. However, in most biological system, van der Waals

forces are fairly weak to have any major significance, especially in high salt concentrations. Although, their effect was seen in low salt concentrations, it is the electrostatic repulsions that have to be enhanced to prevent aggregation, a theory that is reasonably understood. But it was important to realise that this theory has a certain selectivity regarding its application as it cannot be universally employed. DLVO theory was used to predict non-specific interactions based on charge, size and distance (Section 4.6.2). It cannot be applied to systems which have a high degree of specific interactions, otherwise known as protein-protein interactions. Therefore, there is certain degree of empiricism to be utilised in determining whether or not DLVO theory is suitable.

As stated in the introduction the improvement of the vaccine production method was sought with the use of ultra scale down tools and utilising a micro-scale platform; effectively minimising the sample volume used to conduct the experiments described in this chapter. This has been achieved and, more over, addressed the four key process issues highlighted earlier. *Primary recovery* was improved upon with the use of ultra scale down, which allowed the selection of an appropriate continuous centrifuge and alluded to its operating conditions (Section 4.2). *Vesicle recovery* was discovered to be already efficient at 88 % recovery, but could be further increased to 95 % by applying a short amount of high shear attained through homogenisation (Section 4.3). The time spent using *ultra-centrifugation* has been halved by replacing the step with iso-electric precipitation (Section 4.4), a scalable operation which also reduced the DNA contaminant in the product stream (Section 4.5.1). Finally, with DLVO theory it has been possible to minimise aggregation and so increase membrane transmission of the OMVs from 35 % to 80 % through a 0.22µm filter (Section 4.6.4).

In summary the *N. lactamica* fermentation studies described in Chapter 3 and the related downstream processing studies described here demonstrate the potential for micro-scale processing methods to be applied to vaccine process creation. Although verification of the

pilot scale operating condition determined in Table 4.1 for the Carr Powerfuge™ was not conducted the method itself is well understood and has previously been verified in numerous experiments (Boychyn *et al.* 2004;Maybury *et al.* 1998;Salte *et al.* 2006). The methods described here have the potential to be applied to other pharmaceutical processes and may be essential to reduce the time a vaccine spends in development thus reducing its cost to the consumer.

5 Micro-scale Process Application: Investigation into the growth kinetics and antigen production of *B. anthracis*

5.1 Introduction

In the previous two chapters a micro-scale approach has been established and utilised to investigate and optimise a process route for a vaccine that is still in early development phase. In this chapter the micro-scale platform approach is applied to an already existing and indeed well established process in order to increase our understanding of anthrax vaccine production.

As described in Section 1.3, microwell systems and microtitre plates have already been widely used in analytical and high throughput screening applications (Devlin 1997). The challenge here is to develop a micro-scale platform which would confer the many benefits of high throughput screening with scale-up predictability with specific application to the current UK anthrax vaccine. The quality of data attained combined with the small amount of material required makes microwell plates particularly suited for experimentation on Advisory Committee on Dangerous Pathogens (ACDP) Class 3 pathogens. The small foot print of microwell systems means that they can easily fit within an isolator or cabinet. Reducing the experimental volume to a few millilitres also allows for safer experimentation. Furthermore, their ability to fit within existing facilities means that they require no additional capital investment, thus can be considered an inexpensive method of bioprocess creation.

The current UK anthrax vaccine is based on the static fermentation of *B. anthracis* Sterne $34F_2$ in 500 mL glass Thomson bottles (Charlton *et al.* 2007). It uses a partially defined

medium which contains activated charcoal and has been used clinically for over 40 years and licensed in 1979. Due to the restrictions of the license, there has been little process modification and consequently there is limited process understanding. Furthermore, observations have been made of the process (Dr. S. Charlton, Health Protection Agency, personal communication). For example, in some production runs there have been reports of surface pellicle formation. Any disturbance to this pellicle caused the bacteria to cease antigen production. Secondly there is the requirement of charcoal in the media. It was known that the absence of charcoal resulted in poor growth and antigen production, but the precise role of charcoal had yet to be ascertained. The charcoal may serve one of several functions; it could be a nutrient sink, it may absorb harmful waste products or it may be a growth scaffold linked to surface pellicle formation. These are all hypotheses that require further investigation.

5.1.1 Quorum Sensing and cell resuscitation

The formation of a surface pellicle or more accurately a biofilm may indicate that the bacteria are communicating via quorum sensing (De Kievit *et al.* 2001). It is known that bacteria are capable of intercellular communication in order to co-ordinate a response to an environmental stimulus. The basis of this intercellular communication is through the self-generation of small signalling molecules called auto-inducers. Through auto-inducers, bacteria can regulate their behaviour according to population density (de Kievit and Iglewski 2000). Quorum sensing relies on the principle that when a single bacterium releases auto-inducers into the environment their concentration is too low to be detected. However, when sufficient bacteria are present a threshold level is reached allowing the bacteria to detect a critical cell mass and activate or repress certain genes (Miller and Bassler 2001). Several classes of autoinducers have been identified. Auto-inducer class 1 (AI-1) are known to be N-acyl-homoserine lactones in Gram negative bacteria (Bassler 1999). In Gram positive bacteria, such as *B. anthracis*, they are usually small peptide chains detected by a histidine kinase receptor (Kleerebezem *et al.* 1997;Lazazzera and

Grossman 1998). Auto-inducer class 2 (AI-2) molecules have been found in both Gram positive and Gram negative bacteria (Bassler *et al.* 1994;Surette *et al.* 1999). AI-2 molecules are a product of the LuxS gene (Schauder *et al.* 2001) and have been shown to control the response of several genes in *Vibrio harveyi*, (Henke and Bassler 2004;Lilley and Bassler 2000). Quorum sensing can also be inhibited using halogenated furanones such as fur-1. Fur-1 or *(5Z)*-4-bromo-5-(bromomethylene)-3-butyl-2*(5H)*-furanone, has been reported to inhibit AI-2 mediated quorum sensing systems in *Escherichia coli* and *V.harveyi* without affecting bacterial growth (Ren *et al.* 2001). Conversely, Jones *et al* have recently demonstrated the inhibition of *B. anthracis* growth using the quorum sensing inhibitor fur-1 (Jones *et al.* 2005).

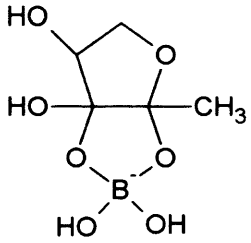

AI-2

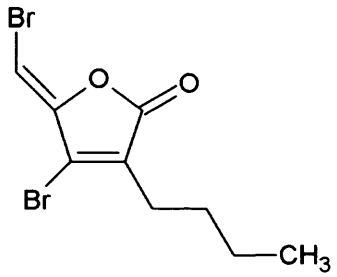

Fur-1

Figure 5.1 The proposed structure of the auto-inducer 2 molecule, (AI-2) and the quorum sensing inhibitor halogenated furanone, *(5Z)*-4-bromo-5-(bromomethylene)-3-butyl-2*(5H)*-furanone, (fur-1). The AI-2 molecule and fur-1 directly compete to bind to the LuxPQ receptor, thus categorising fur-1 as a quorum sensing inhibitor (Jones *et al.* 2005).

It should be noted that quorum sensing is not normally associated with cell growth and so another bacterial cytokine was resuscitation promotion factors (Rpf's). Rpf's are quorum sensing independent utilising different genes (Tufariello *et al.* 2004). They do not depend upon cell density but act rather as bacterial cytokines which enhance the cultivability of the cell (Keep *et al.* 2006). Their importance has been demonstrated in several other species, such as *Micrococcus luteus* and *Mycobacterium tuberculosis* (Mukamolova *et al.* 2006;Zhu *et al.* 2003). Genetic analysis has indicated that *B. anthracis* may share a common genetic lineage with other bacteria with Rpf's. Putative evidence has suggested that one possible Rpf may be a murolytic enzyme of approximately 17kDa (Mukamalova *et al.* 1998).

5.1.2 Aim and objectives

The aim of this chapter is to apply the microwell fermentation approach described in Chapter 3 to increase the understanding of the main factors that contribute to efficient *B. anthracis* growth in Thompson bottles. Since the vaccine is manufactured in static culture the agitation and scale-up principles described in Chapter 3 are not required here. The specific objectives of this chapter are:

- To establish microwell culture for *B. anthracis* that mimics growth and antigen production in static Thompson bottle cultures.

- To investigate the effects of the culture medium and the main factors which enhance *B. anthracis* growth and antigen production using the experimental microwell DOE techniques described in Chapter 3.

- To apply the microwell platform to investigate the presence of intercellular signalling pathways

5.2 Micro-scale B. anthracis cell culture conditions

5.2.1 Microwell and Thompson bottle culture kinetics

As described in Section 5.1.3 the first objective was the use of microwells as mimics of the physiological condition *B. anthracis* experienced during normal vaccine production. It is important to first demonstrate the comparability of microwell and Thompson bottle cultures under static conditions, requiring the same cell growth and antigen production kinetics. The Thompson bottle data used were produced by the Health Protection Agency. Figure 5.2 shows the close correlation between *B. anthracis* growth in microwells and Thompson bottles. Over the twenty-eight hour period, both cultures have a lag phase of approximately eight hours before entering an exponential growth phase. By the twenty-fifth hour both cultures have entered stationary phase. The maximum growth rate of Thompson bottles between eight and 18 hours is $6x10^5$ cfu mL^{-1} hr^{-1}; in microwells the equivalent growth rate is $2x10^6$ cfu mL^{-1} hr^{-1}. Figure 5.3 shows the corresponding antigen expression in both culture systems and again reveals close similarity of Thompson bottle and microwell antigen expression levels. Protective Antigen (PA) expression was first detected at 12 hours in microwells instead of the 16 hours seen in Thompson bottles but this may be explained by the slightly increased inoculum and biomass production seen in microwells. The specific antigen yield per colony forming unit in Thompson bottles and microwell is $8x10^{-6}$ and $3x10^{-6}$ µg cfu^{-1} respectively.

5.2.2 Analysis of microwell plate well to well variability

To provide confidence in the microwell data presented in Figure 5.2 it is important to check that the method was not biased based on well position. This is especially important as each well was to be sacrificed sequentially to generate a time course data shown in Figure 5.2. Therefore *Bacillus cereus* was used as a reporter strain to check that the outer wells of the microwell plate did not favour bacterial growth when compared with the inner wells.

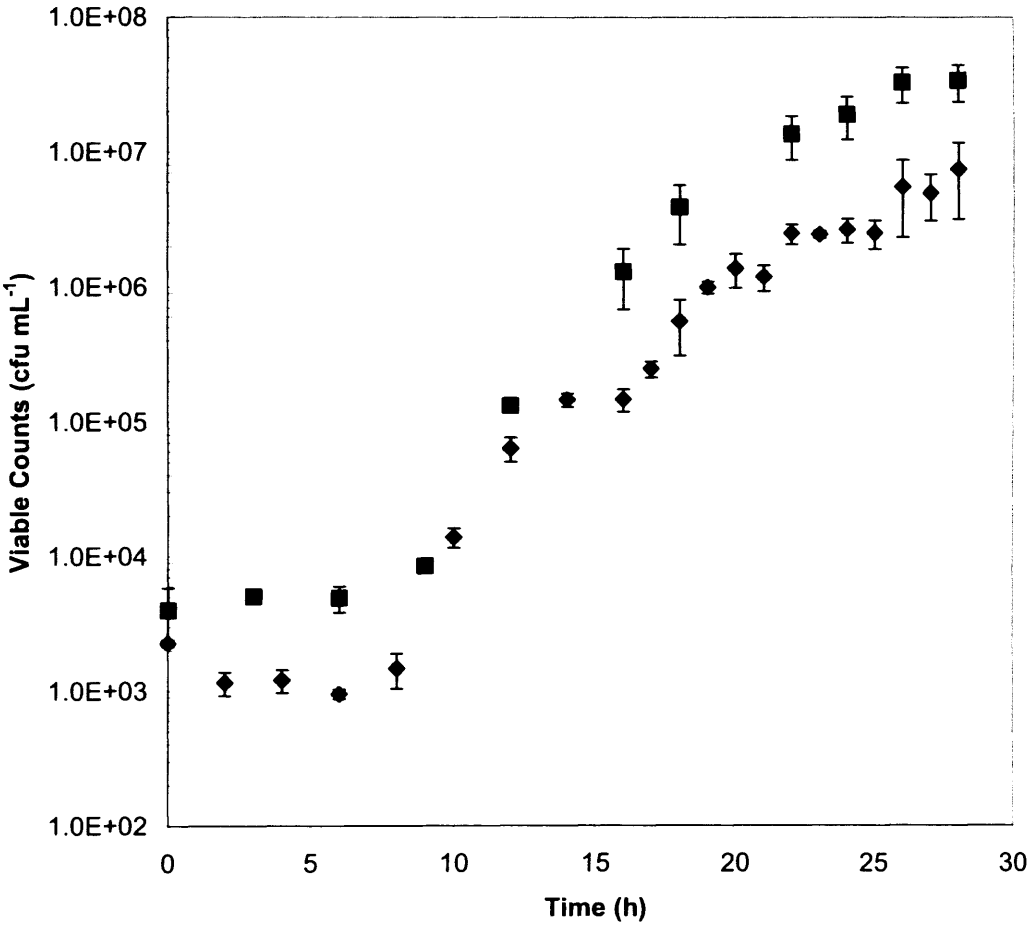

Figure 5.2 *B. anthracis* Sterne $34F_2$ growth kinetics in Thompson bottles and microwell plates: (◆) Thompson bottle, (■) microwell plate. Microwell and Thompson bottle cultures were conducted as described in Section 2.3.6 and 2.3.7 respectively and viable counts determined as in Section 2.6.1. The data represents the average of three independent runs and error bars show one standard deviation about the mean, where n=3. The Thompson bottle data were generously provided by the Health Protection Agency.

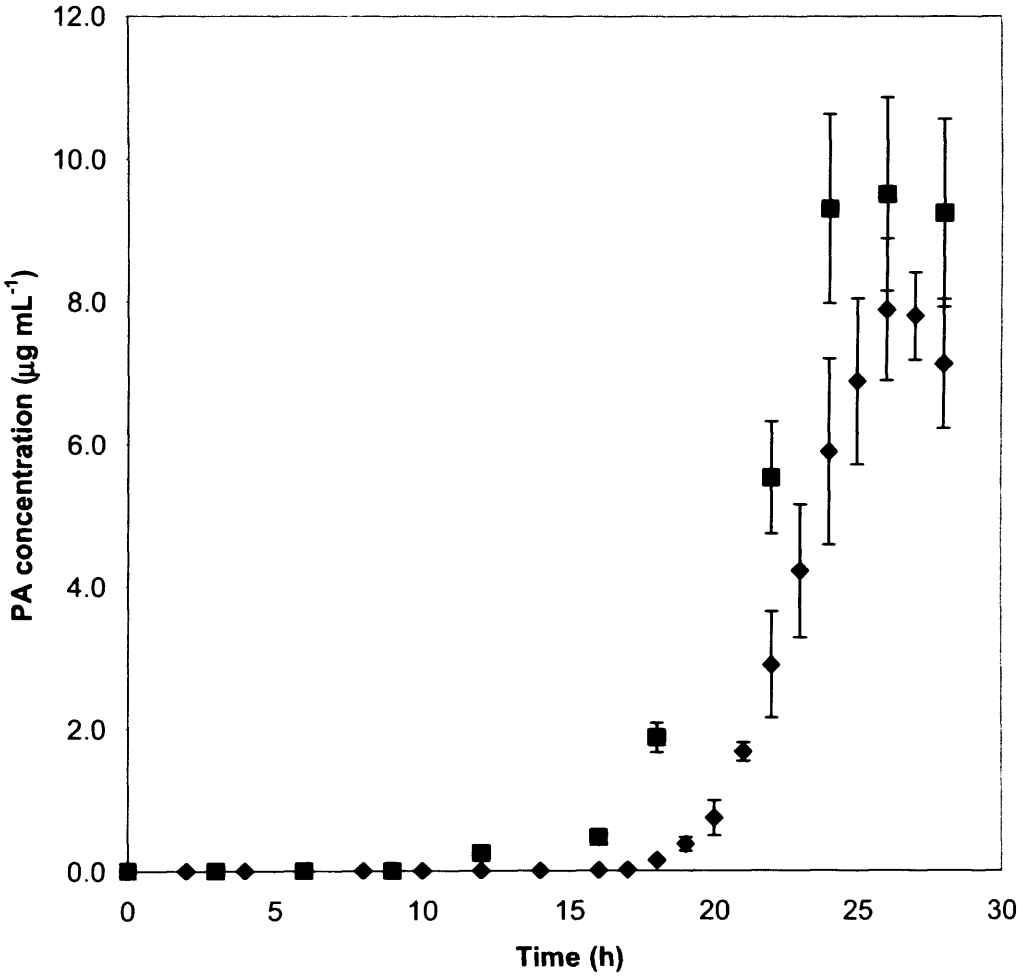

Figure 5.3 PA production in Thompson bottles and microwell plates: (◆) Thompson bottle, (■) microwell plate. Microwell and Thompson bottle PA and LF concentrations were determined as described in Section 2.6.6 and 2.6.7 respectively. The data represents the average of three independent runs and error bars show one standard deviation about the mean, where n=3. The Thompson bottle data were generously provided by the Health Protection Agency.

This was of particular importance as the incubator used for these experiments (Sections 2.3.6, 2.3.7 and 2.3.9.) was rear heated, the hot air circulated with the aid of a fan. Figure 5.4 shows growth profiles generated on different days using the same media and inoculation conditions. The first six hours of growth were monitored and all the growth profiles generated appear to be very similar. The exponential growth rate during this time was calculated and used in a test of equal variance analysis shown in Figure 5.5.

The confidence interval is a range of likely values for the population standard deviation. It is not possible to know the exact value of the population standard deviation so confidence intervals are used as a likely range of values which best describe the population standard deviation based on the sample data (Mathews 2004). The 95% Bonferroni confidence interval allows the determination of the probability that one or more of the confidence intervals failed to describe the population standard deviation to be less then 5%. These confidence intervals are asymmetric because they are based on the chi-squared distribution (Mathews 2004). Two tests are used to determine if the variance is equal, they are the F-test, used when analysing data based on the normal distribution, and Levene's test, used for any continuous data set. Irrespective of the distribution, in both cases a *p*-value greater then 0.8 is recorded which is significantly greater then the error rate of 5% (0.05), demonstrating equal variance. Hence there is no difference between using the inner and outer wells of the microtitre plate.

5.2.3 Analysis of potential evaporation losses

In the previous section it was shown that there was no well-to-well variation from using a sacrificial well approach, (Section 5.2). For such long culture times it is also important to show there is no systemic variation due to evaporation of liquid from each well. Figure 5.6 shows the average percentage volume loss and reveals that a static 12 well microwell plate can lose up to 5.3% in volume over a 24 hour period.

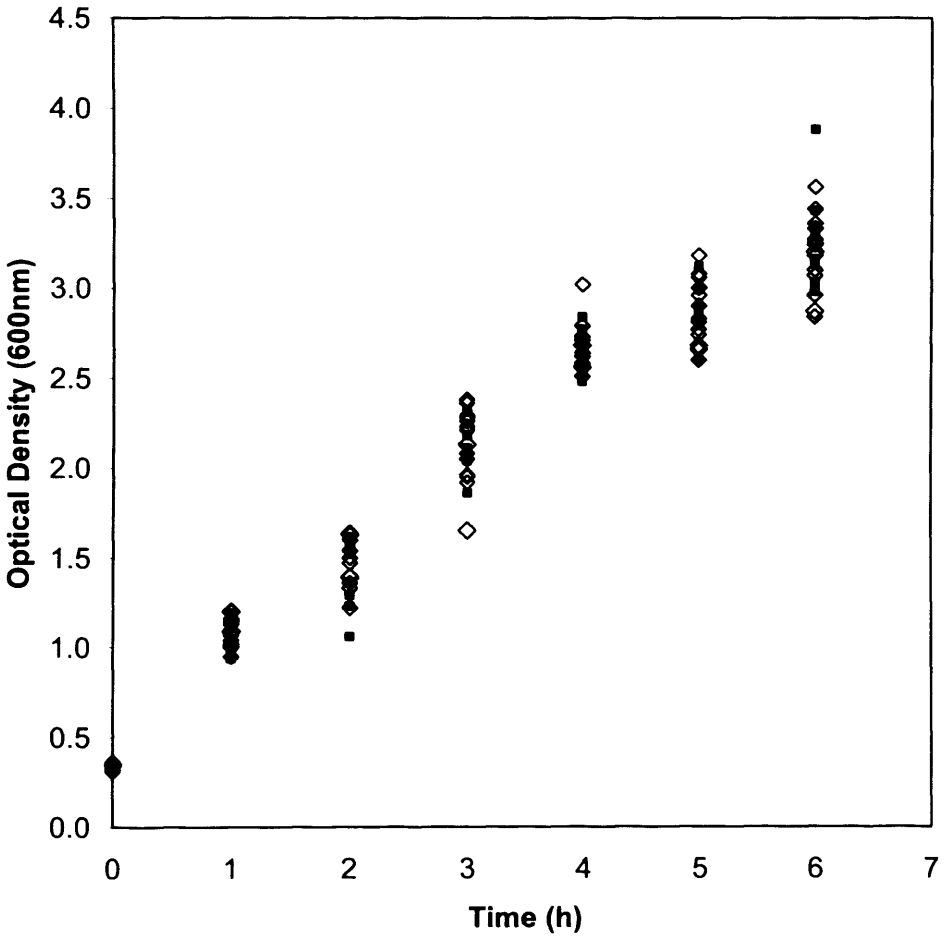

Figure 5.4 Replicate kinetics of *Bacillus cereus* in 12 well microwell plates: (◇) outer wells, (■) inner wells. Experiments performed as described in Section 2.3.9.

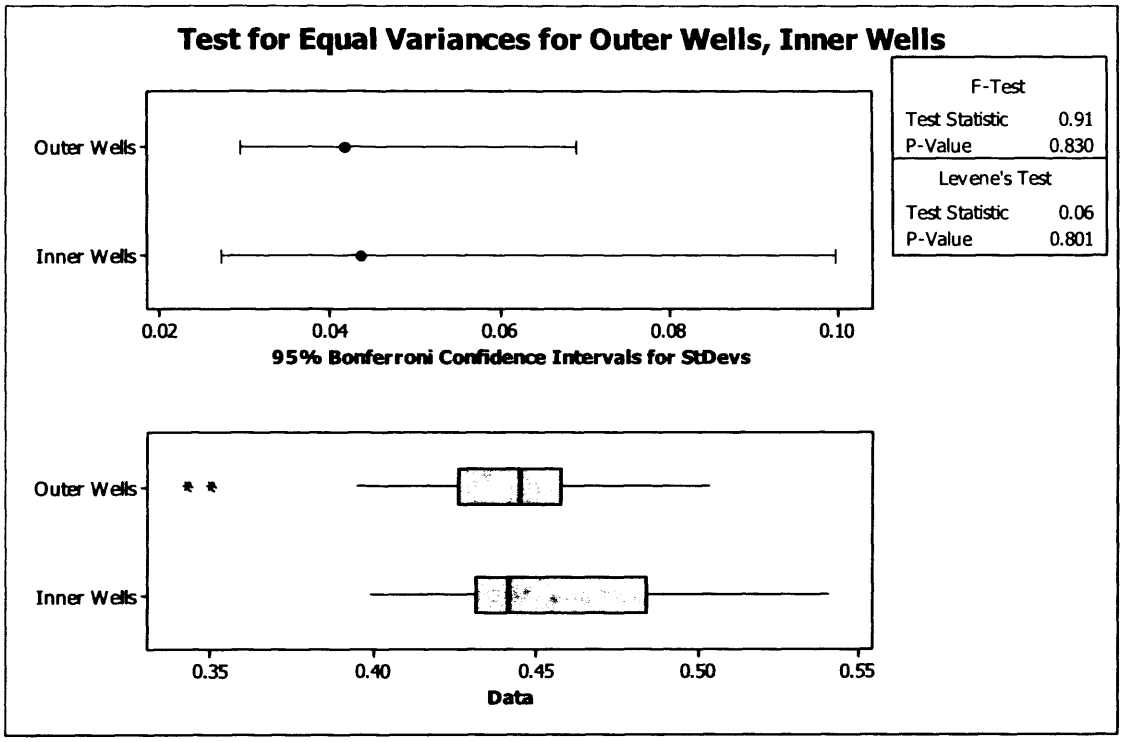


```
95% Bonferroni confidence intervals for standard deviations

              N      Lower      StDev      Upper
Outer Wells  16  0.0295308  0.0416536  0.0690596
Inner Wells   8  0.0272429  0.0435460  0.0997414


F-Test (normal distribution)
Test statistic = 0.91, p-value = 0.830


Levene's Test (any continuous distribution)
Test statistic = 0.06, p-value = 0.801
```

Figure 5.5 Calculation of the Test for Equal Variances. Using a Bonferroni confidence interval of 95% it was observed that the standard deviation of both inner and outer wells were to within 4% of each other with both the lower interval having close similarity. The upper interval is slightly higher in the inner wells however when looking at the significance of this outcome, the F-test and Levene's test indicate this is not a significant variance. The large *p*-value of 0.8 in both cases indicates that the null hypothesis should not be rejected, that the two data sets are of equal variance.

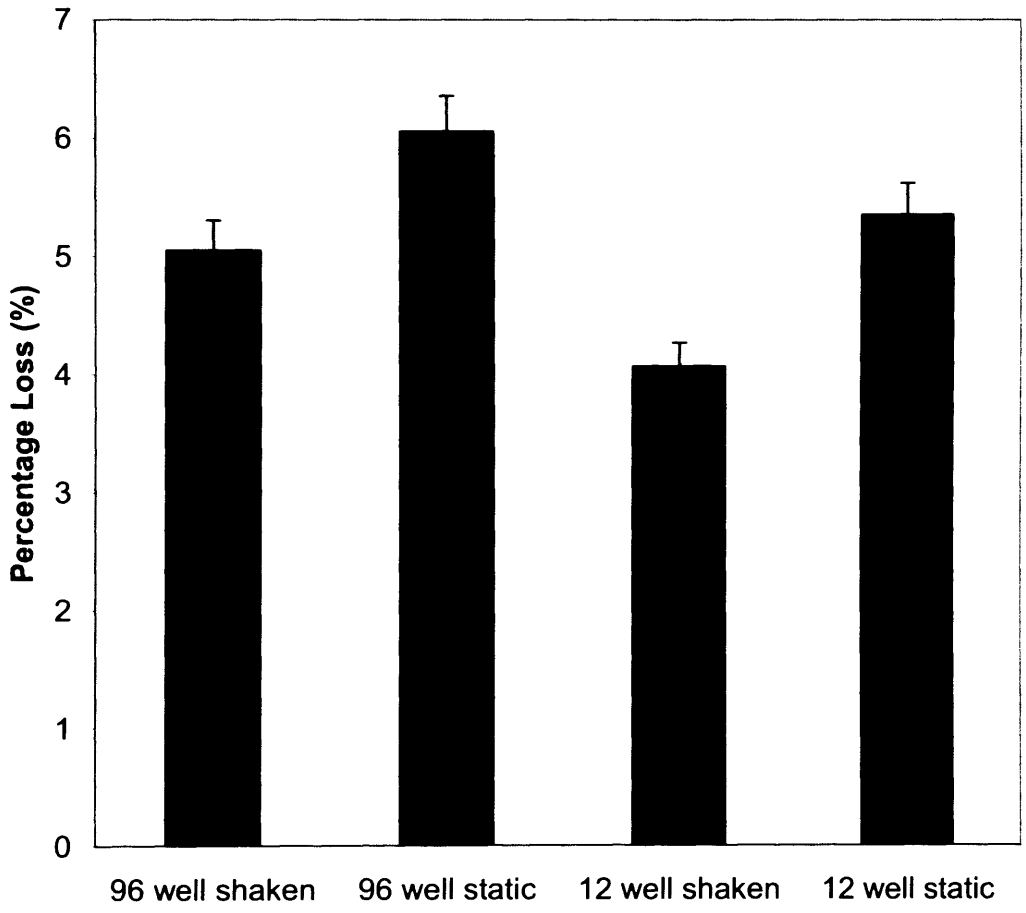

Figure 5.6 The average percentage loss of mass due to evaporation in differing microwell geometries under unshaken and shaken (700rpm) conditions. Experiments were performed using Basal medium over 24 hours. These data are the average of three runs completed on differing days and the error bars represent one standard deviation about the mean.

However, this evaporation error did not have a significant contributory effect on the microwell data and did not detract from the close relationship between the two culture methods described in Section 5.2.1. Hence microwells can be considered satisfactory mimics of the culture system currently used in the vaccine production process.

5.3 Investigation of main factors influencing B. anthracis growth and antigen production

Having established that microwells are satisfactory mimics of static Thompson bottle culture; a 2^4 factorial design experiment was performed. Four factors had been identified for investigation; these were the absence and presence of charcoal, cyclodextrins, agitation (shaking) and high or low inoculum levels. As stated in Section 5.1, previous observations had suggested that agitation, charcoal and inoculum levels might impact on vaccine production and pellicle formation; however, the exact nature this impact takes had yet to be discovered. By monitoring the response of viable counts, protective antigen (PA) and lethal factor (LF) levels, it is possible to detect which factors affect which responses. The rationale for using cyclodextrins was two fold; firstly to evaluate if cyclodextrins could be used to replace charcoal in the media and secondly to help identify the possible role charcoal plays if cyclodextrin substitution was successful. Cyclodextrins have been commonly used in pharmaceutical application to enhance the solubility, stability, and bioavailability of drug molecules (Ghorab and Adeyeye 2001;Loftsson 1998).

Table 5.1 shows the 2^4 experimental design. If all the combinations of factors were to be investigated then this would yield a total of 16 runs per replicate (2^4=16). However, to include more replicates per run a half-factorial experiment was conducted yielding eight runs per replicate (16/2 = 8). Each run order represents a microwell which was subjected to the conditions described in Table 5.1.

		Factors				Responses		
	Run Order	Charcoal (A)	Cyclo-dextrin (B)	Shaking (C)	Inoculum (D)	Viable Count	PA	LF
Replicate 1	1	+1	-1	-1	+1	2590000	3900	750
	2	-1	+1	-1	+1	2480000	920	94
	3	+1	+1	+1	+1	3510000	17	10
	4	-1	-1	-1	-1	230000	1900	290
	5	-1	-1	+1	+1	795000	0	0
	6	+1	-1	+1	-1	840000	0	0
	7	+1	+1	-1	-1	3600	190	31
	8	-1	+1	+1	-1	9400	0	0
Replicate 2	9	+1	-1	-1	+1	2610000	4100	890
	10	-1	+1	-1	+1	2800000	1000	100
	11	+1	+1	+1	+1	3600000	22	12
	12	-1	-1	-1	-1	250000	2100	350
	13	-1	-1	+1	+1	810000	0	0
	14	+1	-1	+1	-1	740000	0	0
	15	+1	+1	-1	-1	3800	250	32
	16	-1	+1	+1	-1	10100	0	0
Replicate 3	17	+1	-1	-1	+1	2200000	4500	720
	18	-1	+1	-1	+1	2700000	900	92
	19	+1	+1	+1	+1	460000	16	10
	20	-1	-1	-1	-1	7100000	1800	300
	21	-1	-1	+1	+1	760000	0	0
	22	+1	-1	+1	-1	2000	0	0
	23	+1	+1	-1	-1	5510000	300	39
	24	-1	+1	+1	-1	14100	0	0

Table 5.1 2^4 factorial design grid to investigate the effect of charcoal, cyclodextrins, agitation and inoculum levels on *B. anthracis* growth, PA and LF expression. (1) indicates the following factor levels present; 7mg L^{-1} charcoal, 10mg L^{-1} methly-beta-cyclodextrin, agitation (shaking) of 500rpm, $2x10^4$ cfu mL^{-1} inoculum. (-1) indicates that charcoal, cyclodextrins and agitation (shaking) was not present and that the inoculum was $2x10^{-3}$ cfu mL^{-1}. Experiment planned, performed and analysed as described in Sections 2.6.17. and 2.3.6.

The analysis of results was split up into the three response factors, viable cell count, PA and LF levels. Figure 5.7 shows the normal probability chart of effects for viable counts. The normal probability chart is used to identify the relative magnitude and statistical significance of the main and interaction effects. The projected line in the middle is where the points should fall if they were to have no effect on the system. The further away each point falls from the line, the greater their effect. However, in order to determine if the points are significant, they must have a *p*-value below the alpha-value of 0.05 as described in Section 3.2.3. Here no effects were labelled as significant, which on first inspection suggests that *B. anthracis* growth was quite robust and can withstand changes in all four factors. However, with the analysis of the numerical response, shaking (agitation) has a *p*-value of 0.086. Thus shaking does become a significant factor if the alpha-value is changed to 0.10, increasing the error rate from 5% to 10%. As shaking has an effect score (T-score) of -1.83 it has a detrimental effect to the viable count and anthrax growth, but when comparing back to the normal probability chart, it is only a short distance away from the projected blue line, thus it was not a major negative effect. This may prove useful later in determining if anthrax culture can be moved into agitated culture.

In analysing the data for the antigens PA and LF, a different response is seen. Figures 5.8 and 5.9 both share common outcomes. The significance and order of significance of all the factors were the same. In both cases increasing the inoculum and the presence of charcoal had a net positive effect on antigen production. Furthermore, both charcoal and the increased inoculum appeared to have a positive interaction effect which further increased antigen production. Shaking had the greatest negative effect on antigen production followed by the addition of cyclodextrins. The latter result perhaps indicates that cyclodextrins are not a suitable replacement for charcoal in the media and that the role of charcoal is not limited to that of a carrier material. The negative effects of shaking and cyclodextrins can be limited with the addition of charcoal, hence their interaction effect are plotted more closely to the blue line of no significance.

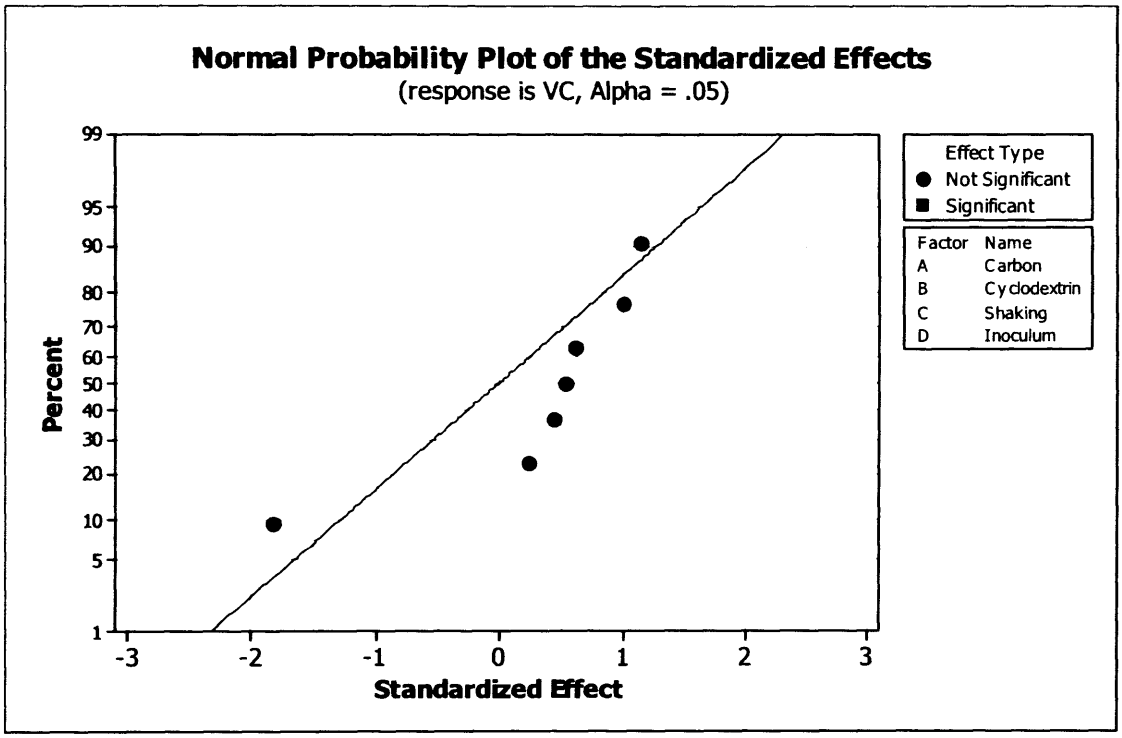

Factorial Fit: Viable Count versus Charcoal, Cyclodextrin, Shaking, Inoculum

Estimated Effects and Coefficients for Viable Count (coded units)

Term	Effect	Coef	SE Coef	T	P
Constant		1674446	389343	4.30	0.001
Charcoal	339991	169995	389343	0.44	0.668
Cyclodextrin	190274	95137	389343	0.24	0.810
Shaking	-1424841	-712420	389343	-1.83	0.086
Inoculum	903109	451555	389343	1.16	0.263
Charcoal*Cyclodextrin	482398	241199	389343	0.62	0.544
Charcoal*Shaking	785702	392851	389343	1.01	0.328
Charcoal*Inoculum	419319	209659	389343	0.54	0.598

S = 1907382 R-Sq = 29.31% R-Sq(adj) = 0.00%

Figure 5.7 Normal probability plot and factorial fit numerical data for the viable cell count. The plot illustrates the significance of each factor based upon their distance from the projected blue line and their respected *p*-value. In this case all the *p*-values are above the critical alpha value of 0.05 hence none of the factors are significant. Experiments performed as described in Table 5.1 and analysed using Minitab (Section 2.6.17). Note plot references to carbon refer to charcoal.

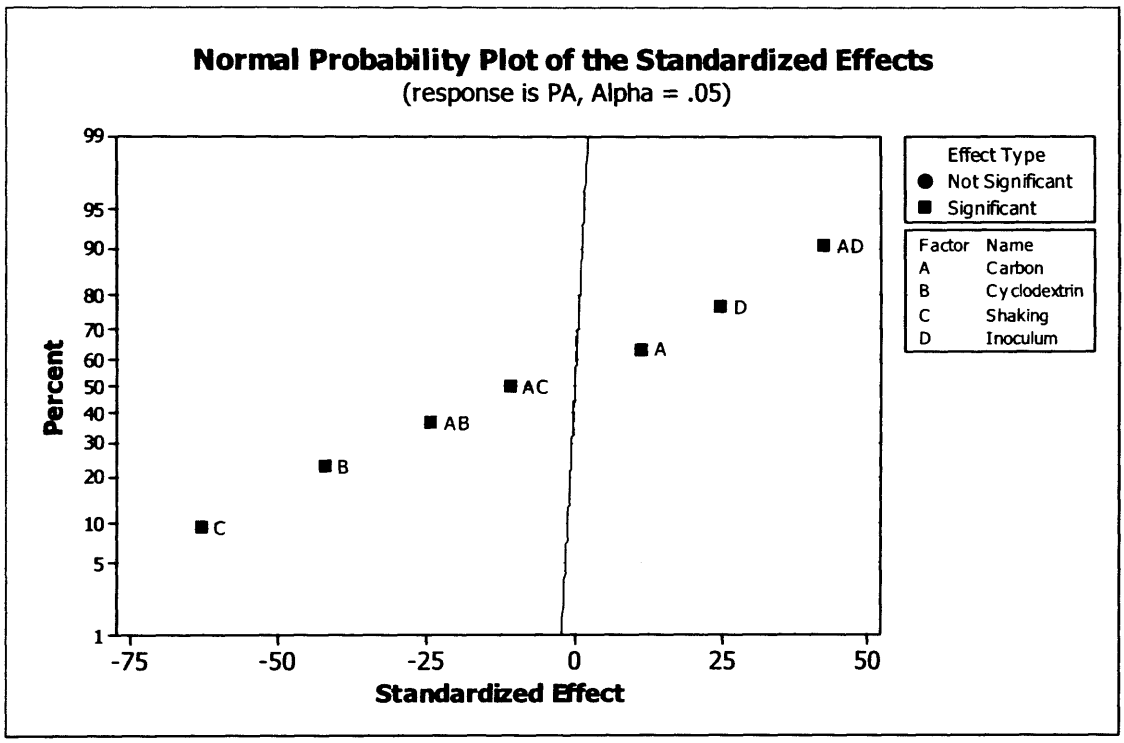

Factorial Fit: PA versus Charcoal, Cyclodextrin, Shaking, Inoculum

Estimated Effects and Coefficients for PA (coded units)

Term	Effect	Coef	SE Coef	T	P
Constant		891.0	14.06	63.36	0.000
Charcoal	318.9	159.5	14.06	11.34	0.000
Cyclodextrin	-1187.6	-593.8	14.06	-42.22	0.000
Shaking	-1772.8	-886.4	14.06	-63.03	0.000
Inoculum	694.2	347.1	14.06	24.68	0.000
Charcoal*Cyclodextrin	-684.9	-342.4	14.06	-24.35	0.000
Charcoal*Shaking	-309.6	-154.8	14.06	-11.01	0.000
Charcoal*Inoculum	1196.9	598.5	14.06	42.56	0.000

S = 68.8955 R-Sq = 99.82% R-Sq(adj) = 99.75%

Figure 5.8 Normal probability plot and factorial fit numerical data for PA. In this case all the factors are significant and their effects determine the relative strength of each term. A negative sign in front of the effect indicates the factor has a detrimental effect while a positive sign indicated the reverse. Experiments performed as described in Table 5.1 and analysed using Minitab (Section 2.6.17). Note plot references to carbon refer to charcoal.

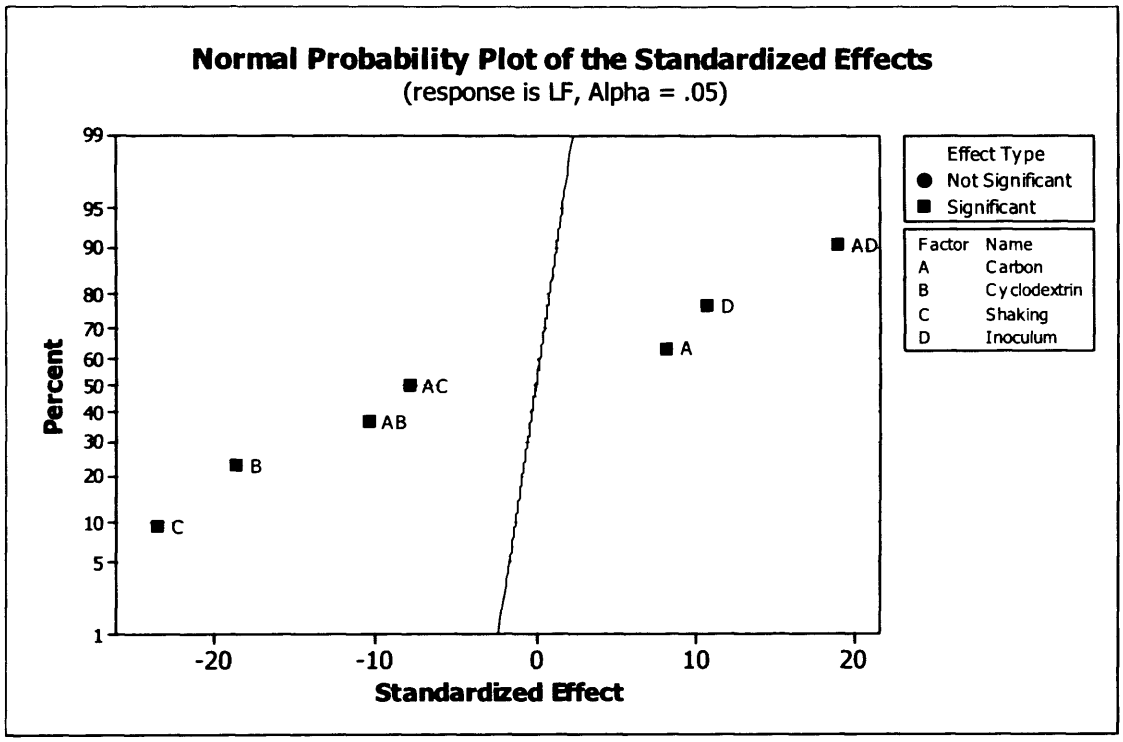

Factorial Fit: LF versus Charcoal, Cyclodextrin, Shaking, Inoculum

Estimated Effects and Coefficients for LF (coded units)

Term	Effect	Coef	SE Coef	T	P
Constant		155.6	6.514	23.88	0.000
Charcoal	107.7	53.8	6.514	8.27	0.000
Cyclodextrin	-242.5	-121.2	6.514	-18.61	0.000
Shaking	-305.9	-153.0	6.514	-23.48	0.000
Inoculum	140.8	70.4	6.514	10.80	0.000
Charcoal*Cyclodextrin	-135.5	-67.7	6.514	-10.40	0.000
Charcoal*Shaking	-102.4	-51.2	6.514	-7.86	0.000
Charcoal*Inoculum	247.8	123.9	6.514	19.02	0.000

S = 31.9136 R-Sq = 99.02% R-Sq(adj) = 98.59%

Figure 5.9 Normal probability plot and factorial fit numerical data for LF. In this case all the factors are significant and their effects determine the relative strength of each term. A negative sign in front of the effect indicates the factor has a detrimental effect while a positive sign indicated the reverse. Experiments performed as described in Table 5.1 and analysed using Minitab (Section 2.6.17). Note plot references to carbon refer to charcoal.

Overall these results have demonstrated that while cultures of *B. anthracis* are quite robust and can grow in many different environments, it is the production of its antigens which are most sensitive to changes in culture conditions. Key to exploiting better antigen production was the increased inoculum and the presence of charcoal (carbon) in the media. This information coupled with previous knowledge of pellicle formation suggested the possibility that anthrax antigen production could be linked to the cell density dependent signalling system known as quorum sensing (de Kievit *et al.* 2001).

5.4 Quorum sensing investigation in B. anthracis

5.4.1 Observations of carbon-cell growth association

It had been noted during growth in microwells that the charcoal appeared to aggregate, forming small clusters, having initially started as a thin layer at the base of the microwell. This type of aggregation has also been reported in Thompson bottles as pellicle formation (Section 5.1.1). In order to understand this phenomenon, the tetrazolium salt WST-1 was used. WST-1 is a soluble salt which is cleaved by metabolically active cells to release a dark orange formazan dye (Johnsen *et al.* 2002). When the WST-1 dye was added to a *B. anthracis* microwell culture which had been incubated for 24 hours, the bulk liquid initially remained colourless. However, after 20 minutes of further incubation the charcoal aggregates and their immediate area were stained orange. This would seem to indicate that the majority of cells aggregate towards charcoal. Due to containment level 3 conditions it was not possible to take an image of this event but it did suggest that the charcoal may have a role of a growth scaffold in *B. anthracis* growth and further suggests an active quorum sensing mechanism as aggregation is a precursor to biofilm formation (Morici *et al.* 2007).

5.4.2 Sterile stationary-phase supernatant additions enhance *B. anthracis* cell growth

In previous quorum sensing experiments (Rivas *et al.* 2005), sterile stationary phase supernatant (SSPS) from a previous bacterial culture was added to bacteria in early lag phase to see if it provoked a response. The rationale is that the signalling molecule in question is in sufficient quantities in the SSPS as to create a response when introduced in early lag phase cultures. Normally, the cultivability of the cells is improved in resuscitation protein factor experiments, where as in quorum sensing mechanisms, gene expression is initiated (Bassler 1999). Consequently in this experiment both viable cell counts and protective antigen production is monitored.

Figure 5.10 shows results from three cultures: one is normal *B. anthracis* growth with no SSPS addition, another had a 15% (v/v) SSPS addition from time zero and the third had a 30% (v/v) SSPS addition also from the beginning of culture. During normal growth, *B. anthracis* had left the initial lag phase by 9 hours, and subsequently entered stationary phase by 22 hours with an exponential growth rate of 9.85×10^5cfu mL^{-1} hr^{-1}. Cultures with the various supernatant additions exhibited a shorter lag time, reduced to just three hours, and an increased growth rate to 1.03×10^6cfu mL^{-1} hr^{-1} with 15% (v/v) SSPS addition and 1.51×10^6cfu mL^{-1} hr^{-1} with a 30% (v/v) addition.

A *box slippage test* was used to determine if the growth data sets were comparable (Mathews 2004). This non-parametric test is a test of medians and applicable in cases where the population sample has the same standard deviation. If the null hypothesis is true then the top of the box plots should be substantially overlapped and the medians similar to each other. In Figure 5.11, it is observed that the median for normal growth was significantly different from that of the two SSPS treatments and that the upper quartile value, Q3, greatly differed from the SSPS treatment values.

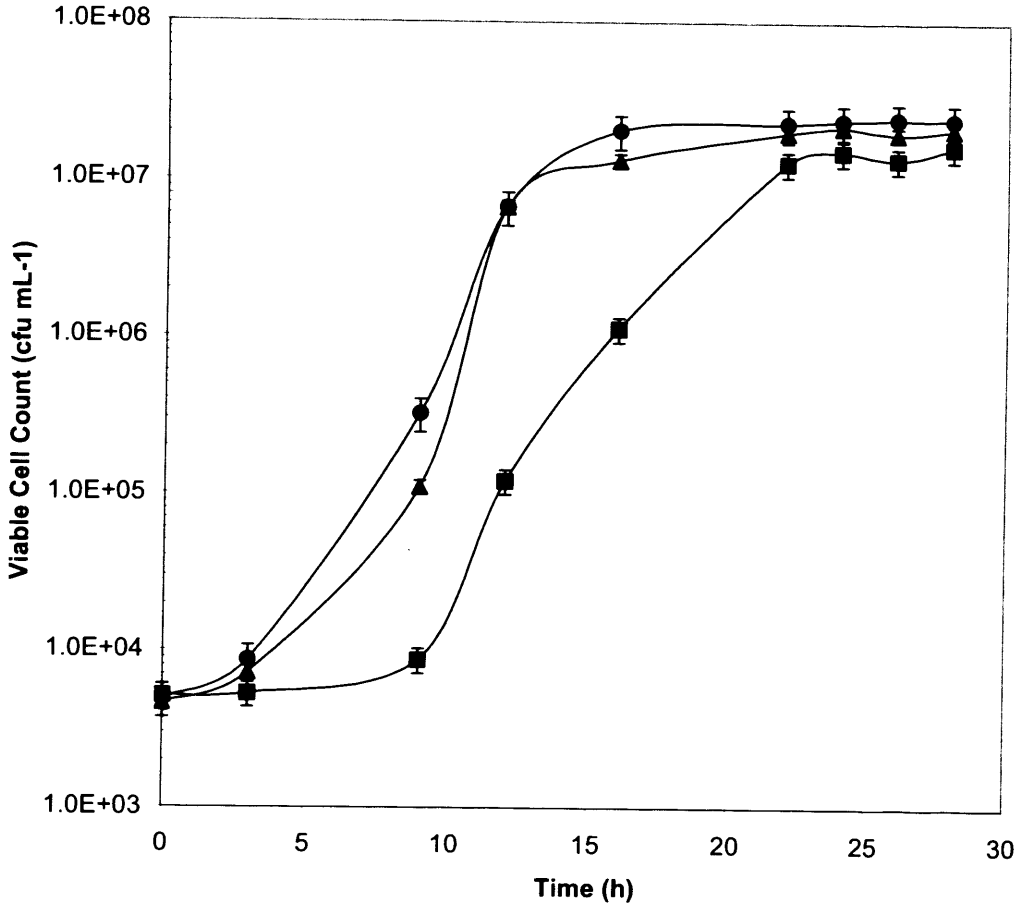

Figure 5.10 Growth kinetics of *B. anthracis* Sterne $34F_2$ with varying SSPS additions in microwell plates: (■) normal growth, (▲) growth with 15% (v/v) SSPS addition, (●) growth with 30% (v/v) SSPS addition. Experiments performed and analysed as described in Sections 2.5.3 and 2.6.1. The data represents the average of three independent microwell runs conducted on different days and error bars show one standard deviation about the mean.

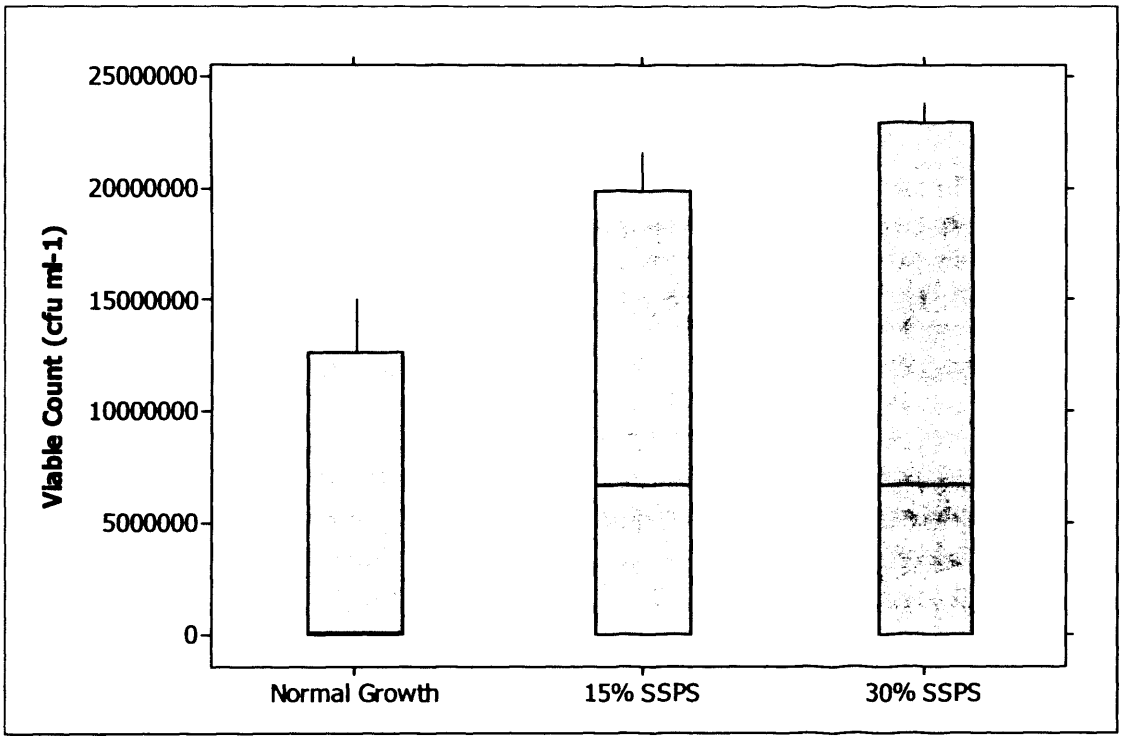

Treatment	Normal Growth	15% SSPS	30% SSPS
Median	$1.2x10^5$	$6.7x10^6$	$6.7x10^6$
Q1	$5.3x10^3$	$7.2x10^3$	$8.7x10^3$
Q3	$1.07x10^7$	$1.99x10^7$	$2.29x10^7$

Figure 5.11 Box plot slippage test of growth data for the three treatments, normal growth, 15% (v/v) SSPS and 30% (v/v) SSPS addition. If there were to be no difference in the data sets, the three medians would all be equal; H_0: $\mu_1=\mu_2=\mu_3$ and each of the box plots would exhibit no slippage. In this instance, it can be seen that the median for normal growth is not equal to that's of the SSPS additions, however, both the 15% and 30% treatments have equal medians and comparable inter-quartile ranges, thus can be considered statistically equal. Experimental conditions as described in Figure 5.10.

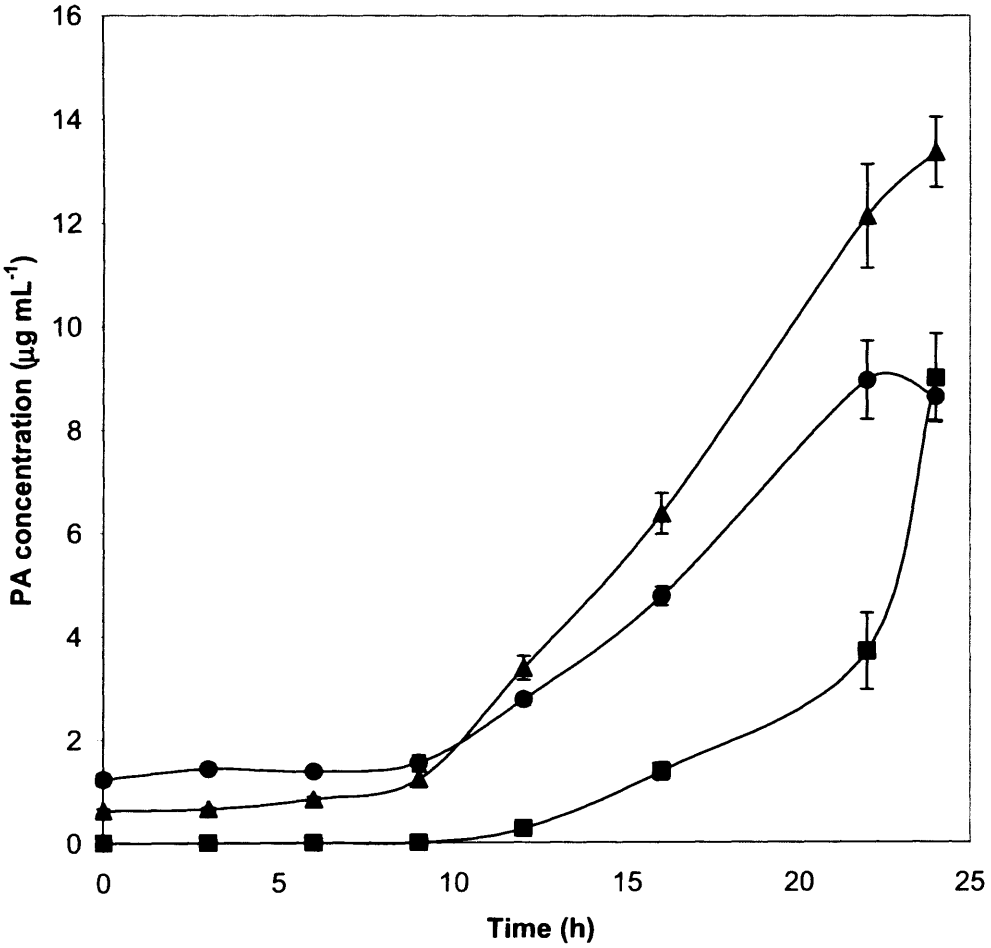

Figure 5.12 PA production of *B. anthracis* Sterne $34F_2$ under varying SSPS conditions in microwell plates: (■) normal growth, (▲) growth with 15% SSPS addition, (●) growth with 30% SSPS addition. Experiments performed and analysed as described in Sections 2.5.3 and 2.6.6. The data represents the average of three independent microwell runs conducted on different days and error bars show the one standard deviation about the mean.

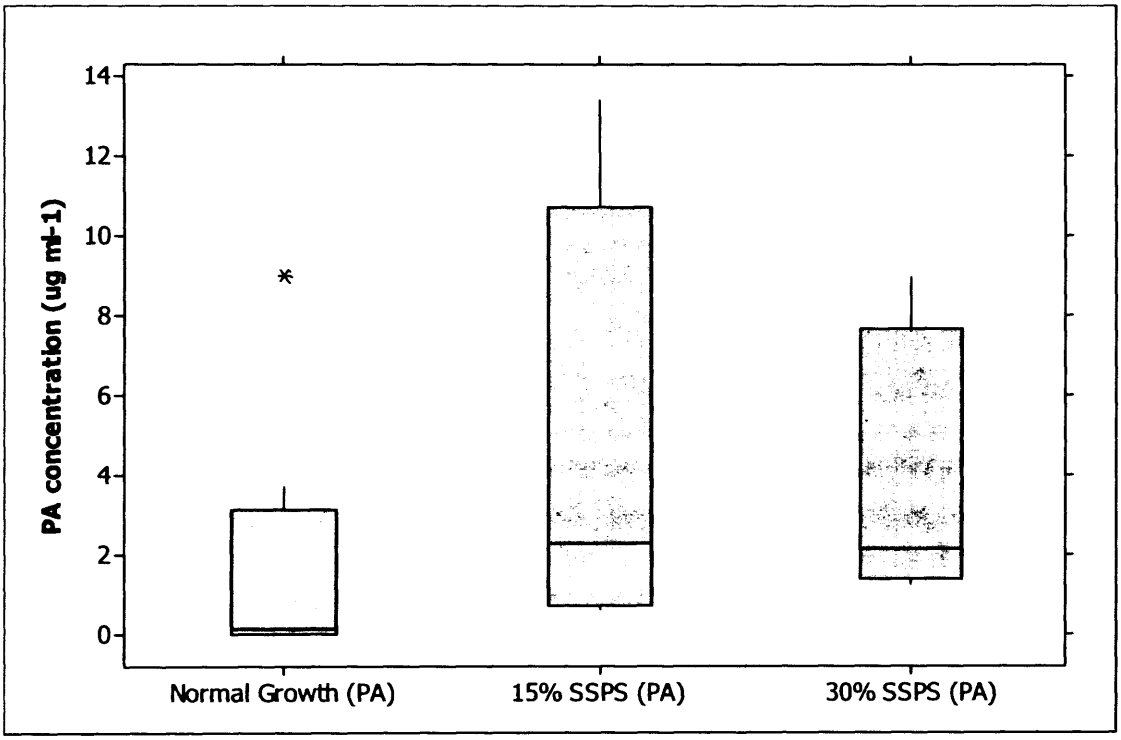

Treatment	Normal Growth	15% SSPS	30% SSPS
Median	0.142	2.31	2.16
Q1	0.0025	0.707	1.40
Q3	3.12	10.69	7.67

Figure 5.13 Box plot slippage test for PA production under the three treatments, normal growth, 15% SSPS and 30% SSPS addition. As observed previously, both SSPS box plots have significant slippage when compared to normal growth and the medians are not equal, thus are statistically different to normal growth. However, when comparing between 15% and 30% SSPS treatments both have a similar median but the slippage between the two box plots is large, accounting for the different PA production rates. Experimental conditions as described in Figure 5.12.

However, the difference between the two SSPS treatments, 15% (v/v) and 30% (v/v) additions, is not significant. Both data sets have similar Q3 values and identical medians. Therefore, it could be stated that there was no real difference between the 15% (v/v) and 30% (v/v) treatments and the growth rate response.

While Figure 5.10 demonstrates that the cultivability of *B. anthracis* can be increased with SSPS additions, a trait associated with resuscitation protein factors, Figure 5.12 further indicates that PA gene expression is also affected. Normally *B. anthracis* cultures began to produce detectable levels of PA after nine hours but it was after 20 hours that production exponentially increased from 3.7μg mL^{-1} to 9μg mL^{-1}. In both the supernatant addition profiles there were already detectable amounts of PA present from time zero, introduced through the SSPS addition. However, after the ninth hour, PA production began to steadily increase in both cases. The variability in the Q1 and Q3 range for PA (Figure 5.13) may be put down to the antigen production rates. The 15% (v/v) SSPS addition had the fastest PA production rate at 0.84μg mL^{-1} hr^{-1}. The 30% (v/v) SSPS addition production rate was lower at 0.57μg.$mL^{-1}hr^{-1}$. Normal anthrax growth achieved the lowest antigen production rate at 0.29μg.mL^{-1} hr^{-1}, as determined from gradient analysis post nine hours.

The *box slippage test* was once again employed to observe if these data sets were statistically different from each other. Figure 5.13 indicates that there is little difference in the median between the two SSPS treatments, suggesting that the null hypothesis should hold. However, when the SSPS medians were compared with the normal growth median, a significant difference was observed, thus confirming that there was a statistical difference in PA production when *B. anthracis* culture was incubated with either of the SSPS additions. Thus the data from Figures 5.12 and 5.13 indicate that quorum sensing is the most likely mechanism of *B. anthracis* intercellular communications and is used to influence growth and antigen production.

5.4.3 Fur-1 inhibits anthrax growth and PA production

In Figures 5.10 and 5.12 it was demonstrated that SSPS addition enhanced both *B. anthracis* growth and PA gene expression. To confirm if the mechanism of action actually was quorum sensing, the quorum sensing inhibitor, fur-1, was utilised (Jones *et al.* 2005).

In Figure 5.14, *B. anthracis* is subjected to four treatments; normal growth, 15% (v/v) SSPS addition, 15% (v/v) SSPS addition plus 20 μg mL^{-1} fur-1 and a 20 μg mL^{-1} fur-1 addition. The viable cell count and PA concentrations are both measured. The first treatment is normal growth, where a six hour lag period is observed before the culture entered exponential phase growth. During this time period, (0-12 hours) there is no detectable PA production. The next showed *B. anthracis* growth with a 15% SSPS addition from the start of culture. It had a starting PA concentration of 5.25ng mL^{-1}, represented by the bar chart below. Here, the lag phase is reduced to 3 hours before the cells entered exponential phase and consequently the amount of PA produced also increased exponentially to reach a value of 1.87μg mL^{-1} by 12 hours. The third trace showed anthrax growth with a 15% SSPS addition as before plus a supplement of 20μg mL^{-1} of fur-1 in the culture. With this latter culture there was a prolonged lag phase of nine hours before growth was observed. Thus there appeared to be some form of inhibition followed by recovery. The same traits are also observed in PA production. At time zero 4.57ng mL^{-1} PA is detected in the spiked fur-1 profile. PA production remained static for the first nine hours after which time some low level PA production is observed, resulting in 18.2ng mL^{-1} PA by the end of the nine hours. By 12 hours 22.43ng mL^{-1} PA had been produced. Finally, with just normal growth plus 20μg mL^{-1} of fur-1 there is no detectable production of PA and the culture did not leave lag phase. From these observations it is concluded that fur-1 has a negative impact on both PA production and *B. anthracis* growth. This with other data in the previous section led to the conclusion that quorum sensing is probably the dominant mechanism for cell growth and antigen production, not Rpf's.

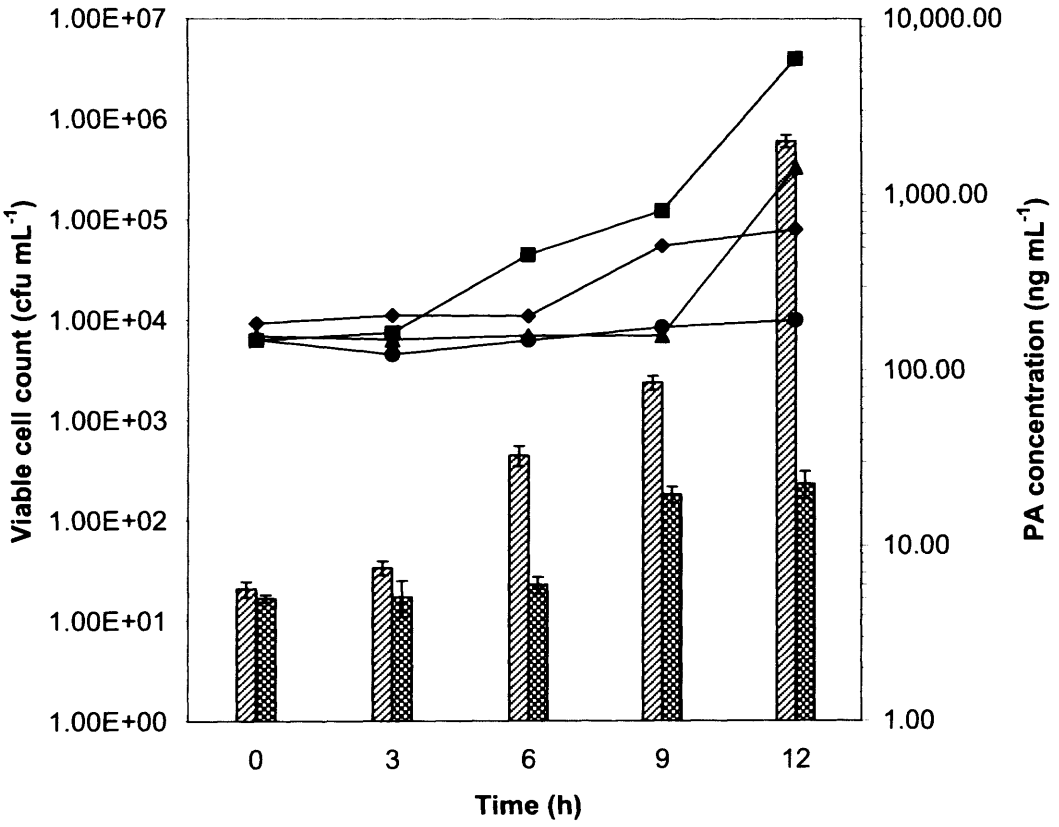

Figure 5.14 Growth and protective antigen (PA) production in *B. anthracis* Sterne $34F_2$ with varying additions of SSPS and fur-1: (■) growth with 15% SSPS addition, (◆) normal growth, (▲) growth with 15% SSPS addition and 20µg mL^{-1} fur-1, (●) growth with 20µg mL^{-1} fur-1 addition, (▨) PA production with 15% SSPS addition, (▩) PA production with 15% SSPS addition and 20µg mL^{-1} fur-1. Experiments performed as described in Sections 2.5.3 and 2.3.6. PA concentrations determined as described in Section2.6.6. Error bars represent one standard deviation about the mean, where n=3.

5.4.4 Identification of potential quorum sensing proteins produced by *B. anthracis* in the sterile supernatant

In order to determine which components of the SSPS had a significant impact on cell growth the SSPS was subdivided into discreet molecular weight fractions as described in Section 2.5.2. Four supernatant fractions are created; 0-50kDa, 0-30kDa, 0-10kDa and finally 0-5kDa. Figure 5.15 shows *B. anthracis* growth with varying fractions of SSPS. Apart from the normal anthrax growth curve, which has no additions made to it, the other growth profiles are all treated with a 15% (v/v) addition of the molecular weight protein fraction from the start of culture. The average growth rate is calculated using viable count data from cultures numbered from between three and 12 hours. The rationale for this was because it excluded the first three hours of lag phase experienced by all the growth profiles, but included a time frame which allows for a comparison of growth profiles. The normal *B. anthracis* growth rate is calculated to be $2.4x10^4$ cfu mL^{-1} hr^{-1}. The average growth rates calculated for each of the three supernatant fractions, 0-50kDa, 0-30kDa and 0-10kDa, are $3.7x10^4$, $4.3x10^4$ and $2.6x10^4$ cfu mL^{-1} hr^{-1} respectively. There appears to be a slight reduction of the growth rate in moving from the 0-30kDa pool to the 0-10kDa pool, though not significant. The most significant reduction in growth rate is between the 0-10kDa fraction, which has a growth rate of $2.6x10^4$ cfu mL^{-1} hr^{-1} to the 0-5kDa fraction, which fell by one order of magnitude to $1.7x10^3$ cfu mL^{-1} hr^{-1}. Clearly, there is some component missing in the 0-5kDa pool which has a profound effect on cell growth. The 0-5kDa protein fraction growth rate is inferior to normal anthrax growth. The poor growth rate may be accounted for due to the purification of waste products or a dilution effect because of an absence of proteins present in the 0-5kDa addition. Overall the finding suggested that the absence of a protein or proteins in the 0-5kDa fraction resulted in poor *B. anthracis* growth.

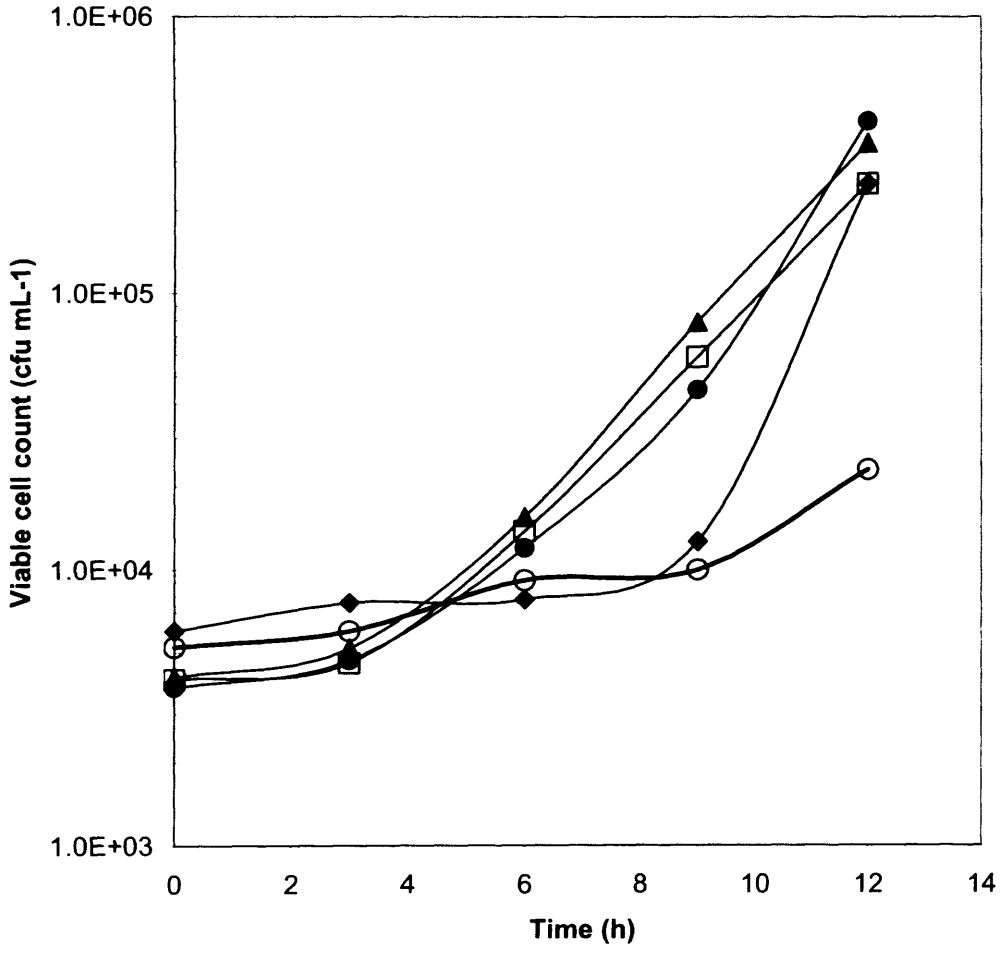

Figure 5.15 *B. anthracis* Sterne $34F_2$ growth monitored over the first 12 hours with varying fractions of SSPS: (◆) normal growth, (▲) 0-50kDa SSPS addition, (●) 0-30kDa SSPS addition, (□) 0-10kDa SSPS addition, (○) 0-5kDa SSPS addition. Experiments performed as described in Section 2.5.3 and viable counts measured as in Section 2.6.1.

5.4.5 Preliminary identification of proteins in the 5-10kDa mass fraction

Proteins in the 0-50 kDa, 0-10kDa and 0-5 kDa pooled supernatant fractions were identified using SELDI-MS, Figure 5.16.

Figure 5.16(a) shows the protein profile of the 0-50kDa fraction. This is used as a reference pool to compare both the 0-10kDa and 0-5kDa fractions. In previous profiling experiments (Appendix A), the 83kDa PA peak broke down during the SELDI-MS process to form several smaller peaks, including one at 3kDa and another at 8kDa. Because these proteins are in such high abundance they had the effect of masking the signal of smaller, low abundance peaks. Therefore by using the 0-50kDa fraction PA is excluded from the SELDI-MS analysis, hence allowing the visualisation of smaller low abundance proteins present in the supernatant. Figure 5.16(a) illustrates that many small molecular weight proteins (4-10kDa) are present; 12 peaks in total are identified. However, when compared with Figure 5.16(b), the 0-10kDa protein fraction, only three peaks are identifiable from the background noise; peaks at 4.8kDa, 5.8kDa and 8.6kDa. Only peaks that had a signal to noise ratio greater than five are included in this analysis in order to have a high confidence that the peaks detected are true proteins rather then artefacts. The fact that nine of these peaks are lost between Figure 5.16(a) and 5.16(b) and that the arbitrary height of the 4.8kDa and 8.6kDa proteins are approximately the same as in Figure 5.16(a), suggests that some of the proteins are absorbed by the spin filters. Only the 5.8kDa peak is slightly diminished from an arbitrary height of 4.1 in Figure 5.16(a) to a height of 2.4 in Figure 5.16(b).

Comparing Figures 5.16(b) and 5.16(c), the only peak present in the 0-5kDa fraction is the 4.8kDa peak; both the 5.8kDa and the 8.6kDa peaks are absent.

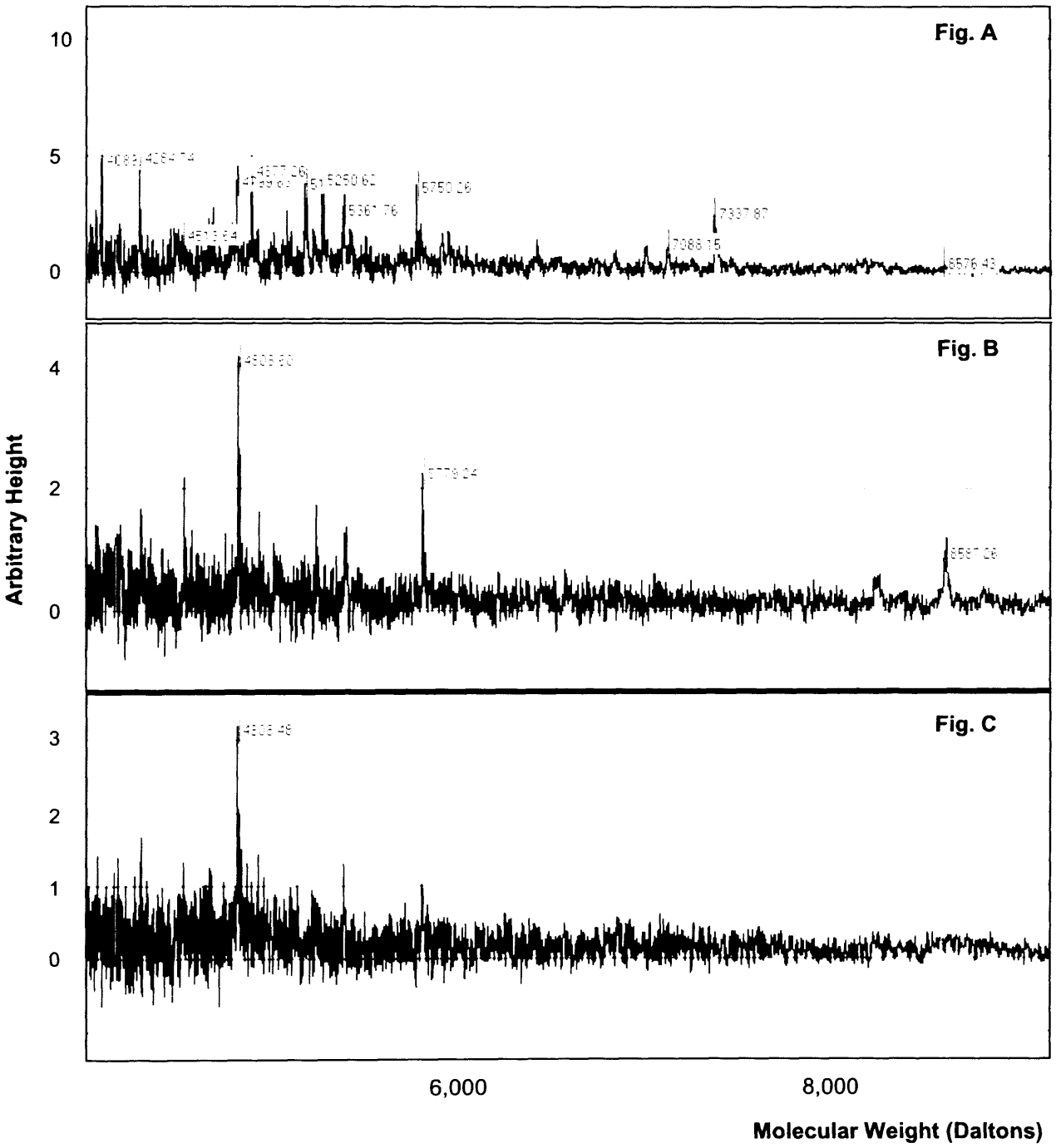

Figure 5.16 SELDI-MS analysis of various fractions of SSPS; (A) 0-50kDa SSPS fraction, (B) 0-10kDa SSPS fraction, (C) 0-5kDa SSPS fraction. A signal to noise ration above 5 was used to identify true peaks. SSPS fractions prepared as described in Section 2.5.2 and SELDI-MS analysis conducted as in Section 2.6.12.

The 50, 30 and 10kDa fractions all increased the growth rate of *B. anthracis* while the 5kDa fraction was unable to produce such a stimulatory effect. Therefore, some component in the first three fractions but not present in the 5kDa fraction must be responsible. Looking at Figure 15.6(b), there appears to be three possible candidates, at 4.8kDa, 5.8kDa and 8.6kDa. The 4.8kDa peak is visible in the 5kDa fraction, Figure 15.6(c), so this can be excluded. This leaves the 5.8kDa and 8.6kDa components, thought the latter is very close to 8.3kDa, the known molecular weight of the PA breakdown product. The difference of 0.3kDa is within the error for dynamic range focusing and therefore may indeed be the same peak. This leaves the peak at 5.8kDa which may be the active component responsible for enhanced *B. anthracis* growth rate.

5.5 Summary

In this chapter microwells have been shown to be excellent tools for the small scale culture of dangerous pathogens such as *B. anthracis* (Figure 5.2 and 5.3). They have proved to be a cheap alternative to bottles and shakeflasks allowing for a greater throughput due to their small footprint and compatibility with ancillary equipment such as multi-tip pipettes, sealing membranes and incubators. They can easily fit within existing flexible film isolators without requiring additional capital investment. Furthermore, Figures 5.4 and 5.5 have demonstrated they can be employed to generate pertinent and reproducible data. The application of microwells in this study expands their usefulness to beyond assays, highlighting their effectiveness as mimics of the Thompson bottle production environment, illustrated in Figures 5.2 and 5.3.

The data demonstrates, through the use of fur-1, that the primary system for the control of growth and antigen production in *B. anthracis* is probably quorum sensing. This contrasts with the traditional view of quorum sensing which suggests that quorum sensing only affects the expression of certain genes, not bacterial growth itself. Through the additions of SSPS, it has been observed that quorum sensing not only increased antigen production in

B. anthracis but also enhanced the cultivability of the cells themselves. The results also implies that two mechanisms are in action, one mediated through the auto-inducer molecule, AI-2 and another that is protein based, AI-1. AI-1 utilises a small post-translationally modified peptide signal which interacts with a sensor element on the cell surface composed of a two-component histidine kinase. AI-2 makes use of the LuxS product, a 3A-methyl-5,6-dihydro-furo (2,3-D)(1,3,2) dioxaborole-2,2,6,6A-tetraol. Its structure is shown in Figure 5.1 (Chen *et al.* 2002). This molecule binds with LuxP and LuxQ, which combine to act as an AI-2 sensor (Bassler *et al.* 1994). With the addition of fur-1, the inhibition of growth was observed in *B. anthracis* (Section 5.4.3). However, with the addition of SSPS, growth was seen to recover. It is possible that fur-1 and AI-2 compete with each other to bind to LuxPQ and that by increasing the concentration of AI-2 the inhibition can be reversed, similar to reversible inhibition in enzymes. The reversion of fur-1 inhibition may be attributed to the molecule being metabolised or the generation of greater amounts of AI-2. In any case, it highlights the limits of fur-1 as an anti-microbial agent, as given enough time the bacteria will recover.

Experiments with the use of size exclusion spin filters indicated that the omission of a certain small molecular weight supernatant protein (possibly at 5.8kDa) also had a detrimental effect on growth. In these examples however, AI-2 was not excluded as it would be small enough to pass through the spin filter membrane, yet a decrease in the growth rate was still observed. This may suggest that the two quorum sensing systems, AI-1 and AI-2, may act in parallel and share a common signalling pathway. Suppression of the signalling pathway, either through the exclusion of these small molecular weight proteins using size exclusion spin filters or fur-1 caused the pathway not to be activated; thus preventing increased cell growth and antigen production. This finding is in agreement with research by Miller *et al* (2002) who demonstrated that AI-1 and AI-2 can act in parallel. Much of the current knowledge on quorum sensing was derived through experimentation on *V. harveyi and V. cholerae*. Though in these bacteria AI-1 uses a homoserine lactone

produced by LuxM and detected by LuxN (Bassler *et al.* 1993), AI-2 remains the same. Both LuxM and LuxN are hybrid two-component proteins that contain a sensor kinase and response regulator domain, similar to the Gram positive peptide sensor and both share the signalling cascades (Freeman *et al.* 2000;Freeman and Bassler 1999a;Freeman and Bassler 1999b). This cascade controls many effects, such as bioluminescence and polysaccharide and metalloprotease secretions in *V. harveyi*. In *B. anthracis* it is possible that this quorum sensing system may control both growth kinetics and antigen expression as perhaps an evolutionary mechanism relating to the pathogenicity of the bacteria.

The use of microwells as an effective mimic of the *B. anthracis* vaccine production environment has been demonstrated in this chapter. Statistical analysis has revealed little intra-plate variation, and where variation from production data was observed it was explained without difficulty. Evaporation proved to contribute a little deviation from production data, but it was monitored and its impact on the general data trends was negligible. With the use of factorial design it was possible to separate out different components of the current vaccine production and deduce that while *B. anthracis* can grow in differing environments, antigen expression is very susceptible to changes in the media and charcoal and inoculum density play an important role in stabilising antigen expression. It was further held that charcoal may play the role of a growth scaffold facilitating antigen expression, visualised using the tetrazolium salt, WST-1. The results obtained clearly demonstrated that viable cell shifted towards the charcoal to form aggregates. The final aim of this chapter, to investigate quorum sensing in *B. anthracis* using microwells has proved successful. It was determined that quorum sensing mechanisms play an important role for both growth and antigen expression and that a dual signal mechanism may be in place requiring both the AI-2 molecule and a small protein of 5.8kDa in order to activate a signal cascade.

6 *B. anthracis* fermentations and vaccine production in a stirred miniature bioreactor

6.1 Introduction

The UK Anthrax Vaccine has been produced under licence from the Secretary of State for Health at the HPA for more than 40 years. It is a cell free alum precipitate of the anthrax culture supernatant and contains the vaccine antigens PA and LF. Cultures of the non-encapsulated *B. anthracis* Sterne $34F_2$ are grown in a partially defined media in Thompson bottles with a 500mL working volume under static conditions. They are maintained at 37℃ until a pH drop below pH 7.6 is detected, at which time the cultures are harvested. This process takes approximately 24-28 hours. However, it is not possible to monitor if each bottle has met the harvest criterion since there is no on-line process monitoring. The culture is then passed through a 0.2 μm filter after which the sterile supernatant is combined with potassium aluminium sulphate and acidified to create a precipitate which is left to settle for approximately one week. After one week the supernatant is aspirated and settling is allowed to proceed for a second week. This precipitate forms the basis of the anthrax vaccine (Hambleton *et al.* 1984). A typical vaccine run consists of 228 bottles and takes approximately 2 hours to inoculate under containment level 3 conditions, which could lead to some batch to batch variability; however HPA data has shown the consistency of the process and product.

The vaccine process uses pH as the harvest criterion which presents an operational problem. In order to measure the pH of a Thompson bottle, a bottle is removed from the incubation room and the pH measured aseptically. If the bottle has reached the harvest pH the batch is harvested, otherwise the bottle is returned to the incubation room. However, because the inoculation process can take up to two hours to complete, the pH value of a

single bottle may not be entirely representative of the other Thompson bottles. Consequently, the implementation of on-line pH monitoring through probed Thompson bottles was investigated by the HPA. The data collected were found to be reproducible and the overall shape of the pH profiles generated were identical to profiles generated from off-line pH measurement, although the absolute values did differ slightly possibly due to the probe not being immersed in sufficient media or the build up of a stagnant layer surrounding the pH probe (HPA, unpublished results). Furthermore, the exclusive use of pH as the harvest criterion results in a vulnerable process as the production batch must be rejected if the pH does not fall below pH 7.6.

A possible improvement to the cultivation process would be the use of stirred tank fermenters. This would allow sampling without sacrifice of the production volume as on-line pH monitoring could be utilised and eliminate bottle to bottle variability as a homogeneous culture environment would be created. However, because the production of *B. anthracis* is a containment level 3 (CL3) operation, the capital investment required to produce a CL3 fermentation suite would be considerable. From a business perspective this would be very risky especially as the route from static culture to stirred tank reactor is unproven. The DOE study conducted in Chapter 5 indicated that anthrax growth was possible in agitated (shaken) conditions (Section 5.3). However, the result also indicated that antigen production was susceptible to a change in the production environment. Therefore, a miniature stirred bioreactor was used to evaluate the factors which would most impact on the vaccine process in an agitated culture environment.

The use of miniaturised bioreactors is gaining increased interest in order to reduce the labour intensity and material costs of bioprocess development (Kostov *et al.* 2001;Kumar *et al.* 2004;Lye *et al.* 2003;Puskeiler *et al.* 2005). Miniature bioreactors have been created as early stage process evaluation tools and as an alternative to microtitre plates and shake flasks to overcome the limitations of mixing and scale up (Betts *et al.* 2006;Doig *et al.*

2002). The quality of data obtained, combined with the small amount of required material makes miniature bioreactors particularly suited for experimentation on ACDP Class 3 pathogens. Their small foot print means that they can easily fit within a CL3 isolator or cabinet and reducing the experimental volume to millilitres allows for safer experimentation.

6.1.1 Aim and objectives

The aim of this chapter is focused on the investigation of *B. anthracis* Sterne $34F_2$ cultivation and antigen production in a homogeneous, stirred culture system. In this work a novel miniature bioreactor designed in house (Gill 2007a) is employed to evaluate the possibility of moving anthrax vaccine production from static culture to stirred tank conditions. The miniature bioreactor used is geometrically similar to conventional fermenter designs and thus the results are readily scaleable to laboratory and pilot scales (Gill *et al.* 2007b). It is already known from work conducted in Section 5.3 that antigen production was susceptible to changes in the culture environment; hence the specific objectives of this chapter are:

- To establish conditions for the cultivation of *B. anthracis* in a miniature stirred bioreactor

- To compare cell growth, PA and LF antigen production kinetics in static and stirred cultivation systems

- To characterise and identify other potential harvest criteria for vaccine production in addition to pH

6.2 Thompson Bottle Culture Kinetics

In order to provide a basis for later comparison the typical fermentation kinetics of *B. anthracis* Sterne $34F_2$ in static Thompson bottle culture conducted by the Health Protection Agency is shown in Figure 6.1. The same charcoal medium (Basal medium, Section 2.3.7) used in the previous chapter was used here as well. The culture required between 24-28 hours during which time the change in pH was closely monitored. Culture pH is a critical control parameter as described in Section 6.1 and obtaining representative samples in a static environment proved to be an issue. Agitation of the Thompson bottle was not possible due to limits in design space. Thus, in order to attain accurate pH measurements sequential bulk sacrifice of Thompson bottles was required to generate the data presented in Figure 6.1. Under these static culture conditions an increase in pH is observed from 7.9 to 8.5 over the first 16 hours, after which time the pH dropped to a low of 7.6 by the twenty-fifth hour. Glucose depletion is also monitored which initially remained static until the sixteenth hour where upon it declined corresponding to the drop in pH. Glucose is also monitored using a hand held glucose meter which made it possible to add confidence to the harvest process by eliminating the possibility that the transient pH drop may be missed. It would appear for the initial exponential phase amino acid in the medium are used as the primary carbon source for growth as the pH increases from 7.9 to 8.7 over the first 16 hours. *B. anthracis* culture itself had a lag phase of eight hours followed by an exponential phase of 12 hours where upon it entered stationary phase. During this time it is observed that the charcoal was not uniformly distributed in the Thompson bottle which may be an indicator of cellular aggregation, visualised using the tetrazolium salt, WST-1 (Section 5.4.1).

6.3 Miniature bioreactor culture kinetics

The initial stirred bioreactor experiments were designed to mimic Thompson bottle culture conditions except that the cultures were agitated. Consequently, all the gas ports are sealed and no air is sparged into the bioreactor; nor is any gas allowed to escape. The rationale for this is the acid released from glucose metabolism would react with the bicarbonate in the media to create a carbon dioxide rich environment. Carbon dioxide is known to positively increase PA and LF expression through the anthrax toxin attenuator, AtxA (Uchida *et al.* 1997). The key difference from Thompson bottle culture was the mechanical agitation applied to create a homogeneous culture environment which allowed for accurate pH readings. Visual observations showed the carbon and biomass to be uniformly distributed throughout the bioreactor and there was no dispersed gas phase as a result of surface air entrapment.

Figure 6.2 shows typical fermentation kinetics for *B. anthracis* in unaerated agitated culture using the miniature bioreactor. It can be clearly seen that the key traits in terms of pH, glucose and optical density in the miniature bioreactor mirrored those observations in Thompson bottle cultures. The characteristic minimum in pH, reinforced through the decline in glucose is still visible. However the decrease in pH value from 8.7 to 7.5 occurred in only nine hours, not 25 hours as previously recorded in Thompson bottles. Furthermore, a higher optical density is attained in the bioreactor most probably due to the reduction in the duration of the lag phase. It is possible that as a consequence of agitation growth kinetics were much faster because the diffusion of nutrients was no longer limited by cellular aggregation.

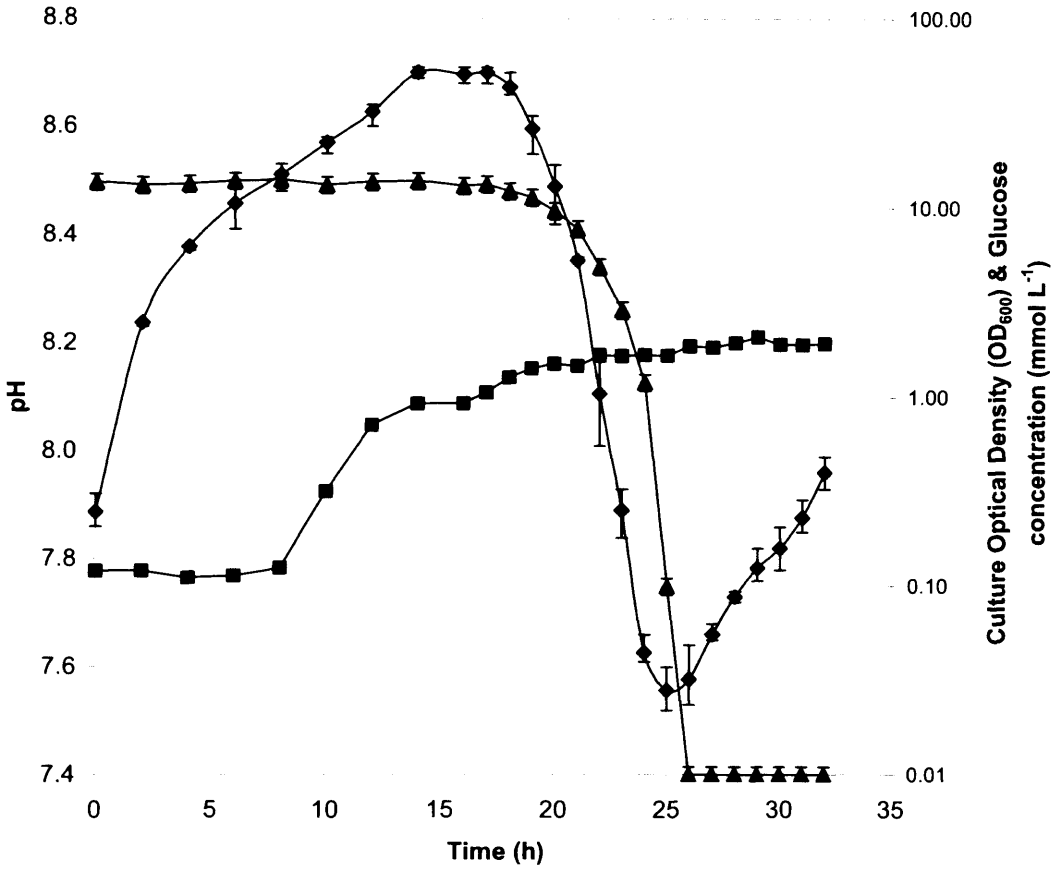

Figure 6.1 Batch fermentation kinetics of a typical *B. anthracis* Sterne $34F_2$ culture in a static Thompson bottle: (■) culture optical density, (◆) culture pH, (▲) glucose concentration. Cultures performed as described in Section 2.3.7 and analysed as in Section 2.6.3. This data shown is the average of three independent runs using different bottles and the error bars represent one standard deviation about the mean. The Thompson bottle data were generously provided by the Health Protection Agency.

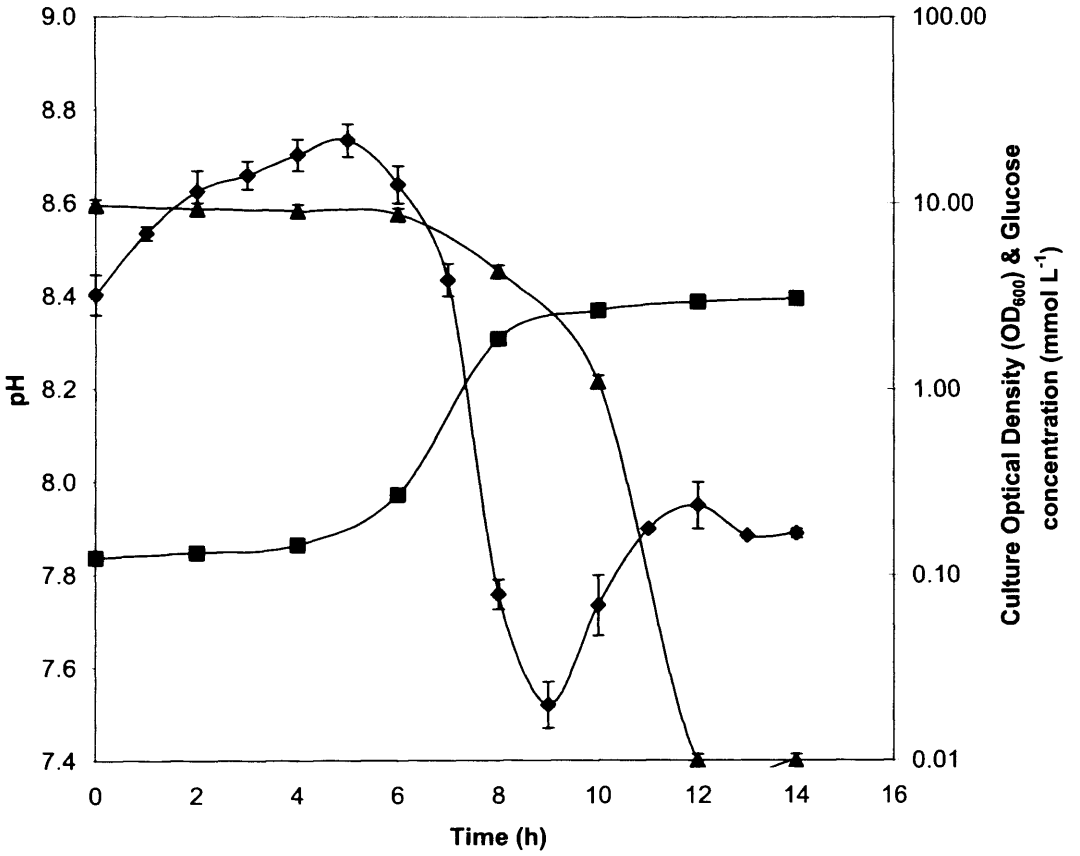

Figure 6.2 Batch fermentation kinetics of a typical *B. anthracis* Sterne $34F_2$ culture in the miniature bioreactor: (■) culture optical density, (◆) culture pH, (▲) glucose concentration. No aeration was used and the agitation rate was set at 700 rpm. Cultures performed as described in Section 2.3.8 and analysed as in Section 2.6.3. This data shown is the average of three independent runs and the error bars represent one standard deviation about the mean.

6.4 Comparison of Antigen Titres in Static and Stirred Cultures

For vaccine production it is vital that stirred cultures produced equivalent PA and LF antigen titres as in Thompson bottle culture. These antigens are key components of the anthrax vaccine (Section 1.5.2) and thus to consider transfer from one culture method to another it is important to demonstrate equivalent if not increased antigen expression. Figure 6.3 shows that not only were equivalent antigen titres reached in the miniature bioreactor, but they surpassed Thompson bottle yields. More importantly from the commercial perspective, the culture time was halved to 14 hours. At 28 hours an optical density of 1.94 OD_{600} is attained in Thompson bottles and antigen concentrations of 7.13μg mL^{-1} PA and 1.61μg mL^{-1} LF are realised. Comparatively, the bioreactor culture achieved an optical density of 3.08 OD_{600} and antigen concentrations of 10.3μg mL^{-1} PA and 3.6μg mL^{-1} LF by 14 hours. This increased antigen yield can be accounted for by increased biomass production as the antigen production rate per unit of culture optical density remained approximately the same. For example PA production in Thompson bottles was 3.68μg mL^{-1} OD^{-1}; in stirred culture it was 3.54μg mL^{-1} OD^{-1}.

6.5 Proteolytic degradation of Antigens in Bioreactor Culture

The ELISA method used to quantify PA and LF concentrations in Figure 6.3 used a polyclonal antibody as described in Section 2.6.5. Consequently, it is necessary to conduct western blots, (Figures 6.4 and 6.5) in order to determine whether antigen degradation had occurred throughout the bioreactor culture. The western blots showed PA_{83} breaking down to PA_{63} (Miller *et al.* 1999) and LF degradation was also detected.

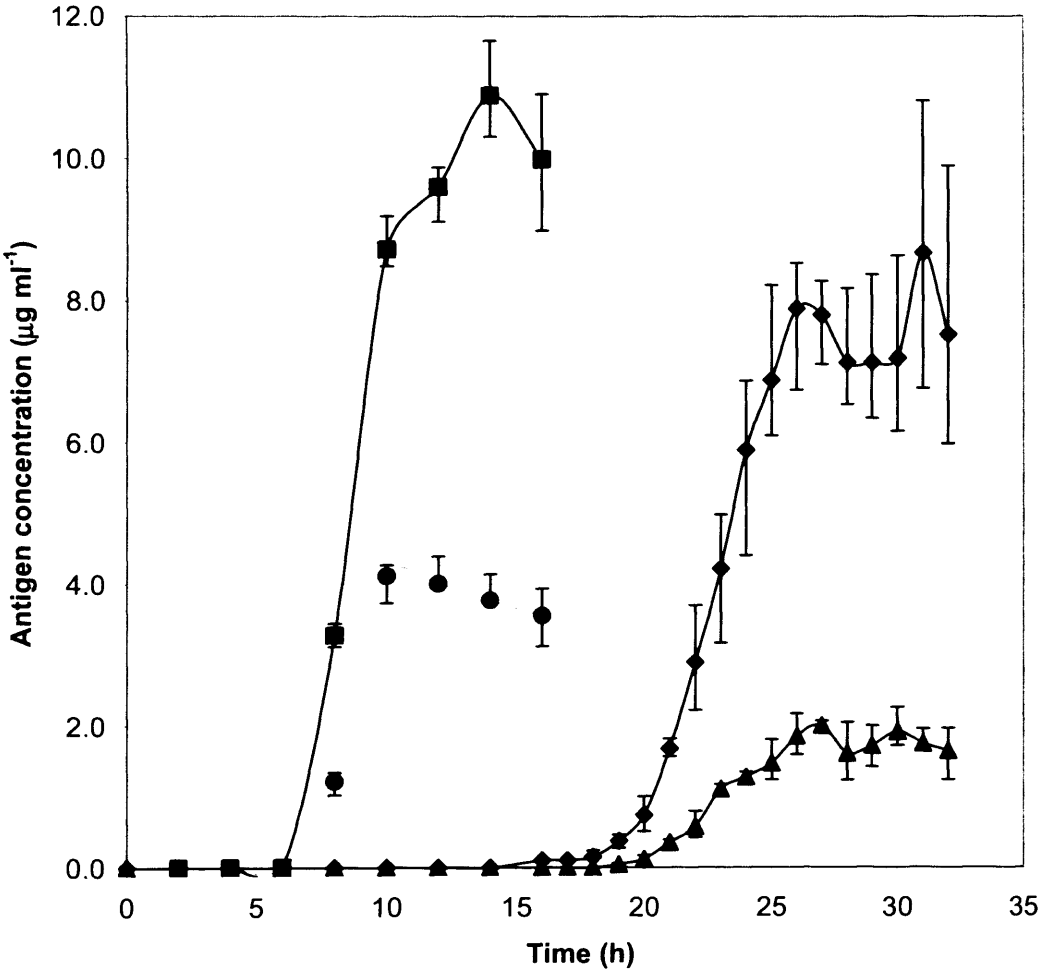

Figure 6.3 Kinetics of antigen production in unaerated Thompson bottles and unaerated miniature bioreactor cultures of *B. anthracis* Sterne $34F_2$; (■) bioreactor PA, (●) bioreactor LF, (◆) Thompson bottle PA, (▲) Thompson bottle LF. Experiments performed as in Sections 2.3.5.and 2.3.6. PA and LF quantified as in Sections 2.6.6 and 2.6.7. The data is the average of three experimental runs and the error bars represent one standard deviation about the mean. The Thompson bottle data were generously provided by the Health Protection Agency.

In miniature bioreactor cultures the first signs of PA degradation are visible from hour 10; however, LF degradation is first detected two hours earlier at hour 8, (Figures 6.4 and 6.5). PA breakdown had not been previously observed in Thompson bottle cultures though some LF degradation had been monitored in the past, (HPA, personal communication), however PA_{63} is still a valuable form which is known to confer immune protection (Hepler *et al.* 2006).

Zymograms were used to assay for protease activity in Thompson bottle culture supernatants, but none was detected (data not shown). In order to check for any signs of antigen degradation in stirred bioreactor cultures a zymogram (Figure 6.6) was used to detect proteases which may account for the degradation. Two types of zymogram were performed each using different substrates, casein and gelatine and time point samples between 0-16 hours were run on both gels as described in Section 2.6.10. The casein zymogram detected no protease activity whatsoever (data not shown) but the gelatine zymogram did detect proteases over the same time period. More over, it appeared that the intensity of the band increased with increased antigen titres, thus initially it is thought that the zymogram may be assaying for LF, which is a metalloprotease. However, the molecular weight of the gelatinase is too low to be LF. LF has a molecular weight of 90kDa, whereas this enzyme had a molecular weight of approximately 70kDa. Therefore the protease is not LF but it may account for PA and LF degradation.

6.5.1 Influence of bioreactor aeration on antigen production

Based on the results of the Section 6.4, it would appear that antigen concentrations are linked to biomass production. Thus by increasing biomass production through aeration and glucose concentrations it may be possible to increase titres of PA and LF. Hence bioreactor experiments were performed over a range of operating condition. Figures 6.7 and 6.8 show a bioreactor run where the culture was initially aerated for the first thirteen hours after which time aeration was stopped.

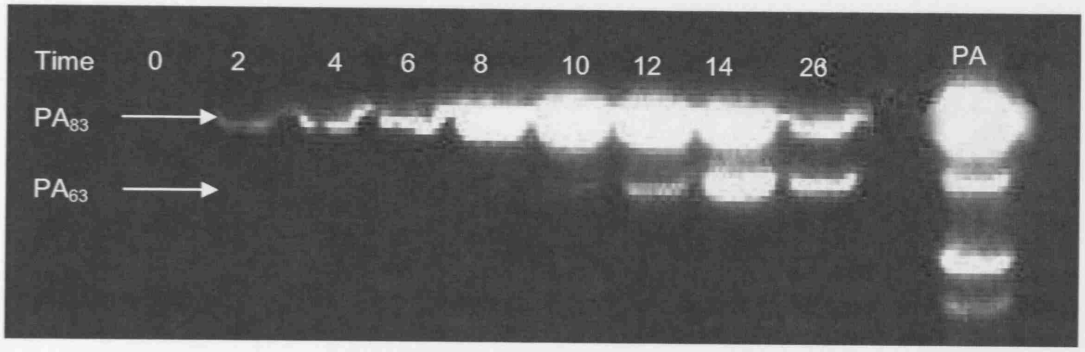

Figure 6.4 A Western Blot showing the time course of PA degradation in the miniature bioreactor under unaerated conditions. The numbers above each well correspond to the fermentation time in hours at which the sample was taken. The lane marked PA was created using rPA and shows several low molecular weight bands which are break down products of PA_{83}. Cultures performed as described in Figure 6.2. Western blot performed as described in Section 2.6.8.

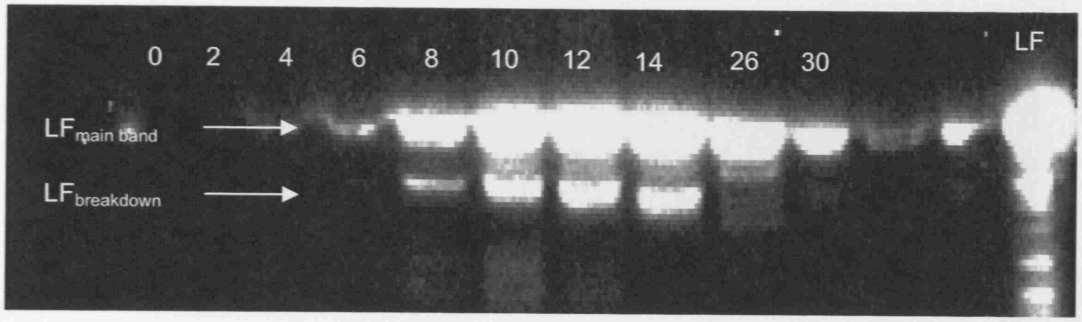

Figure 6.5 A Western Blot showing the time course of LF degradation in the miniature bioreactor under unaerated conditions. The number above each well indicates the fermentation time in hours at which the sample was taken. The LF standard was created using rLF and shows several low molecular weight bands which are break down products. Cultures performed as described in Figure 6.2. Western blot performed as described in Section 2.6.8.

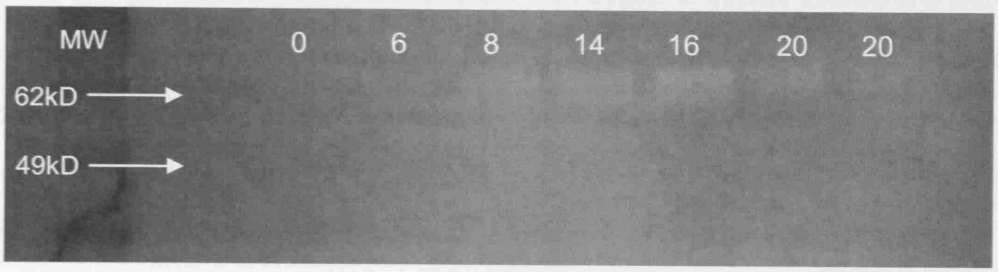

Figure 6.6 A zymogram showing the level of protease activity during the time course of a typical bioreactor run under unaerated conditions. The numbers above each well correspond to the fermentation time in hours at which the sample was taken. Cultures performed as described in Figure 6.2. Zymogram performed as described in Section 2.6.10.

This was done to evaluate the potential of using a two stage operation for vaccine production; where initially the bioreactor is aerated to quickly produce biomass after which point aeration is stopped to promote antigen production. In Figure 6.7 the culture is aerated for the first 13 hours during which time bacterial growth is in exponential phase. There appears to be no lag in cell growth. The pH increases rapidly to 9.2 a result of the air reacting with the bicarbonate in the media but then begins to decline steadily and glucose is also slowly depleted. Once aeration is stopped there is a sharp decline in glucose and in response pH as well. Figure 6.8 shows that there was poor PA production and no LF production during aeration. It appears antigen production is hindered by aeration. When aeration is stopped PA production begins to recover.

In order to prove that the initial increase in pH observed in Figure 6.7 was due air reacting with the bicarbonate in the medium, pH was monitored in aerated sterile growth medium (Figure 6.9). There was no aeration for the first five minutes but after this time, air was sparged through the bioreactor at 0.6vvm and consequently an increase in pH was seen. It is possible that the combination of heat and aeration is causing the sodium bicarbonate in the medium to break down forming a mild alkaline solution. The bicarbonate ion itself has a pK_a value of 6.3 causing it to form a base in water. This reaction would release carbon dioxide into the media which would explain the initial low level expression of PA observed in Figure 6.8, as within the first few hours a high CO_2 environment would have been created. Yet as aeration continued, most of the carbon dioxide in the media and head space would have been stripped out of the liquid phase. Consequently a slow down in PA expression was monitored, which reached zero by 14 hours. However, when aeration was stopped at 13 hours there was a small recovery in PA expression along with a steady decline in pH. This may be due to a small amount of acid released into the media through glucose metabolism reacting with residual bicarbonate to release carbon dioxide once again, but because the amount of carbon dioxide evolved was so low, antigen expression remained within the nanogram range.

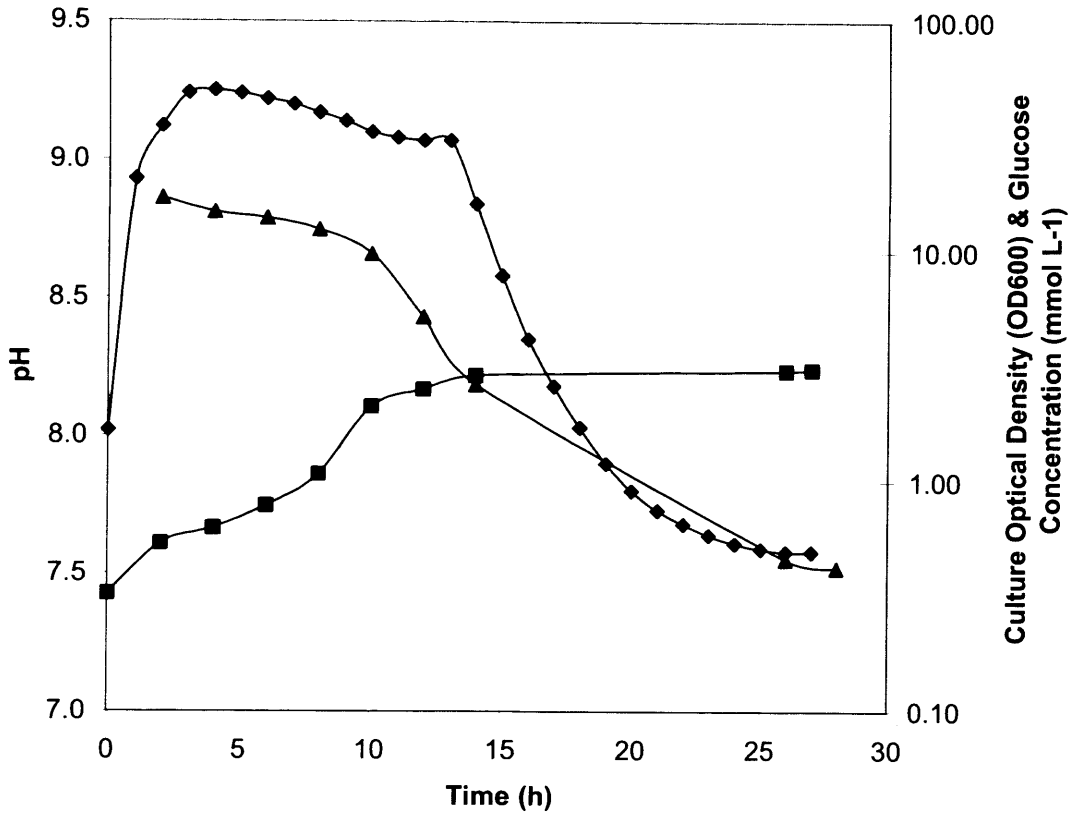

Figure 6.7 Batch fermentation kinetics of an intermittently aerated *B. anthracis* Sterne $34F_2$ culture in the miniature bioreactor: (■) culture optical density, (◆) culture pH, (▲) glucose concentration. Experiment performed as described in Section 2.3.6. The culture was continuously agitated at 700rpm and initially aerated at 0.68 vvm, but aeration was stopped after 13 hours.

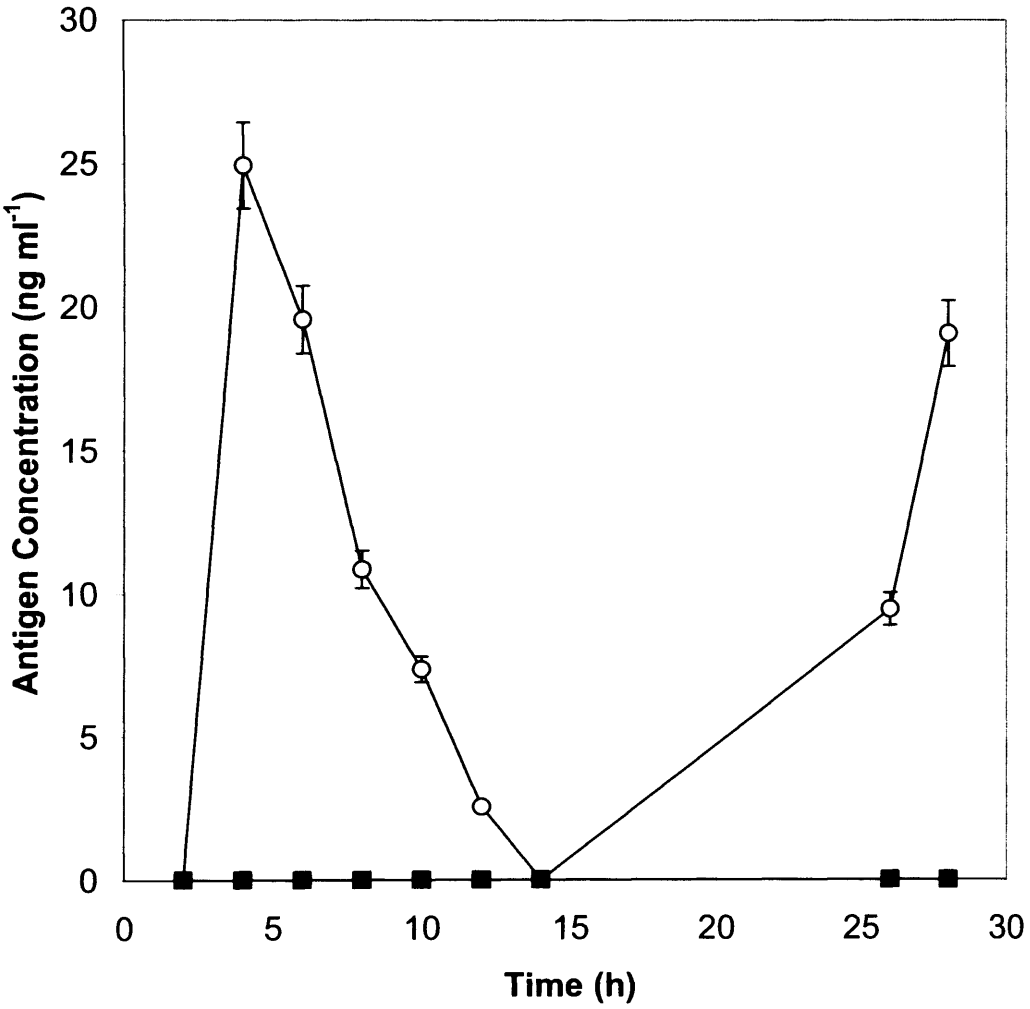

Figure 6.8 PA and LF production during the intermittently aerated miniature bioreactor culture described in Figure 6.7: (○) PA titres, (■) LF titres. PA and LF quantified as in Sections 2.6.6 and 2.6.7. The error bars represent one standard deviation about the mean, where n=3.

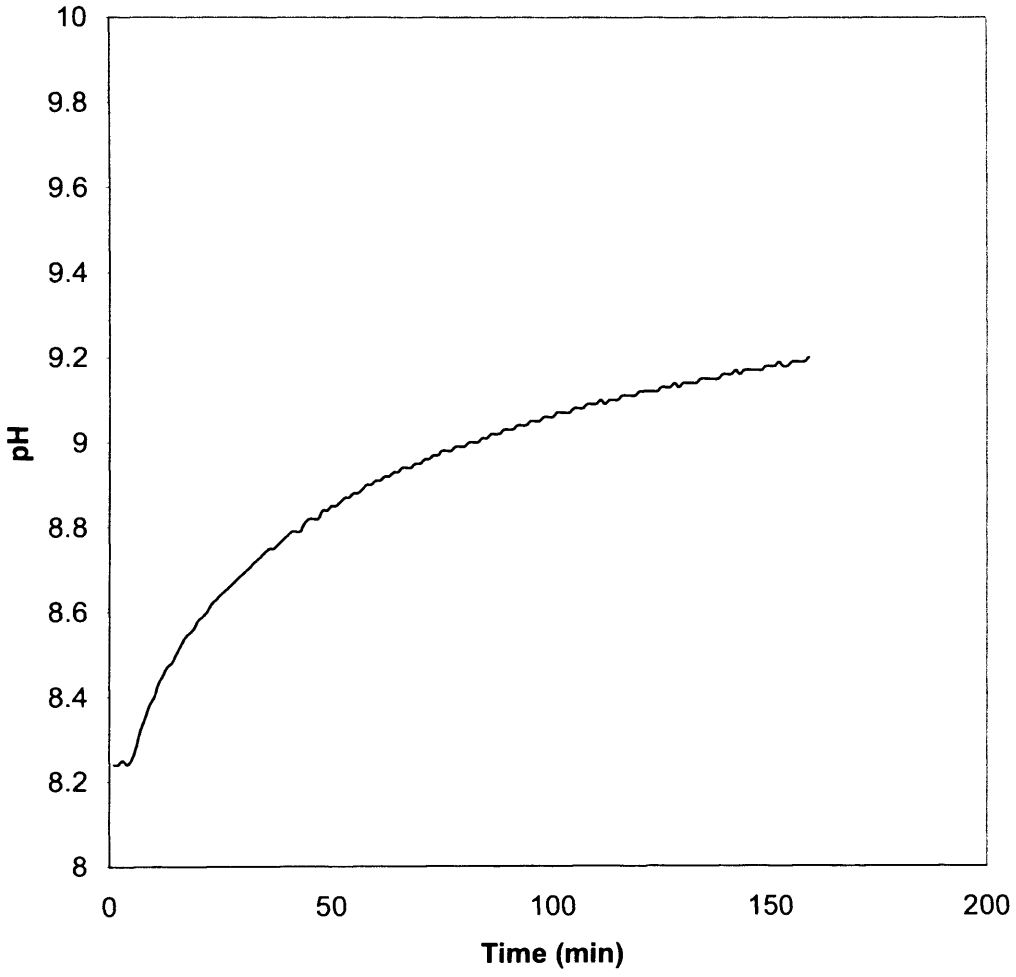

Figure 6.9 The effect of aeration on sterile basal medium. The pH probe was given five minutes to equilibrate to pH 8.25 before the media was aerated at 0.6vvm. Experiment performed as described in Section 2.3.6.

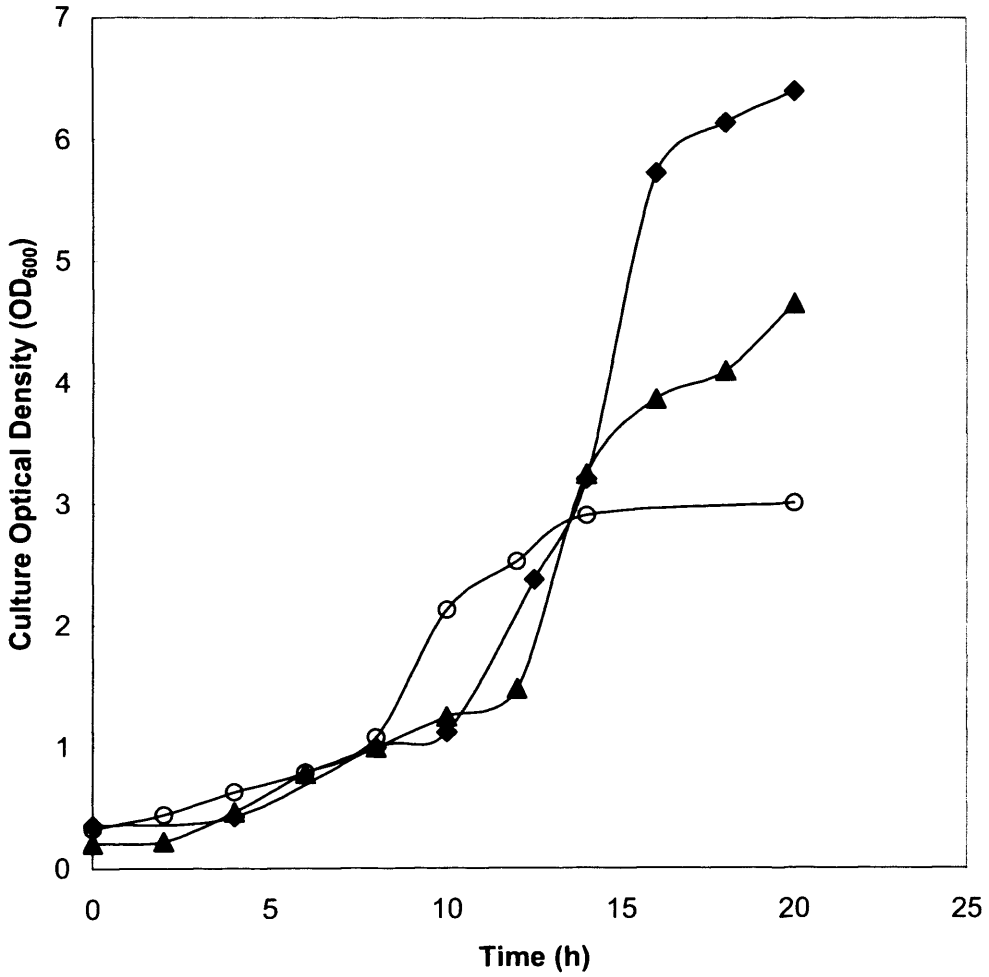

Figure 6.10 The effect of glucose concentration in the growth medium on biomass production: (◆) 10gL^{-1} glucose (▲) 5gL^{-1} glucose, (○) 2gL^{-1} glucose. Experiments performed as described in Section 2.3.6.

Biomass production can be increased in the usual manner by altering the amount of glucose in the media and increasing aeration. As seen in Figure 6.10 *B. anthracis* is grown in media with different initial concentrations of glucose. As glucose concentration is increased the biomass concentration also increased and reached a maximum optical density of 6.4 OD_{600} with 10g L^{-1} glucose after 20 hours. This requires the culture to be aerated as without it *B. anthracis* growth was limited and yielded a similar growth profile as seen in Figure 6.2. It is not possible however to increase antigen yields. In fact, with any amount of aeration a rapid decline in PA and LF titres was observed. Hence, the data indicates that aeration itself has a detrimental effect on antigen expression as there was sufficient glucose available in the media to support antigen expression.

6.6 Characterisation of the negative effects of aeration

To further investigate the effect of aeration on antigen stability a non-aerated culture was performed in the miniature bioreactor as previously described in Section 6.3. However, the bioreactor was aerated at 0.44vvm between 16-17 hours, after which time the gas ports were once again sealed.

As shown in Figure 6.11 and 6.12, during the first 16 hours the fermentation behaved as previously seen in Figure 6.2. The culture entered exponential phase by the fourth hour and by the sixth hour glucose and subsequently pH began to decline, an indication of primary metabolism. By the fourteenth hour all the glucose had been depleted, pH began to increase and the culture entered stationary phase; there was a constant optical density of 2.6 OD_{600} and PA titres reached 10μg mL^{-1}. When aeration was applied between 16 and 17 hours, PA titres diminish from 12μg mL^{-1} to 0.8μg mL^{-1}. At the same time there is a decrease in pH from 8.1 to 7.8, but this is within the normal range for vaccine production. As soon as aeration is stopped antigen titres recovered slightly, but gradually declined over time. Meanwhile, the culture optical density increases from 2.73 OD_{600} at 17 hours to

4.01OD_{600} at 26 hours. Assays for protease activity using a zymogram (Figure 6.13) with time points before, during and after aeration, detect a steady build up of proteases up to 16 hours, but protease titres decline during aeration and never recover after aeration was stopped. Post 17 hours, proteases were still present in the media which may have accounted for the low PA titres witnessed even after aeration is discontinued.

It is possible that three separate phenomena are being observed in this experiment. The first is that the initial drop in antigen titres is related to aeration itself, causing the marked fall from 12µg mL^{-1} to 0.8µg mL^{-1}. The second is that after an initial recovery, the continued fall in titres was linked to amino acid metabolism, which would also explain the increase in both pH and biomass production. It is known that *B. anthracis* is a chemoheterotroph (Todar 2005), and is capable of metabolising a variety of carbon sources. Considering that all the glucose had been metabolised by this stage it is possible that the bacteria had shifted to using amino acids as their primary carbon source. This would explain both the increase in biomass and pH as free ammonia was released into the media. Finally, as a consequence of opening the gas ports and allowing aeration, the previous high carbon dioxide environment was lost, thus creating an atmosphere not conducive for antigen expression.

6.7 Scale-up considerations

Based on the assumption that the HPA wishes to maintain the current production level at 228 bottles, each with a volume of 500mL, the present production volume is 114 litres. Since the vaccine can be cultured in half the time in a stirred tank reactor, a vessel only half the size would be required to produce the same amount of vaccine in the same time frame. Therefore, one 70 litre bioreactor should be sufficient to meet demands, with a working volume of 57 litres as described in Appendix A. This strategy enhances process

safety as the total volume of *B. anthracis* handled at any one time is halved from 114 litres using Thompson bottles to just 57 litres using a bioreactor.

Kinematic scale up can be achieved by maintaining constant power per unit volume. The miniature bioreactor used an impeller diameter of 0.02m at 700rpm and generated a P/V= $445Wm^{-3}$. In order to maintain the same ratio the 70 litre fermenter, calculated to have an impeller diameter of 0.22m will require a minimum rotational speed of 115 rpm. This of course would require experimental verification.

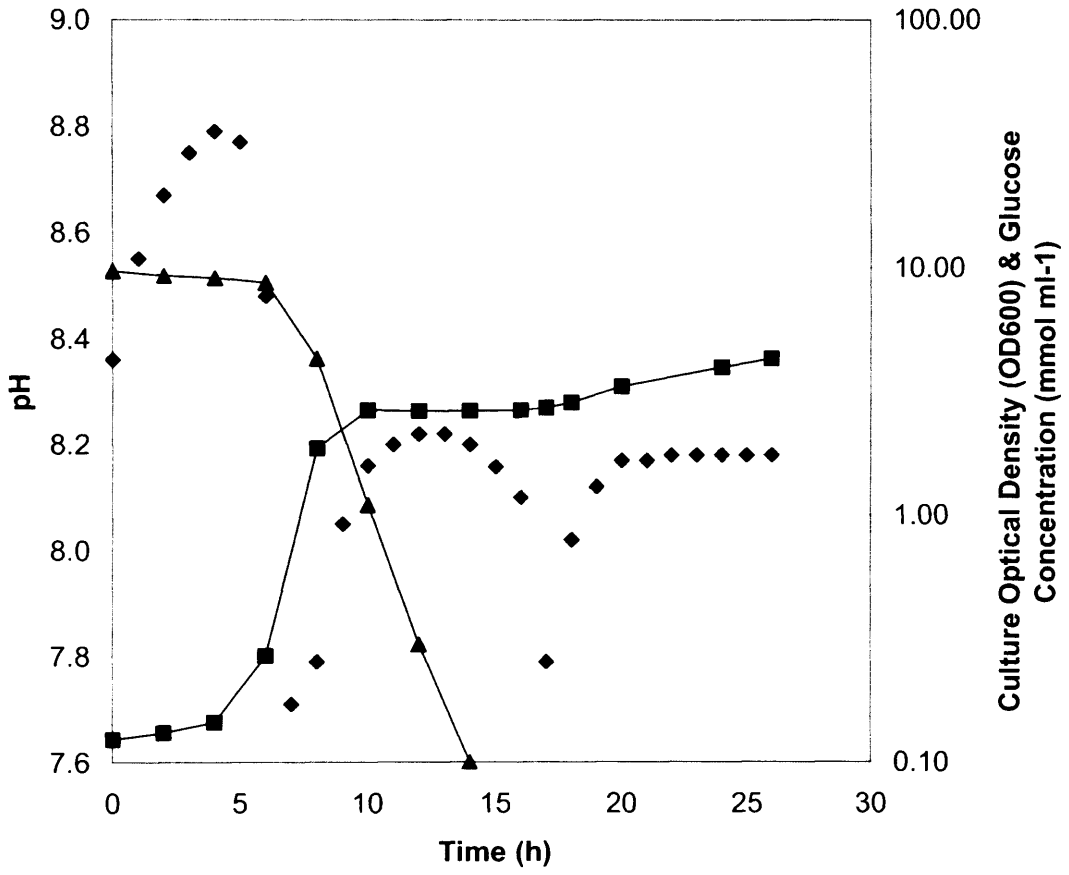

Figure 6.11 Batch fermentation kinetics of *B. anthracis* Sterne $34F_2$ culture in the miniature bioreactor aerated between hours 16 and 17, as represented by the shaded region: (■) culture optical density, (◆) culture pH, (▲) glucose concentration. Experiment performed as described in Section 2.3.6, except that between hours 16 and 17 the gas ports were opened and air was sparged into the bioreactor at 0.44vvm.

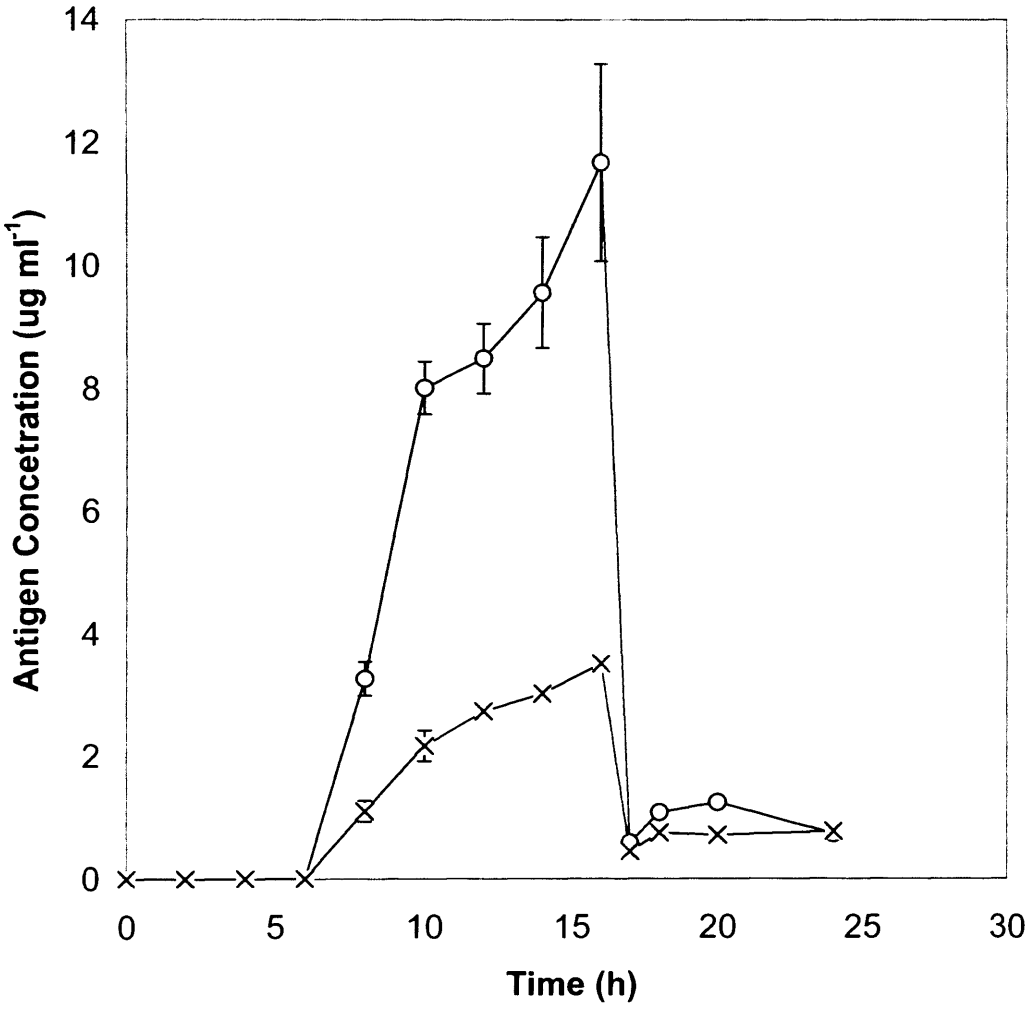

Figure 6.12 Antigen production during the miniature bioreactor run described in Figure 6.11: (○) PA titres, (×) LF titres. The grey shading represents the period of time when the culture was aerated at 0.44 vvm. Experiment performed as described in Figure 6.11. PA and LF quantified as in Sections 2.6.6 and 2.6.7. The error bars represent one standard deviation about the mean, where n=3.

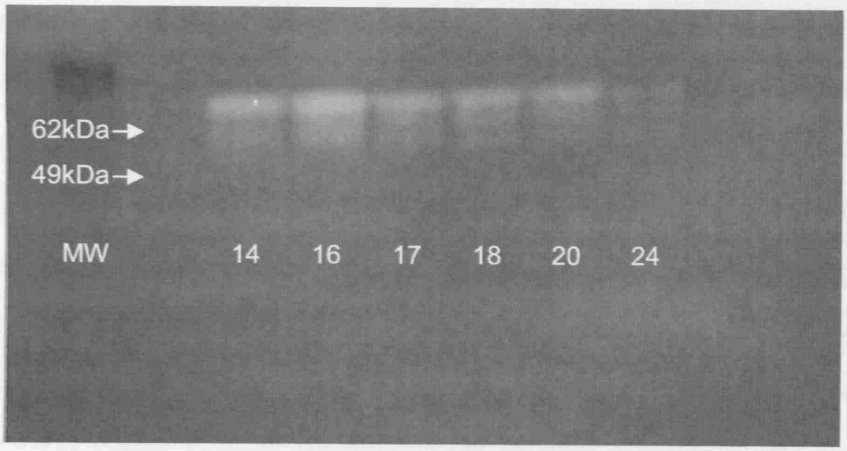

Figure 6.13 A zymogram showing the level of protease activity before, during and after aeration of the bioreactor culture in Figure 6.11. Culture performed as described in Figure 6.11 and zymogram performed as described in Section 2.6.10.

6.8 Summary

Thompson bottles are not readily scaleable which means that the only possible increase in production was through sideways expansion of present production methods. Unfortunately, because the vaccine is already licensed the production method remains locked. Therefore, any deviation from the current manufacturing method would require a re-evaluation of that license and clinical trials using the two-animal model (FDA 2001). Moving production into stirred tank reactors may be ideal, but before adopting this approach it was important to evaluate the costs versus benefits. It must be shown that the benefits that changes may bring outweigh the costs associated with changing the license, coupled with loss of revenue and investing in a containment level 3 production scale bioreactor. Though there is precedent of *B. anthracis* being grown in stirred tank reactors, established by the US production of Biothrax™, the strain and production methods are different. Biothrax™ uses the *B. anthracis* Vollum V770-NP1-R strain under nitrogen sparging (Puziss *et al.* 1963), whereas *B. anthracis* Sterne $34F_2$ has yet to be cultivated in stirred tank reactors.

The miniature bioreactor has allowed the evaluation of potential process transfer to stirred tank reactors without any significant capital costs. Due to its small footprint, it can be easily placed within existing containment level 3 facilities allowing investigation before investment. The use of the miniature bioreactor revealed that not only is vaccine production possible in bioreactors (Figure 6.2), but that it can potentially increase antigen titres and reduce production time (Figure 6.3). The main reason for this is that growth kinetics were no longer diffusion limited in a stirred tank system, which accounts for halving the production time. Antigen degradation may be an issue. Theoretically greater antigen titres could be realised through prolonged culture times but this leads to greater antigen degradation (Figures 6.4 and 6.5). Although it should be noted that there is no clinical evidence to suggest that intact PA or LF elicits a better immune response then their

degraded counterparts. In fact PA_{63} has been demonstrated to confer protection in rabbit and primate inhalation anthrax challenge experiments (Hepler *et al.* 2006).

Aeration has proven to be a major detrimental factor in anthrax toxin production. Based on the observations made in Figures 6.11 and 6.12, two mechanisms are hypothesised to be active during aeration, one hydrodynamic and the other physiological. It is well documented that globular proteins in solution are remarkably resilient to hydrodynamic shear forces (Thomas and Dunnill 1979). However, when the intense mixing that generally occurs in bioreactors is coupled with an air-liquid interface, alterations to the protein structure can occur (Hoare and Dunnill 1989;Virkar *et al.* 1981). It may be that PA and LF are both sensitive to the destructive effects of the gas-liquid interface, since once aeration was stopped an initial recovery of PA titres was observed allowing its accumulation in the media. A feasible remedy is the use of shear protectants, such as Pluronic F68 commonly used in mammalian cell culture to reduce the effects of shear on cells and proteins (Keane *et al.* 2003). The physiological effect may be related to the activation of the anthrax toxin attenuator (AtxA). Though the exact mechanism has yet to be determined it is known that a high carbon dioxide environment has a positive effect on AtxA which in turn causes the expression of the anthrax toxin proteins, PA, LF and EF (Mignot *et al.* 2003). These results add weight to a CO_2/O_2 switch. AtxA expression is CO_2 dependent (Hoffmaster and Koehler 1997) and during aeration any carbon dioxide evolved from the culture is expelled. Even after aeration is stopped the result is a highly oxygenated culture post hour 17 in Figure 6.12. PA levels begin to decline, especially after 20 hours. However, this is not due to proteolytic effects, nor the mechanical effects of a gas-liquid interface. The result must be due to physiological effects and knowing that a high O_2 / low CO_2 environment is present after aeration has stopped may account for the drop in PA through AtxA decay.

The factorial design experiment from Section 5.3 indicated that *B. anthracis* vaccine production in a stirred tank may be possible. The experiments conducted in the miniature

bioreactor have allowed the investigation of these reasons and allowed the advancement of process conditions to overcome these limitations. The work presented in this chapter has shown that anthrax vaccine production by *B. anthracis* Sterne $34F_2$ is feasible in a stirred tank reactor and it has allowed for the definition of a detailed harvest criteria. The switch to a more highly instrumented bioreactor culture allows more criteria to be added and monitored, which will increase confidence in each production run. Not only should pH be used as a harvest criterion, but monitoring for the glucose to drop below 1mmol L^{-1} and to limit culture kinetics to the fourth hour of stationary phase allows for a more sophisticated process which should minimise vaccine variability.

The miniature bioreactor has achieved all of the chapter objectives, but its main benefits are speed and cost. It has also identified potential process pitfalls which may occur in a commercial scale bioreactor using only millilitres of material.

7 Conclusions and future work

7.1 Conclusion

The main findings of the thesis are summarised with respect to the specific aim and objectives identified in Section 1.6.

The identified need of a micro-scale platform which can generate quantitative results was achieved by using microtitre plates of different geometries with statistical DOE. Chapter 3 specifically focused on applying this newly established microwell platform to *N. lactamica* fermentations. The first aspect was media development with respect to *N. lactamica* growth. This was improved upon through the creation of two new media, MCD and MC7, both of which improved upon biomass yields produced by the original Frantz medium (Figure 3.5). However, upon analysis of the antigen profile using SELDI-MS it was noted that MC7 medium generated the best profile overall. This was confirmed in the purified OMVs, improving on NspA, RmpM and PorB titre by three, six and three fold respectively, when compared with Frantz medium (Figure 3.10). The scale-up of microwell data was achieved in *N. lactamica* by exploiting its trait as a strict aerobe. By establishing that *N. lactamica* growth is a function of aeration in 2 L bioreactors (Figure 3.12) it was then possible to develop a scale up correlation using dimensionless analysis (Equation 3.8). Tested, this proved to be effective for a wide range of bioreactor scales (Figure 3.17).

Combining the micro-scale platform with USD tools created a method of analysing potential downstream purification route and indeed proposing a new purification routes (Figure 4.1). The ability to mimic the key traits of a unit operation, rather then the unit operation itself has allowed the assessment of product loss due to the hydrodynamic forces the purification stream would experience. The quantification of shear especially and its impact on product loss allows the inclusion or exclusion of certain unit operations based on shear effects.

Using the methods developed in the microwell culture platform from Chapter 3, the generic application of the technique was applied to create a Thompson bottle mimic in microwells (Figure 5.2). This mimic allowed the investigation of the anthrax vaccine process and specifically identifies the main factors responsible for cell growth, PA and LF production (Section 5.3). The newly created microwell mimic also allowed for the investigation of quorum sensing in *B. anthracis* demonstrating that it this cell density dependent signalling mechanism controlled growth and antigen production (Section 5.4).

Finally, a miniature bioreactor cultivation system was created in a containment level 3 conditions to evaluate the effect of a stirred, homogeneous culture environment on *B. anthracis* cell growth and antigen production. The results proved to be very encouraging as a side by side comparison of static and stirred culture environments illustrated that stirred culture achieved the same cell growth and antigen titres in half the time (Section 6.2 and 6.3). The miniature bioreactor also revealed that antigen production was susceptible to hydrodynamic shear effects. Repeated bioreactor runs show that bioreactor cultivation would increase antigen titres (Figure 6.3) but prolonged culture leads to increased antigen degradation and protease activity (Figures 6.4-6.6) not previously measured in Thompson bottles.

7.2 Future Work

The outcome of this research has shown the potential benefits of the micro-scale platform approach to vaccine development. It has also provided areas for further investigations. Specifically these are:

- For *N. lactamica*, further experiments into the scale-up correlation generated in Chapter 3. The basis of scale-up was to use biomass generation as an indication

of oxygenation. Optical probes could be employed to directly measure dissolved oxygen in microwell cultures to verify the model.

- Fermentations were conducted under non-oxygen limiting conditions to measure the maximum growth and biomass generation possible in *N. lactamica*. Fermentations should be conducted under oxygen-limiting condition to test the model, as lower oxygenation should push the data points in Figure 3.17 further left – confirming if oxygenation is the basis of the model.

- Chapter 4 outlined a potential downstream purification route for N. lactamica OMV using USD tools and micro-scale experiments. The route improved route identified (Figure 4.1(c)) has yet to be verified on the commercial scale. It is important to verify the predicted results and calculated antigen yields as this will validate the method.

- Quorum sensing proved to be a very interesting phenomenon that may impact on *B. anthracis*, but it has produced many more questions. At the end of Chapter 5 a 5.8kDa protein was identified as possibly being involved in quorum sensing. This protein may be further processed, cleaved or indeed have nothing to do with quorum sensing. Efforts should be made to characterise the lower molecular weight proteins present in *B. anthracis* culture supernatant and identify those which have links to quorum sensing.

- In applying the quorum sensing work to *B. anthracis* culture in Thompson bottles, it would be interesting to measure the effect of increased inoculum levels upon Thompson bottle culture and monitor if this reduced the time required for cell growth, PA and LF production. By definition, quorum sensing is a population

density dependent form of signalling, thus by increasing the starting inoculum level could this may allow the cells to reach competence earlier.

- Chapter 6 revealed that *B. anthracis* culture is possible in stirred culture, but that aeration had a detrimental effect on antigen production. To test the hypothesis that antigen degradation was linked to hydrodynamic shear forces, cultures of *B. anthracis* should be conducted using a shear protectant, such as Pluronic F68 commonly used in mammalian cell culture, should be conducted to measure the effect upon PA and LF concentrations.

- This work has identify the key traits required of a quantitative micro-scale platform for vaccine development, but has not looked into its automation. The next step would be to integrate the platform into automated liquid handling systems and evaluate the throughput and time benefits possible.

8 References

Alexander,A.E. and Posner,A.M. (1950) A method of integrating the Gibbs adsorption isotherm. *Nature* **166**, 432-433.

Allison, N. and Tranter, H. S. (2003) From vaccine research to manufacture. In *Vaccine Protocols: Methods in Molecular Medicine (Vol 87)* ed. Robinson,A. pp. 391-407. Totowa, NJ, USA: Humana Press Inc.

Axton,J.M.H. (1972) Six cases of poisoning after a parenteral organic mercurial compound (merthiolate). *Postgrad Med J* **48**, 417-421.

Ball,L.K., Ball,R. and Pratt,R.D. (2001) An assessment of thimerosal use in childhood vaccines. *Pediatrics* **107**, 1147-1154.

Banks, G. T. (1979) Scale up of fermentation processes. In *Topics in Enzyme and Fermentation Biotechnology* ed. Wiseman,A. pp. 170-267. Chichister: Ellis Horwood.

Bartholomew,W.H., Karrow,E.O., Sfat,M.R. and Wilhelm,R.H. (1950) Oxygen transfer and agitation in submerged fermentations. Mass tranfer of oxygen in submerged fermentations of *Streptomyces griseus*. *Ind. Eng. Chem.* **42**, 1801-1809.

Bassler,B.L. (1999) How bacteria talk to each other: regulation of gene expression by quorum sensing. *Curr. Opin. Microbiol.* **2**, 582-587.

Bassler,B.L., Wright,M., Showalter,R.E. and Silverman,M.R. (1993) Intercellular signalling in *Vibrio harveyi*: sequence and function of genes regulating expression of luminescence. *Mol. Microbiol.* **9**, 773-786.

Bassler,B.L., Wright,M. and Silverman,M.R. (1994) Multiple signaling systems controlling expression of luminescence in *Vibrio harveyi*: sequence and function of genes encoding a second sensory pathway. *Mol. Microbiol.* **13**, 273-286.

Beall,F.A., Taylor,M. and Thorne,C.B. (1962) Rapid lethal effect in rats of a third component found upon fractionating the toxin of *Bacillus anthracis*. *J Bacteriol.* **83**, 1274-1280.

Bell,G.H. and Gallo,M. (1971) Effect of impurities on oxygen transfer. *Process Biochem.* **6**, 33-35.

Betts,J.I., Doig,S.D. and Baganz,F. (2006) Characterization and application of a miniature 10 mL stirred-tank bioreactor, showing scale-down equivalence with a conventional 7 L reactor. *Biotechnol. Prog.* **22**, 681-688.

Boccazzi,P., Zhang,Z., Kurosawa,K., Szita,N., Bhattacharya,S., Jensen,K.F. and Sinskey,A.J. (2006) Differential gene expression profiles and real-time measurements of growth parameters in *Saccharomyces cerevisiae* grown in microliter-scale bioreactors equipped with internal stirring. *Biotechnol Prog.* **22**, 710-717.

Boulding,N., Yim,S.S., Keshavarz-Moore,E., Shamlou,P.A. and Berry,M. (2002) Ultra scale-down to predict filtering centrifugation of secreted antibody fragments from fungal broth. *Biotechnol. Bioeng.* **79**, 381-388.

Boychyn,M., Doyle,W., Bulmer,M., More,J. and Hoare,M. (2000) Laboratory scale-down of protein purification processes involving fractional precipitation and centrifugal recovery. *Biotechnol. Bioeng.* **69**, 1-10.

Boychyn,M., Yim,S.S., Bulmer,M., More,J., Bracewell,D.G. and Hoare,M. (2004) Performance prediction of industrial centrifuges using scale-down models. *Bioprocess. Biosyst. Eng* **26**, 385-391.

Boychyn,M., Yim,S.S.S., Shamlou,P.A., Bulmer,M., More,J. and Hoare,A. (2001) Characterization of flow intensity in continuous centrifuges for the development of laboratory mimics. *Chemical Engineering Science* **56**, 4759-4770.

Brachman,P.S. (2002) Bioterrorism: an update with a focus on anthrax. *Am. J. Epidemiol.* **155**, 981-987.

Bruge,J., Bouveret-Le Cam,N., Danve,B., Rougon,G. and Schulz,D. (2004) Clinical evaluation of a group B meningococcal N-propionylated polysaccharide conjugate vaccine in adult, male volunteers. *Vaccine* **22**, 1087-1096.

Büchs,J. (2001) Introduction to advantages and problems of shaken cultures. *Biochemical Engineering Journal* **7**, 91-98.

Buckingham,E. (1914) On physically similar systems; illustrations of the use of dimensional equations. *Physical Review* **4**, 345-376.

Cao,Y. (2006) Optimization of expression of *dha*T gene encoding 1,3-propanediol oxidoreductase from *Klebsiella pneumoniae* in *Escherichia coli* using the methods of uniform design and regression analysis. *J. Chem. Technol. Biotechnol.* **81**, 109-112.

Cartwright,K., Morris,R., Rumke,H., Fox,A., Ray,B., Begg,N., Richmond,P. and Poolman,J. (1999) Immunogenicity and reactogenicity in UK infants of a novel meningococcal vesicle vaccine containing multiple class 1 (PorA) outer membrane proteins. *Vaccine* **17**, 2612-2619.

Catlin BW. (1973) Nutritional profiles of Neisseria gonorrhoeae, Neisseria meningitidis, and Neisseria lactamica in chemically defined media and the use of growth requirements for gonococcal typing. *Journal of Infectious Diseases* **128**, 178-194.

Charlton,S., Herbert,M., McGlashan,J., King,A., Jones,P., West,K., Roberts,A., Silman,N., Marks,T., Hudson,M.J. and Hallis,B. (2007) A study of the physiology of *Bacillus anthracis*

Sterne during manufacture of the UK acellular anthrax vaccine. (2007) *J. Appl. Microbiol.* ***103***,1453-1460.

Chen,X., Schauder,S., Pelczer,I., Bassler,B.L., Hughson,F.M., Potier,N. and Van Dorsselaer,A. (2002) Structural identification of a bacterial quorum-sensing signal containing boron. *Nature* **415**, 2-69-2-70.

Coen,P.G., Cartwright,K. and Stuart,J. (2000) Mathematical modelling of infection and disease due to *Neisseria meningitidis* and *Neisseria lactamica*. *Int. J. Epidemiol.* **29**, 180-188.

Danve,B., Lissolo,L., Mignon,M., Dumas,P., Colombani,S., Schryvers,A.B. and Quentin-Millet,M.J. (1993) Transferrin-binding proteins isolated from *Neisseria meningitidis* elicit protective and bactericidal antibodies in laboratory animals. *Vaccine* **11**, 1214-1220.

de Kievit,T.R., Gillis,R., Marx,S., Brown,C. and Iglewski,B.H. (2001) Quorum-sensing genes in *Pseudomonas aeruginosa* Biofilms: Their role and expression patterns. *App. Environ. Microbiol.* **67**, 1865-1873.

de Kievit,T.R. and Iglewski,B.H. (2000) Bacterial Quorum sensing in pathogenic relationships. *Infect. Immun.* **68**, 4839-4849.

Devlin, J. P. (1997) *High throughput screening; the discovery of bioactive substances.* Marcecl Dekker.

Doig,S.D., Avenell,P.J., Bird,P.A., Gallati,P., Lander,K.S., Lye,G.J., Wohlgemuth,R. and Woodley,J.M. (2002) Reactor operation and scale-up of whole cell Baeyer-Villiger catalyzed lactone synthesis. *Biotechnol. Prog.* **18**, 1039-1046.

Doig,S.D., Ortiz-Ochoa,K., Ward,J.M. and Baganz,F. (2005) Characterization of oxygen transfer in miniature and lab-scale bubble column bioreactors and comparison of microbial growth performance based on constant k(L)a. *Biotechnol Prog.* **21**, 1175-1182.

Doran, P. M. (2003) Mass Transfer. In *Bioprocess Engineering Principles* pp. 192-193. London: Academic Press.

Dudley,G. and McFee,R.B. (2005) Preparedness for biological terrorism in the United States: Project BioShield and beyond. *Journal of the American Osteopathic Association* **105**, 417-424.

Duesbery,N.S., Webb,C.P., Leppla,S.H., Gordon,V.M., Klimpel,K.R., Copeland,T.D., Ahn,N.G., Oskarsson,M.K., Fukasawa,K., Paull,K.D. and Vande Woude,G.F. (1998) Proteolytic inactivation of MAP-kinase-kinase by anthrax lethal factor. *Science* **280**, 734-737.

Elmahdi,I., Baganz,F., Dixon,K., Harrop,T., Sugden,D. and Lye,G.J. (2003) pH control in microwell fermentations of *S. erythraea* CA340: influence on biomass growth kinetics and erythromycin biosynthesis. *Biochem. Eng. J.* **16**, 299-310.

FDA. New Drug and Biological Drug Products; Evidence needed to demonstrate effectiveness of new drugs when human efficacy studies are not ethical or feasible (Animal Rule). 21 CFR Parts 314 and 610. 2001.
Ref Type: Statute

Fenner, F., Henderson, D. A., Arita, I., Jezek, Z. and Ladnyi, I. D. Smallpox and its erradication. 1988. Geneva, World Health Organisation.
Ref Type: Report

Ferreira-Torres,C., Micheletti,M. and Lye,G.J. (2005) Microscale process evaluation of recombinant biocatalyst libraries: application to Baeyer–Villiger monooxygenase catalysed lactone synthesis. *Bioprocess. Biosyst. Eng* **28**, 83-93.

Food and Drug Administration - CDER. Guidance for Industry, Investigators, and Reviewers Exploratory IND Studies. 2006.

Fredriksen,J.H., Rosenqvist,E., Wedege,E., Bryn,K., Bjune,G., Froholm,L.O., Lindbak,A.K., Mogster,B., Namork,E. and Rye,U. (1991) Production, characterization and control of MenB-vaccine "Folkehelsa": an outer membrane vesicle vaccine against group B meningococcal disease. *NIPH Ann.* **14**, 67-79.

Freeman,J.A. and Bassler,B.L. (1999a) A genetic analysis of the function of LuxO, a two-component response regulator involved in quorum sensing in *Vibrio harveyi. Mol. Microbiol.* **31**, 665-677.

Freeman,J.A. and Bassler,B.L. (1999b) Sequence and function of LuxU: a two-component phosphorelay protein that regulates quorum sensing in *Vibrio harveyi. J Bacteriol.* **181**, 899-906.

Freeman,J.A., Lilley,B.N. and Bassler,B.L. (2000) A genetic analysis of the functions of LuxN: a two-component hybrid sensor kinase that regulates quorum sensing in *Vibrio harveyi. Mol. Microbiol.* **35**, 139-149.

Fu,J., Bailey,F.J., King,J.J., Parker,C.B., Robinett,R.S., Kolodin,D.G., George,H.A. and Herber,W.K. (1995) Recent advances in the large scale fermentation of *Neisseria meningitidis* group B for the production of an outer membrane protein complex. *Biotechnol.* **13**, 170-174.

Fuller,E.N., Schettler,P.D. and Giddings,J.C. (1966) New method for the prediction of binary phase-gas diffusion coefficients. *Ind. Eng. Chem.* **58**, 18-27.

Fuqua,C., Winans,S.C. and Greenberg,E.P. (1996) Census and consensus in bacterial ecosystems: the LuxR-LuxI family of quorum-sensing transcriptional regulators. *Annu. Rev. Microbiol.* **50**, 727-751.

Ghorab,M. and Adeyeye,M.C. (2001) Enhancement of ibuprofen dissolution via wet granulation with beta-cyclodextrin. *Pharm Develop Technol* **6**, 303-312.

Gill, N. K. Design and characterisation of parallel miniature bioreactors for bioprocess optimisation and scale up. (2007a).
Ref Type: Thesis/Dissertation

Gill,N.K., Appleton,M., Baganz,F. and Lye,G.J. (2007b) Design and characterisation of a miniature stirred bioreactor system for parallel microbial fermentations. *Biochem. Eng. J. In press.*

Girard,P., Jordan,M., sao,M. and urm,F.M. (2001) Small-scale bioreactor system for process development and optimization. *Biochem. Eng. J.* **7**, 117-119.

Gold,R., Goldschneider,I., Lepow,M.L., Draper,T.F. and Randolf,M. (1978) Carriage of *Neisseria meningitidis* and *Neisseria lactamica* in infants and children. *J. Infec. Dis.* **137**, 112-121.

Goldschneider,I., Gotschlich,E.C. and Artenstein,M.S. (1969) Human immunity to the meningococcus. II. Development of natural immunity. *J. Exp. Med.* **129**, 1327-1348.

Gorringe,A., Halliwell,D., Matheson,M., Reddin,K., Finney,M. and Hudson,M. (2005a) The development of a meningococcal disease vaccine based on *Neisseria lactamica* outer membrane vesicles. *Vaccine* **23**, 2210-2213.

Gorringe,A.R., Reddin,K.M., Funnell,S.G., Johansson,L., Rytkonen,A. and Jonsson,A.B. (2005b) Experimental disease models for the assessment of meningococcal vaccines. *Vaccine* **23**, 2214-2217.

Grabenstein,J.D. (2003) Anthrax vaccine: a review. *Immunol. Allergy Clin. North Am.* **23**, 713-730.

Gram,L., de Nys,R., Maximilien,R., Givskov,M., Steinberg,P. and Kjelleberg,S. (1996) Inhibitory effects of secondary metabolites from the red alga *Delisea pulchra* on swarming motility of *Proteus mirabilis*. *J Bacteriol.* **178**, 6618-6622.

Griffiss,J.M., Yamasaki,R., Estabrook,M. and Kim,J.J. (1991) Meningococcal molecular mimicry and the search for an ideal vaccine. *Trans. R. Soc. Trop. Med Hyg.* **85 Suppl 1**, 32-36.

Guidi-Rontani,C., Weber-Levy,M., Labruyere,E. and Mock,M. (1999) Germination of *Bacillus anthracis* spores within alveolar macrophages. *Mol. Microbiol.* **31**, 9-17.

Hajduk,P.J. and Greer,J. (2007) A decade of fragment-based drug design: strategic advances and lessons learned. *Nat Rev Drug Discov* **6**, 211-219.

Hambleton,P., Carman,J.A. and Melling,J. (1984) Anthrax: the disease in relation to vaccines. *Vaccine* **2**, 125-132.

Harris, E. L. V. (1989) Concentration of the extract. In *Protein Purification Methods* ed. Harris,E.L.V. IRL Press.

Helting,T.B., Guthohrlein,G., Blackkolb,F. and Ronneberger,H. (1981) Serotype determinant protein of *Neisseria Meningitidis*. Large scale preparation by direct detergent treatment of the bacterial cells. *Acta Pathol. Microbiol. Scand. [C.]* **89**, 69-78.

Henke,J.M. and Bassler,B.L. (2004) Quorum sensing regulates type III secretion in *Vibrio harveyi* and *Vibrio parahaemolyticus*. *J Bacteriol.* **186**, 3794-3805.

Hepler,R.W., Kelly,R., McNeely,T.B., Fan,H., Losada,M.C., George,H.A., Woods,A., Cope,L.D., Bansal,A. and Cook,J.C. (2006) A recombinant 63-kDa form of *Bacillus anthracis* protective antigen produced in the yeast *Saccharomyces cerevisiae* provides protection in rabbit and primate inhalational challenge models of anthrax infection. *Vaccine* **24**, 1501-1514.

Hermann,R., Walther,N., Maier,U. and Büchs,J. (2001) Optical method for the determination of the oxygen transfer capacity of small bioreactors based on sulfite oxidation. *Biotechnol. Bioeng.* **74**, 355-363.

Hermanson, G. T. (1996) *Bioconjugate Techniques*. Academic Press Inc. London.

Hoare,M. and Dunnill,P. (1989) Biochemical engineering challenges of purifying useful proteins. *Philos. Trans. R. Soc. Lond B Biol. Sci.* **324**, 497-507.

Hoffmaster,A.R. and Koehler,T.M. (1997) The anthrax toxin activator gene atxA is associated with CO2-enhanced non-toxin gene expression in *Bacillus anthracis*. *Infec. Immun.* **65**, 3091-3099.

Hughmark,G.A. (1980) Power requirements and interfacial area in gas-liquid turbine agitated systems. *Ind. Eng. Chem. Process Des. Dev.* **19**, 638-641.

Israelachvili, J. (1991) Electrostatic Forces Between Surfaces in Liquids. In *Intermolecular and Surface Forces* pp. 213-254. Academic Press.

Israelachvili,J. and Pashley,R. (1982) The hydrophobic interaction is long range, decaying exponentially with distance. *Nature* **300**, 341-342.

Jackson,N.B., Liddell,J.M. and Lye,G.J. (2006) An automated microscale technique for the quantitative and parallel analysis of microfiltration operations. *Journal of Membrane Science* **276**, 31-41.

Jodar,L., Feavers,I.M., Salisbury,D. and Granoff,D.M. (2002) Development of vaccines against meningococcal disease. *The Lancet* **359**, 1499-1508.

Johnsen,A.R., Bendixen,K. and Karlson,U. (2002) Detection of Microbial Growth on Polycyclic Aromatic Hydrocarbons in Microtiter Plates by Using the Respiration Indicator WST-1. *App. Environ. Microbiol.* **68**, 2683-2689.

Jones,M.B. and Blaser,M.J. (2003) Detection of a luxS-signaling molecule in *Bacillus anthracis*. *Infec. Immun.* **71**, 3914-3919.

Jones,M.B., Jani,R., Ren,D., Wood,T.K. and Blaser,M.J. (2005) Inhibition of *Bacillus anthracis* growth and virulence-gene expression by inhibitors of quorum-sensing. *J. Infect. Dis.* **191**, 1881-1888.

Joyce,E.A., Kawale,A., Censini,S., Kim,C.C., Covacci,A. and Falkow,S. (2004) LuxS Is Required for Persistent Pneumococcal Carriage and Expression of Virulence and Biosynthesis Genes. *Infec. Immun.* **72**, 2964-2975.

Kaprelyants,A.S. and Kell,D.B. (1996) Do bacteria need to communicate with each other for growth? *Trends Microbiol.* **4**, 237-242.

Keane,J.T., Ryan,D. and Gray,P.P. (2003) Effect of shear stress on expression of a recombinant protein by Chinese hamster ovary cells. *Biotechnol. Bioeng.* **81**, 211-220.

Keep,N.H., Ward,J.M., Cohen-Gonsaud,M. and Henderson,B. (2006) Wake up! Peptidoglycan lysis and bacterial non-growth states. *Trends Microbiol.* **14**, 271-276.

Kensy,F., Zimmermann,H.F., Knabben,I., Anderlei,T., Trauthwein,H., Dingerdissen,U. and Büchs,J. (2005) Oxygen transfer phenomena in 48-well microtitre plates: Determination by optical monitoring of sulfite oxidation and verification by real time measurement during microbial growth. *Biotechnol. Bioeng.* **89**, 698-708.

Khan,A., Jonsson,B. and Wennerstrom,H. (1985) Phase-equilibria in the mixed sodium and calcium di-2-ethylhexylsulfosuccinate aqueous system - an illustration of repulsive and attractive double-layer forces. *J. Phys. Chem.* **89**, 5180-5184.

Kim JJ, Griffiss JM and Mandrell RE (1989) *Neisseria lactamica* and *Neisseria meningitidis* share lipooligosaccharide epitopes but lack common capsular and class 1, 2, and 3 protein epitopes. *Infec. Immun.* **57**, 602-608.

Kleerebezem,M., Quadri,L.E., Kuipers,O.P. and de Vos,W.M. (1997) Quorum sensing by peptide pheromones and two-component signal-transduction systems in gram-positive bacteria. *Mol. Microbiol.* **24**, 895-904.

Kostov,Y., Harms,P., Randers-Eichhorn,L. and Rao,G. (2001) Low-cost microbioreactor for high-throughput bioprocessing. *Biotechnol. Bioeng.* **72**, 346-352.

Kumar,S., Wittmann,C. and Heinzle,E. (2004) Minibioreactors. *Biotechnol. Lett.* **26**, 1-10.

Lazazzera,B.A. and Grossman,A.D. (1998) The ins and outs of peptide signaling. *Trends in Microbiology* **6**, 288-294.

Leppla,S.H. (1984) Bacillus anthracis calmodulin-dependent adenylate cyclase: chemical and enzymatic properties and interactions with eucaryotic cells. *Adv. Cyclic. Nucleotide. Protein Phosphorylation. Res* **17**, 189-198.

Lilley,B.N. and Bassler,B.L. (2000) Regulation of quorum sensing in *Vibrio harveyi* by LuxO and sigma-54. *Mol. Microbiol.* **36**, 940-954.

Loftsson,T. (1998) Increasing the cyclodextrin complexation of drugs and drug biovailability through addition of water-soluble polymers. *Pharmazie* **53**, 733-740.

Longworth,E., Borrow,R., Goldblatt,D., Balmer,P., Dawson,M., Andrews,N., Miller,E. and Cartwright,K. (2002) Avidity maturation following vaccination with a meningococcal recombinant hexavalent PorA OMV vaccine in UK infants. *Vaccine* **20**, 2592-2596.

Lye,G.J., Ayazi-Shamlou,P., Baganz,F., Dalby,P.A. and Woodley,J.M. (2003) Accelerated design of bioconversion processes using automated microscale processing techniques. *Trends Biotechnol.* **21**, 29-37.

Magnuson,R., Solomon,J.M. and Grossman,A.D. (1994) Biochemical and genetic characterization of a competence pheromone from *B. subtilis*. *Cell* **77**, 207-216.

Manny,A.J., Kjelleberg,S., Kumar,N., de Nys,R., Read,R.W. and Steinberg,P. (1997) Reinvestigation of the sulfuric acid-catalysed cyclisation of brominated 2-alkyllevulinic acids to 3-alkyl-5-methylene-2(5H)-furanones. *Tetrahedron* **53**, 15813-15826.

Marra,J. (1986) Direct measurement of the interaction between phosphatidylglycerol bilayers in aqueous electrolyte solutions. *Biophys. J.* **50**, 815-825.

Mathews, P. (2004) DOE Language and Concepts. In *Design of Experiments with Minitab* ed. O'Mara,P. pp. 93-142. Milwaukee, Wisconsin: ASQ Quality Press.

Maybury,J.P., Mannwelier,K., Tichner-Hooker,N.J., Hoare,M. and Dunnill,P. (1998) The performance of a scaled down industrial disc stack centrifuge with a reduced feed material requirement. *Bioproc. Eng.* **18**, 191-199.

Meares,P. (1984) Mass transfer and reactions at interfaces. *Faraday Discuss. Chem. Soc.* **77**, 7-16.

MHRA (2002) EU guidance on manufacture. In *Rules and guidance for pharmaceutical manufacturers and distributors* pp. 51-294. London: TSO.

Micheletti,M., Barrett,T., Doig,S.D., Baganz,F., Levy,M.S., Woodley,J.M. and Lye,G.J. (2006) Fluid mixing in shaken bioreactors: Implications for scale-up predictions from microlitre-scale microbial and mammalian cell cultures. *Chem. Eng. Sci.* **61**, 2939-2949.

Micheletti,M. and Lye,G.J. (2006) Microscale bioprocess optimisation. *Curr. Opin. Biotechnol.* **17**, 611-618.

Mignot,T., Mock,M. and Fouet,A. (2003) A plasmid-encoded regulator couples the synthesis of toxins and surface structures in *Bacillus anthracis*. *Mol. Microbiol.* **47**, 917-927.

Miller,C.J., Elliott,J.L. and Collier,R.J. (1999) Anthrax protective antigen: Prepore-to-pore conversion. *Biochem.* **38**, 10432-10441.

Miller,G.L. (1959) Use of dinitrosalycylic acid reagent for determination of reducing sugars. *Anal. Chem.* **31**, 426-428.

Miller, H. Vaccine development a casualty of flawed public policy. The Daily Report Ed-Op[Online]. 2003. The Hoover Institution Office of Public Affairs.
Ref Type: Electronic Citation

Miller,M.B. and Bassler,B.L. (2001) Quorum sensing in bacteria. *Annu. Rev. Microbiol.* **55**, 165-169.

Miller,M.B., Skorupski,K., Lenz,D., Taylor,R.K. and Bassler,B.L. (2002) Parallel quorum sensing systems converge to regulate virulence in *Vibrio cholerae. Cell* **110**, 303-314.

Mitchell,M.S., Rhoden,D.L. and King,E.O. (1965) Lactose fermenting organisms resembling *Neisseria meningitidis. J Bacteriol.* **90**, 560.

Mock,M. and Fouet,A. (2001) Anthrax. *Annu. Rev. Microbiol.* **55**, 647-671.

Mock,M. and Mignot,T. (2003) Anthrax toxins and the host: a story of intimacy. *Cell Microbiol.* **5**, 15-23.

Moe,G.R., Zuno-Mitchell,P., Lee,S.S., Lucas,A.H. and Granoff,D.M. (2001) Functional activity of anti-Neisserial surface protein A monoclonal antibodies against strains of *Neisseria meningitidis* Serogroup B. *Infec. Immun.* **69**, 3762-3771.

Morici,L.A., Carterson,A.J., Wagner,V.E., Frisk,A., Schurr,J.R., zu Bentrup,K.H., Hassett,D.J., Iglewski,B.H., Sauer,K. and Schurr,M.J. (2007) *Pseudomonas aeruginosa* AlgR represses the Rhl quorum-sensing system in a biofilm-specific manner. *J. Bacteriol.* ***189***, 7752-7764.

Morley,S.L. and Pollard,A.J. (2001) Vaccine prevention of meningococcal disease, coming soon? *Vaccine* **20**, 666-687.

Mukamalova,G.V., Kaprelyants,A.S., Young,D.I., Young,M. and Kell,D.B. (1998) A bacterial cytokine. *Proc. Natl. Acad. Sci. USA* **95**, 8916-8921.

Mukamolova,G.V., Murzin,A.G., Salina,E.G., Demina,G.R., Kell,D.B., Kaprelyants,A.S. and Young,M. (2006) Muralytic activity of *Micrococcus luteus* Rpf and its relationship to physiological activity in promoting bacterial growth and resuscitation. *Mol. Microbiol.* **59**, 84-98.

Mukhopadhyay, T. K. Stop clinical trials in developing nations. *Chemistry and Industry* 2006 [22], 17. 2006.

Mukhopadhyay,T.K., Halliwell,D., O'Dwyer,C., Shamlou,P.A., Levy,M.S., Allison,N., Gorringe,A. and Reddin,K.M. (2005) Rapid characterization of outer-membrane proteins in *Neisseria lactamica* by SELDI-TOF-MS (surface-enhanced laser desorption ionization-time-of-flight MS) for use in a meningococcal vaccine. *Biotechnol. Appl. Biochem.* **41**, 175-182.

Neal,G., Christie,J., Keshavarz-Moore,E. and Shamlou,P.A. (2003) Ultra scale-down approach for the prediction of full-scale recovery of ovine polycolonal immunoglobulins used in the manufacture of snake venom-specific Fab fragment. *Biotechnol. Bioeng.* **81**, 149-157.

Neiditch,M.B., Federle,M.J., Pompeani,A.J., Kelly,R.C., Swem,D.L., Jeffery,P.D., Bassler,B.L. and Hughson,F.M. (2006) Ligand-induced asymmetry in histidine sensor kinase complex regulates quorum sensing. *Cell* **126**, 1095-1108.

Neiditch,M.B. and Hughson,F.M. (2007) The regulation of histidine sensor kinase complexes by quorum sensing signal molecules. *Methods Enzymol.* **423**, 250-263.

Nikerel,I.E., Toksoy,E., Kirdar,B. and Yildirim,R. (2005) Optimizing medium composition for TaqI endonuclease production by recombinant *Escherichia coli* cells using response surface methodology. *Process Biochem.* **40**, 1633-1639.

NIST/SEMATECH. Process Improvment. Engineering Statistics Handbook. 2003. Information Technology Laboratories.

Norheim,G., Aase,A., Caugant,D.A., Hoiby,E.A., Fritzsonn,E., Tangen,T., Kristiansen,P., Heggelund,U. and Rosenqvist,E. (2005) Development and characterisation of outer membrane vesicle vaccines against serogroup A *Neisseria meningitidis*. *Vaccine* **23**, 3762-3774.

O'Dwyer,C.A., Reddin,K., Martin,D., Taylor,S.C., Gorringe,A.R., Hudson,M.J., Brodeur,B.R., Langford,P.R. and Kroll,J.S. (2004) Expression of heterologous antigens in commensal *Neisseria* spp.: preservation of conformational epitopes with vaccine potential. *Infect. Immun.* **72**, 6511-6518.

O'Hallahan,J., Lennon,D. and Oster,P. (2004) The strategy to control New Zealand's epidemic of group B meningococcal disease. *Pediatr. Infect. Dis. J* **23**, S293-S298.

Oliver,K.J., Reddin,K.M., Bracegirdle,P., Hudson,M.J., Borrow,R., Feavers,I.M., Robinson,A., Cartwright,K. and Gorringe,A.R. (2002) *Neisseria lactamica* protects against experimental meningococcal infection. *Infect. Immun.* **70**, 3621-3626.

Olsen,S.F., Djurhuus,B., Rasmussen,K., Joensen,H.D., Larsen,S.O., Zoffman,H. and Lind,I. (1991) Pharyngeal carriage of *Neisseria meningitidis* and *Neisseria lactamica* in households with infants within areas with high and low incidences of meningococcal disease. *Epidemiol. Infect.* **106**, 445-457.

Parsek,M.R. and Greenberg,E.P. (2000) Acyl-homoserine lactone quorum sensing in gram-negative bacteria: a signalling mechanism involved in associations with higher organisms. *Proc. Natl. Acad. Sci. USA* **97**, 8789-8793.

Pichichero,M.E., Cernichiari,E., Lopreiato,J. and Treanor,J. (2002) Mercury concentrations and metabolism in infants receiving vaccines containing thimerosal: a descriptive study. *Lancet* **360**, 1737-1741.

Pillai,S., Howell,A., Alexander,K., Bentley,B.E., Jiang,H.Q., Ambrose,K., Zhu,D. and Zlotnick,G. (2005) Outer membrane protein (OMP) based vaccine for *Neisseria meningitidis* serogroup B. *Vaccine* **23**, 2206-2209.

Pollard,A.J. and Frasch,C. (2001) Development of natural immunity to *Neisseria meningitidis. Vaccine* **19**, 1327-1346.

Pollard,A.J. and Moxon,E.R. (2002) The meningococcus tamed? *Arch. Dis. Child* **87**, 13-17.

Puskeiler,R., Kusterer,A., John,G.T. and Weuster-Botz,D. (2005) Miniature bioreactors for automated high-throughput bioprocess design (HTBD): reproducibility of parallel fed-batch cultivations with *Escherichia coli. Biotechnol Appl Biochem.* **42**, 227-235.

Puziss,M., Manning,L.C., Lynch,J.W., Barclay,E., Abelow,I. and Wright,G.G. (1963) Large-Scale Production of Protective Antigen of *Bacillus anthracis* in Anaerobic Cultures. *Appl. Microbiol.* **11**, 330-334.

Ren,D., Bedzyk,L.A., Setlow,P., England,D.F., Kjelleberg,S., Thomas,S.M., Ye,R.W. and Wood,T.K. (2004a) Differential gene expression to investigate the effect of (5Z)-4-bromo-5-(bromomethylene)-3-butyl-2(5H)-furanone on *Bacillus subtilis. App. Environ. Microbiol.* **70**, 4941-4949.

Ren,D., Bedzyk,L.A., Ye,R.W., Thomas,S.M. and Wood,T.K. (2004b) Differential gene expression shows natural brominated furanones interfere with the bacterial signaling system of autoinducer-2 bacterial signaling system of *Escherichia coli*. *Biotechnol. Bioeng.* **88**, 630-642.

Ren,D., Sims,J.J. and Wood,T.K. (2001) Inhibition of biofilm formation and swarming of *Escherichia coli* by (5Z)-4-bromo-5-(bromomethylene)-3-butyl-2(5H)-furanone. *Environ. Microbiol.* **3**, 731-736.

Ren,X., Yu,D., Han,S. and Feng,Y. (2006) Optimization of recombinant hyperthermophilic esterase production from agricultmethodologyural waste using response surface. *Bioresour. Technolog.* **97**, 2345-2349.

Rivas,M., Seeger,M., Holmes,D.S. and Jedlicki,E. (2005) A Lux-like quorum sensing system in the extreme acidophile *Acidithiobacillus ferrooxidans*. *Biol. Res.* **38**, 283-297.

Salte,H., King,J.M.P., Baganz,F., Hoare,M. and Titchener-Hooker,N.J. (2006) A methodology for centrifuge selection for the separation of high solids density cell broths by visualisation of performance using windows of operation. *Biotechnol. Bioeng.* **95**, 1218-1227.

Schauder,S., Shokat,K., Surette,M.G. and Bassler,B.L. (2001) The LuxS family of bacterial autoinducers: biosynthesis of a novel quorum-sensing signal molecule. *Mol. Microbiol.* **41**, 463-476.

Schmidt,M. and Bornscheuer,U.T. (2005) High-throughput assays for lipases and esterases. *Biomol. Eng.* **22**, 51-56.

Showalter,R.E., Martin,M.O. and Silverman,M.R. (1990) Cloning and nucleotide sequence of luxR, a regulatory gene controlling luminescence in *Vibrio harveyi*. *J Bacteriol.* **172**, 2946-2954.

Sirard,J.C., Mock,M. and Fouet,A. (1994) The three *Bacillus anthracis* toxin genes are coordinately regulated by bicarbonate and temperature. *J Bacteriol.* **176**, 5188-5192.

Sircili,M.P., Walter,M., Trabulsi,L.R. and Sperandio,V. (2004) Modulation of enteropathogenic *Escherichia coli* virulence by quorum sensing. *Infec. Immun.* **72**, 2329-2337.

Smith, A. Vaccines: Hot 'new' business for drugmakers. 2007.
Ref Type: Internet Communication

Smith,K.A. (2005) Wanted, an Anthrax vaccine: Dead or Alive? *Med. Immunol.* **4**, 5.

Solomon,J.M., Lazazzera,B.A. and Grossman,A.D. (1996) Purification and characterization of an extracellular peptide factor that affects two different developmental pathways in *Bacillus subtilis*. *Genes Dev.* **10**, 2014-2024.

Solomon,J.M., Magnuson,R., Srivastava,A. and Grossman,A.D. (1995) Convergent sensing pathways mediate response to two extracellular competence factors in *Bacillus subtilis*. *Genes Dev.* **9**, 547-558.

Stanbury, P. F. and Whitaker, A. (1984a) Aeration and Agitation. In *Principles of Fermentation Technology* pp. 169-191. Oxford: Pergamon Press.

Stanbury, P. F. and Whitaker, A. (1984b) Media for industrial fermentation. In *Principles of fermentation technology* pp. 74-87. Oxford: Pergamon Press Ltd.

Stanley,J.L. and Smith,H. (1961) Purification of factor I and recognition of a third factor of the anthrax toxin. *J. Gen. Microbiol.* **26**, 49-63.

Stephens, L. J. (2004) Analysis of Variance. In *advanced statistics demystified* ed. Bass,J. pp. 57-106. New York: Mc Graw-Hill.

Stolberg, S. G. FDA approves costly meningits shots. New York Times. 2000.

Surette,M.G., Miller,M.B. and Bassler,B.L. (1999) Quorum sensing in *Escherichia coli*, *Salmonella typhimurium* and *Vibrio harveyi*: a new family of genes responsible for autoinducer production. *Proc. Natl. Acad. Sci. USA* **96**, 1639-1644.

Swalley,S.E., Fulghum,J.R. and Chambers,S.P. (2006) Screening factors effecting a response in soluble protein expression: Formalized approach using design of experiments. *Anal. Biochem.* **351**, 122-127.

Thomas,C.R. and Dunnill,P. (1979) Action of shear on enzymes: studies with catalase and urease. *Biotechnol. Bioeng.* **21**, 2279-2302.

Todar, K. The Genus *Bacillus*. 2005. Online textbook reference: http://textbookofbacteriology.net/Bacillus.html

Tondella,M.L., Popovic,T., Rosenstein,N.E., Lake,D.B., Carlone,G.M., Mayer,L.W., Perkins,B.A. and The Active Bacterial Core Surveillance Team (2000) Distribution of *Neisseria meningitidis* Serogroup B Serosubtypes and Serotypes Circulating in the United States. *J. Clin. Microbiol.* **38**, 3323-3328.

Tornberg,E. (1977) Absorption of Surfactants in dilute aqueous solutions. Anomalous oscillating jet phenomena. *J. Colloid. Interf. Sci.* **60**, 50-53.

Troncoso,G., Sanchez,S., Criado,M.T. and Ferreiros,C.M. (2002) Analysis of *Neisseria lactamica* antigens putatively implicated in acquisition of natural immunity to *Neisseria meningitidis*. *FEMS Immunol. Med. Microbiol.* **34**, 9-15.

Tufariello,J., Jacobs Jr.,W. and Chan,F. (2004) Individual *Mycobacterium tuberculosis* resuscitation-promoting factor homologues are dispensable for growth in vitro and in vivo. *Infec. Immun.* **72**, 515-526.

Uchida,I., Hornung,J.M., Thorne,C.B., Klimpel,K.R. and Leppla,S.H. (1993) Cloning and characterization of a gene whose product is a trans-activator of anthrax toxin synthesis. *J. Bacteriol.* **175**, 5329-5338.

Uchida,I., Makino,S., Sekizaki,T. and Terakado,N. (1997) Cross-talk to the genes for *Bacillus anthracis* capsule synthesis by atxA, the gene encoding the trans-activator of anthrax toxin synthesis. *Mol. Microbiol.* **23**, 1229-1240.

Urban,A., Ansmant,I. and Motorin,Y. (2003) Optimisation of expression and purification of the recombinant Yol066 (Rib2) protein from *Saccharomyces cerevisiae*. *J. Chromatogr. Biomed. Sci. Appl.* **786**, 187-195.

Urwin,R., Russell,J.E., Thompson,E.A.L., Holmes,E.C., Feavers,I.M. and Maiden,M.C.J. (2004) Distribution of surface protein variants among hyperinvasive meningococci: Implications for vaccine design. *Infec. Immun.* **72**, 5955-5962.

van't Riet,K. (1979) Review of measuring methods and results in non-viscous gas-liquid mass transfer in stirred vessels. *Ind. Eng. Chem. Process Des. Dev.* **18**, 357-364.

Vignaux, G. A. (1991) Dimensional analysis in data modelling. In *Maximum Entropy and Bayesian Methods* ed. Smith,C.R., Erickson,G.J. and Neudofer,P.O. pp. 1-9. Seattle: Kluwer Academic Publishers.

Virkar,P.D., Narendranathan,T.J., Hoare,M. and Dunnill,P. (1981) Studies of the effect of shear on globular proteins: extension to high shear fields and to pumps. *Biotechnol. Bioeng.* **23**, 425-429.

Welty, J. R., Wicks, C. E. and Wilson, R. E. (1995) Dimensionless analysis. In *Fundementals of momentum, heat and mass transfer.* pp. 150-162. Chichester: John Wiley & Sons.

Wenner,K.A. and Kenner,J.R. (2004) Anthrax. *Dermatol. Clin.* **22**, 247-56, v.

West,D., Reddin,K., Matheson,M., Heath,R., Funnell,S., Hudson,M., Robinson,A. and Gorringe,A. (2001) Recombinant *Neisseria meningitidis* transferrin binding protein A protects against experimental meningococcal infection. *Infect. Immun.* **69**, 1561-1567.

Wright,J.C., Williams,J.N., Christodoulides,M. and Heckels,J.E. (2002) Immunization with the recombinant PorB outer membrane protein induces a bactericidal immune response against *Neisseria meningitidis*. *Infec. Immun.* **70**, 4028-4034.

Xavier,K.B. and Bassler,B.L. (2005) Regulation of uptake and processing of the Quorum Sensing autoinducer AI-2 in *Escheichia coli*. *J Bacteriol.* **187**, 238-248.

Zhu,W., Plikaytis,B.B. and Shinnick,T.M. (2003) Resuscitation factors from mycobacteria: homologs of *Micrococcus luteus* proteins. *Tuberculosis* **83**, 261-269.

Zollinger,W.D., Mandrell,R.E., Altieri,P., Berman,S., Lowenthal,J. and Artenstein,M.S. (1978) Safety and immunogenicity of a *Neisseria meningitidis* type 2 protein vaccine in animals and humans. *J Infect. Dis.* **137**, 728-739.

Zwartouw,HT. and Smith,H. (1956) Polyglutamic acid from *Bacillus anthracis* grown in vivo; structure and aggressin activity. *Biochem. J* **63**, 437-442.

9 Appendix A – Supplementary data

9.1 Media and analytical calibration standards

9.1.1 Media Used

Summarised below are all the media formulations used in this study, complete with the supplier details. Two media, Basal and Addition, were supplied directly by the Media Prep Division at the Health Protection Agency, Porton Down, UK and have been indicated as such.

MC7 Medium

Component	Amount ($g\ L^{-1}$)	Supplier
L – Glutamic acid	3.90	Sigma
NaCl	5.80	BDH
K_2SO_4	1.00	Sigma
$MgCl_2.6H_20$	0.40	Sigma
NH_4Cl	1.00	BDH
Yeast Extract	0.80	Oxoid
K_2HPO_4	2.00	Sigma
L - Cystine. 2HCl	0.10	Sigma
$CaCl_2.2H_2O$	0.03	Sigma
Glucose	10.00	Sigma

Table A1.1 Formulation of MC7 medium used for *N. lactamica* fermentations.

Frantz Medium

Component	Amount ($g\ L^{-1}$)	Supplier
L – Glutamic acid	1.60	Sigma
NaCl	6.00	Sigma
KCl	0.09	BDH
$MgCl_2.6H_20$	0.60	Sigma
NH_4Cl	1.25	Sigma
Yeast Extract	2.00	Oxoid
$NaHCO_3$	2.5	BDH
L - Cystine. 2HCl	0.01	Sigma
Glucose	5.00	Sigma

Table A1.2 Formulation of Frantz medium used for *N. lactamica* fermentations.

MCD Medium

Component	Amount ($g\ L^{-1}$)	Supplier
L – Glutamic Acid	3.70	Sigma
NaCl	5.80	BDH
K_2SO_4	1.00	Sigma
$MgCl_2.6H_20$	0.40	Sigma
NH_4Cl	0.20	BDH
Glycine	0.25	Sigma
K_2HPO_4	4.00	Sigma
L - Cystine. 2HCl	0.10	Sigma
$CaCl_2.2H_2O$	0.04	Sigma
$NaHCO_3$	0.04	Sigma
L – Aspartic acid	0.50	Sigma
Sodium acetate	2.00	Sigma
Choline Chloride	0.01	Sigma
Biotin	0.01	Sigma
Myo - Inositol	0.04	Sigma
Glucose	10.00	Sigma

Table A1.3 Formulation of MCD medium used in *N. lactamica* fermentations.

Basal Medium

Component	Amount ($g\ L^{-1}$)	Supplier
Casamino acids	5.956	HPA
KOH	0.518	HPA
Activated charcoal	0.0695	HPA
DL-serine	0.052	HPA
$MgSO_4.7H_2O$	0.025	HPA
$CaCl_2.6H_2O$	0.0245	HPA
L-cystine	0.020	HPA
Thiamine.HCl	0.000167	HPA

Table A1.4 Formulation of basal medium used in *B. anthracis* culture, supplied by the Health Protection Agency.

Addition Medium

Component	Amount ($g\ L^{-1}$)	Supplier
$NaHCO_3$	60	HPA
Glucose	20	HPA
$MnSO_4.4H_20$	0.01	HPA

Table A1.5 Formulation of addition medium, supplied by the Health Protection Agency, for use in *B. anthracis* culture.

9.1.2 Glucose Calibration Curve

A typical calibration curve for the DNS glucose assay as described in Section 2.6.3 is shown below. The assay mixture was calibrated against known concentrations of glucose, from which the glucose concentration of the fermentation supernatant could then be determined.

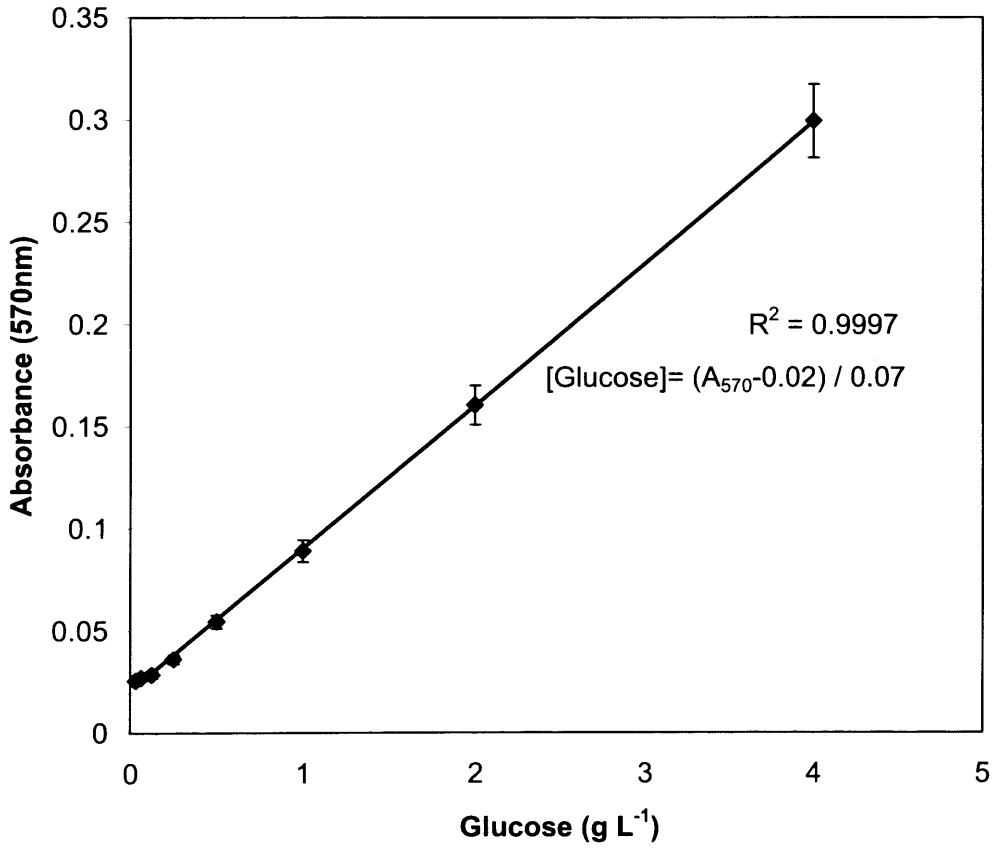

Figure A1.1 Calibration curve of DNS glucose assay. Error bars represent one standard deviation about the mean, where n=3. Solid line fitted by linear regression.

9.1.3 BCA Total Protein Assay

A typical BCA calibration curve as described in Section 2.6.4 is shown below. The assay mixture was calibrated against known concentrations of BSA, from which the total protein concentration of the fermentation supernatant could then be determined.

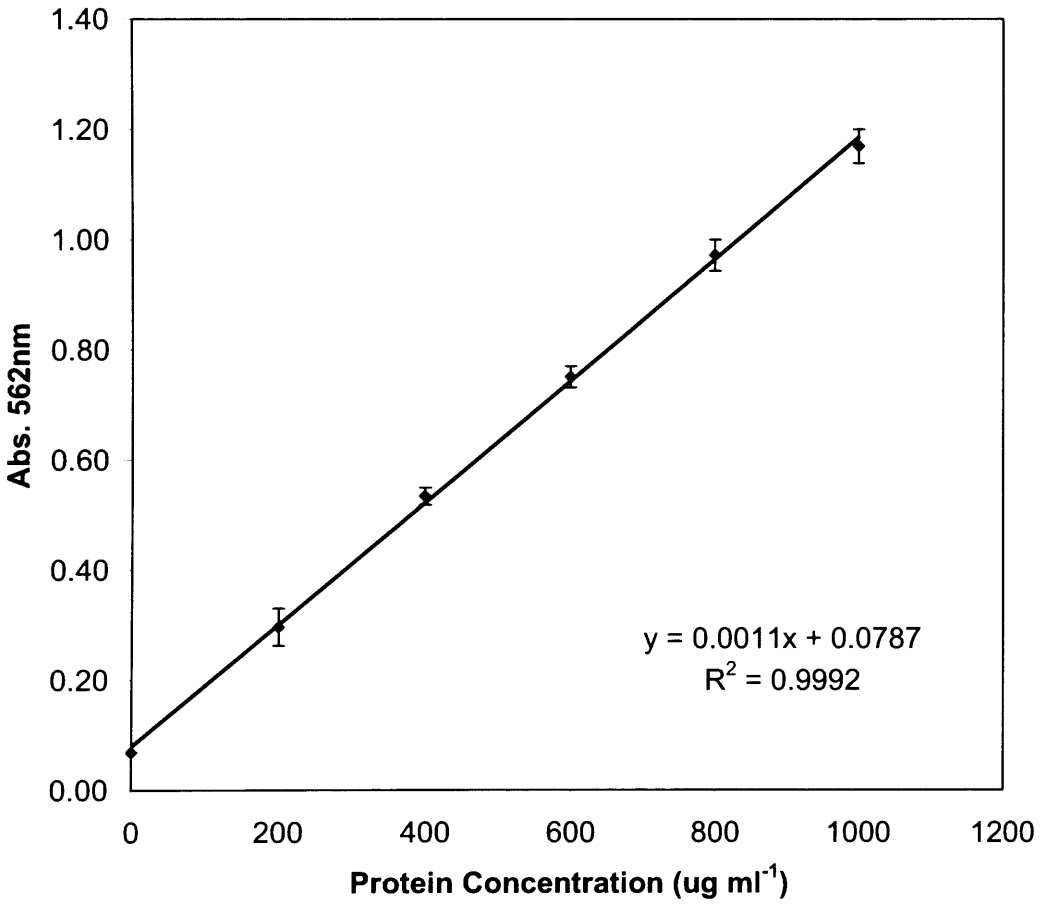

Figure A1.2 Calibration curve of BCA total protein assay. Error bars represent one standard deviation about the mean, where n=3. Solid line fitted by linear regression.

9.1.4 PA ELISA Standards Curve

A typical standards curve used for the determination of PA concentration in *B. anthracis* fermentation samples. Samples were serially diluted and compared with the standards curve. Sample points of closest parallelism to the standards curve were used to calculate the PA concentration.

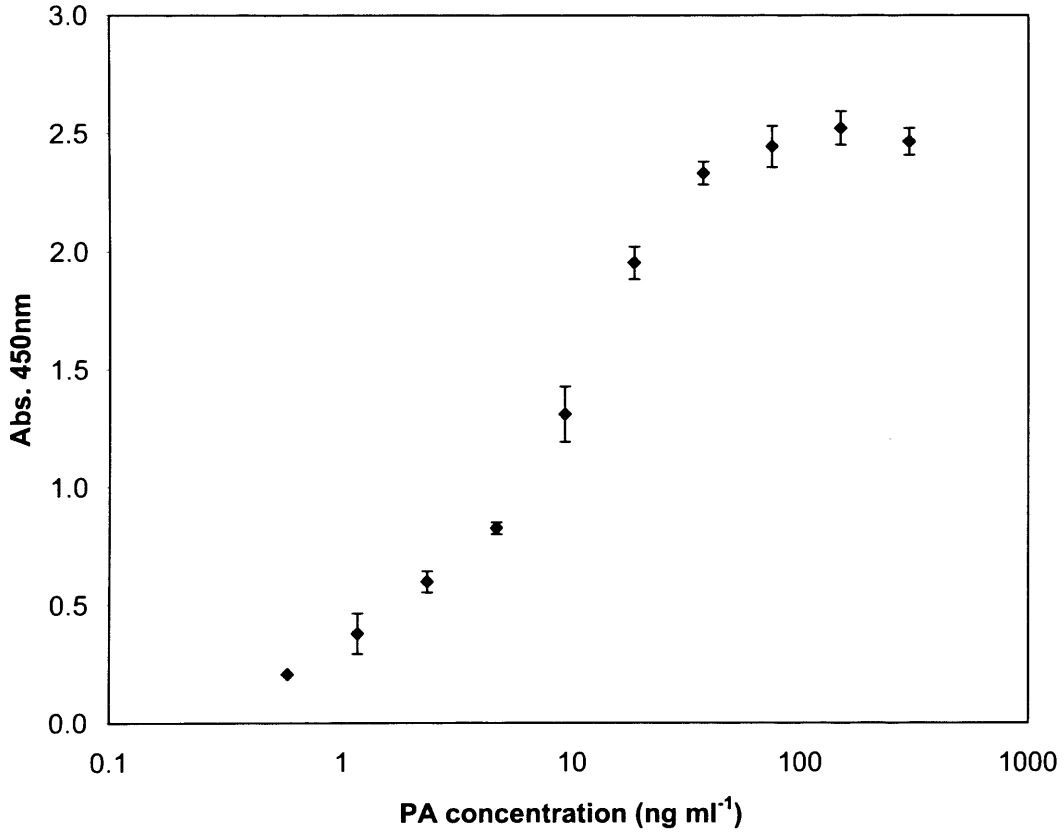

Figure A1.3 A standard curve generated from the PA ELISA. Error bars represent one standard deviation about the mean, where n=3. The ELISA is analysed using Ascent software, V2.6, which fits the curve with a four parameter logistic fit: $y=b+(a-b)/(1+xc)^{d}$.

9.1.5 LF ELISA Standards Curve

A typical standards curve used for the determination of LF concentration in *B. anthracis* fermentation samples. Samples were serially diluted and compared with the standards curve. Sample points of closest parallelism to the standards curve were used to calculate the LF concentration.

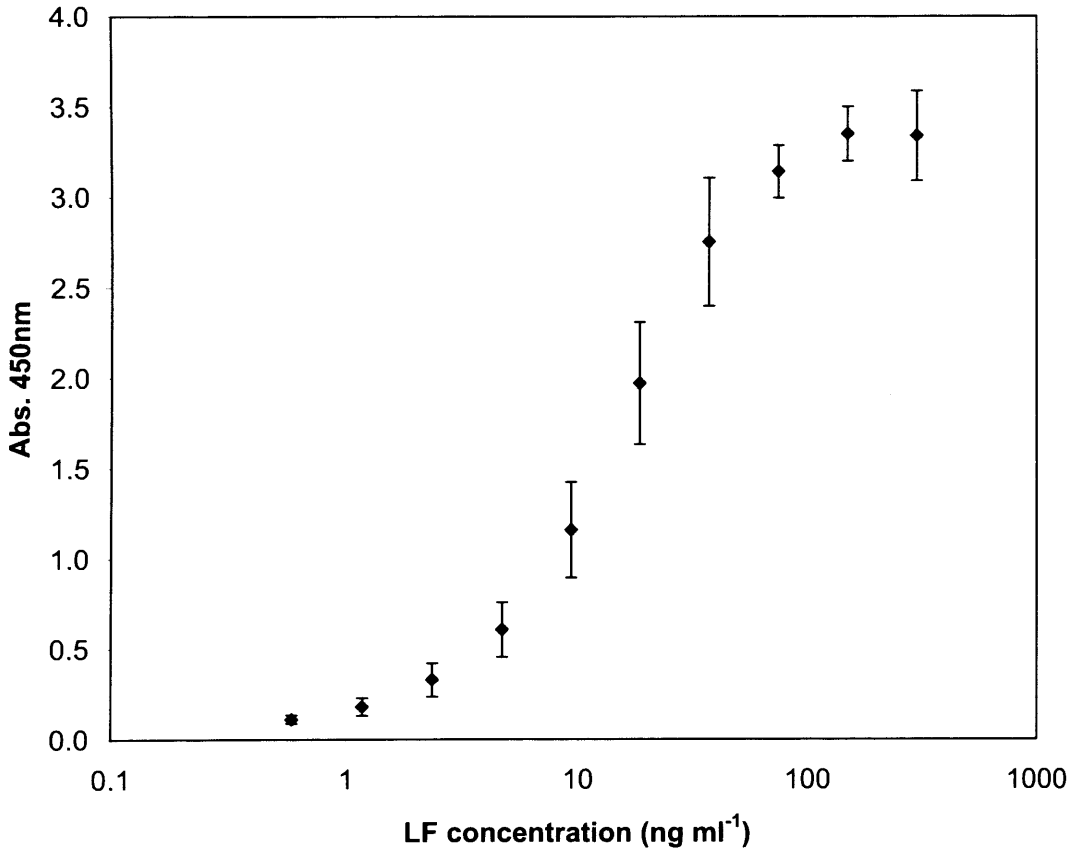

Figure A1.4 A standard curve generated from the LF ELISA. Error bars represent one standard deviation about the mean, where n=3. The ELISA is analysed using Ascent software, V2.6, which fits the curve with a four parameter logistic fit: $y=b+(a-b)/(1+xc)^d$.

9.2 Supplementary data (Chapter 5)

9.2.1 PA_{83} degradation during SELDI-MS analysis

As described in Section 5.4.5, PA_{83} break down products were identified using the gel band extraction protocol and analysed through SELDI. Briefly, the PA_{83} band was excised from a SDS-PAGE gel and the protein purified and analysed through SELDI-MS. Figure A3.1 shows a gel of the protective antigen reference, used to generate the SELDI profile in Figure A3.2 and the purified PA_{83} component, (extracted band) from the reference used to generate Figure A3.3.

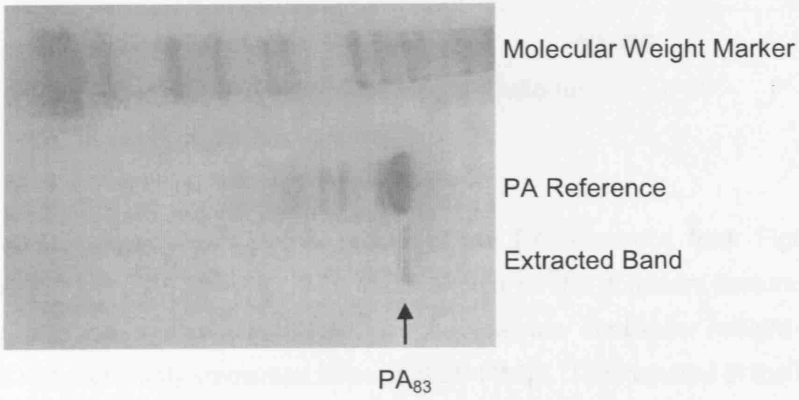

Figure A2.1 A gel showing the purified PA83 component obtained through SDS-PAGE band extraction. The protective antigen reference was the protein component used in the vaccine. In order to identify the break down products, the 83kDa band was extracted and analysed using SELDI-MS as described in Sections 2.6.12 and 2.6.13.

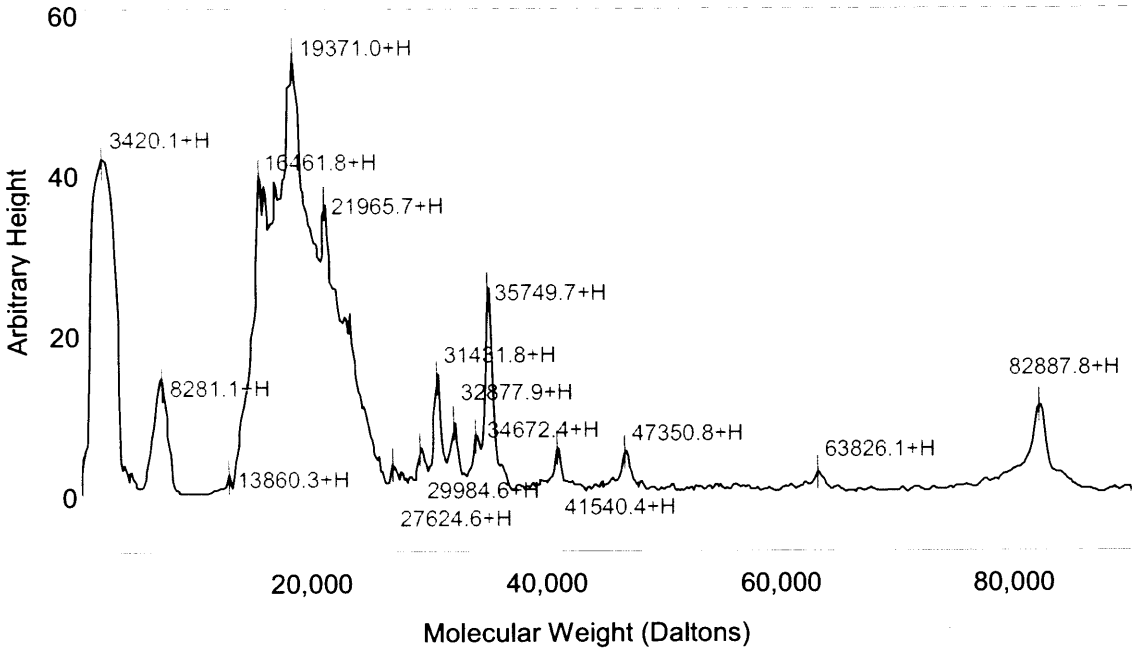

Figure A2.2 A typical SELDI-MS profile of the PA reference from Figure A3.1. With reference to Figure A3.1 the 82.9kDa peak should be the dominant feature on this profile, however, this peak was diminished and several low molecular weight proteins were identified not previously visualised through SDS-PAGE. This resulted in the hypothesis that the SELDI-MS process may be breaking down the vaccine antigen. Analysis performed as described in Section 2.6.12.

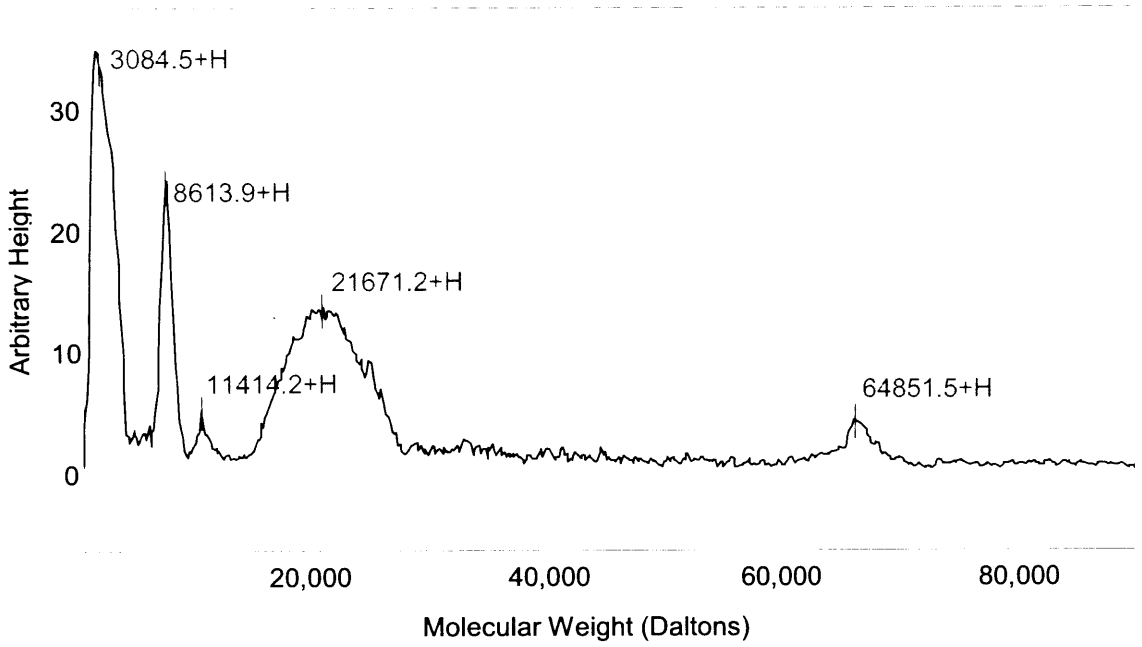

Figure A2.3 A typical SELDI-MS profile of the extracted PA band. The extracted 83kDa protein has been completely broken down into several smaller peaks. PA_{63} and PA_{20}, represented here at 64.9kDa and 21.7kDa respectively, are known break down products of PA_{83}. The other breakdown products identified are peaks at 3.1kDa, 8.6kDa and 11.4kDa. Analysis performed as described in Sections 2.6.12 and 2.6.13.

9.3 Supplementary Data (Chapter 6)

9.3.1 Scale Up Calculations

Geometric and kinematic ratios will be used to scale up the fermentation process from the miniature bioreactor to a commercial stirred tank bioreactor. In order to do this, the manufacturing capacity required per batch will be used, assuming the HPA wishes to maintain its current production level.

Current anthrax vaccine production volume, per batch	= 114 L
Assume 2 vessels used, working volume per vessel	= 57 L
Assume 20% head space (57 x 1.20)	= 68.4 L
Vessel volume	≈ 70 L

Thus, in order to maintain the current production volume, two 70 L vessels should be used per batch. Alternatively, because production time is halved in bioreactors, one 70 L bioreactor could be used, and the number of batches doubled.

9.3.2 Geometric Scale Up of Production Vessel

In order to facilitate kinematic scale up, geometric scale up must first be considered. This is achieved by making the following assumptions:

- Vessel is cylindrical
- Vessel height to diameter ratio is 3:1
- Vessel diameter to impeller diameter is 3:1

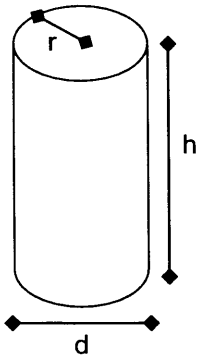

$$V = \pi r^2 h$$

$$V = \pi\left(d/2\right)^2 3d$$

$$V/\pi = 3/4\, d^3$$

$$d = \sqrt[3]{\frac{0.7}{\pi}\cdot\frac{4}{3}}$$

$$d = 0.67m$$

Vessel Height	= 2.00 m
Vessel Diameter	= 0.67 m
Impeller Diameter	= 0.22 m

9.3.3 Kinematic Scale Up

Using the vessel dimensions calculated from Section 9.3.2, kinematic scale up is possible by calculating the power input per unit volume in the miniature bioreactor first, and then to calculate the impeller speeds required in the 70 L bioreactor to achieve the same kinematic conditions.

Assumptions:

- Media density is 1000kg m^{-3}
- Media viscosity is 0.01Pa s^{-1}

Determining Reynolds number of the miniature bioreactor:

Miniature bioreactor impeller diameter, D_i=0.02m and N=700rpm.

$$\mathrm{Re} = \frac{\rho N D_i}{\mu}$$

$$\mathrm{Re} = \frac{1000 \times \left(700/60\right) \times 0.02}{0.01}$$

$$\mathrm{Re} = 2.3 \times 10^4$$

Conditions are turbulent, power number, N'_p = 3.5

Normally a power number of 7 would be expected in bioreactors under turbulent conditions, however, this is lower in the miniature bioreactor due to thicker impeller blades and a disk at the base of the impeller shaft.

$$P = N'_p \rho N^3 D_i^5$$

$$P = 3.5 \times 1000 \times \left(700/60\right)^3 \times 0.02^5$$

$$P = 0.018 \text{ W}$$

$$P/V = 225 \text{ Wm}^{-3}$$

Hence the power per unit volume in the miniature bioreactor is 225Wm^{-3}, which must be maintained in the larger production vessel to ensure the cell experience the same culture conditions. This is controlled by impeller speed.

9.3.4 Determining the impeller speed for the 70L vessel based on constant power input per unit volume

P/V = 225 Wm^{-3}

Working volume = 0.057 m^3

Total power = 12.83 W

$$N = \sqrt[3]{\frac{P}{N_p' \rho D_i^5}}$$

$$N = \sqrt[3]{\frac{12.83}{7 \times 1000 \times 0.22^5}}$$

$$N = 1.53 s^{-1}$$

$$N = 92 rpm$$

Therefore, in order to maintain the same culture conditions experienced in the miniature bioreactor, the impellers of the 70 L bioreactor should operate at a minimum of 92 rpm.

10 Appendix B – Formal course requirements

10.1 The Commercialisation of Vaccines and Development costs

10.1.1 Introduction

In the 1980's vaccine research and development was primarily conducted by public sector institutes. This is because vaccines such as BCG, measles and diphtheria were based on complex molecules which required a high level of investment[1]. However, vaccine prices had already been established at $1-3 per dose reducing the return possible. This made vaccines appear unprofitable and deterred the private sector from investing.

Twenty years later, vaccines are now considered very profitable provided enough capital is available for investment. Vaccines such as Prevnar® and Gardasil® are considered to reach blockbuster status as individuals and governments become more willing to pay higher prices, between $15-50 per dose. Annual vaccine sales in 1982 at $2 billion[3] have now risen to an estimated $5.4 billion[4]. Today vaccine sales only account for less then 1.7%of the total pharmaceutical market[2] but it is projected to have an annual growth of 12%.

The cost components of modern vaccine commercialisation can be broken down into four main areas: (i) Research and development, (ii) Intellectual Property, (iii) Clinical trials and (iv) Regulation, each of which will be considered in turn.

10.2 Research and development

As discussed in the main body of the thesis, the research and development process can hold a vaccine back from commercialisation and incorporates a major cost component into the process. The development of high throughput screening helped to make drug discovery more economical, but created a bottle neck further down the line as an equivalent platform was not available for the research and development phases. This is now changing, as this thesis has demonstrated. The application of an automated micro-scale platform combined with statistical methodology, allows the conversion of what once was a qualitative research tool into a quantitative one. A trait that is essential in order to determine critical process parameters (CPP) and critical quality attributes (CQA) for vaccine production. By applying the philosophy of ultra scale down to the micro-scale platform, the key is not to mimic the entire unit operation, but the crucial attributes which control CPP and CQA. The reduced consumption of materials and increased throughput will undoubtedly reduce costs. However, further cost reduction may be possible be eliminating a verification step. Normally, after micro-scale experiments are conducted, verification of the results is carried out before transition to a commercial scale. At some point in the future our knowledge and confidence in the micro-scale process may reach a point where pilot scale verification is no longer required. This would mean processes could leap from micro-scale studies directly into commercial production. This may be considered far-sighted, but not inconceivable.

10.3 Intellectual property rights

Whether it is the defence of a patent or a licensing of technology, intellectual property usually adds a cost component to a pharmaceutical product. However, vaccines may prove to be a more interesting example as fewer vaccines are licensed from third parties and those with the original patents are facing legal challenges. Biogen obtained a patent for its DNA recombinant Hepatitis B vaccine for expression in either yeast or mammalian cell lines. This patent was struck down in 1996 by the House of Lords for being 'too broad,' as

technology overtook the original patent [5,6]. This allowed new manufactures to enter the market resulting in increased competition. With the impact of Trade Related Intellectual Property Rights (TRIPs) setting a global minimum on the application of intellectual property law, the vaccine sector will become increasingly more competitive for smaller emerging manufacturers. For larger manufacturers, TRIPs may not have the same impact as vaccines require a specific knowledge on how to create and consistently manufacture a safe and potent vaccine, which larger manufacturers retain. On all levels TRIPs is making the vaccine sector more competitive and increasing a demand on methods to reduce development and manufacturing costs.

10.4 Clinical trials

The cost of clinical trials is spiralling due to the number of subjects required, post-market monitoring and globalisation.

More and more subjects are required in order to generate enough data to make the clinical trial statistically significant and to develop the safety profile. The tetravalent rotavirus vaccine, Rotashield®, licensed in 1998 used over 10,000 subjects in clinical trials, but this proved to be insufficient to detect the adverse side effect of intussusception[7]. Therefore the FDA is considering the expansion of Phase 3 trials to further develop the safety profile of a vaccine, especially those for children[8]. Consequently, the importance of post-market monitoring or Phase 4 studies is adding further cost to vaccine development.

The third cost component to clinical trials is globalisation. Previously, market sector populations were considered as one homogeneous group but sub-populations exist which may react very differently to a vaccine. Therefore, safety and immunogenic data must be obtained using the candidate vaccine in specific populations[9]. This has applied to a 9 and

11 valent conjugant pneumococcal vaccine developed in the US design to benefit both the indigenous population and migrants of other nationalities[10].

Due to the complexity of compliance and expanding guidelines contract research organisations are becoming increasingly popular. 60% of pharmaceutical companies outsource some part of their drug development creating a $5 billion market, with projected growth of 20% per annum. Clinical trials now account for 45% of the total research and development budget for a new drug (PricewaterhouseCoopers).

10.5 Regulation

Since 1997 the Code of Federal Regulations, Chapter 21 has been updated in the form to two new pieces of US legislation, the Food and Drug Modernisation Act (FDMA) and the Prescription Drug Users Fee Act (PDUFA). Since then there has been an increased effort to incorporate International Committee on Harmonisation standards into 21CFR better regulations on genetic stability, viral clearance and validation methods and pre-clinical data collection. It is the review of the pre clinical data and the consideration of an investigational plan that forms the basis of an IND application. After the IND application has been approved, the vaccines can then enter clinical trials after which time the product is launched. 21CFR Section 312 considers the points required for IND submission, which 21 CFR 600 outlines the investigation parameters which should be taken into account during the clinical trials along with any outline test, as described in 21 CFR 610.

Pre-clinical data and data which is collected for the IND application should demonstrate product quality and control. It must include the manufacturing method, characterisation of the master seed, in process tests and include a tentative product specification. At each step quality, safety and risk factor must be considered. Release tests also have to be developed during the development process including sterility testing, safety testing, vaccine

purity, identity testing, stability and potency. In some rare cases adjuvants may need to undergo toxicity testing. However, the IND must describe the vaccine, its method of manufacture, release control tests, animal data and a proposed study protocol.

With regards to clinical trials, phase one should be small enough to measure any lethal effects, while phase two should be large enough to detect common adverse vaccine reactions, such as inflammation of the injection site and fever. Phase three should be large enough to be able to detect uncommon side effects and adverse reactions. At the end of each phase, all the data should be analysed and evaluated for a benefit versus risk assessment.

10.6 Future considerations

In the past vaccines have been produced in industrialised nations but this may change with more vaccines being produced for developing markets making them region specific, impacting on markets sizes. Due to the identification of overseas markets, there will be an increasing role for outsourcing, potentially being co-ordinated by virtual companies. Due to activities in different markets and the impact of TRIPs, competition will increase and so will regulation.

However, the future trend is for a growing vaccine market which should open new sources of funding. Instead of either public or private investment, an opportunity exists for Public-Private Partnerships, especially those for developing markets.

References

1. MR Hilleman, The business of science and the science of business in the quest for an AIDS vaccine.Vaccine (1999), *17*, 1211-1222.

2. Sana Siwolop, Big Steps for Vaccine Industry, http://www.nytimes.com/2001/07/25

3. JB Milstien, P Evans, and A Batson, Discussion on paper Vaccine Development in Developing Countries, Vaccination and World Health, FT Cutts and PG Smith, eds. John Wiley & Sons, Chichester, 1994, p. 62

4. SN Glass, A Batson, and R Levine, Issues Paper: Accelerating New Vaccines. (GAVI)

5. European & UK Case Law Review in the area of Biotechnology, World Biotech Supplement (4 October 1999).

6. Toshika Takenaka, Highly Anticipated UK Decision of Biogen v. Medeva about Validity of Biotechnology Patents, 1997 University of Washington, School of Law

7. RM Jacobson, A Adegbenro, VS Pankratz, GA Poland. Adverse events and vaccination-the lack of power and predictability of infrequent events in pre-licensure study. Vaccine (2001), *19*: 2428-2433.

8. CDC. Intussusception among recipients of Rotavirus Vaccine – United States, 1998-1999. MMWR (1999), *48*: 577-581.

9. KL Goldenthal, JM Vaillancourt, DR Lucey. Preventive HIV type 1 vaccine clinical trials: a regulatory perspective. AIDS Res Hum Retroviruses (1998), *14 (Suppl 3)*, S333-S340.

10. D Klein, Development and Testing of *Streptococcus pneumoniae* Conjugate Vaccines. The Jordan Report (2000). Pp 111-130